The Effect of Montmorillonite Clay on the Mechanical Properties of Kenaf Reinforced Polypropylene Composite

S.GOVINDEN

A dissertation submitted to the Faculty of Engineering and the Built Environment, University of the Witwatersrand, Johannesburg, in fulfilment of the requirements for the degree of Master of Science in Engineering.

Johannesburg, October 2017

Declaration

I declare that this dissertation is my own, unaided work, except where otherwise acknowledged. It is being submitted for the degree of Master of Science in Engineering in the University of the Witwatersrand, Johannesburg. It has not been submitted before for any degree or examination at any other university.

Signed this 15th day of October 2017

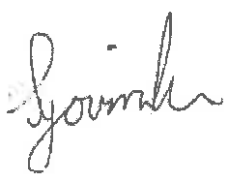

S.GOVINDEN

Acknowledgements

I would like to thank the following people:

My brothers, Megandran and Thiren Govinden for their constant support and care.

My mum, Radhamani, for always encouraging me.

My supervisor, Robert Reid, for his efforts in assisting me to finish my Masters. Without him, and the funding he provided, this dissertation would not have been possible.

The lab staff, all the staff always offered encouragement, a lot of laughs which made this masters all the more bearable. Shaun, Lionel, Buthi, Marius, and Norman, it was amazing having you as the lab staff. Thanks for always seeing to my project manufacturing problems.

Morne Swart and Brian Sole, from Sasol, for donating many bags of polypropylene and providing assistance with extruding.

Mike Formo, from Southern Chemicals, for providing all the required bonding agents for free as well as advice on how to use them.

The Wits Microscopy and Microanalysis Unit in Biology. Deran Reddy and Jacques Gerber were very good teachers. They taught me how to operate a SEM, TEM, Ultramicrotome and a Fluorescence Microscope.

My Neelam, for assisting me with completing this report and always being there.

Abstract

An investigation was carried out to determine the effect of the addition of clay on the mechanical properties of a Natural Fibre Composite consisting of a polypropylene matrix with kenaf fibre reinforcement. The kenaf fibres were treated using various chemical treatments to improve the strength of the composites manufactured. Four treatments using different 3-Mercaptopropyltrimethoxy silane (MPS) concentrations were investigated to determine which treatment resulted in the best mechanical properties. The treated kenaf fibres were manufactured into fibre mats having a density of 350 g/m^2. Clay was mixed into the polypropylene using a twinscrew extruder and then turned into matrix sheets having a thickness of 0.5 mm, using a sheet extruder. The matrix and fibre mats were then joined using a combination of a film stacking technique and compression moulding. The composites investigated were made using two types of matrices namely; a virgin polypropylene matrix and a clay matrix with a clay content of 4%. The composites were then subjected to three mechanical tests, namely; tensile, impact and short beam shear testing.

The results showed that a kenaf fibre chemical treatment consisting of a 6% sodium hydroxide and 0.25% MPS silane solution resulted in the highest mechanical properties for composites using both types of matrices. The effect of a variation of fibre weight fraction on the mechanical properties of the composite was also investigated. It was found that the optimum fibre weight fraction was 25%, as any further addition of fibre resulted in poor wetting of the fibres, reducing the load capability of the composite. The amount of clay in the composite was varied and it was found that a clay concentration of 2% resulted in the best mechanical properties. Further addition of clay into the polypropylene matrix resulted in the reduction of fracture toughness, which limited the tensile strength capability. It was also found that the impact energy of the NFC decreased with the addition of clay. The shear strength data showed that the addition of clay helped improved the interfacial shear strength of the composite when compared to a composite using a virgin polypropylene matrix. A composite consisting of a polypropylene matrix with 2% clay content and fibres treated with a 6% sodium hydroxide treatment showed the greatest improvement in

mechanical properties whilst still being cost effective. This improvement in strength will be useful in the ever increasing demand for natural fibre composites.

Contents

List of Figures

List of Tables

List of Symbols

W_f - Fibre Weight Fraction

℃ - Degree Celsius

List of Acronyms

SEM	Scanning Electron Microscope
TEM	Transmission Electron Microscope
XRD	X-ray Diffraction
PP	Polypropylene
RPM	Revolutions per minute
FTIR	Fourier Transform Infrared Spectroscopy
TGA	Thermogravimetric Analysis
APS	3-Aminopropyltriethoxy Silane
NaOH	Sodium Hydroxide
MPS	3-Mercaptopropyltrimethoxy Silane
PTFE	Polytetrafluoroethylene
DAQ	Data Acquisition Device
FWF	Fibre Weight Fraction
STD	Standard of Deviation
MMT	Montmorillonite Clay
PP-g-MA	Polypropylene-Graft-Maleic Anhydride
MFI	Melt Flow Index
GPS	3-Glycidoxypropyltrimethoxy Silane
PHR	Parts per Hundred
MMU	Microscopy and Microanalysis Unit
HDPE	High Density Polyethylene
kN	Kilo-Newton
NFC	Natural fibre composites
GFRP	Glass Fibre Reinforced Plastic

1 Introduction

With ongoing developments in the mechanical and aviation industry, the need for materials which are cost effective and sustainable whilst still displaying favourable mechanical properties has become increasingly important. This need for eco-friendly materials have drawn much attention to natural fibre composites (NFC). NFC's have mainly attracted research communities as a sustainable alternate solution to depleting petroleum resources [1].

NFC's are the most abundant raw material on earth with a primary production of 2×10^{11} tons per year compared to the production of synthetic polymers which is estimated to be 1.5×10^{8} tons per year [2]. In addition to their wide availability, natural fibres are also inexpensive and eco-friendly. They also have the advantages of having a low density, competitive specific mechanical properties and reduced energy consumption when compared to synthetic fibres such as glass and carbon. The use of NFC's in the automotive industry has helped reduce energy consumption by as much as 80% [3].

Due to the need for natural fibre composites, much focus is placed on kenaf fibres due to its good mechanical properties which have been highlighted by several researchers [4, 5, 6]. In addition to meeting mechanical requirements, the use of kenaf fibres in materials fulfils several social and environmental roles as well. An acre of a kenaf plantation has the potential to produce up to eight tonnes of raw material in a single season. This has the added benefit of having a positive effect on global warming. There is a strong drive in the South African Department of Agriculture behind growing kenaf fibres and the creation of kenaf plantations. This is due to the good climate conditions available in SA, which are ideal for growing kenaf, and the employment potential which is associated with kenaf farming. This is particularly important in a country such as South Africa, where unemployment rates are high. The climatic conditions available in S.A yield fibres that are stronger, resulting in composites which display better strength properties. This ongoing interest in kenaf plantations provides the need for further research to be done on NFC composed of kenaf fibres and a polymer matrix.

Natural fibres are a suitable form of reinforcement in plastics due to their high strength and stiffness and low density [7]. The modulus of cellulose based fibres can range from 40 GPa to as much as 250 GPa depending on the component of the fibre. The fibre itself can be divided into microfibrils which have a modulus of 70 GPa. These microfibrils can be further subdivided into cellulose chains, which have a modulus of 250 GPa. No technology is currently available that allows the processing of microfibrils into these cellulose chains [7].

Previous research has been carried out on the development of natural fibres as a reinforcement in thermoplastic resin matrices [3, 8]. Thermoplastics are cheap, biodegradable and renewable. The decision to use polypropylene as a matrix for the NFC stems from several known advantages including; abundance of the material, low cost, low density and the fact that it is highly recyclable.

Researchers [2, 3, 8, 9] agree that although natural fibres are renewable and widely available, they also display some drawbacks such as poor wettability, incompatibility with some polymer matrices, high moisture absorption and poor repeatability of mechanical properties [9].

Most of these drawbacks associated with natural fibres can be overcome through the use of chemical treatments [1, 10, 11]. Chemical treatments help remove debris from the surface of the fibre whilst creating more sites for interlocking with the matrix. This improves the mechanical bond between the fibre and matrix. Additionally, waxy substances on the surface of the fibre that promote moisture absorption are removed, which in turn reduces the fibre's affinity for moisture [4, 10].

Knowledge of this concept led to the research previously done by PhD student Oscar Asumani [4], who investigated NFC using kenaf fibre and polypropylene. He treated kenaf fibres with alkali solutions as well as aminopropylethoxy silanes to improve the interfacial strength between the kenaf fibres and polypropylene. The alkali solution strips the kenaf fibers of debris, which creates a rough surface so that better bonding sites are available for the polypropylene to bond to the kenaf fibres. The silane helps create a chemical bond between the fibres and the matrix, which consequently results in the improvement of mechanical properties of the composite.

In recent years several automotive components which were previously made with Glass Fibre Reinforced Plastic (GFRP), are now being manufactured using NFC [9]. The strength of treated natural fibres is currently comparable to glass fibres with the added advantage that it can be produced on a larger scale. A further development in natural fibre composites, is the introduction of clay into polymers. The benefit of clay is that it has a high aspect ratio [12] and it acts as reinforcement within the polymer, thereby increasing the overall mechanical

strength [13]. An example of this development is the door bolsters of the Ford Focus which feature polymers used in conjunction with clay.

The preparation of an organic-inorganic nanocomposite has received considerable attention for its great promise in industrial applications [14]. An addition of as little as 3-5% clay to a polymer can increase its mechanical properties up to 20% [15]. The most characteristic feature of such a composite, is the fact that very little clay is required to improve the strength of the material.

Previous research by Asumani et al. [4] uses chemical treatments to improve the bond strength between the kenaf and polypropylene matrix, whilst previous research into clay nanocomposites [14, 15] shows that the strength of a polypropylene matrix can increase with the addition of clay. It is thus possible that an improved composite can be manufactured using research by Asumani et al. [4] in conjunction with the research related to clay nanocomposites [14, 15].

The purpose of this investigation is to further research nanocomposites and determine the effect of clay loading on the mechanical properties of a NFC consisting of a mixture of clay and polypropylene as a matrix and kenaf fibres which serve as reinforcement to the matrix. Chemical treatments are used to improve the interaction between the matrix and fibre. However, since the matrix will be modified to have a clay component, the interactions between the fibres and the modified matrix, together with the mechanical properties of the composite are expected to differ from the results obtained by Asumani et al. [4]. Although a comparison to the work of Asumani et al. is not a main objective, their results form a baseline for comparison since the same basic materials were used.

2 Literature Survey

Natural fibre composites (NFC) comprise a combination of natural fibres and a polymer matrix which act together as a single material. The NFC investigated in this work has three main constituents; kenaf fibres, polypropyiene and clay. Each of these constituents are discussed individually as well as the combination of all three, which is required to form a NFC.

2.1 Kenaf Fibres

Natural fibres can be found in the stems, leaves and seeds of plants. There are a wide range of natural fibres available for the production of NFC. Kenaf fibres are one such example. These fibres were chosen for the NFC used in this work based on their good mechanical properties as well as the social benefits associated with kenaf farming in the context of South Africa.

2.1.1 Background to Kenaf Fibres

Kenaf fibre is produced from the bast of the Hibiscus Cannabinus plant [16], which is also known as a stockroot in South Africa [8]. It is commonly used for the production of NFC and can be seen in Figure 2.1.

The Hibiscus Cannabinus plant reaches full growth in a mere three months and can grow under a wide range of weather conditions [5]. The plant reaches heights of up to 3.5 m with stems up to 5 cm in diameter. The plant has a unique combination of long bast (bark) fibres with short core fibres [8]. In terms of energy consumption, it takes 15 MJ of energy to make 1 kg of kenaf fibre whilst it takes 54 MJ to make 1 kg of glass fibre [17]. Kenaf fibre is used in the making of paper, rope, twine, cloth, animal bedding and in the making of engineering materials, namely, natural fibre composites.

Figure 2.1: Kenaf Plants [5]

2.1.2 Structure of Kenaf Fibres

Natural fibres are ligno-cellulosic meaning they are mainly composed of three constituents, cellulose, hemicellulose and lignin [18]. Cellulose is the major framework component of the fibre structure, providing strength, stiffness and structural stability to the fibre. Cellulose is hydrophilic and comprises polymer chains which contain three types of hydroxyl groups. Two of the hydroxyl groups form hydrogen bonds, which are intramolecular bonds that attach to the cellulose. The third group also forms hydrogen bonds to link up to all the other cellulose which can be seen as an intermolecular bond. These hydrogen bonds described above are responsible for the fibres characteristic high affinity for water. The full structure of the kenaf fibre can be seen in Figure 2.2.

The strength and stiffness of a fibre depends on the angle between the longitudinal axis of the fibre and fibril of the fibre [2], called the fibril angle seen in Figure 2.2. Small angles result in higher mechanical strength, whilst low angles indicate a lower mechanical strength. The natural cellulose fibre in itself, is a composite, as it consists of microfibril fibres held together by an amorphous matrix of lignin and hemicellulose [19]. The cellulose consists of crystalline and amorphous regions. The crystalline region is hard to penetrate with resins or solvents due to its closely knit structure resulting from the hydrogen bonds which hold the cellulose together. The amorphous region also consists of lignin and hemicellulose with hemicellulose acting as the connection between the microfibrils, creating the primary structural network [20]. When this component is removed, the interfibrillar region is likely to be less dense and less rigid, which allows the fibrils to rearrange themselves along the direction of the tensile force. This allows the fibres to achieve higher stresses before failure [7]. Hemicellulose is also responsible for the biodegradation, moisture absorption and thermal degradation of the

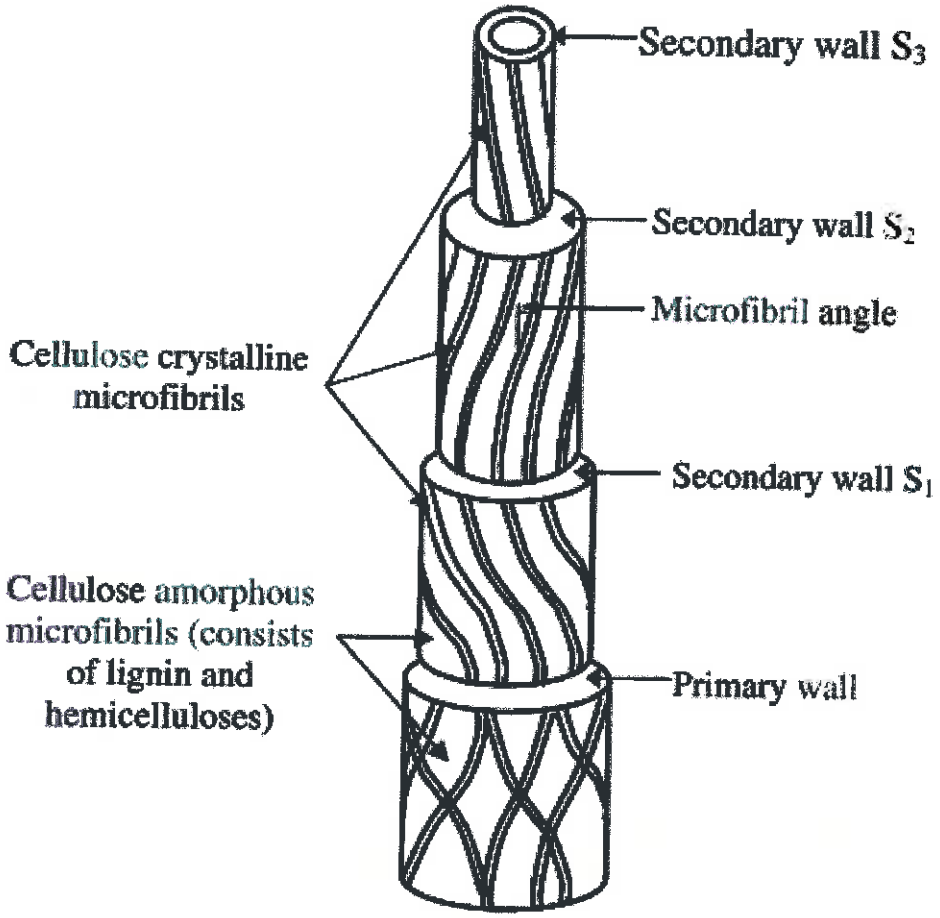

Figure 2.2: Structure of Kenaf Fibre [10]

fibre [19]. Lignin bonds the cellulose and hemicellulose together [18] and also controls UV degradation of the fibre [19]. Hemicellulose and lignin allow for the absorption of dyes and resins and is also responsible for the water absorption characteristics of natural fibres. Hemicellulose, lignin, pectin and waxy substances normally contain water molecules. This makes the fibre hydrophilic and polar, lowering its compatibility with the non-polar/hydrophobic matrix [10]. The hemicellulose in the fibre is responsible for the thermal degradation in the natural fibre, which occurs at approximately 200°C [10].

Natural fibres also have low repeatability in mechanical performance. The physical and mechanical properties of natural fibres depend on a number of factors including planting condition, place of origin, climatic condition and the method used to extract and store fibres [16]. The factors mentioned above influence the amount of cellulose in the fibre as well as the microfibril angle which ultimately dictates the mechanical strength of the fibre. The mechanical and chemical composition of kenaf fibres can be found in Table 2.1.

Table 2.1: Mechanical and Chemical Composition of Kenaf Fibres [1]

Fibre	Tensile strength (MPa)	Young's modulus (GPa)	Cellulose (wt%)	Hemicellulose (wt%)	Lignin (wt%)	Waxes (wt%)	Density (g/cm^3)
Abaca	400	12	56-63	20-25	8	3	1.5
Alfa	350	22	45.4	38.5	14.9	2	0.89
Bagasse	290	17	55.2	16.8	25.3	-	1.25
Bamboo	140-230	-	26-43	30	21-31	-	0.6-1.1
Banana	500	12	63-64	19	-	-	1.35
Coir	175	-	32-43	0.15-0.25	40-45	-	1.2
Cotton	287-597	5.5-12.6	85-90	5.7	-	0.6	1.5-1.6
Curauna	500-1,150	11.8	73.6	9.9	7.5	-	1.4
Date palm	97-196	2.5-5.4	-	-	-	-	1-1.2
Flax	345-1,035	27.6	71	18.6-20.6	2.2	1.5	1.5
Hemp	690	70	68	15	10	0.8	1.48
Henequen	500 70	13.2 3.1	60	28	8	0.5	1.2
Isora	500-600	-	74	-	23	1.09	1.2-1.3
Jute	393-773	26.5	61-71	14-20		0.5	1.3
Kenaf	930	53	72	20.3	9	-	-
Nettle	650	38	-	-	-	-	-
Oil Palm	248	3.2	65	-	29	-	1.5
Piassava	134-143	1.07-4.59	28.6	25.8	45	-	1.4
Pineapple	1.44	400-627	81	-	12.7	-	0.8-1.6
Ramie	560	24.5	68.6-76.2	13-16	0.6-0.7	0.3	1.5
Sisal	511-635	9.4-22	65	12	9.9	2	1.5

2.2 Polypropylene

2.2.1 Background to Polypropylene

Polypropylene (PP) is a thermoplastic material which is low cost, widely available and highly recyclable. It is used to manufacture several products including packaging, textiles, reusable containers, laboratory equipment and stationery. PP has a low surface energy which implies that substances such as common glues will not stick to it.

There are three grades of PP; Homopolymers, block copolymers and random copolymers. The homopolymer grade is the strongest and most stiff, whilst the copolymer has better impact properties and is transparent because it is amorphous. This research makes use of homopolymer PP as it is the strongest of the three grades.

2.2.2 Structure and Properties of Polypropylene

PP has the chemical formula CH_3 with a melting point of 163°C for a formulation with a Melt Flow Index (MFI) of 5.3. The datasheet for this particle formulation can be found in Appendix A. PP is susceptible to degradation when exposed to UV light such as that found in sunlight. The processing temperature of polypropylene is between 160°C and 200°C. Manufacturing NFC composites between these temperatures avoids thermal degradation of the natural fibres as this occurs at 200°C [19]. Crystallization is defined as the aligning of polymer chains and it is a major factor in the processing of PP. Longer cooling times promote this phenomenon which results in stronger materials. This is due to the fact that the aligned chains give the polymer a structured region which in turn helps make PP stronger. MFI is another property of a polymer which is a measure of the ease of flow of a thermoplastic polymer, measured using the ASTM 1238 standard. In this standard, the polymer is heated up to a specified temperature and pushed through a hole under a specified force. The amount of polymer that exits the exit hole in 10 min is measured and recorded and this defines the MFI in g/10 min. It is also an indirect measure of molecular weight, where a high MFI corresponds to a low molecular weight and a low viscosity.

2.3 Composite Manufacturing

Several methods have been cited for combining kenaf fibres and polypropylene. These methods include extrusion and compression, compression moulding and injection moulding [4, 21].

The underlying principle of all these methods is similar and involves heating the polypropylene to lower it's viscosity so that it can flow between the fibres. Pressure is required to help assist the matrix to penetrate the fibres. After the fibres are sufficiently wetted out with matrix, the heat is removed and the composite is allowed to cool. There is a relationship between the manufacturing method used and the fibre length. For extrusion based manufacturing, the fibre length is between 53-540 micrometres whilst injection moulding works for fibres between 2-51 mm in length. Alternatively, compression moulding covers a larger range of fibres than extrusion or injection moulding [22].

2.4 Shortcomings of Natural Fibres and Surface Treatments

The surface adhesion between the fibre and the polymer plays a vital role in the transmission of stress from matrix to the fibre, which ultimately contributes towards the composite's mechanical performance [19]. The fibres and the matrix are incompatible which results in poor adhesion between the two elements. This poor interaction is attributed to the fibres being hydrophilic and the matrix being hydrophobic [19]. The hydrogen bonds in the fibres cause the fibres to agglomerate, making it more difficult for the matrix to penetrate the fibres. In addition, there is debris on the fibres which is essentially a cover of dirt. During the moulding process, the polypropylene is prevented from penetrating through to the fibre surface by the layer of dirt which results in a weak bond. Another shortcoming is the high affinity for moisture associated with the fibres. This causes a dimensional increase in the fibre, consequently decreasing the dimensional stability of the composite [23]. The mechanical properties of the fibres, the aspect ratio of the fibres and the fibre-matrix interface dictate the properties of the composite.

A way to overcome this shortcoming is to introduce chemical treatments. These treatments clean the surface of the fibres and chemically modify the fibre which improves it's strength and the bond between the fibre and matrix. Cleaning removes the waxes and oils from the fibre which aids in lowering the moisture absorption. A silane treatment is another way of improving the matrix-fibre bond strength. The treatment is a chemical grafting method which modifies the chemical composition of the kenaf fibre surface, allowing it to link up with the polymer chains of the polypropylene matrix.

2.4.1 Akali Treatment

The alkali treatment uses sodium hydroxide which reacts with the hydroxyl part of the fibre to remove some of the lignin, wax and oils covering the fibres. The fibrils rearrange themselves,

aligning more with the axis of the fibre [24]. This decrease in angle consequently corresponds to an increase in strength and stiffness of the fibre [1]. The treatment causes a rough surface on the fibre thereby allowing for additional sites for interlocking with the polymer matrix [25]. The treatment also modifies the crystal structure of the fibre, changing the crystalline arrangement of the fibrils into an amorphous state on the surface of the fibre. This allows for better penetration of the silane treatment which can be seen in Figure 2.3.

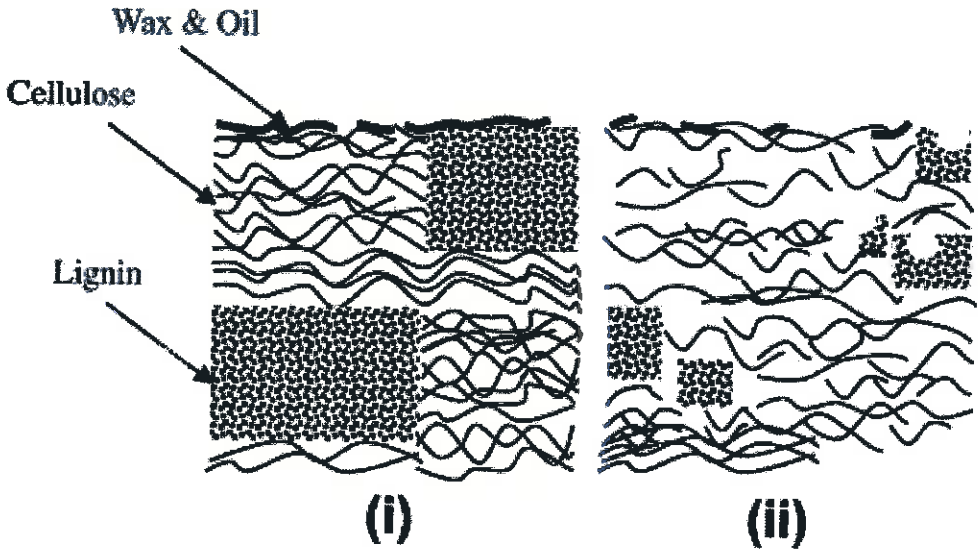

Figure 2.3: Typical structure of (i) untreated and (ii) alkalized cellulose fibres [10]

Edeerozey et al. [26] analysed the effect of the alkali treatment using a 3%, 6% and 9% sodium hydroxide solution. The surface of the fibres were viewed after the treatment using a scanning electron microscope (SEM) with a 800 times magnification. This magnification gives insight to the surface morphology of the composite and the bonding between the matrix and fibres. There were two parameters that were varied in the application of this treatment by Edeerozey et al. [26], which are; the variation in temperature at which the treatment is carried out and the concentration of the solution. They found that the alkali treatment is most effective in cleaning the fibres at temperatures higher than room temperature and that alkali concentrations greater than 6% cause fibre damage. Asumani et al. [4] also conducted several sodium hydroxide treatments ranging from a 1% to 10% in concentration. They concluded that a concentration of 6% was the most effective [4, 26] for a duration of 24 hours.

2.4.2 Silane

Silane consists of an alkoxy, organofunctionality, alkyl bridge and a silicon atom that holds these functions together [38]. A non-reactive akyl group is attracted to the matrix due to both molecules having similar non-polar properties . The organofunctionality is physically compatible with the matrix, where by its long chains can get entangled within the polymer chains. The interlocking of the chains of the polymer to the chains of the silane form a mechanical bond. Typically, organofunctionalites are amino and vinyl groups. There is much literature for the use of the amino based silane, which has the ability to get entangled in the polypropylene matrix. It is possible to graft the silane onto the fibres first and through thermal compounding, which is the application of heat, covalently bond the silane to the polypropylene. This mechanism which occurs during the administration of silane is mentioned by Xie et al. [27], although this joining mechanism is not fully explained. Asumani et al. [4] used 3-Aminopropyltriethoxy Silane (APS) (silane having an amino functionality) as a result of work done by Huda et al. [28] who used APS in conjunction with a sodium hydroxide treatment and found a 60% improvement in composite strength.

2.4.2.1 The Chemical Process of using Silane on Fibres

A small amount of silane, typically 1% of weight relative to the weight of the fibres being treated, is mixed into a mixture of alcohol and water. Thereafter a complex process between all of the elements occurs. This process can be summarised by the following interactions explained by Xie et al. [27] and can also be seen in Figure 2.4.

1. Hydroloysis : The silane is mixed with water and the catalyst (normally the corresponding alkoxy alcohol). During the mixing the silane breaks down into reactive silanols.
2. Self Condensation : Hydrolysis and condensation simultaneously take place. During this process the free silanols attract to other silanol groups in a Si-O-Si- bond while attempting to attract to the hydroxyls in the fibres through hydrogen bonding. The condensation is controlled by keeping the solvent slightly acidic, between a pH of 3 and 6.
3. Adsorption : During this process reactive silanols are adsorbed into the fibres. These free silanols also react with each other to form a rigid polysiloxane structure which prevents any further silanols from penetrating the fibres. This helps seal the micropores of the fibre, decreasing its ability to absorb water.

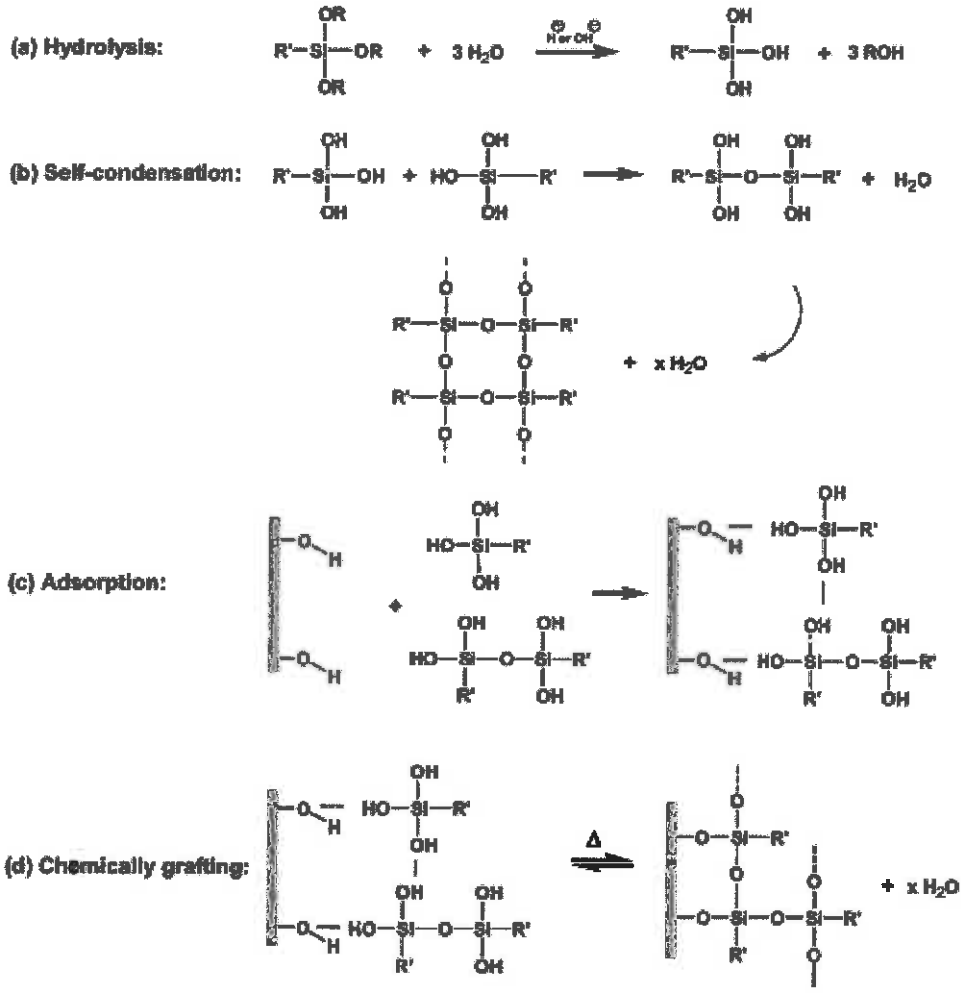

Figure 2.4: Chemical Process of Silane [27]

4. Grafting : Under heating, typically at 110°C for 2 hours, the hydrogen bonds between the silanols and the hydroxyl groups turn into covalent Si-O-C- bonds and liberate water. These bonds are reversible in the presence of water.

2.4.2.2 Mechanism of Silane Treatment

Silane hydrolyzes in the presence of water and the alcohol corresponding to the alkoxy group, thereby releasing the reactive silano groups [27]. Typical alkoxy groups are methoxy and ethoxy. Methoxy hydrolizes much faster than ethoxy thereby reducing processing time. Di- and tri- alkoxy produce stronger adhesion to the natural fibre than mono-alkoxy groups since there are more binding sites after they are hydrolised [27]. To deliver the functional groups of the silane to the interior of the fibre, the silane has to be dissolved in the corresponding alkoxy alcohol, eg, methoxy in methanol. Additionally water should be used to hydrolize

the silane. When the hydrolysis takes place, the reactive silonals exist in solution. During the condensation of the silanols, the silanols attract each other through (Si-O-Si) bonds and form a siloxane polymer network. If condensation occurs too quickly, the siloxane network consisting of large chains will coat the surface of the fibres, preventing the silanol groups from attaching to the hydroxyl groups of the fibre. The condensation can be controlled by an acidic solution in the pH range of 3-6, which Asumani et al. did within a range of 4 and 5, using an acetic acid solution. The condensation process must be as long as possible to allow the small silanols to penetrate the fibre and attach to the hydroxyls before they become incorporated into the large polysiloxane layer, preventing any further penetration of the silanols. The treatment by Asumani et al. [4] is almost exactly the same as that of Xie et al. [27], except for the different liberating alcohol, which is referred to in step 1 of the silane process. Asumani et al. made use of methanol despite the fact that silane has an ethoxy in it. The alcohol helps liberate the reactive alkoxy silanols. A methoxy group hydrolyses faster than ethoxy but methoxy releases a toxic methanol molecule. It would be interesting to investigate the same procedure that Asumani et al. [4] used but using the silanes with the corresponding liberating alcohols to the alkoxy groups. The grafting process was not done by Asumani et al. Although this step is not done immediately by Asumani, it might not be necessary to make use of a separate grafting process, as the treated fibres later undergo thermal compounding in the composite manufacturing process. During this, the temperatures exceed that of the 110°C.

2.4.2.3 Choice of Silane Treatment

Different silane treatments were investigated to find the optimum concentration of silane which would improve the strength of the composite whilst still being economically viable. Cho et al. [29] showed that 3-Aminopropyltriethoxy Silane (APS), 3-Mercaptopropyltrimethoxy Silane (MPS) and 3-Glycidoxypropyltrimethoxy Silane (GPS) yield mechanical improvements with kenaf fibres. These results can be seen in Figure 2.5.

It can be seen that MPS and GPS treatments yield almost the same strength at a concentration of 0.5 wt% and that both treatments yield greater strengths than the APS treatment.

2.4.2.4 Combination of Akali and Silane Treatments

The alkali treatment reacts with the fibres to create a rough surface which improves the mechanical bond between the fibres and the matrix. It also creates more amorphous regions on the surface of the fibre, which aids in allowing the silane to penetrate the fibres. Silane provides a chemical medium to join the fibre and matrix. It chemically grafts onto the

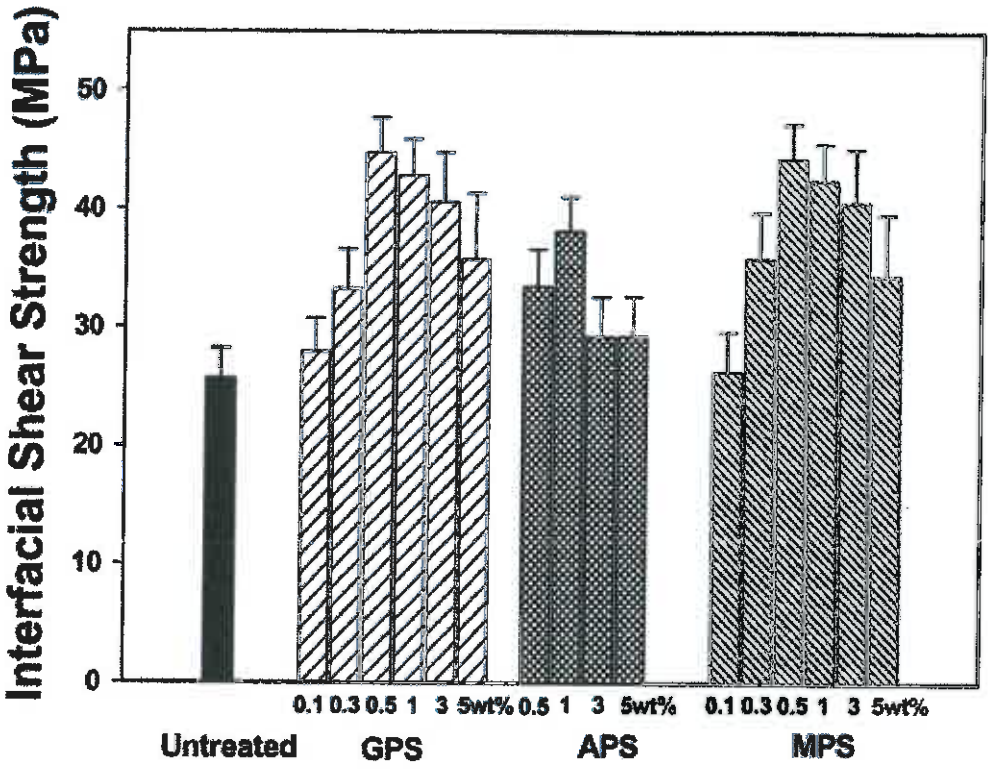

Figure 2.5: Interfacial shear strength measured for Kenaf Fibre and PP composite [29]

fibre and intertwines into the polymer chains and with the application of heat, the chains become a covalent bond. It can be seen that the combined alkali and the silane treatment offers two different mechanisms for improving the bond strength between the fibre and the matrix. Combining the two mechanisms therefore helps to create an improved composite. This method has been carried out by authors [4, 28].

2.5 Polypropylene-clay nanocomposites

For the past decade, the preparation of organic-inorganic nanocomposites has received considerable attention for their great promise in industrial applications [14]. 3-5% clay added to a polymer can increase the tensile strength of the composites by up to 20% [15]. Successful pioneering work was done using a nylon-6/Montmorillonite Clay (MMT) clay system by Toyota [30]. The resultant nanocomposite showed improvements in strength, modulus and heat distortion temperature compared to the virgin polymer [30]. As mentioned previously, the most characteristic feature of this composite is the fact that very little clay is needed to get improvements in the strength of the material.

2.5.1 MMT

Montmorillonite (MMT) is of interest as it is often used in conjunction with polypropylene [14, 30, 31, 32, 33]. Montmorillonite clay is a smectite which is a group of clay minerals that has an affinity for absorbing water which causes the clay to swell. Hectorite and montmorillonite are amongst the most common smectite-type layered silicates used in the preparation of nanocomposites. Smectites are also a valuable mineral class for industrial applications due to their high cation exchange capacities, surface area, surface reactivity and adsorptive properties. Each of the layers of montmorillonite are separated by water molecules, thus it is called hydrated montmorillite clay. It is able to act as a reinforcement material due to its high aspect ratio as well as its platelet structure [32]. It has a large surface area to volume ratio (700 m^2/g) and has layers measuring 1 nm in thickness, 500 nm in width with an interlayer spacing of 1 nm.

MMT is a 2:1 aluminosilicate [34] which means that it has an octahedral aluminium oxide sheet sandwiched between two tetrahedral silicon sheets, which together form a layer. This can be seen in Figure 2.6. MMT clay, consists of clay sheets with a gap between the layers called the interlayer distance/gap. The combination of the layer and the interlayer spacing is a repeat unit of the clay and it is called a d-spacing or basal spacing d_{001}. This is a common term used in X-Ray diffraction studies which can determine the interlayer distance [35].
The benefit of mixing clay into polypropylene is that the clay serves as secondary reinforcement which improves the mechanical properties of the composite. However, the incompatibility between the clay and polypropylene is one of the shortcomings. MMT is hydrophilic which is problematic as polypropylene is hydrophobic [12, 36, 37]. This interaction makes the two incompatible and modification of the MMT structure is required to facilitate dispersion of the clay layers within the polypropylene matrix.

As mentioned previously, MMT clay in its original inorganic state does not mix well into polypropylene due to the hydrophilic nature of MMT clay and the hydrophobic nature of polypropylene. This causes the MMT clay to agglomerate during mixing of MMT clay into polypropylene which negates the strength benefits of the nanocomposite. The most popular surface treatment to help with the dispersion of clay layers, is an ion exchange treatment called a surfactant, which chemically modifies the inorganic clay into an organic clay [39]. The surfactant first causes the central aluminium cation to be exchanged with a less positive sodium cation containing water. This causes the overall structure to be negative as the central ion is less positive compared to the original aluminium ion. Thereafter, another exchange process occurs, whereby the sodium ion is exchanged with alkyl ammonium so as to maintain neutrality in the structure. This final step causes the clay to become hydrophobic. [33, 40]. This increases the distance between the layers as well as decreases the surface energy. Since

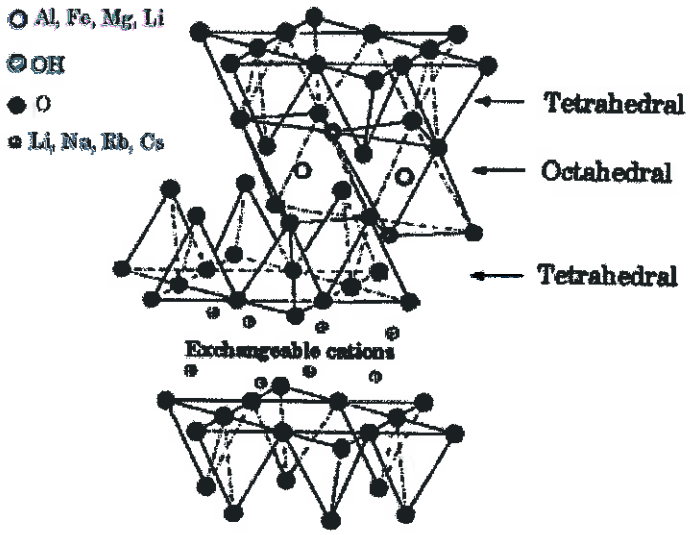

Figure 2.6: Montmorillonite Clay Structure [38]

the montmorillonite clay is to be used as a filler within a polyolefin matrix, the hydrophobic nature will improve bonding with the polyolefin matrix. Without the alkyl ammonium cation exchange, or any other ion to create the hydrophobic nature, the clay will not disperse in the polyolefin matrix. It should be noted that alkyl ammonium is thermally unstable above 200°C [40], which causes degradation, called Hoffmann degradation [41]. Mixing chemically modified MMT clay and polypropylene above 200°C will destroy the surfactant, eliminating the benefits of the surfactant. This causes the MMT clay to be more hydrophilic and the interlayer space to decrease, causing the clay layers to agglomerate. Consequently, this results in a microcomposite, rather than a nanocomposite. Ka et al. [42] found that the surfactant helps reduce the surface energy, lowering the forces between the clay layers, which facilitates dispersion of the clay layers within a polypropylene matrix.

When polypropylene is mixed together with clay, the polypropylene chains enter the interlayer gap of the clay and separate the layers of clay, also known as platelets. Figure 2.7 shows the different types of separation that can occur when polypropylene is mixed with clay.

A tactoid of clay is a phase separated microcomposite, where the clay layers are clumped together [43] and this can be seen in Figure 2.7. If the polymer chains move in between the platelets causing less than 20-30 angstrom separation, the clay is said to be intercalated. Once the distance increases to 80-100 angstrom, the clay is then said to be exfoliated [15]. Exfoliation is the required result when mixing the clay into the polymer, as it results in the best mechanical properties [36]. Since improvements are directly related to the degree of exfoliation and intercalation, it is important to measure these through two common techniques; X-Ray diffraction and Transmission Electron Microscope (TEM).

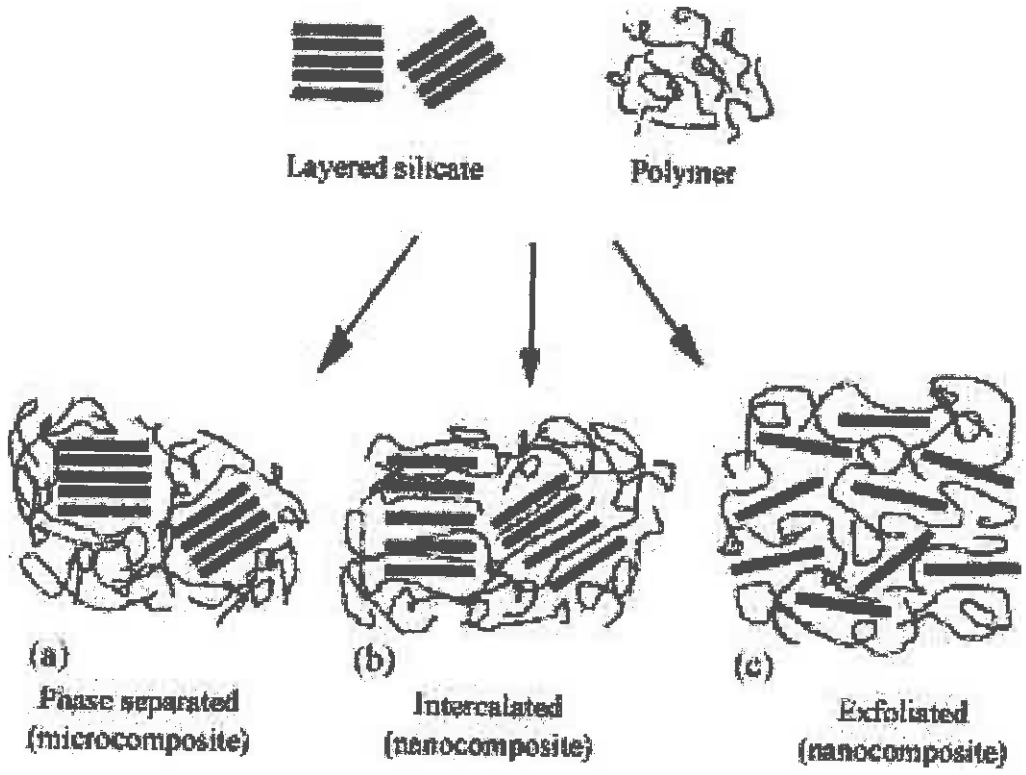

Figure 2.7: Montmorillonite Clay Structure [43]

Garca-Lpez et al. [12] found that clay modified with a surfactant is not enough to provide an appropriate nanometric dispersion. Despite the organoclay having a larger interlayer distance than inorganic clay, the clay agglomerates. This is due to the fact that PP does not include any polar groups in its backbone and it is not compatible with organic montmorillonite modified with a surfactant. To assist with the dispersion, a third component, known as a compatabiliser, is used in the mixing of PP and clay, which assists in the intercalation of polymer chains [13, 14, 30, 33]. The compatabiliser used in this work is polypropylene-graft-maleic anhydride.

2.5.2 Compatabilisation

Polypropylene has a very low polarity, making it difficult to disperse a polar material such as clay into homogenous mixture of the two components [36]. The compatabiliser, known as Polypropylene-Graft-Maleic Anhydride (PP-g-MAH), contains PP that is grafted onto a Maleic Anhydride (MA) chemical. The one end of the compatabiliser which contains maleic anhydride (MA), intercalates between the platelets and chemically bonds to the oxygen group, or the negative charge of the platelets [44]. The other end of the compatabiliser is the PP chain which can intertwine together with the matrix polymer chains. This process can be seen in Figure 2.8.

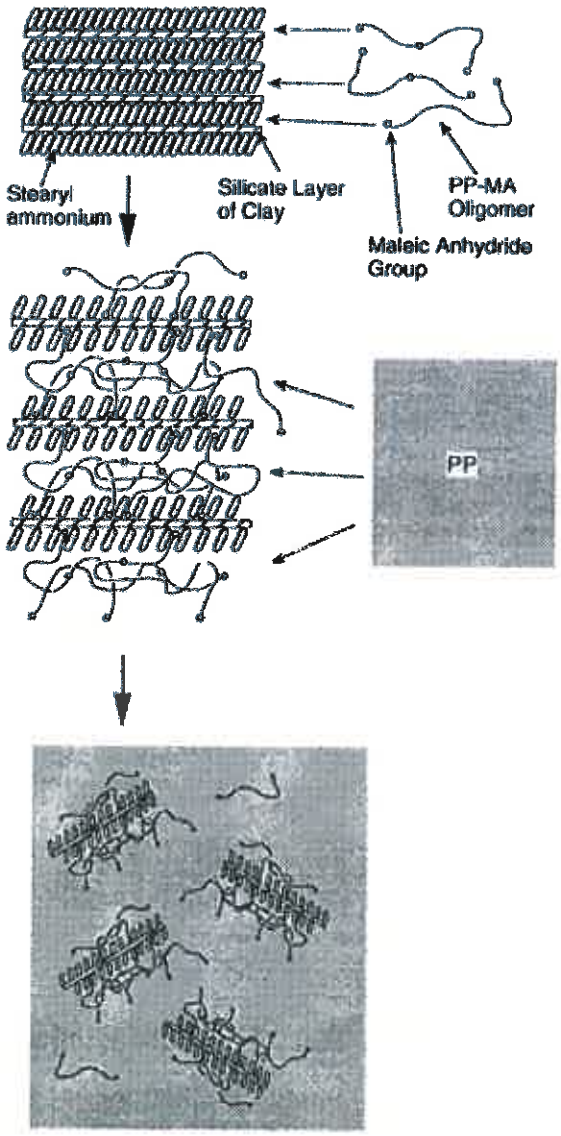

Figure 2.8: Delamination of clay through the use of PP-g-MAH [30]

During the first stage of mixing the maleic anhydride goes into the interlayer gap, causing the interlayer gap to increase, consequently decreasing the interaction of the platelets. The properties of PP/organoclay nanocomposites are directly affected by the exfoliation levels of the nanocomposite. These levels depend on the method of mixing, speed and temperature of mixing and content of compatabiliser and clay [44].

Chiu et al. [14] investigated the effect of the content of MA within the compatabiliser on the degree of dispersion of clay layers within a polypropylene matrix. They used two compatabilisers, one consisting a MA content of 50 mol% and the other consisting of a MA content of 0.24 mol%. The compatabiliser with the lower MA promoted better exfoliation than the compatabiliser with higher MA content. They also found that a higher MA content

within a compatabiliser results in a large difference in the polarity between the compatabiliser and the PP. This results in poor interaction between the two components. A large quantity of MA also hampers the dispersion of organoclay [45]. There is a high affinity of MA for the organoclay and this causes the MA to saturate the interlayer, making it impossible for the PP to penetrate it [45]. Further shear stress imposed through mixing may flatten the chain conformations which reduces the interlayer distance. Sathe et al. [46] mentioned that the compatabiliser has a saturation limit which effects the interaction mechanism, whereby exceeding the limit negates the effect of the compatabiliser. They also found that the dispersal of excess compatabiliser in the matrix affects the homogeneity of the nanocomposite, reducing the mechanical strength.

2.5.2.1 Effects of Compatabiliser

Several methods are available to mix organoclay with PP-g-MAH into polypropylene to obtain a nanocomposite. Generally the clay, compatabiliser and polypropylene are mixed in a high temperature mixer. Several parameters are varied including; the mixing time, temperature of the mix and the quantities of each component. Each parameter has an effect on the overall composition of the nanocomposite which ultimately affects its mechanical properties. It is beneficial to highlight the effects and limitations of a compatabiliser to ensure that the compatabiliser is used correctly. These effects are as follows:

1. The compatabiliser and the shearing forces of the mixing process assist with delamination (intercalation and exfoliation) of the nanoclay.
2. An anhydride with a lower acid count is more immiscible within polypropylene than a anhydride with a higher acid count [30].
3. Polymers with large organic chains result in a larger interlayer distance as well as a higher packing density [45]. Kim et al. [45] found that the anhydride has a high affinity to the clay due to hydrogen bonds and as a result accumulates within the interlayer.
4. Excessive MA hampers the diffusion of PP molecules due to the large difference in polarity between the MA and PP [45].

2.5.3 Effect of Clay Content

The purpose of this research is to investigate the effect of the addition of clay on a polypropylene composite with kenaf reinforcement. It is useful to be aware of quantities of clay that

improve the mechanical properties of the composite found in previous research . They are as follows:

Chow et al. [47] found that four parts per hundred (PHR) organoclay together with five PHR or ten PHR compatabiliser (PP-g-MA) significantly improved the strength results of the composite.

Tarapow et al. [15] investigated the effect of different clay loading on a polypropylene matrix, results of which can be seen in Figure 2.9. This figure shows that 1% clay content results in the best tensile strength. Poor improvement in material properties can be attributed to poor interfacial adhesion between the PP and MMT [15]. They found that a maximum stiffness is reached at 5wt% clay content.

Tarapow et al. [15] showed that the increase in impact strength of polypropylene is due to the intercalation of the clay layers which hinders the crack path caused by impact.

Clay content (wt %)	σ_u (MPa)	E (GPa)	ε_b (%)	E_{izod} (kJ/m)	X_{cr} (%)
0	33.6 ± 1.0	1.43 ± 0.07	30.8	1.58 ± 0.18	51.0
0.5	33.5 ± 1.5	1.52 ± 0.06	17.6	1.72 ± 0.21	53.4
1.0	34.1 ± 0.6	1.62 ± 0.05	16.3	1.75 ± 0.32	48.8
3.0	33.9 ± 0.8	1.86 ± 0.06	13.1	1.75 ± 0.20	49.7
5.0	32.8 ± 1.9	1.88 ± 0.07	7.2	1.65 ± 0.11	48.2

Figure 2.9: Effect of clay content on the properties of PP/MMT Nanocomposite [15]

2.5.4 Preparation of Clay/Polypropylene Nanocomposite

The most appreciable benefits from the addition of clay in a polyolefin matrix is found in the range of clay loadings of 1-10 wt% [13, 14, 15, 30, 33, 36, 39]. The addition of more clay leads to aggregation of the clay, making the overall composite more brittle [15]. Since there are several variations in the method of mixing MMT clay, compatabiliser (PP-g-MA) and PP, it will be useful to present this information to help establish the quantities and parameters involved in producing the nanocomposite. The methods employed are as follows:

Tarapow et al. [15] mixed PP, MMT clay and compatabiliser in samples weighing 38 g with specific weights of the constituents to obtain the desired composite. The weight ratio of organoclay to compatabiliser was 1:3 in all cases and the mixing was done at 175°C for 40 min. These authors mentioned that delamination of clay yields much more surface area with high aspect ratio particles, which is essential in improving the mechanical properties in nanocomposite materials. To achieve an effective intercalation, a compatabiliser to organoclay

ratio of 3:1 is needed [15]. Kawasumi et al. [30] and Kim et al. [45] used the same ratio for mixing.

For effective interaction between the clay and PP it was found [36] that the best mechanism to introduce the clay into the PP, is through a two stage process. First a master batch is prepared in which the organoclay and compatabiliser are mixed and presumably the MA in the compatabiliser penetrates into the organoclay interlayer. Thereafter, in another mix, the PP penetrates into the larger interlayer to form an exfoliated structure. Tarapow et al. [15] showed that an exfoliated clay composite has enhanced mechanical strength compared to virgin PP.

Chiu et al. [14] investigated the effect of temperature on exfoliation of the montmorillonite clay. It was found that a processing temperature of 190°C reduced the ordered structures better than a processing temperature of 210°C. This was attributed to the higher viscosity incurred through a lower temperature and thus a higher shear stress in mixing. In this case, the screw speed was 300 rpm.

The final process for manufacturing is of the utmost importance as it found that there are differences in results for injection moulding and compression moulding. Compression moulding sometimes decreased the interlayer spacing between clay platelets and consequently decreased the overall properties of the composite [35].

Ding et al. [48] made the clay and PP composite using a 2 wt% graft anhydride whilst varying the clay amount from one to six part per hundred (phr). They found that using a two phr clay results in the best mechanical properties. These results can be seen in Figure 2.10.

Xu et al. [49] investigated the effect of compatabiliser whilst keeping the content of organoclay constant at 2 wt%. A maximum tensile strength of 40.2 MPa and an impact strength of 24.3 J/m was achieved with a 10% and 20% graft anhydride content respectively.

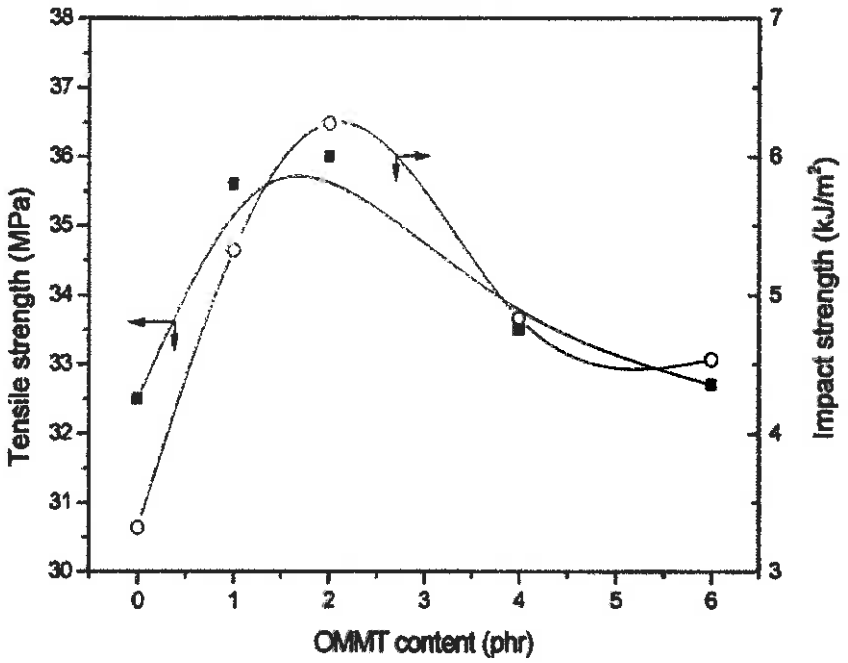

Figure 2.10: The effect of clay loading on the flexural, tensile and impact strengths of a MMT Clay/PP composite [48]

3 Objectives

It is clear from the preceding chapters that the properties of a clay/NFC/PP composite depends on a wide range of factors that include processing conditions, clay dispersion and surface treatments of the fibres. These factors need to be investigated further as part of the investigation on the mechanical properties of the composite. Accordingly the objectives of this work are listed as follows:

1. Determine the best manufacturing temperature.
2. Determine the best fibre treatment using silane as well as the optimum silane concentration for a composite using a fixed fibre weight fraction of 25% for both a polypropylene matrix and a polypropylene/4% clay matrix.
3. Determine the optimum clay content in polypropylene using a fibre weight fraction of 25%.
4. Manufacture composites using fibre weight fractions of 15%, 20% and 30% and determine the optimum fibre weight.
5. Investigate the tensile, shear and impact properties of the manufactured composites.

4 Experimentation

Before providing further details, it is useful to provide an overview of the methodology used in this work. Essentially the composite is made up of two components; the fibre and the matrix. Fibres were treated using various chemical treatments to help improve their mechanical properties as well as improve their compatibility with the matrix. Thereafter the treated fibres were made into fibre mats using the mat manufacturing jig.

Two types of matrices were used for this study; a matrix consisting of clay and another without the presence of clay. The matrix without clay consisted of virgin polypropylene. The clay and polypropylene were mixed using a twin screw compounding extruder to form a clay matrix. These two types of matrices were shaped into sheets of 0.5 mm thickness using a sheet extruder.

Thereafter the fibre and the matrix sheets were cut and placed into the mould to form a charge. The mould was then placed into the compression moulding oven. A method consisting of a series of pressures and temperatures was applied to the mould using the compression moulding oven to obtain the composite plate. This plate was cut into mechanical test pieces to obtain tensile, impact and shear properties.

4.1 Fibre Treatments

The fibres were treated using a method described by Asumani et al. [4]. The fibres were originally 30 mm in length, however fibres of this length are difficult to make into fibre mats using the mat manufacturing rig which will be explained in detail later. The longest fibre that successfully could be processed in the rig was 15 mm and this length was used throughout the investigation. The fibres were cut to this length using scissors.

4.1.1 NaOH Treatment

An eight litre solution of 6% NaOH comprising 7 520 ml of distilled water and 480 g of NaOH pellets was mixed into a 10 litre plastic container. 400 g of cut kenaf fibre was placed in the solution, the container was covered with a sheet of Polytetrafluoroethylene (PTFE) and placed in a convection oven at 45°C for 24 hours. Two scales were used for mass measurements in the fibre treatments and general composite manufacturing. These were the Shimadzu mass scale with a capacity of 3200 g and a resolution of 0.01 g. The other scale, made by BEL, has a capacity of 160 g and a resolution of 0.001 g.

Thereafter, the fibres were removed from the solution and placed in a 10 litre bucket filled with tap water. The fibres were washed and mixed by hand so that the sodium hydroxide solution was rinsed from the fibres. Thereafter, the water containing the sodium hydroxide was poured into a container for storage and subsequent disposal. The rinsing process was repeated three times to ensure maximum removal of the sodium hydroxide solution.

4.1.1.1 Acetic Acid Treatment

The fibres were placed in a 1% acetic acid solution to neutralise any remaining NaOH. After the NaOH treatment and rinsing of fibres, approximately 320 g of fibres remained. An eight litre solution of 1% acetic acid was made to neutralise the fibres of the NaOH treatment. The required solution consisted of 7 920 ml of distilled water and 80 g of acetic acid which were mixed in a 10 litre bucket. The fibres were placed in the bucket containing the solution, covered with a sheet of PTFE and left for three hours at room temperature. Thereafter, the acetic acid solution was rinsed in the same manner as it was done for the NaOH treatment. The fibres were then heated at 70°C for a minimum of twelve hours to ensure that they were completely dry.

4.1.2 Silane Treatments

The silane treatments were intended to improve the bonding between the fibre and the matrix of the NFC. The treatments were similar except for the different types of silane used and the duration of the treatments. Two silane treatments were of interest. The first was 3-Aminopropyltriethoxy Silane (APS) which was used by Asumani et al. [4]. This treatment used a large quantity of silane compared to the alternative silane treatment. The alternative silane treatment was 3-Mercaptopropyltrimethoxy Silane (MPS). This was beneficial because less silane was needed to improve the bonding strength in the composite. Since the two types

of silanes were similar in price and both expensive, it was proposed that the MPS treatment would yield good results so that the cost of the treatment could be reduced. This is an important issue because cost is a significant factor in the viability of any potential treatment.

4.1.2.1 APS treatment

This treatment was performed in accordance with the procedure described by Asumani et al.[4]. 280 g of treated NaOH fibres were treated with silane. A 6.4 litre solution was used consisting of 5% APS in a 50/50 solution by volume of distilled water/methanol. This solution comprised 3.2 litres of distilled water, 3.2 litres of methanol and 14 g of APS. The APS weight was 5 wt% of the dry mass of the kenaf fibre subjected to NaOH treatment. Before submersing the fibres into the solution, the pH of the solution was checked using a Jenway Model 3510 pH meter, which can be seen in Figure 4.1. The pH was maintained below 4 using approximately 1 g of acetic acid for every 70 g of fibre. Under acidic conditions, the hydrolysis rate of silanes forming silanol groups is greater than the condensation rate of the silanols forming siloxane bonds [27]. After submersion of the fibres, the pH was maintained at a value of less than 6 using acetic acid. The pH of the treatment needs to be acidic to ensure that the silane grafting can occur, and to prevent the early formation of the polysiloxane layer. The solution was covered with a sheet of PTFE and left for four hours at room temperature. Thereafter, the fibres were rinsed using the same rinsing method previously described.

4.1.2.2 MPS treatment

Four MPS treatments were used in the investigation, three of which were based on the findings from literature [29, 50, 51]. The fourth treatment was a modification of the treatment carried out by Cho et al. [29], which was modified by changing the liberating alcohol from ethanol to methanol, as methanol is a cheaper solvent. Xie et al. [27] indicated that delivery of an alkoxy functional silane to the interior of the fibre can be accomplished by dissolving the silane in the appropriate alcohol i.e methanol for methoxy and ethanol for ethoxy silane. Consequently, for MPS, it is preferable to use methanol rather than ethanol. This modification of the treatment formed the fourth treatment. Further details of the four treatments used can be found in Table 4.1.

Treatment 1

70g of fibres treated with NaOH were used for this treatment based on the work of Abdelmouleh et al. [50]. The treatment comprised a 1.6 litre solution consisting of 80/20 by volume of ethanol/distilled water. The treatment required 3% MPS mass related to the dry

Figure 4.1: pH Meter

mass of the treated kenaf fibre, which was calculated to be 2.1 g of MPS. Condensation was controlled by keeping the solvent slightly acidic; the pH was kept below 4 before the fibres were submersed in the solution. This was done by adding 1 ml of acetic acid to the solution. Once the fibres were placed in the solution, they were covered with a sheet of PTFE and left for a duration of two hours at room temperature.

Treatment 2

This treatment used 70 g of fibres treated with NaOH and is based on the work of Sever et al. [51]. This treatment required a 1.6 litre solution comprising acidic water with a pH of 4.5. This treatment differed from the other treatments as the MPS content was calculated on the volume of the solution rather than the mass of the kenaf fibres to be treated. The MPS content was calculated to be 0.3% of the total volume of the solution and in this case, it related to 4.8 ml of MPS silane. 2 ml of acetic acid was added to the solution to ensure that the pH was approximately 4.5. Thereafter, the fibres were placed in the solution, and left at room temperature for an hour. The solution was then covered with a sheet of PTFE.

Treatment 3

This treatment was similar to treatment one and was based on the work of Cho et al. [29]. It made use of a solution consisting of a 50/50 volume of ethanol/distilled water, and 0.5% MPS silane, which related to 0.35 g of MPS silane.

Treatment 4

As mentioned earlier, this treatment is similar to Treatment 3, except for the liberating alcohol, which was changed from ethanol to methanol due to it's economic benefit.

A summary of the treatments described can be seen in Table 4.1.

Table 4.1: MPS treatments

Treatment	Alcohol	Ratio by Volume (Alcohol/Water)	MPS wt%	MPS weight (g)	References
M1	Ethanol	80/20	3	2.1	[50]
M2	None	0/100	0.3% vol	6.43	[51]
M3	Ethanol	50/50	0.5	0.35	[29]
M4	Methanol	50/50	0.5	0.35	

4.2 Fibre Mat Manufacturing

After the fibres were chemically treated, they had to be made into fibre mats of an uniform thickness. Non-uniform thicknesses result in inconsistent fibre volume fractions and lead to variations in the mechanical properties of the composites. Rinsing of the fibres to remove the surface treatment solutions caused the fibres to cling together. Fibre separation was thus required before the mat manufacturing rig could be used.

4.2.1 Fibre Separation

Fibres were placed in an oven for 12 hours at 70°C to ensure that they were completely dry prior to fibre separation. Fibre separation was done with the cyclone bucket which can be seen in Figure 4.2. The setup consists of a bucket covered with a lid that has a hole in the centre. 14 g of dried fibres were placed in the cyclone bucket. An airline was inserted into the lid of the bucket and held at an angle of 45°relative to the lid, whilst the lid was secured in place. The airline was then opened, creating a tornado effect. The rapidly moving air

mixed and separated the fibres, removing any clumps which had formed during the chemical treatments. The lid was held firm enough to allow the air to escape whilst trapping the fibres in the bucket. A supply pressure of 6.8 bar was used and it was found that approximately two minutes of operation was sufficient to fully separate the fibres.

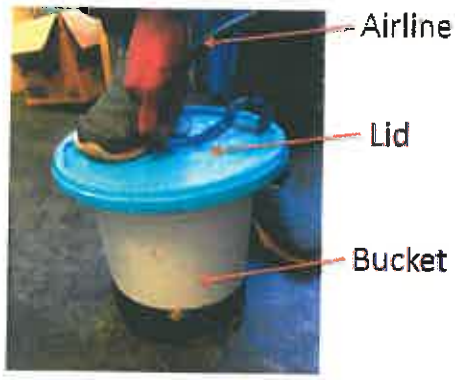

Figure 4.2: Fibre Separation Setup

4.2.2 Mat Manufacture

The separated fibres were converted into fibre mats using a rig designed by Paiken [52], which can be seen in Figure 4.3. A hose was passed through the bottom of the frame and connected to the base of the rig. This was done to ensure that the pipe would not have any obstacles that would possibly hamper it's rotation when it was rotated end on end. The fibres were placed in the pipe and tap water was allowed to fill the pipe. The initial filling of the pipe was rapid to ensure that the turbulent water flow separated the fibres. To create a better mixing effect, the pipe was shaken by hand as the pipe filled with water. The mesh filter was placed at the top of the pipe and was orientated such that the mesh was pointing to the bottom. It was secured in position with two steel pins. Once the water began overflowing at the top of the pipe, the tap was closed. The pipe was then rotated end on end and the hose connected to the pipe was disconnected. This caused an outrush of water, leaving the fibres to collect against the mesh. Once the water had drained from the pipe, the mesh was removed. The mat was then taken from the mesh and placed into an oven to dry for a minimum of twelve hours at 70°C.

4.3 Manufacture of Matrix Sheets

The parameters used to mix the clay and polypropylene to form a nanocomposite were derived from literature. Kawasumi and Tarapow et al. [15, 30] found that using a ratio of 3:1 of compatabiliser to organoclay provides the best intercalation and exfoliation of the clay within

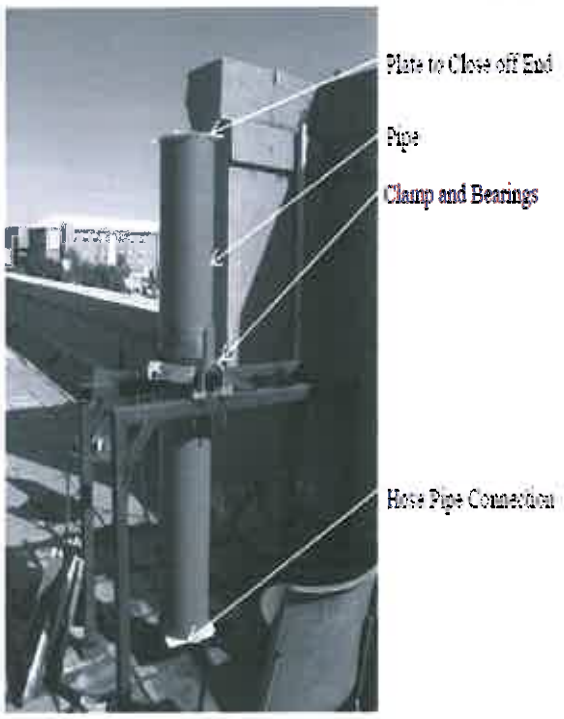

Figure 4.3: Mat Manufacturing Rig

the polymer matrix. Lopez et al. [12] found that mixing the compatabiliser into the clay to form a masterbatch, and then later introducing the PP to dilute the mix, provided better intercalation of the clay. Chiu et al. [14] found that having a lower mixing temperature of 190°C created higher shear mixing stress which dispersed the organoclay better than at higher temperatures. These parameters were used to mix the matrix which was used to manufacture the composite. Two sets of equipment were used in order to mix the nanocomposite matrix and to extrude the PP matrix into sheets, namely; twin screw compounding mixer and multilayer cast film line.

The initial step of mixing involved creating the masterbatch using a twin screw extruder. Normally the masterbatch would consist of clay and compatabiliser, however the compatabiliser purchased had a high concentration of maleic anhydride and the only way to reduce the content was to dilute it with polypropylene. Therefore, the masterbatch consisted of polypropylene, PP-g-MA and clay. Thereafter TGA was used to determine the actual clay content in the masterbatch before it was diluted to the required clay content using the sheet extruder.

4.3.1 Twin Screw Compounding Extruder

The TE-30 co-rotating twin screw extruder (Nanjing Only Extrusion Machinery Co.Ltd) can be seen in Figure 4.4a. The diameter of the screw is 30 mm and the length to diameter ratio is 40. It is located in the Nano Technology Unit at the Council for Scientific and Industrial Research (CSIR) in Pretoria. It has instrumented gravimetric dosing feeders which were used in the melt intercalation process. The feeders were used to introduce the three constituents mentioned above at different mass flow rates according to the desired ratios. The heating zone was divided into several sections, and individually controlled by use of a temperature controller. The extrudent was fed into a pelletiser which can be seen in Figure 4.4b, resulting in pellets.

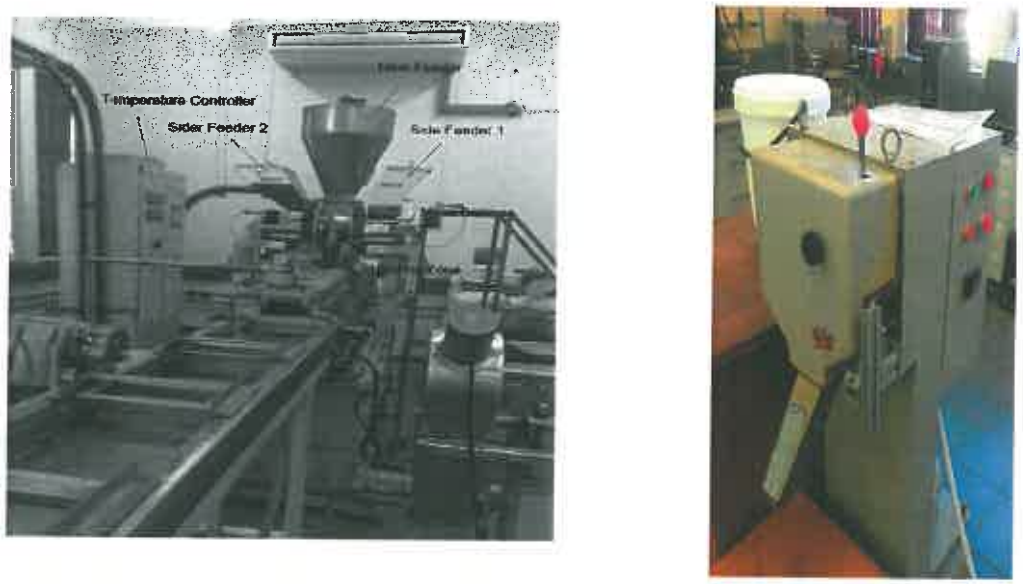

(a) Overview of Twin Screw Extruder (b) Pelletiser

Figure 4.4: Twin Screw Compounding Equipment

Before mixing it was important to establish the melting temperature of the components, as this is a crucial factor in mixing and creating a homogeneous mixture.
Temperature and rotation speed affect the shearing forces on the montmorillonite clay layers, and thereby affect their separation. The shearing force is greater for lower temperature mixing, which results in better dispersion of the clay platelets [14]. Polypropylene (PP) and Polypropylene-Graft-Maleic Anhydride (PP-g-MAH) have melting temperatures of 163°C and 156°C [36], respectively. Specification sheets for these materials can be found in Appendix A. No clear information was found indicating the melting temperature of MMT however, this detail was not required for the intercalation of the MMT platelets. The temperature for mixing had to be greater than the melting point of PP but not greater than the thermal

degradation of the three constituents. An upper mixing temperature of 190°C was thus used in the mixing which was based on the work of Chiu et al. [14].

The compatabiliser purchased for this project consisted of 10% maleic anhydride whilst the compatabiliser used in previous work [12, 36, 53] had concentrations of approximately 1% maleic hydride. The gravimetric feeders were controlled so that the maleic anhydride concentration was reduced from 10% to 1% by diluting it with polypropylene. The feeders also ensured that a compatabiliser to clay ratio of 3:1, as specified in previous work [15, 30], was achieved.

It was observed on the gravitational feeder monitor that the gravimetric feeders were effective in controlling the mass rate of polypropylene and the compatabiliser. However, there were lumps in the clay powder which made it difficult for the gravimetric feeders to release the clay at a constant mass rate. This resulted in slight variations in the clay content in the mixtures. To ensure good consistency in the mixing process, the master batch was collected in smaller batches where the clay mass rate was constant. The extrudent was fed into the pelletisor to form pellets, which was required to feed the sheet extruder.

4.3.2 Analysis on the compounded extruded plastic using TGA

A Perkin-Elmer STA6000 TGA machine shown in Figure 4.5 was used to check the quality of the clay/polypropylene mix which is made of three components; polypropylene, montmorillonite clay, and compatabiliser. This equipment is capable of measuring the weight of the sample placed in a capsule whilst simultaneously heating the sample until decomposition. Each component has its own disintegration temperature and the final composition of the mix can be calculated by heating the sample until disintegration, which occurs at approximately 600°C.

Each sample tested had a mass of approximately 10 mg. This weight was measured by the TGA equipment and used by the instrument as the reference weight. The weight was then continuously measured as the instrument heated the sample from room temperature to 600°C. Two samples from each batch were tested and an average of these values were used. The TGA results of the masterbatch and its three constituents are shown in Figure 4.6.

Figure 4.6 shows that above 500°C, clay has 71% mass remaining and that the masterbatch has approximately 15% mass remaining. This remaining mass corresponds to the inorganic content in the clay as the polypropylene and the compatabiliser are completely degraded above 450°C. Using this information, the composition of the pellets from the twin screw extruder could be determined. The assumption made in this calculation is that the feeders

Figure 4.5: TGA equipment

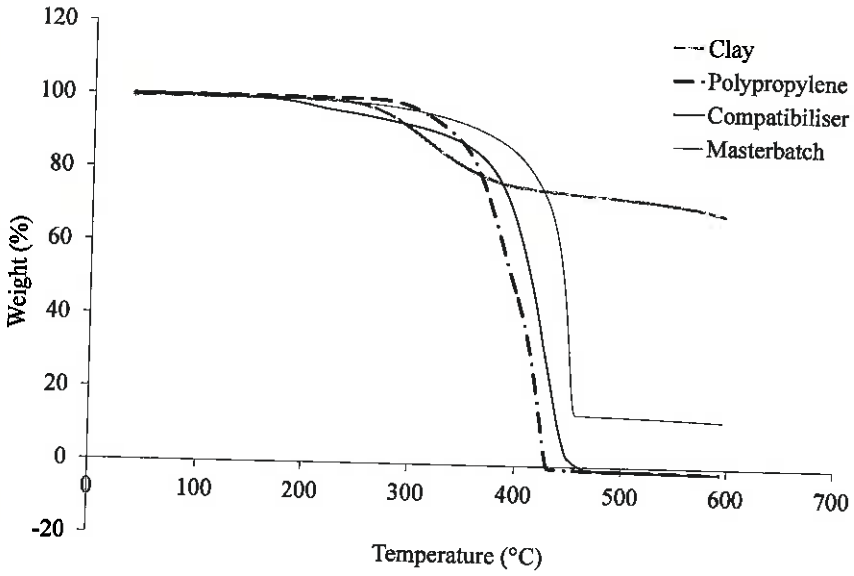

Figure 4.6: TGA Results for Polypropylene, Compatabiliser and Clay

were effective in diluting the concentration of maleic anhydride from 10% to 1%.

Five batches of masterbatch were collected from the twin screw extruder and subjected to TGA testing. The results are presented in Figure 4.7.

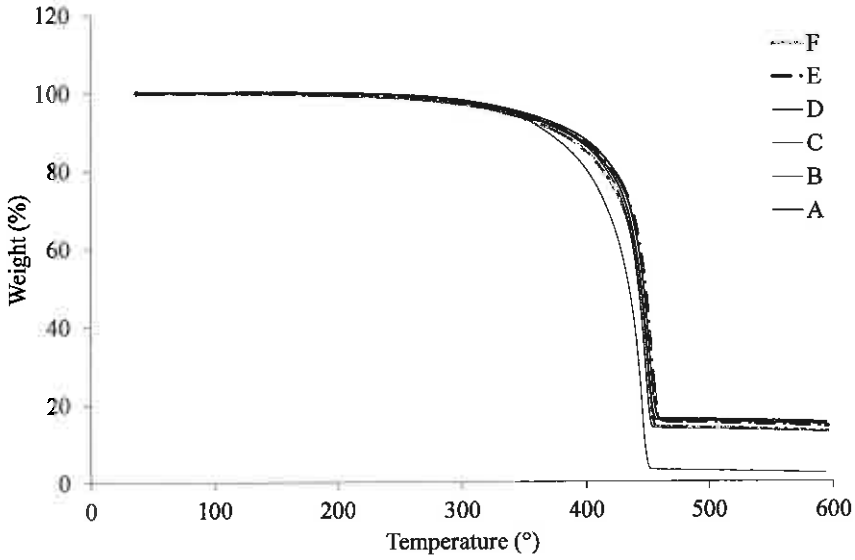

Figure 4.7: TGA Results for the Master batches

The TGA results for the clay and the masterbatch A were tabulated from 500°C to 594°C, and these can be seen in Table 4.2.

Table 4.2: TGA results for batch A

	Actual			Calculated		
Temp °C	Percentage Inorganic in Clay	Percentage Inorganic in A1	Percentage Inorganic in A2	Percentage Inorganic in A Avg	Percentage Inorganic in Clay	Ratio
500	73.28	15.46	15.16	15.31	20.89	3.79
520	72.71	15.33	15.03	15.18	20.88	3.79
540	72.07	15.20	14.88	15.04	20.87	3.79
560	71.25	15.05	14.70	14.88	20.88	3.79
580	70.13	14.84	14.49	14.67	20.91	3.78
594	69.17	14.68	14.30	14.49	20.95	3.77
Avg	71.43	15.09	14.76	14.93	20.90	3.79

It is seen in Table 4.2 that at 500°C, there is 73.28% inorganic content in clay and on average 15.31% of inorganic content in master batch A. At this temperature, polypropylene and compatabiliser have completely degraded. It is for this reason that it can be concluded that

the 15.31% inorganic content represents the 73.28% inorganic content in clay. The actual clay in the mixture was calculated to be 20.89%, and the remaining 79.11% is a representation of the compatabiliser in the mixture. From this, the ratio of compatabiliser to clay was calculated to be 3.79:1. Although the aim was to obtain a ratio of 3, this result is sufficient for the continuation of this investigation.

The desired clay mixture percentages were 1%, 2%, 4%, 6% and 8%. Polypropylene had to be added into the masterbatch to dilute it to the required clay percentage. The required dilutions and batch details can be seen in Table 4.3.

Table 4.3: TGA results indicating batch composition and mixing details

Desired Clay %	1	2	4	6	8
Masterbatch	A	E	D	D	B
Clay %	20.90	21.40	20.75	20.75	18.43
Masterbatch Amount (g)	170	400	740	990	660
Polypropylene (g)	3383	3880	3099	2434	860
Clay Amount (g)	36	86	154	205	122
Compatabiliser Amount (g)	134	314	586	785	538
Total Mass (g)	3553	4280	3839	3424	1520
Ratio	3.79	3.67	3.82	3.82	4.43

Making reference to dilution mixture number one in Table 4.3, it is seen that batch D had 20.75% clay content. This batch had to be diluted to 4% clay content by adding virgin polypropylene. It is shown that 740 g of batch D had to be mixed with 3099 g of virgin polypropylene to obtain 4% clay content in the overall mixture.

4.3.3 Sheet Extruder

The pellets were used as the input for the Multilayer Cast Film Line, which converted the pellets into matrix sheets. This system can be seen in Figure 4.8.

The Cast Film System has a maximum of five separate feeders equipped with individual rotational screws that feed to a single die. Each feeder provides a layer of the extruded sheet, and if required can provide a sheet that has five layers of different materials. The feed rate into the heated die ultimately dictates the thickness of the extruded sheet.

The sheet extruder was used to dilute the master batches to the desired clay content. The quantities needed for making the matrix sheets were presented earlier in Table 4.3. The quantity of masterbatch and polypropylene required to achieve the desired clay content were

Figure 4.8: Overview of the Multilayer Cast System

placed in a sealed container and shaken. The mixture was then placed into the feeders of the sheet extruder. The sheet extruder was set to 190°C with an extruding rate of 90 rpm. The upper temperature limit of extrusion could not exceed 200°C to prevent Hofmann degradation. The resultant sheet thickness was, on average, 0.5 mm with a width of 30 mm.
The TGA results for different clay percentages can be seen in Figure 4.9, and the tabulated summary can be seen in Table 4.4.

4.4 Manufacture of Composite Plates

The manufacturing process of the NFC consisted of a film stacking process combined with thermal compression moulding as used by Asumani et al. [4]. A mould was used to hold the composite charge, consisting of the matrix mixture and fibre mat. The mould is then placed

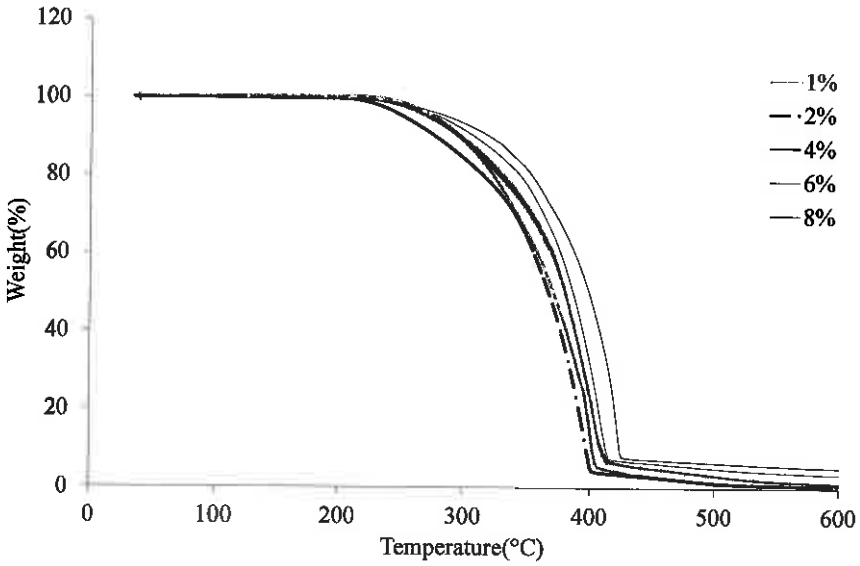

Figure 4.9: TGA results for the different Clay Percentages

Table 4.4: Desired vs Actual Clay Content

Desired Clay Percentage	Actual Clay Percentage
1	1.53
2	1.64
4	3.98
6	6.63
8	8.65

in a compression moulding oven to form the composite plate. The mould seen in Figure 4.10 was manufactured by Paiken [52], and is made from mild steel, consisting of male and female parts. The internal measurement of the mould is 170 mm by 130 mm.

A Thermal Compression Oven consists of two pieces of equipment; an oven and a press which can be seen in Figure 4.11. The oven manufactured by Thermopower Furnaces supplies the heat required to melt the polypropylene. The press essentially comprises a single acting hydraulic cylinder connected to a 10 ton hydraulic jack. The press applies pressure onto the polypropylene so that it can penetrate into the fibres. These two pieces of equipment were assembled to make a single piece of equipment so that heat and pressure can simultaneously be applied to the charge, to form a composite plate.

Figure 4.10: Composite Mould

Figure 4.11: Thermal Compression Oven

After the composite plate is made, the mould is separated using a hydraulic jack. The process of manufacturing the composite plates can be summarised in the following points.

1. Two sheets of PTFE were cut into rectangular pieces with dimensions of 170 mm by 130 mm.

2. Two kenaf fibre mats were cut into a rectangle measuring 170 mm by 130 mm. Each mat weighed 7.8 g, resulting in a total weight of 15.6 g of fibre in each composite plate.

3. Using the appropriate fibre weight fraction of 15%, 20%, 25% and 30%, the quantity of matrix required to make the composite can be determined.

4. The spacer corresponding to the set fibre weight fraction is chosen and placed on the side wall of the base. Table 4.5 shows the details of quantities used in manufacturing the composites as well as the spacer thickness required.

Table 4.5: Fibre Sheet Composite - Requirements for Composite Manufacture

Fibre Weight Fraction	30	25	20	15
Fibre Mass(g)	15.6	15.6	15.6	15.6
Polypropylene Excess(g)	4.5	7.5	10.5	13.5
Polypropylene Needed(g)	36.4	46.8	62.4	88.4
Polypropylene to be placed rounded up(g)	41	55	73.0	102
Spacer Thickness for Mould(mm)	2.6	3.1	3.9	5.2
Estimated Composite Thickness(mm)	2.3	2.8	3.6	4.9

5. A PTFE sheet was placed inside the mould. Thereafter the charge, which comprises a sandwich of polypropylene and fibre, was placed into the mould. This charge was made of $\frac{1}{3}$ of the matrix, a fibre mat, $\frac{1}{3}$ of the matrix, a fibre mat and then finally the last $\frac{1}{3}$ of the matrix. The matrix sheet was cut in the centre to allow for the trapped air in the charge to escape during the moulding process. Thereafter another PTFE sheet was placed on top of the charge. Finally the ram was placed in position to compress the charge.

6. The mould was placed in the oven set to a temperature of 280°C with no pressure being applied. After 52 minutes the oven was switched off. The internal temperature of the mould at this point is 175°C, which is the optimum moulding temperature. The derivation of this temperature was determined in a separate investigation which is explained in further detail in Appendix B. The oven was switched off due to the mould having thermal inertia, which causes the internal temperature to increase further even though the oven is switched off. To reduce this temperature increase to some extent, a fan was used to cool the mould and oven for a duration of one minute.

7. The oven was switched on again and set to a temperature of 185°C which aids in maintaining the mould's internal temperature at 175°C for 15 minutes.

8. Hydraulic pressure was gradually applied for 15 minutes at 4 bar per minute up to a maximum of 60 bar, which relates to a maximum pressure in the mould of 7.7 bar. This pressure causes the matrix to penetrate the fibres, thereby making the composite plate.

9. The last step consists of compressing the mould with a hydraulic pressure of 200 bar, switching the oven off, and finally using a fan to cool the mould. This relates to a

maximum pressure of 25.6 bar in the mould. The pressure causes the mould to close on the spacers, and the composite to have an even thickness with the correct fibre weight fraction.

10. The mould was left to cool to room temperature and then removed from the oven.

11. The summary of the moulding procedure can be seen Table 4.6.

Table 4.6: Moulding Procedure

Step	Duration (min)	Temp setting of Oven (°C)	Oven Pressure(Bar)
1	52	280	0
2	1	Off- Place Fan	0
3	15	185	0
4	15	185	60
5	30	Off- Place Fan	200
6	120	Remove Mould and Cool	

12. The mould was then separated and the composite plate removed.

13. The composite plate was marked with the proper identification mark and weighed to establish the final fibre weight fraction.

4.5 Manufacture of Test Specimens

The manufactured composite plates measured 170 mm by 130 mm. A bandsaw is used to cut the manufactured composite plate into rectangular strips which are then shaped into specimens for tensile, impact and short beam shear tests.

4.5.1 Tensile Specimens

The tensile specimens were cut according to the ASTM638 specifications which are shown in Figure 4.12. Type one specimens specifically relate to orthotropic laminates. According to the specifications, at least five specimens should be tested for each configuration of composite material. The composite plate was cut into sections of 21 mm by 166 mm using a bandsaw. Thereafter, the strips were stacked and clamped in the holder of the shaping machine which had the desired tensile specimen shape. The shaping machine consists of a pneumatic grinder and guides that allowed the holder to slide in a set path which grind the strips into the required shape. The shaping machine can only fit three strips at a time. The transition from the grip length to the gauge length of the specimen has to be ground to a very smooth finish, as any imperfections may cause stress concentrations, which can result in premature failure.

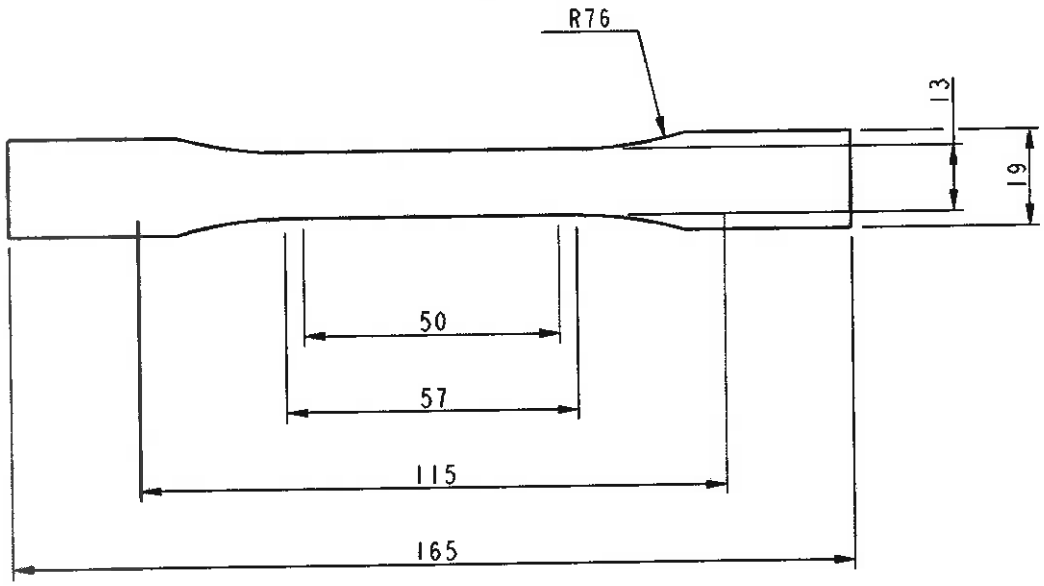

Figure 4.12: Dimensions for the Tensile Specimen [54]

4.5.2 Impact Specimens

For impact testing, the composite plate was cut into six samples measuring 65 mm by 15 mm using a bandsaw. These were given to a machining shop, where they were ground to the required length and width (Dimensions C and E, respectively, shown in Figure 4.13), and then notched according to the ASTM D256 standard which can be seen in Figure 4.13.

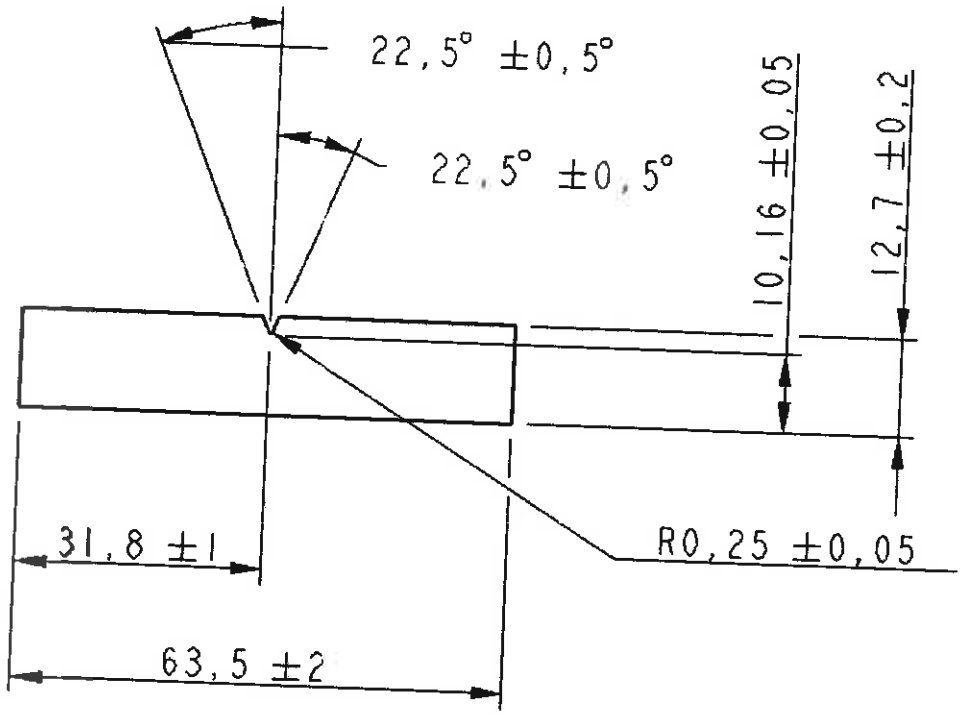

Figure 4.13: Dimensions for the Impact Specimens [55]

4.5.3 Shear Specimens

The short beam shear specimens requirements are outlined in the ASTM D2344 standard [56] and it shows that a minimum of five samples is required for testing. The standard highlights that the width and length are a function of the thickness of the composite plate. The dimensions of the specimen are given in equations 4.1 and 4.2 These equations highlight that the width of the shear specimen is required to be twice the thickness of the specimen and accurate to two decimal places.

The composite plates varied the least in thickness across the width, so strips were cut from the end that had the most even thickness. A milling machine was used to shape the specimens to the required width. The machined strips were then cut into shear specimens using a bandsaw. The length of the specimens does not matter as long as the overhang in testing is greater

than the thickness. The resultant strips can be seen in Figure 4.14. The distance between the supports of the short beam shear jig is four times the thickness of the specimen.

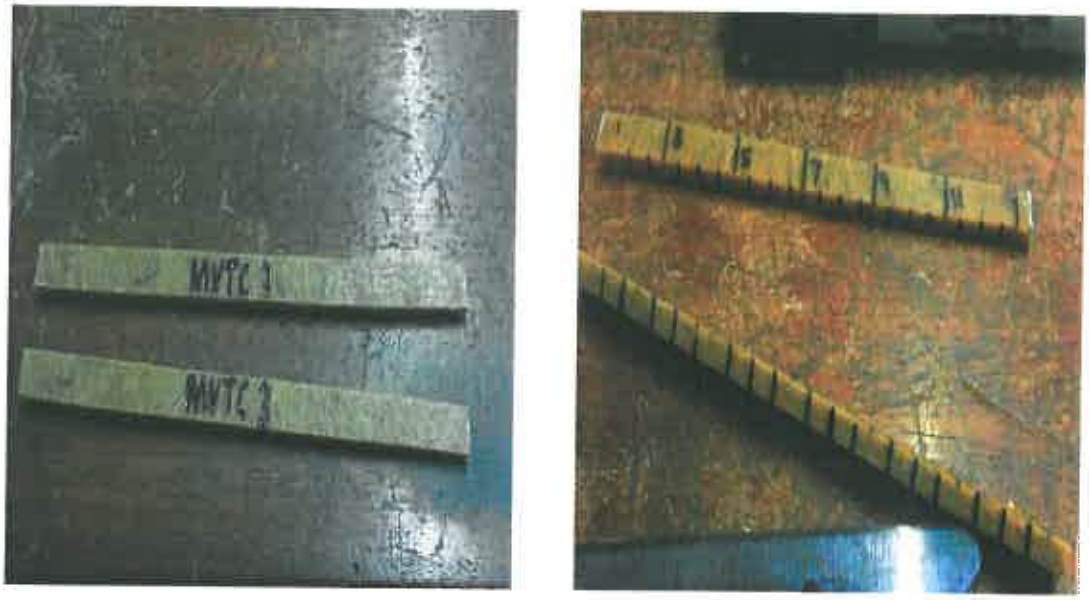

(a) Strips after grinding

(b) Strips marked for cutting

Figure 4.14: Machined Shear Specimen Strips

$$Length = 6 \cdot Thickness \tag{4.1}$$

$$Width = 2 \cdot Thickness \tag{4.2}$$

4.6 Mechanical Testing

The testing procedure used for the three mechanical tests is highlighted below.

4.6.1 Tensile Testing

The setup for the tensile tests performed can be seen in Figure 4.15a. A Shimadzu tensile testing Machine (Model : AC-IC 20kN/50kN) was used to load the specimen. The rated load for the loadcell used in this research is 20 kN. The Epilson Tech Laser Extensometer, Model LE-05, together with reflective tape on the specimen was used to measure strain in the specimen. A National Instruments Data Acquisition Device (Model : NI SCXI-1000) was used to record the force data from the Tensile Testing Machine and the strain data from the extensometer simultaneously. The Data Acquisition Device (DAQ) can be seen in Figure 4.15b.

(a) Shimadzu Tensile Testing Machine

(b) DAQ used to collect force and deflection data

Figure 4.15: Tensile Testing Equipment

According to the ASTM D638 standard, a minimum of five samples is required per test to provide adequate results. Generally, however, six specimens were tested so that in the event that a specimen was destroyed without getting useful results, a minimum of five specimens were still available. Prior to switching all the equipment on, it was necessary to check that all components were properly connected. The laser extensometer was turned on and calibrated before use. The speed of testing was set to 2 mm/min. The procedure for testing can be summarised as follows:

1. Retro-reflective tape was placed on the specimen marking a gauge length of 40 mm.
2. The specimen was placed into the grips of the tensile machine, ensuring that the longitudinal axis of the specimen lined up with the axis of the testing machine. The grips were tightened until they were tight enough to prevent the specimen from slipping.
3. The distance between the face of the laser extensometer and the specimen was set to 351 mm, thereafter the laser was switched on. It is necessary to check that the vertical red light projected by the extensometer is aligned with the longitudinal axis of the specimen.
4. Caution should be taken to avoid looking at the laser light at any time as this can cause permanent eye damage.
5. The force and displacement were zeroed.
6. Tensile testing was initiated by pressing the start button which causes the cross-head to begin moving.
7. After the specimen snaps, the testing machine was stopped and the load and strain data saved.
8. The process was repeated until all specimens were tested.

The output file from the DAQ was processed using a Matlab code to obtain the maximum tensile strength, elastic modulus, secant modulus at 0.01 strain and the secant modulus at failure. The code used can be seen in Appendix C.

The DAQ simultaneously recorded the force applied to the specimen and the distance between the reflective tapes. As mentioned earlier, the reflective tape used by the laser extensometer marked off the gauge length of the specimen. Consequently, the measured distance under no load corresponds to the gauge length of the specimen. The strain of the specimen was calculated by subtracting gauge length from the distance between the reflective strips, which was then divided by the gauge length. The stress data were calculated by dividing the force data by the cross sectional area of the specimen, measured using a micrometer. The stress-strain data can be seen in Figure 4.16.

The original data seen in Figure 4.16 shows that the strain data has an initial negative gradient, which changes to a positive gradient with an increase in load. This initial negative gradient is erroneous and is due to the clamping of the specimen. Another issue is the negative strain at the start of test. These issues relate to the grips of the tensile testing machine move inwards, towards the specimen as it clamps the specimen, putting the specimen in compression. The compression causes out-of-plane bending in the specimen, as the thickness

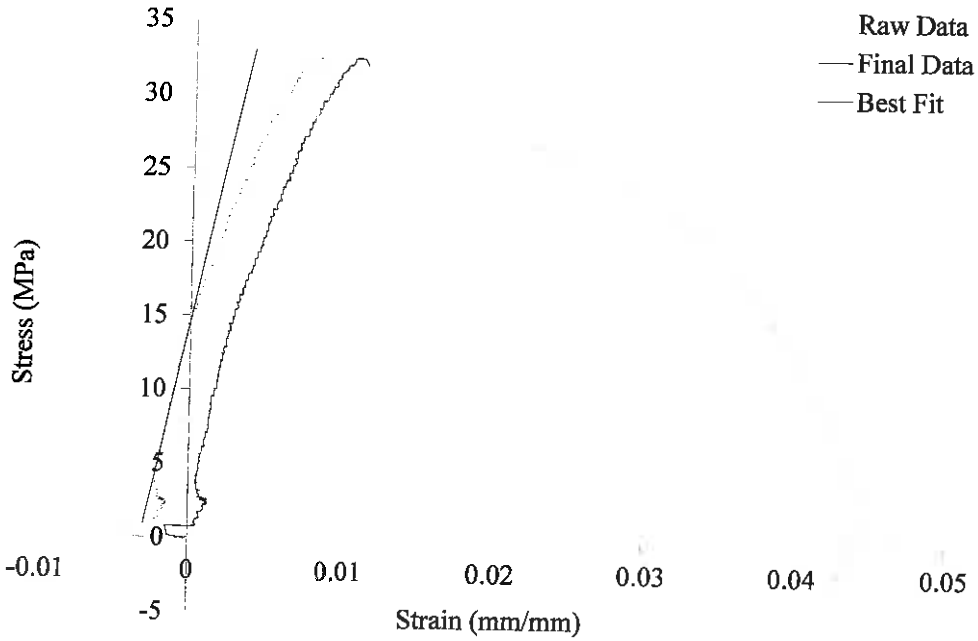

Figure 4.16: Original Data and Adjustment

of the specimen is relatively small compared to the width. This results in erroneous values of distance being measured, as the laser extensometer can not measure out-of-plane bending.

These issues were resolved by shifting the data as well as finding an optimum region to calculate the modulus data. Further explanations for the methods used to address these shortcomings in tensile testing can be found in Appendix D. The adjustment to the tensile data can be seen in Figure 4.16.

4.6.2 Impact Testing

The setup seen in Figure 4.17 was used to impact test the specimens of the manufactured composite. The following is a list of components used in the Impact Rig which was developed in-house.

1. Izod Impact Testing Rig, which can be seen in Figure 4.17
2. PCB Piezotronics Model 353B03 Accelerometer
3. PCB ICP 482A Power Supply
4. Hantek DSO 2090 Oscilloscope

The specification sheet for the accelerometer can be seen in Appendix A. The accelerometer is attached to the impactor of the pendulum, which is in turn connected to the PCB amplifier, connecting to the oscilloscope. This connects to a computer installed with the Hantek oscilloscope software. The trigger is a set point in the oscilloscope, with the sole purpose of indicating to the device when to start recording the data. It is set to ten times the acceleration of gravity, which is the minimum acceleration that occurs for impact specimens. As soon as the set point acceleration is reached, the oscilloscope begins to record.

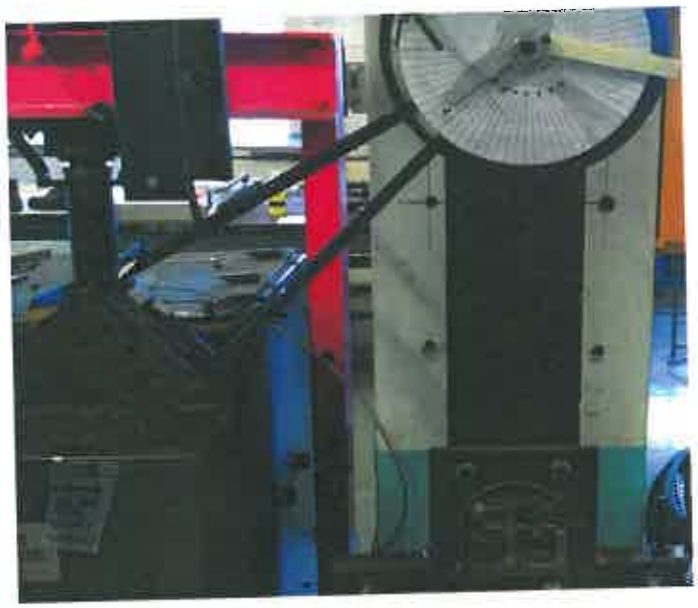

Figure 4.17: Impact Rig Setup and Accessories

ASTM D256 standard requires five specimens to be tested, although for this research six specimens were tested for reasons previously mentioned. The connections in the impact rig setup were straightforward, however, caution was taken to ensure that the cables were not in the space of the pendulum's swinging motion. The equipment is very sensitive to electrical interference which made the presence of the laptop charger a contributor to noise in the data. The laptop was run on battery power but the amplifier was still connected to the main power source. Electrical components in a 1 m vicinity of the impact rig were removed due their propensity to cause electrical interference. The procedure for impact testing can be summarised as follows:

1. The Hantek DSO 2090 software was opened and the setup for impact testing was selected.

2. The setup had three adjustable parameters; the x-axis time scale which was set to 4 ms, the y-axis, or the voltage scale, which was set to 20 mV, and the setting of the placement of the trigger which was crucial in collecting the impact data. The trigger was set to

just above the noise level in the collected data, to prevent premature triggering of the system.

3. The hammer was raised and secured in position using a latch mechanism.

4. The sample was placed in the centre of the vice of the impact test rig. The horizontal line behind the notch was positioned to be parallel to the horizontal edge of the vice.

5. The play button in the Hantek software was selected. The latch was then moved to release the hammer, which impacted the specimen, throwing the unclamped part of the impacted specimen across the room.

6. The specimen was removed from the vice, and replaced with a new specimen, and the above procedure was repeated.

A Hantek DSO2090 DAQ collected the data from the accelerometer and an example of the raw data collected can be seen in Figure 4.18. This figure shows the superposition of the impact data and noise generated during the testing. This noise is caused by impact waves propagating forwards and backwards in the hammer.

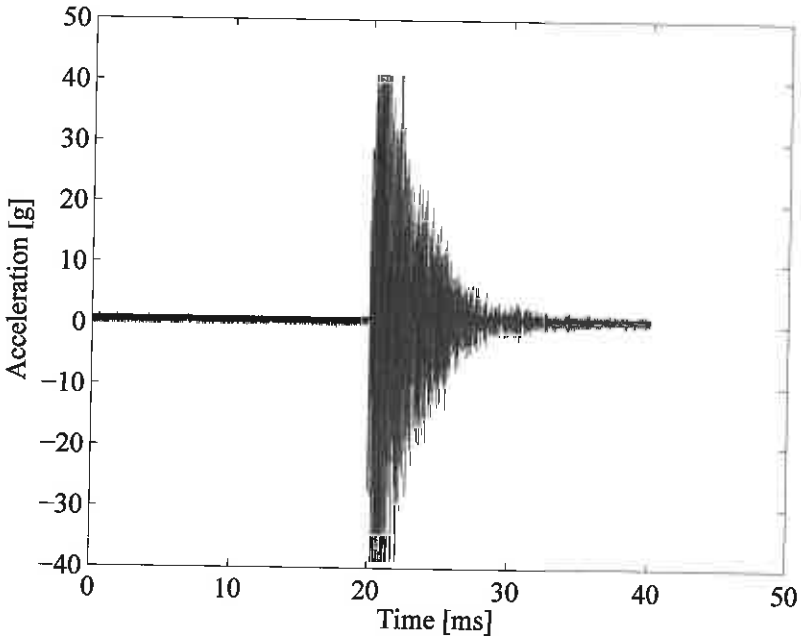

Figure 4.18: Raw Impact Data

It was difficult to differentiate between the impact and noise data. Consequently, a butterworth function in Matlab was used to filter the high frequency noise, the result of which can be seen in Figure 4.19.

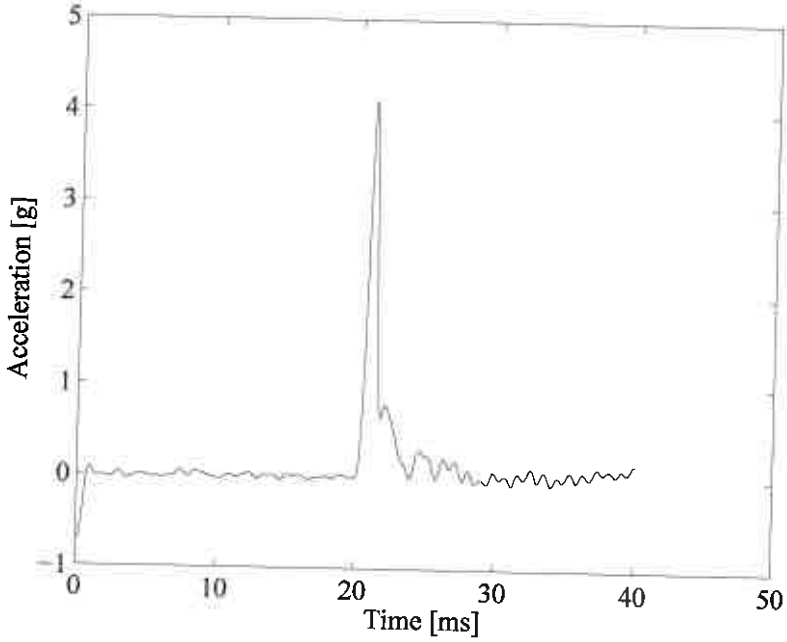

Figure 4.19: Filtered Impact Data

This was processed further to determine the impact energy. The starting of the impact occurred at 20 ms, as the trigger of the oscilloscope was placed at that point. The trapezoidal rule was used to integrate the acceleration data to obtain the velocity vs time data. A high speed camera was used to determine the initial velocity of the pendulum just before impact. The energy was calculated using Equation 4.3.

$$E = \frac{m \cdot v^2}{2} \tag{4.3}$$

where m = mass of the hammer (kg)
v = velocity of the impactor (m/s)

Figure 4.20 shows the final impact data for an impact specimen. It highlights the acceleration and energy through the duration of the impact. The energy absorbed prior to the peak acceleration was considered to be the initial energy whilst the remaining energy is considered to be the propagative energy. This impact rig was developed in-house and all the short comings in using the rig are explained in greater detail in Appendix E.

4.6.3 Shear Testing

The shear rig testing setup and the specimen with all the markings can be seen in Figure 4.21. The shear rig consisted of two support components and a loading pin component. The

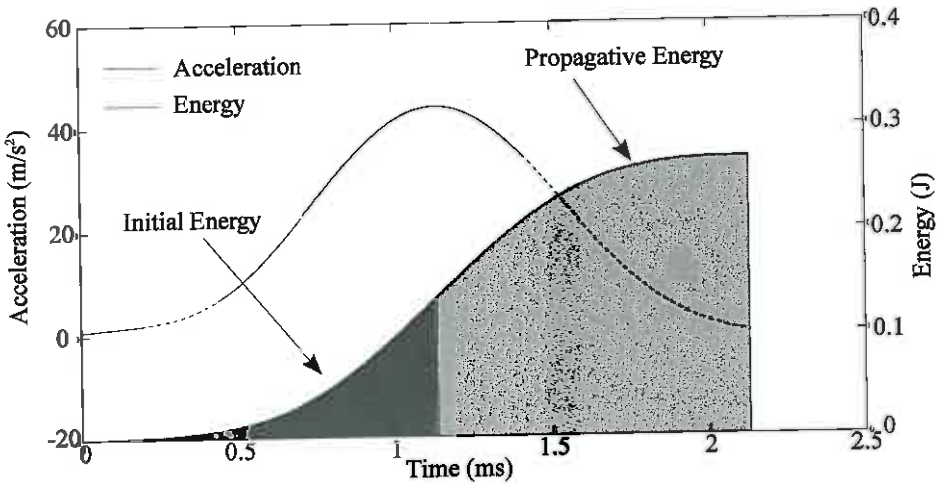

Figure 4.20: Final Impact Data

mechanism was developed in-house according to the ASTM D2344 standard. The dimensions were scaled appropriately to accommodate the low thickness of the test specimens. The shear rig was used in conjunction with the Shimadzu tensile testing machine which applied the load.

Figure 4.21: Short Beam Shear Rig

On average of eight samples were used for this test, although a minimum of five samples were required by the ASTM 2344 standard. The specimens had small dimensions which required careful placement in the testing rig for mechanical testing. Samples were marked off in three places; the two support points and the loading point.

The span distance between the supports is four times the thickness of the specimen according to the standard. The setup of the test with the required distances can be seen in Figure 4.22. The testing of the specimens is similar to that of tensile testing as the Shimadzu tensile testing machine was used to conduct this test as well. A testing speed of 1 mm/min was used [57]. Although the standard recommends 2 mm/min, a slower speed was chosen to reduce the chance of premature failure.

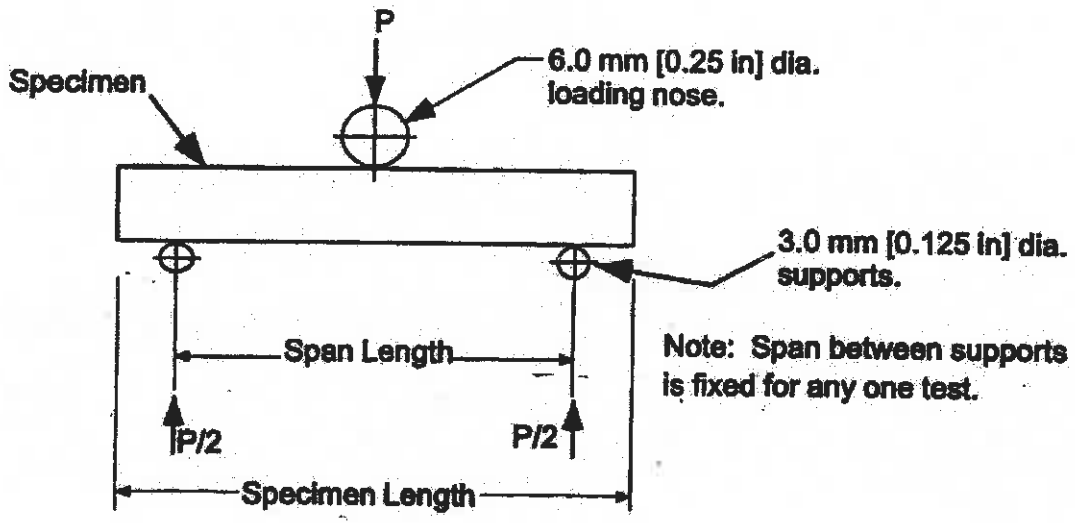

Figure 4.22: Set up for Short Beam Shear Specimen [56]

The shear testing procedure is as follows:

1. The left and right supports were positioned such that the span gap was four times the thickness of the specimen, and that supports were equidistant from the loading nose.
2. The left and right supports were then fixed in place using a spanner, and the shear rig was then secured in the tensile testing machine using the available pins.
3. The specimen was placed in position until the marks on the specimen matched the marks drawn on the rig. This can be clearly seen in Figure 4.21.
4. The loading nose was aligned with the centre mark drawn on the specimen.
5. The test was started by clicking the start button.
6. Once a maximum force was achieved, the test was stopped, and the specimen was replaced with another one.
7. The procedure was repeated until all specimens were tested.

After following the above mentioned procedure, a '.csv' file was generated by the Shimadzu Tensile Testing Machine. A sample of typical force vs deflection data can be seen in Figure 4.23.

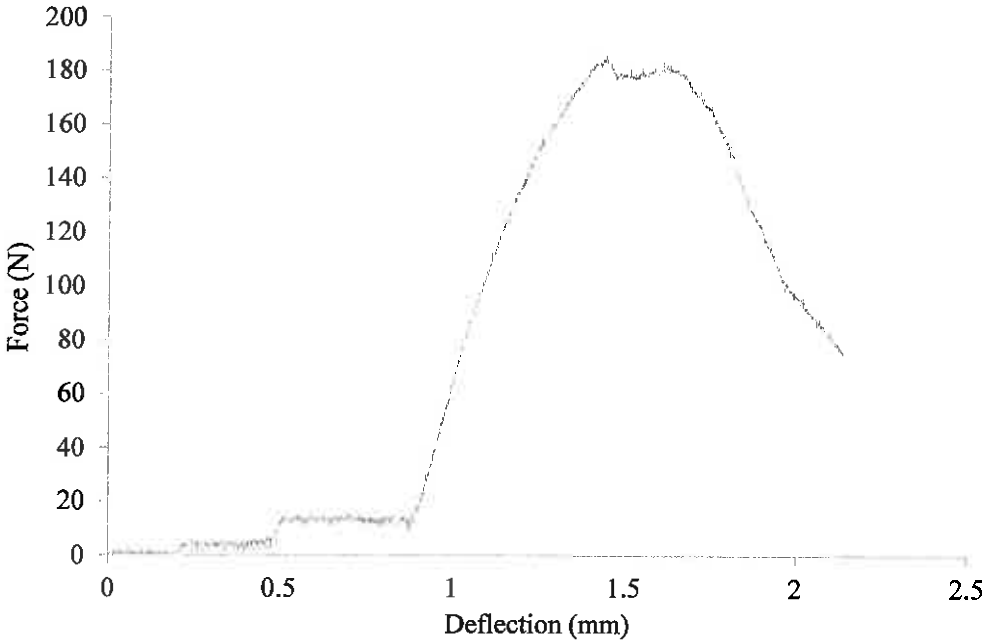

Figure 4.23: Original Shear Force Data

The area of the specimen was calculated using the thickness and width of the cross section of the shear specimen. The force data was converted into stress data using Equation 4.4 which is obtained from the ASTM 2344 standard for short beam shear testing [56]. This result can be seen in Figure 4.24.

$$\tau_{\max} = \frac{0.75 \cdot F_{\max}}{b \cdot h} \tag{4.4}$$

where $\tau_{\max}$ = max shear stress (MPa)
$F_{\max}$ = max force (N)
h = width of specimen (mm)
b = thickness of specimen (mm)

Figure 4.25 was used to calculated the shear angle in radians due to the shearing force. The modulus was determined in the range of 4 MPa to 6 MPa. It could not be determined at low stresses as a consequence of the non-linearity associated with bedding-in of the specimen. Equation 4.5 was used to determine the apparent modulus. The deformation measured is

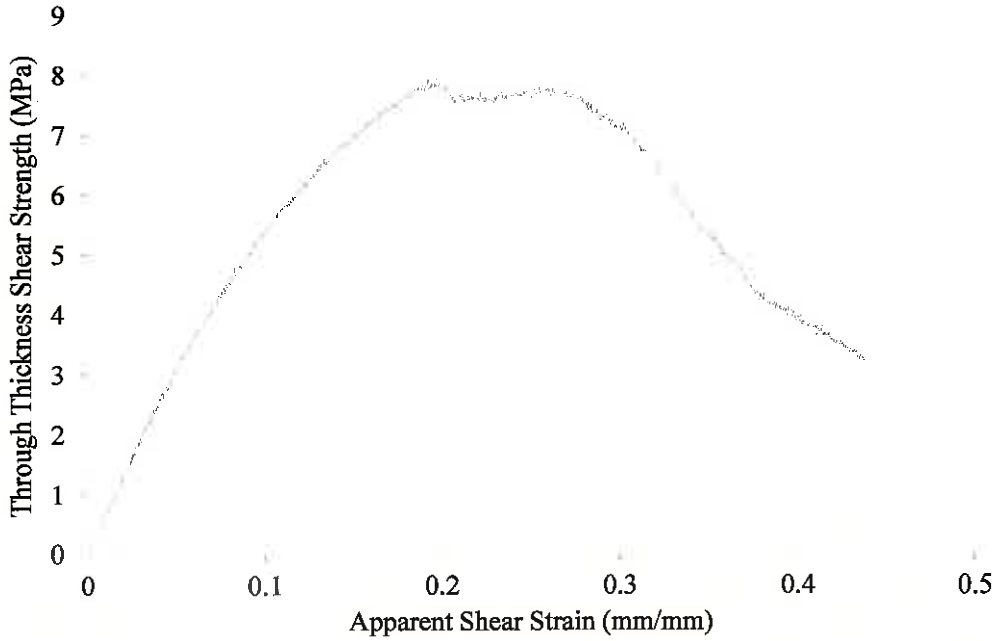

Figure 4.24: Through Thickness Shear Strength

not correct due to the influence of bending in the test, therefore the associated strain and modulus values will be incorrect. However, all specimens were made and tested in a similar manner, therefore this data is comparable, and can be used to provide information about the stiffness of the composite.

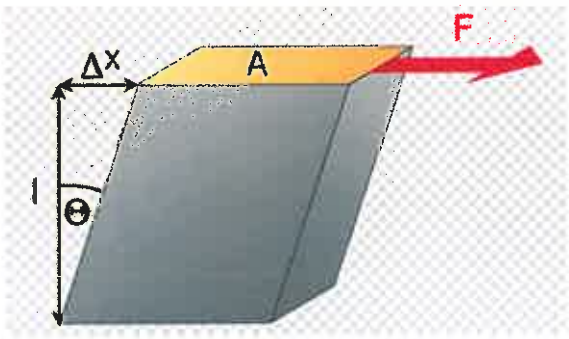

Figure 4.25: Calculating shear angle [58]

$$G = \frac{F \cdot l}{A \cdot \Delta X} \tag{4.5}$$

where l = half of the distance between the testing supports (mm)
F = half of the max force (N)
A = Cross sectional Area (mm^2)

ΔX = Change in displacement (mm)

4.7 Post Processing

A scanning electron microscope (SEM) was used to view the failure surfaces of the tested specimens to gain greater insight into their failure modes as well as the bonding between the matrix and the fibres. FTIR was used to investigate the bond formation resulting from the chemical treatments of the fibres.

4.7.1 SEM

A FEI Nova Nanolab 600 SEM microscope was used in this research project. This instrument assisted in indicating the type of bonding between the fibre and the matrix. The size of specimen that can fit in the microscope can be approximated to an area of 20 mm by 40 mm, with a height of 20 mm.

Natural fibre composites are non-conductive materials which is a problem for electron microscopes as they require a conductive surface. A sputter coater, Quorum Emitech SC7620, was thus used to coat the samples to make them conductive, which prevents charging of the sample. Charging is defined as the accumulation of charge on the specimen and appears in the SEM picture as bright spots. The fractured test pieces were cut and placed on stubs for microscopy. The stubs together with test samples were sputter coated with two coats of carbon and one coat gold/palladium to improve their conductivity in the SEM.

The SEM makes use of an electron gun which interacts with the sample and reflects electrons back to the detector. The detector receives this information and translates it into a picture. Operation of the NOVA SEM is outlined in a manual provided by the University of Witwatersrand Microscopy and Microanalysis Unit (MMU) department. Typical magnifications of the sample are approximately 800-1200X which was sufficient to observe failure modes and bonding of the fibres in the composites. A summary of the procedure used is presented below:

1. The SEM was first vented to release the vacuum in the chamber.
2. Once the chamber was vented, the door of the chamber could be opened by sliding it out.
3. The sample was placed on a stub using carbon tape and inserted into the SEM chamber.

4. A gauge was permanently placed inside the SEM chamber to check the height of the sample.

5. A screw that holds the stub was adjusted until the height of the sample was lower than that of the gauge.

6. The infrared camera which shows the inside of the chamber was activated.

7. The door was then closed by sliding it slowly and monitoring the IR view to ensure that the specimen does not make contact with the electron lens.

8. Once the door was closed, the pump button could be selected, which created a vacuum in the chamber.

9. It took 7 minutes to create a vaccuum, during which time the stage was raised to approximately 5 mm from the electron gun, corresponding with the optimum focal length.

10. After a vacuum was created, the electron gun could be activated by selecting the 'Beam On' button.

11. The magnification, brightness and contrast control knobs were then adjusted to obtain a clear focused picture of the sample.

12. It is important to be careful of specimen charging, which is indicated by bright spots in the picture. A clearer picture can be obtained by decreasing the spot size which in turn decreases the current.

13. The desired image of the specimen was then saved.

14. At the end of the operation, the chamber was vented, the specimen removed, and the pump activated to recreate a vacuum in the chamber.

4.7.2 FTIR

A Bruker Tensor 27 was used for Fourier Transform Infrared Spectroscopy (FTIR) and the setup of which can be seen in Figure 4.26. This instrument was used to investigate the chemical bonds created during the fibre treatments and provide qualitative information about the characteristics of the chemical bonds present on the surface of the kenaf fibre. Table 4.7 lists the functional groups expected in this work with their relevant wavenumber.

The quantity of fibres used in each test was 0.3 g. The FTIR has two pins that hold the sample and these contact pins were cleaned with isopropanol before any measurement could be made. A measurement was taken prior to the samples being placed, which served as a

(a) FTIR Equipment

(b) Computer for FTIR

Figure 4.26: FTIR Setup

Table 4.7: FTIR peaks for kenaf fibre

Component	Wavenumber(cm^{-1})
COOH	664
-Si-O-Si-	1135
Si-O-Cellulose	1200
C-O	1239
CH	1432
Lignin Peak	1500
C=O	1730

reference point. Thereafter, a sample was placed in the FTIR instrument and the procedure was repeated.

During the FTIR analysis, a signal is sent through the pin, which passes through the fibres into a collecter which measures the transmittance. The FTIR data is determined from the transmittance information measured. It is important to note that the amount of fibres placed in the instrument determines the amount of transmittance that occurs. If a lot of fibres of a particular treatment are placed in the instrument, the transmittance will be low for the bonds present in the treatment. Essentially this will cause larger peaks of the bonds associated with the treatment, than in the instance where less fibres were placed in the FTIR instrument.

When the FTIR equipment was used, much effort was placed on keeping the quantity of fibres constant, however the slight variations in the quantity of fibres causes different peak magnitudes. From an analysis point of view, the magnitude of the peaks can be disregarded due to the slight variations in the quantity that was measured. However, the formation

and disappearance of peaks are an indication of the formation and disappearance of chemical bonds. The FTIR instrument generated a file containing the measured transmittance between 650 cm^{-1} and 4000 cm^{-1} wavelength.

5 Results and Discussion

The following discussion is split into six parts. Each part investigates the effect of a particular parameter on the mechanical properties of the composite. Each parameter is varied to find the best mechanical properties for the composite. The first part discusses the effect of temperature on manufacturing so as to obtain the optimum manufacturing temperature that results in the best mechanical properties and this was used for the remaining investigations. The second part investigates the effect of conditioning of the composite. The third part considers four different variations of MPS treatments which were applied to composites using two types of matrices, namely; a virgin polypropylene matrix and a polypropylene matrix with a 4% clay content. The treatment that yields the best mechanical properties is investigated further in the fourth part of this discussion, by varying the silane content to find the effect on mechanical strength. The fifth part discusses the effect of the clay content on a composite and the sixth part considers the effect of the variation of fibre weight fraction. The raw data for all the mechanical tests can be seen in Appendix F.

5.1 Effect of Temperature on Manufacturing

Many fabrication problems were experienced during the manufacture of the composites for this research project. These included; poor penetration of matrix into the fibres of the composite, non-uniform thickness of the composite and fibre tearing. Most of these factors are dependent on the flow of the matrix which is driven by temperature. Consequently, an optimum manufacturing temperature was critical for making composites.

The manufacturing procedure was a follow on from that of Paiken [52]. He made use of a single sheet of fibre with half of the matrix on top and the remaining half beneath the fibres, which made up the 'charge'. He treated the fibres with a 6 % sodium hydroxide solution and 5 % APS silane solution. He then compression moulded the charge. Despite his efforts to improve the penetration of matrix within the composites, there was room for improvement. Thus, fabrication using two sheets of fibre was investigated, so that a third of the matrix

would be placed between the layers of fibre and the matrix would therefore not have to penetrate as far as for a single sheet of fibre. Although this logic only works if each fibre sheet has half the areal mass of Paiken, the matrix content was split into three parts which should have some benefit over splitting it into two parts.

The investigation had a lower limit temperature of 170°C which was 7°C more than the melting temperature of polypropylene matrix. The specification sheet of the polypropylene matrix which can be seen in Appendix A, highlights detail such as the melting temperature. The maximum upper limit was 180°C which relates to the maximum temperature that kenaf fibres can be subjected to before thermal degradation occurs [11]. The tensile strength and modulus measured in this investigation can be seen in Figures 5.1 and 5.2, respectively. The fibre weight fraction was kept constant at 25%.

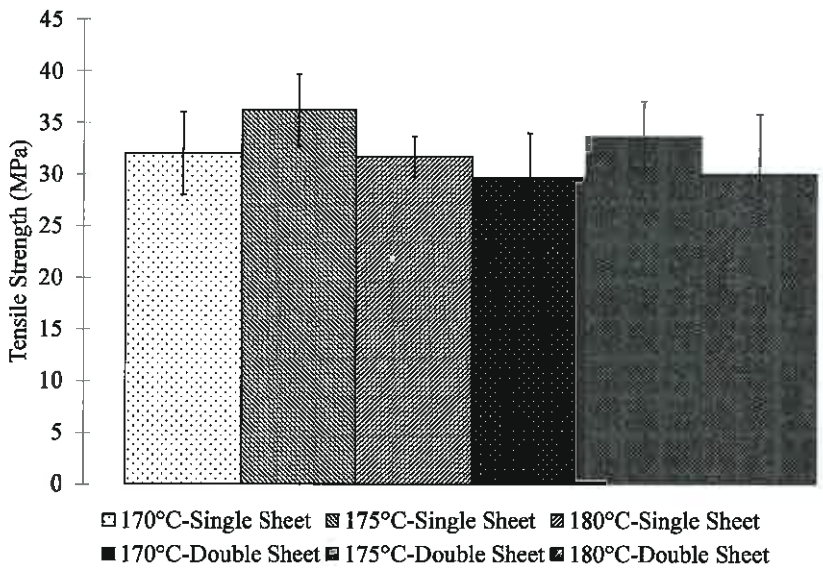

Figure 5.1: Tensile Strength - The effect of temperature in a composite using APS treated fibres

Figure 5.1 shows the variation in tensile strength with different manufacturing temperatures for composites made using both single and a double sheet of kenaf fibre. It is apparent from Figure 5.1 that 175°C is the optimum temperature for composite manufacturing as it results in the maximum tensile strength for composites using a single layer and a double layer of kenaf fibre. The error bars represent the variability of the data or the uncertainty in the measurement. Figure 5.1 also shows that manufacturing at temperatures higher or lower than 175°C results in a lower tensile strength and this trend is seen in both types of composites i.e single layer fibre mat and double layer fibre mat. The data show that

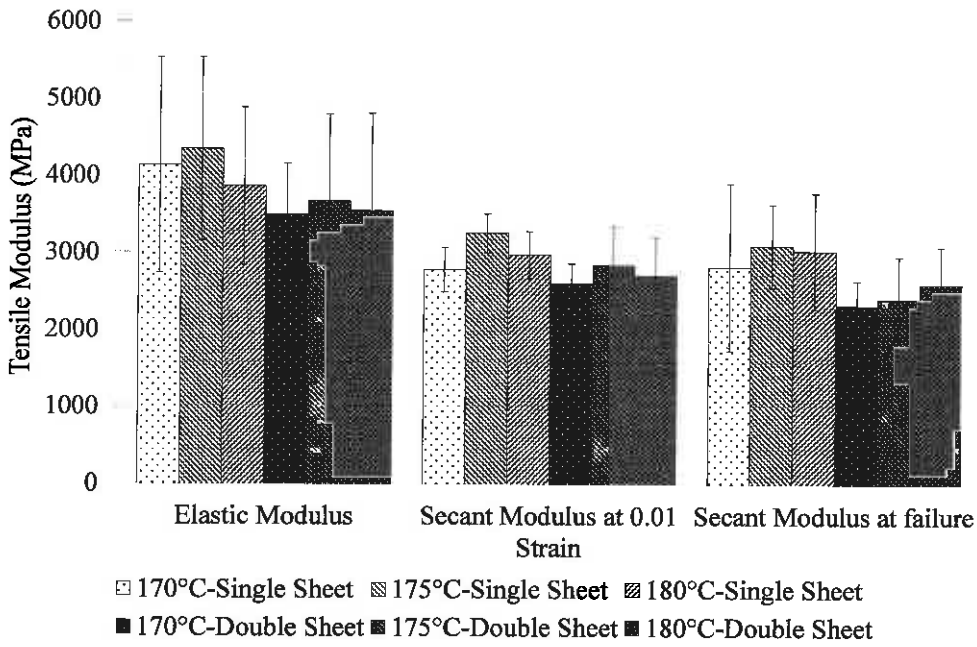

Figure 5.2: Tensile Modulus - The effect of temperature in a composite using APS treated fibres

composites consisting of a single sheet fibre mat are stronger than composites manufactured using a double sheet fibre mat. These composites are identical except for the thickness, as composites that use a double fibre sheet have a larger through-thickness compared to those made using a single fibre sheet. It is probable that the reduction in strength of the double fibre sheet composite is due to the composite thickness. Thin composites display plane stress characteristics i.e no stress through the thickness and have a higher fracture toughness than thicker materials [59]. It is possible that in the event of a brittle fracture, a thin composite which has a higher fracture toughness allows the composites to achieve a higher strength before failure compared to thicker specimens. Despite the marginal improvement in tensile strength for composites using a single fibre sheet compared to that using a double fibre sheet, composites were manufactured with two fibre sheets as thicker specimens satisfy the dimensional requirements for short beam shear testing. It is, of course, also possible that the reduction in strength of the thicker specimens could be the result of manufacturing defects, however. This will be investigated at a later stage through the use of SEM imagery.

It is hypothesised that the poor results obtained at a temperature of 170°C are a consequence of poor impregnation of the matrix into the fibres, and those obtained at 180°C are a result of thermal degradation of silane and/or the kenaf fibres within the composite.

This hypothesis can be investigated further through the use of SEM images. SEM images are useful in obtaining a greater understanding of the mode of failure as they can provide

visual evidence of brittle or ductile failure as well as the quality of fibre-matrix bonding. Figure 5.3 shows the fracture surface of a tensile specimen manufactured at 170°C. This fracture surface shows matrix drawing which is characteristic of a ductile failure [47]. This indicates that fracture toughness did not influence the failure of the composite. It is probable that the reduction in strength for the thicker specimens is a results of manufacturing defects or statistical variation in the data. The fracture surface also shows that there is fibre agglomeration and some fibre pull-out, which suggests poor matrix impregnation. Fibre pull-out is an indication of weak fibre-matrix adhesion [2]. As soon as the fibre-matrix bond fails, the fibres can slip relative to the matrix, resulting in fibre pull-out.

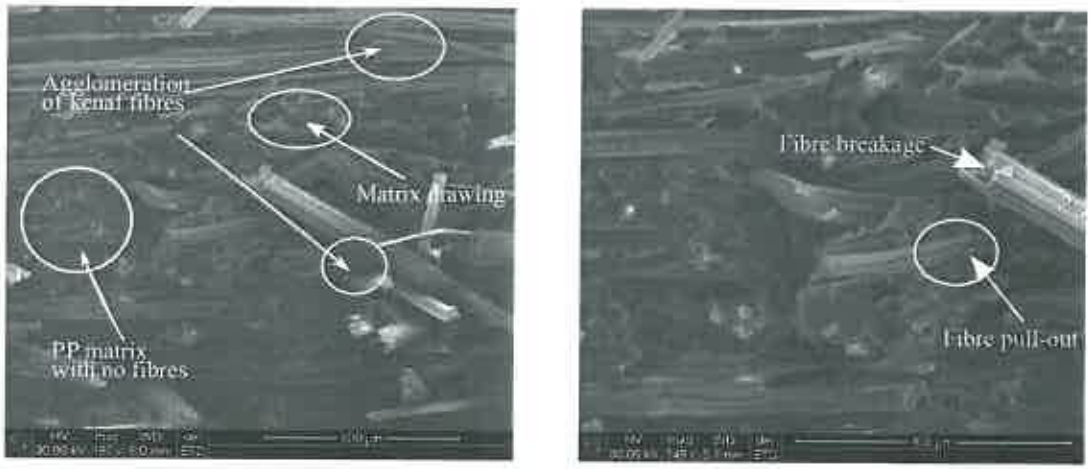

(a) Composite surface overview

(b) Middle section magnification

Figure 5.3: SEM images of composite manufactured at 170°C using APS silane

Ho et al. [60] reported that as temperature increases, the shear viscosity of a polymer decreases, making the flow into the fibres easier. Therefore, the impregnation of the matrix is a direct result of heating and applying pressure to the matrix to penetrate the fibres. Another benefit of manufacturing at high temperatures is the gasification of water molecules which are trapped inside the natural fibres. The water molecules begin to gasify and turn into air bubbles due to the heat supplied during compression moulding. The air bubbles move upwards in the liquid matrix as they are buoyant and then move laterally across the ram when pressure is applied, as it is easier for the bubbles to move laterally than for the liquid matrix to move in the fibre mat. Using higher temperatures in the moulding process makes the matrix less viscous, which in turn makes it easier for the bubbles to escape the matrix. If these bubbles do not exit by the end of the compression moulding cycle, they then exist as voids within the composite, decreasing the overall mechanical strength. The presence of voids in a composite is a manufacturing issue for natural fibres, and was evident in the laminates made by Paiken [52]. In essence, manufacturing at higher temperatures reduces the potential for voids resulting from moisture in the fibres.

Figure 5.1 shows that the composites manufactured at 180°C have inferior mechanical properties compared to those manufactured at 175°C. It is hypothesised that this decrease in tensile strength is possibly linked to the degradation of silane and/or the degradation of the kenaf fibres within the composite. It is possible that degradation of the silane will remove bonds associated with silane in the kenaf fibre. FTIR is thus useful in validating this hypothesis as it is capable of determining bond formation and bond removal, hence it was used to determine whether the kenaf fibres and the silane on the fibres underwent degradation during manufacturing.

Kenaf fibres were treated according to the procedure outlined by Paiken [52]. This treatment consisted of a 6 % sodium hydroxide treatment and 5 % aminopropylethoxy silane(APS). The fibres were heated to 170°C, 175°C and 180°C for one hour, and were labelled APS 170, APS 175 and APS 180, respectively. Untreated kenaf fibres were heated to 25°C and 175°C and were labelled kenaf 25 and kenaf 175, respectively. These results can be seen in Figure 5.4 and a zoomed in section of these results can be seen in Figure 5.5. The results of fibres treated at different temperatures are included so that they can be compared.

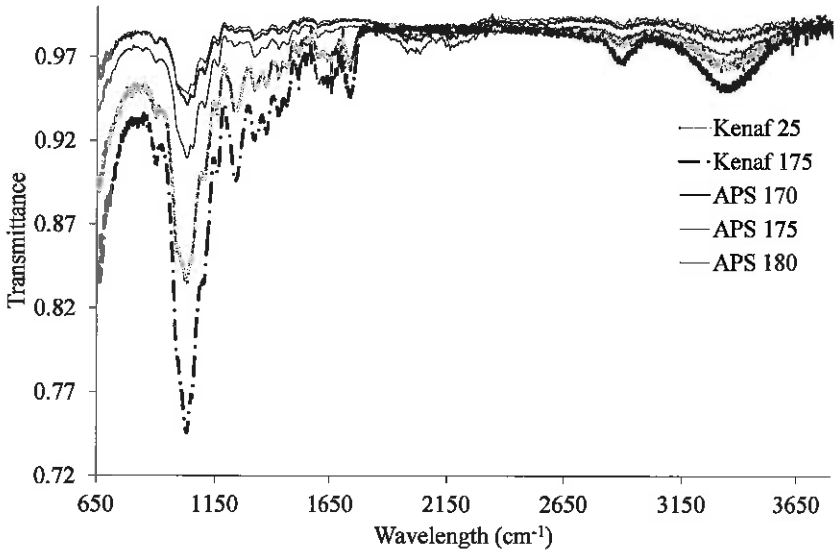

Figure 5.4: Full spectrum of FTIR results for APS treated fibres

Table 4.7 shows that the peaks associated with silane bonding are 1135 cm^{-1} and 1200 cm^{-1} [61, 62]. Figure 5.5 shows that there is no difference in the peaks of these curves, thus implying that the manufacturing temperature did not influence the chemical bonds in the fibres. At this stage, it is uncertain whether silane is present, but if it is present, it was not

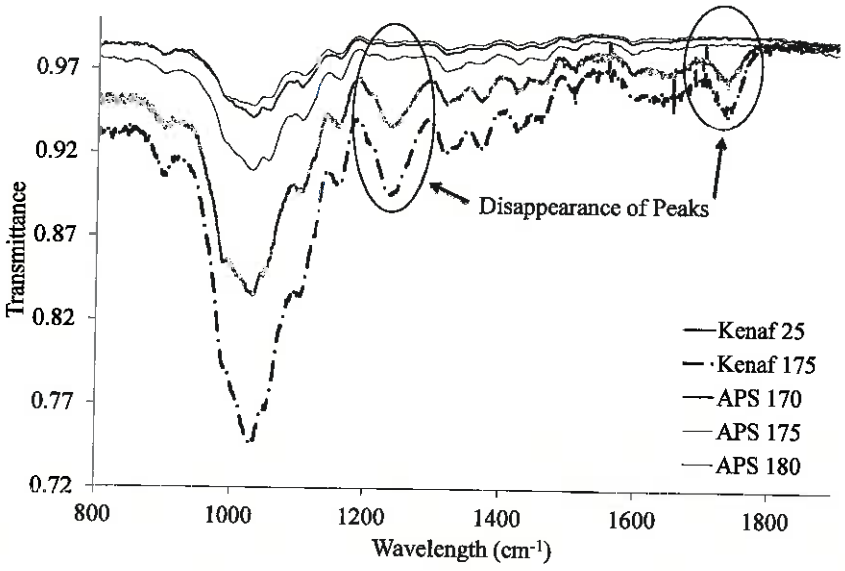

Figure 5.5: FTIR results for 800 cm^{-1} to 1900 cm^{-1} range for APS treated fibres

influenced by temperature. This is because no silane bonds were removed, implying no silane degradation. The effect of silane will be discussed later.

Another aspect to consider regarding the low strength values obtained at 180°C was the degradation of the kenaf fibres within the composite through the heat of manufacture. Ochi et al. [63] concluded that the tensile strength of kenaf fibres decreases when they are subjected to a manufacturing temperature of 180°C for one hour. They concluded that a moulding temperature of 160°C is optimum, whereas in Figure 5.1, it is seen that 175°C is the optimum moulding temperature. The optimum temperature found in this research is thus much higher than the optimum found by Ochi et al. [63], implying that there is possible kenaf fibre degradation. The FTIR results will once again be discussed to determine if the kenaf fibres degraded or not.

Figure 5.5 shows the FTIR results of untreated kenaf fibres left at room temperature and untreated kenaf fibres that were heated at 175°C for one hour. This figure shows no difference in peaks, implying that there is no degradation of the kenaf fibres. This allows the conclusion to be drawn that a moulding temperature of 175°C does not lead to thermal degradation of the kenaf fibres. However, this can be investigated further by considering the tensile modulus data.

The degradation of the fibres should affect the stiffness of the fibres, thereby influencing the modulus of the composites. The modulus data for the variation of composite manufacturing temperatures is presented in Figure 5.2. The elastic modulus would be a better indication of the stiffness of the kenaf fibre without load application, however, the data set has large standards of deviation making it difficult to comment on any trend. The secant modulus at 0.01 strain has smaller standards of deviation making it easier and more reliable for comparison. The secant modulus at 0.01 strain of the composite manufactured at 175°C is higher than the composite manufactured at 180°C. This implies that the kenaf fibres underwent thermal degradation at 180°C as the stiffness of the composite has decreased from that manufactured at 175°C, which agrees with the findings of Ochi et al. [63]. Although the FTIR does not agree with the tensile modulus data, it should be kept in mind that FTIR is a qualitative tool and not a quantitative tool. This implies that degradation will cause some bonds to be destroyed, but since the remainder of that particular bond is still present in the fibre, it will still show in the FTIR data and thereby show no difference in bond formation for the different manufacturing temperatures.

Further details regarding the effect of manufacturing at a temperature of 180°C can be seen in the SEM images. Figure 5.6 shows the surface of a sample manufactured at 180°C which indicates some fibre debonding. This is clearly seen in Figure 5.6b which shows a zoomed in section of the specimen manufactured at 180°C. The debonding seen is possibly a result of fibre degradation which destroys the kenaf fibre components that link to the silane bonding agent.

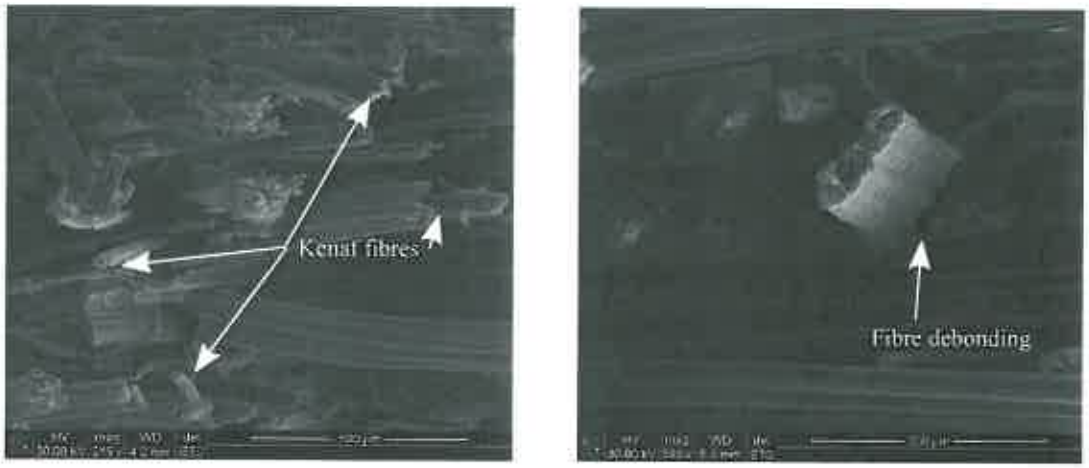

(a) Composite surface overview (b) Middle section magnification

Figure 5.6: SEM images of composite manufactured at 180°C using APS silane

Figure 5.7 shows the fracture surface of a tensile specimen manufactured at 175°C. The surface shows a lot of fibre breakage in the overall view of the surface. Figure 5.7b shows a zoomed in section of the composite manufactured at 175°C. This surface shows the matrix tightly holding onto the fibre, indicating good bonding.

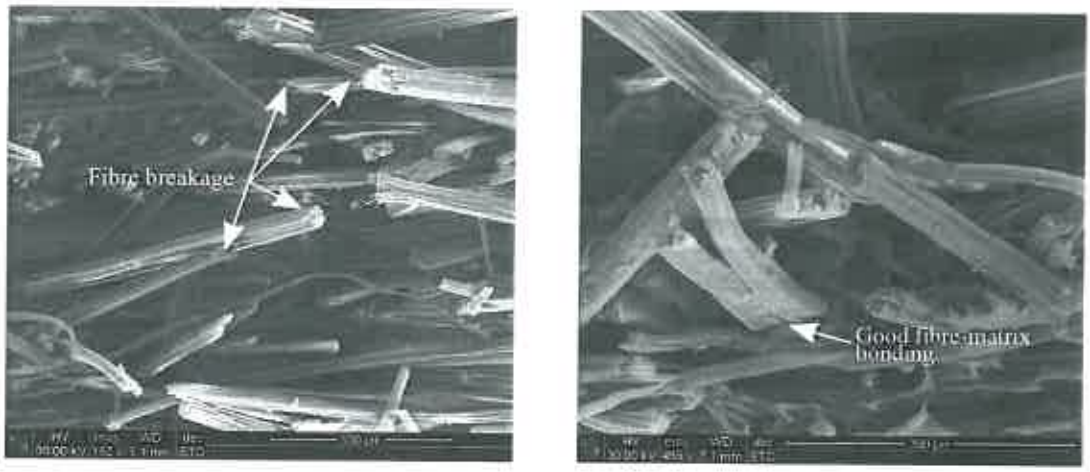

(a) Composite surface overview (b) Middle section magnification

Figure 5.7: SEM images of composite manufactured at 175°C using APS silane

Composites manufactured at 175°C and 180°C show better impregnation of polypropylene compared to those manufactured at 170°C, and this impregnation give the composites a good mechanical bond. However, despite a good mechanical bond, high temperatures cause degradation of the kenaf fibre according to Ochi et al. [63], resulting in a weaker composite.

In summary, manufacturing kenaf based composites in a polypropylene matrix is optimumally performed at 175°C. The failures present in the manufacturing of composites at 170°C are due to the poor impregnation of polypropylene, which results in a poor mechanical bond, whilst manufacturing composites at 180°C causes kenaf fibre degradation, reducing the strength of the composite. The process is a trade-off between better impregnation of the matrix and thermal degradation of the fibre. A manufacturing temperature of 175°C was thus used for all remaining investigations.

Repeatability of the experiments was concerning as the tensile strength data has large standards of deviation, hence this was investigated.

5.2 Repeatability and the Effect of Moisture on Mechanical Properties

Preliminary testing was conducted to determine the repeatability of the manufacturing process. This was tested by making two specimens of the same configuration and performing tensile testing. Each configuration comprised a particular chemical treatment. The first plate, manufactured using a particular fibre chemical treatment, was tested immediately whilst the

remaining plate was tested approximately one week later. The results showed that the tensile strength of composites tested a week after manufacture showed improvements in strength compared to those tested immediately after manufacture. The factor that was varied was time, which would imply conditioning of the composite. Identifying time as a variable indicated that moisture absorption was responsible for the improvement in strength, as natural fibres have a high affinity for water molecules. Consequently, these fibres absorb moisture from the atmosphere.

All of the composites that were tested some time after manufacture showed an improvement in tensile strength, whilst composites tested later did not have any obvious improvements in tensile modulus. The results of this investigation can be seen in Appendix G.

It is hypothesised that the additional moisture present in the fibres makes them more elastic [64], delaying the fracture of the composite, thereby allowing a higher tensile strength to be achieved. Espert et al. [64] found that water molecules act as a plasticizer agent in composite material which leads to an increase in the maximum strain of the composite after moisture absorption.

The moisture may have had an effect on the mechanical properties of composites, but ultimately there was repeatability, as all the composites of a particular configuration that was tested sometime later had a slight increase in strength compared to those tested immediately. There is a chance that the second composite of each configuration was stronger due to other factors associated with the day of manufacture. These variables were not known, therefore further evidence was required to determine the effect of moisture on mechanical strength of the composite.

This effect was investigated further by making two composite plates of the same configuration. The treatment developed by Asumani et al. [4] was used and this consisted of 6% sodium hydroxide and 5% APS. Thereafter, half of the first plate and half of the second plate was tensile tested immediately and the remaining specimens were tested a week later. Each plate was cut and shaped into six tensile specimens, yielding a total of twelve specimens for both plates. Three tensile specimens were taken from each plate and tested immediately after shaping them into tensile specimens. The remaining six specimens were tested a week later. The tensile results of this investigation can be seen in Figures 5.8 and 5.9.

Figure 5.8 shows that the tensile strength increased for every specimen and Figure 5.9 shows that the tensile modulus decreased, confirming the hypothesis. Since the amount of moisture absorbed from the atmosphere was a variable, all composites manufactured for subsequent investigations were cut into the respective testing specimens and left to age under atmospheric conditions for a duration of three weeks before testing.

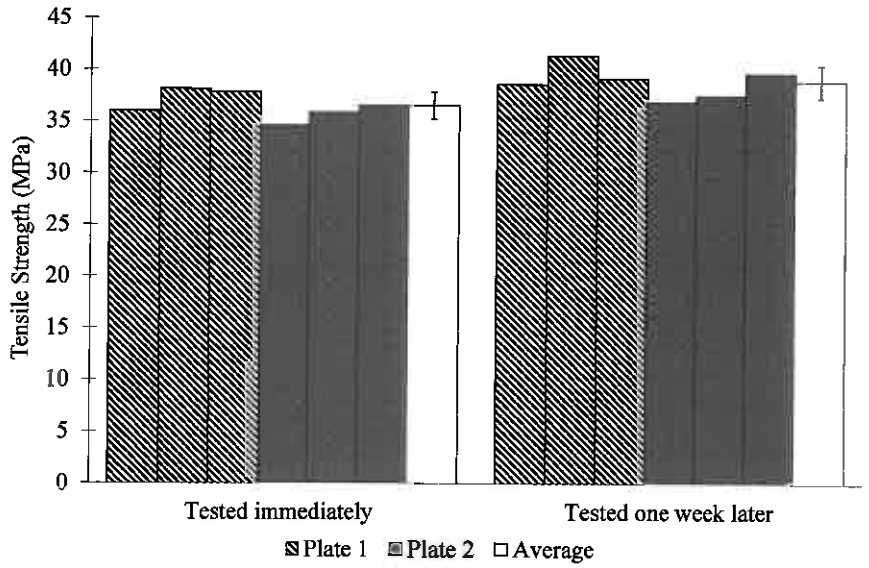

Figure 5.8: Tensile Strength - The effect of conditioning in a composite

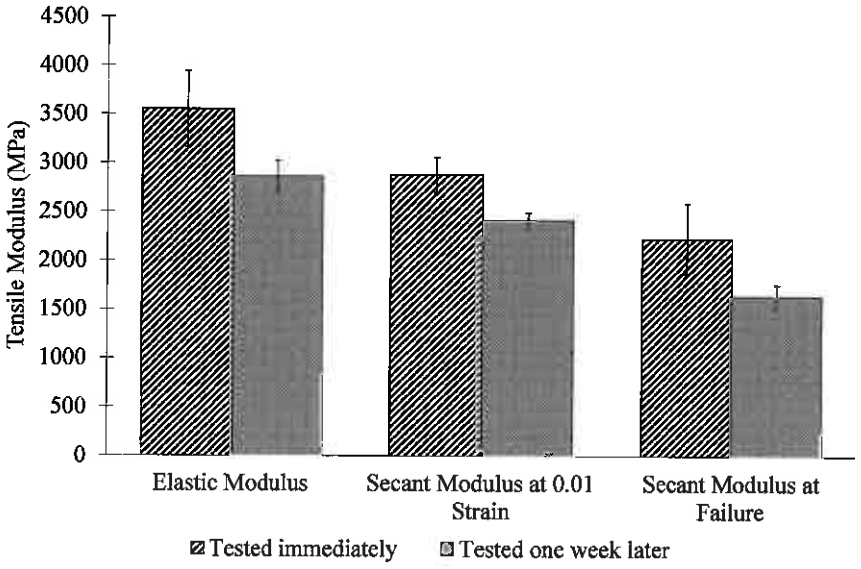

Figure 5.9: Tensile Modulus - The effect of conditioning in a composite

5.3 Investigating the Effect of different MPS treatments and the addition of MMT Clay

The improvement in mechanical properties of composites is primarily driven by the amount of silane used, as silane bonds the polymer matrix to the kenaf fibre reinforcement. In the previous investigation related to conditioning, 5% APS silane was used to treat the fibres. Cho et al. [29] found that as little as 1% APS silane was sufficient to improve the mechanical properties of natural fibre composites. They also found better improvements using 0.5% MPS, which was sufficient to improve the shear strength by as much as 50% compared to untreated kenaf fibres.

Based on the improvements found by Cho et al. [29], MPS was preferred over APS as less silane is required for mechanical improvement. Consequently, MPS became the focus of this project since it was cheaper to administer MPS silane treatments and cost effectiveness is an important aspect in this research project.

Four different MPS treatments were investigated to find the optimal MPS treatment. A full summary of the derivations of the MPS treatments can be found in section 4.1.2.2. Asumani et al. [4] found that silane treatments are most effective when combined with a sodium hydroxide treatment. Consequently this was done and a full breakdown of the treatments together with the corresponding abbreviations used in this report can be seen in Table 5.1. The fibre weight fraction was kept constant at 25%.

Table 5.1: Abbreviation for MPS chemical treatments

Treatments	Abbreviation
Untreated fibres	Unt
6% Sodium Hydroxide	NaOH
6% Sodium Hydroxide + M1	T1
6% Sodium Hydroxide + M2	T2
6% Sodium Hydroxide + M3	T3
6% Sodium Hydroxide + M4	T4

The following investigation was done with two types of matrices. The first matrix consisted of virgin polypropylene (no-clay) and the other was a modified matrix with clay. The modified matrix consisted of a clay content of 4% as this was considered to be the optimal clay concentration by Shariatpanahi et al. [13]. Composite plates were also made with untreated fibres and sodium hydroxide treated fibres using both types of matrices to compare against MPS treated fibres.

This section is divided into four sections highlighting: the effect of using kenaf fibre as reinforcement in a polypropylene matrix, the effect of a sodium hydroxide treatment, the effect of MPS chemical treatments and the addition of the clay in the kenaf based composite.

5.3.1 The Effect of kenaf fibre reinforcement

The effect of different chemical treatments on the mechanical properties of composites using two types of matrices; virgin polypropylene and 4% clay matrix, is presented in Figures 5.10, 5.11, 5.15, 5.18 and 5.19. Figure 5.10 shows the tensile strength results obtained for various chemical treatments on composites using the two types of matrices previously mentioned. This discussion will focus on the effects of using a virgin polypropylene matrix.

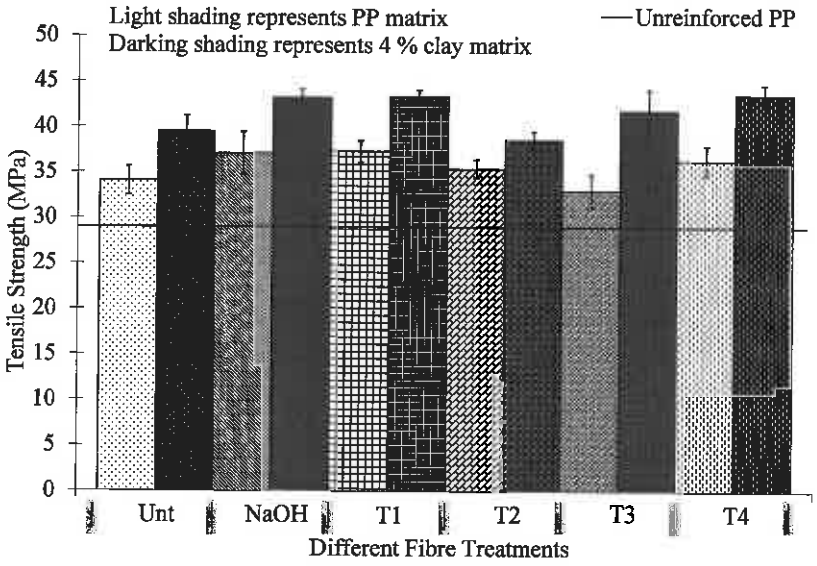

Figure 5.10: Tensile strength - The effect of different MPS treatments on kenaf fibres using virgin PP and PP with 4% clay.

Figure 5.10 shows that a composite consisting of untreated kenaf reinforcement displays an increase in tensile strength compared to composites consisting of an unreinforced pure polypropylene matrix, which is a result observed by other researchers [4, 5, 63] as well. Kenaf fibre is a stiffer and stronger material than the polypropylene matrix [5] and the fibres provide an alternate path for load to transfer, thus allowing the composite to withstand a larger load. If load is successfully transferred from the matrix to the fibres of the composite, the elastic modulus of the composite should be greater than that of unreinforced polypropylene, as the modulus of the kenaf fibre is greater than the unreinforced polypropylene matrix.

Consequently, it will be interesting to look at the modulus data to find evidence of this load transfer and confirm that the fibres are working within the composite. The tensile modulus data for the various fibre treatments done on the kenaf fibres can be seen in Figure 5.11.

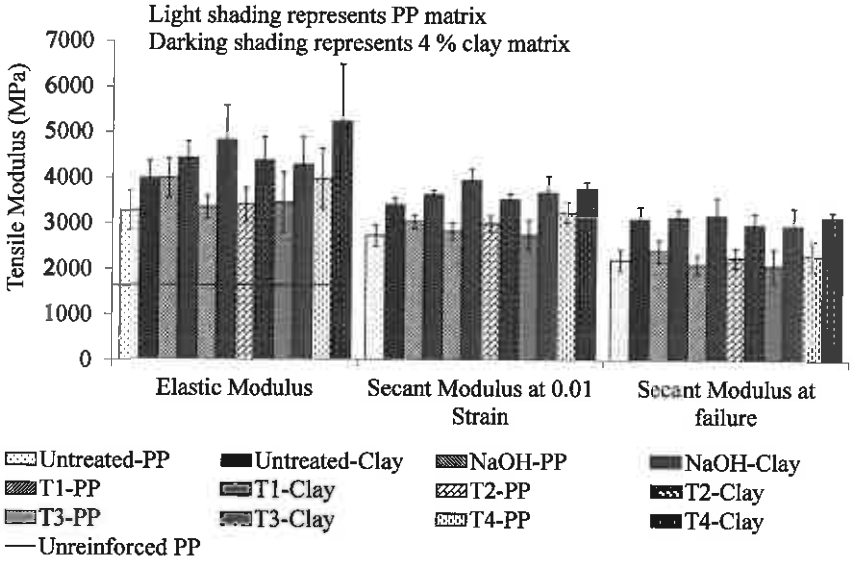

Figure 5.11: Tensile modulus - The effect of different MPS treatments on kenaf fibres using virgin PP and PP with 4% clay.

Figure 5.11 shows that the modulus of a composite consisting of untreated fibres in a polypropylene matrix is larger than that of an unreinforced pure polypropylene. This indicates that there is load transfer between the fibres and matrix, indicating bonding between the matrix and fibres.

5.3.2 The Effect of the Sodium Hydroxide Treatment

The discussion to follow focuses on the effects of using a pure polypropylene matrix in conjunction with fibres treated using sodium hydroxide.

Figure 5.10 shows that some chemical treatments administered to the kenaf fibres improved the strength of the composites whilst others led to a decrease in strength, when compared to untreated fibres. The alkali treatment represented by NaOH, shows the largest improvement of strength when compared to untreated fibres.

Mohanty et al. [11] obtained similar improvements with the use of alkali treated natural fibres, attributing this improvement to the removal of natural and artificial impurities. This results in rough topography and fibre fibrillation which is the breaking down of fibre bundles into small fibrils in turn increasing the effective contact surface area with the matrix polymer. This also increases the fibre aspect ratio, which offers better fibre-matrix adhesion. Farahani et al. [65] mentioned that alkali treatments improve the interfacial bonding by increasing sites for mechanical interlocking between matrix and fibre. SEM images will be helpful in finding evidence of these surface characteristics as the SEM provides a high resolution picture of the fracture surface which is capable of showing the quality of bonding between the matrix and fibres, amongst other effects. These images should provide evidence for some of the mechanical results. Figures 5.12 and 5.13 show the fracture surface of composites manufactured with untreated fibres and sodium hydroxide fibres, respectively, with both types of matrices.

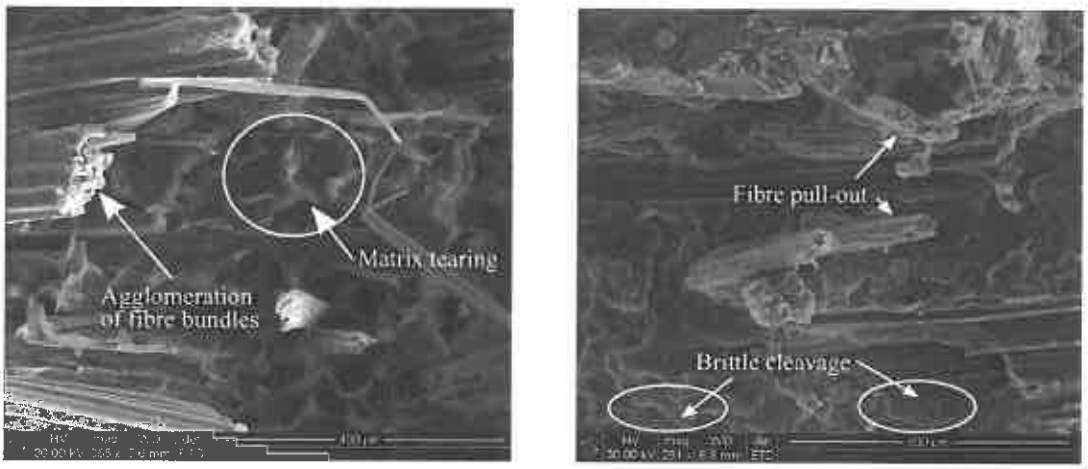

(a) Unt - PP Matrix

(b) Unt - Clay matrix

Figure 5.12: SEM images of tensile specimens using untreated fibres with polypropylene matrix and polypropylene/clay matrix

Figures 5.12a and 5.13a show the fracture surfaces of composites consisting of a virgin polypropylene matrix and untreated fibre reinforcement and the same composite with sodium hydroxide treated fibres, respectively. The surface of the composite with untreated fibre reinforcement displays matrix tearing and agglomerated fibre bundles, whilst the surface of the fibre consisting of sodium hydroxide treated fibres shows fibrillation of fibres. A zoomed in section of the composite using sodium hydroxide fibres can be seen in Figure 5.14.

This fracture surface shows matrix bonded to the fibres and highlights fibres that have a rough topology, similar to the findings by Mohanty et al. [11]. The rough topology of the surface of the kenaf fibre aids the fibres in creating a good mechanical bond with the matrix, thereby increasing the overall strength of the composite. The matrix bonded to the fibres indicate that there is a good bond between the matrix and fibres [4]. Kabir et al. [10] found

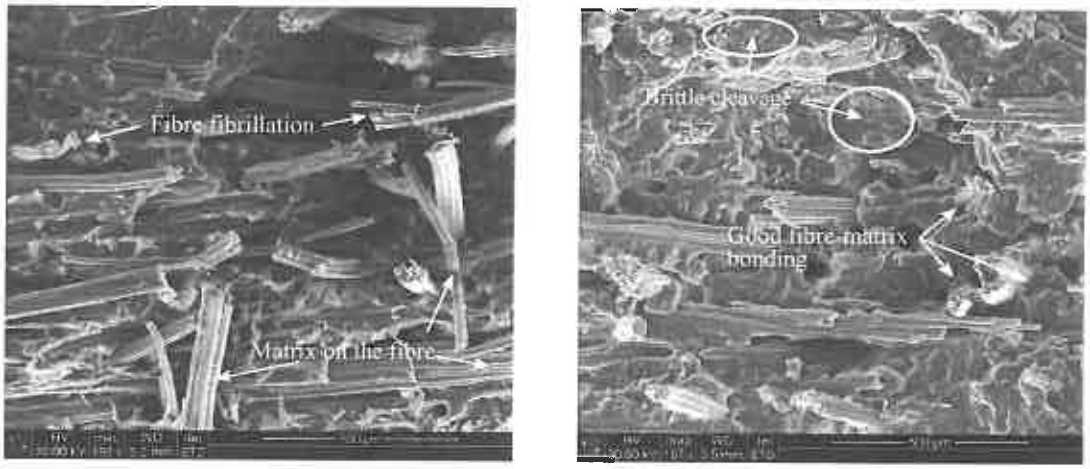

(a) NaOH - PP Matrix (b) NaOH - Clay matrix

Figure 5.13: SEM images of tensile specimens using NaOH treated fibres with polypropylene matrix and clay matrix

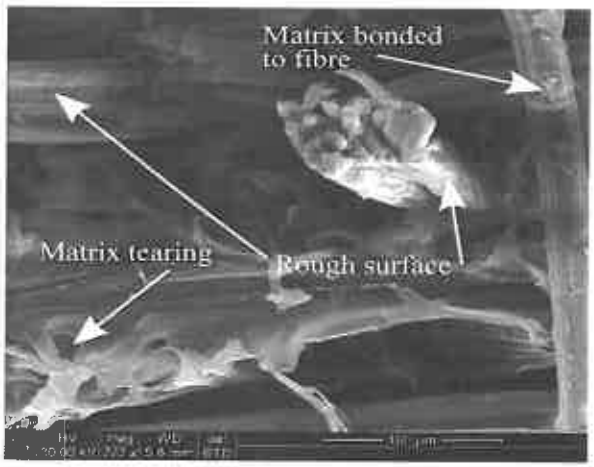

Figure 5.14: NaOH - PP Matrix - zoomed in section of tensile specimen

that an alkali treatment increases the strength and stiffness of the kenaf fibre. This increase in fibre stiffness should lead to an increase in the modulus of the composite which should be apparent in the modulus data.

Figure 5.11 shows that the tensile modulus of a composite consisting of sodium hydroxide treated fibres with a virgin polypropylene matrix is higher than that of the same composite manufactured using untreated fibres. This shows that a sodium hydroxide fibre treatment improves the stiffness of the composite, which is a result that has been observed by other researchers [4, 62, 65]. This treatment decreases the fibril angle in the kenaf fibre [24] which increases its tensile strength and modulus [1]. Therefore, a stiffer fibre will increase the modulus of the overall composite. Further details regarding the fibril angle and chemical properties of the kenaf fibre were discussed in subsection 2.4.1. As mentioned previously, the sodium hydroxide solution helps to create a rough topology on the surface of the fibre

[24, 66], which increases the mechanical bond strength between the fibres and the matrix. This improvement in interfacial strength allows for better load transfer between the matrix and fibres compared to untreated fibres. An increase in interfacial strength allows a larger load to be transferred to the fibres, thereby increasing the modulus of the composite. Asumani et al. [4] showed that a strong fibre-matrix bond can improve the tensile modulus of a composite. Consideration of the impact data obtained can provide a better indication of the bonding between the matrix and the fibres.

Impact strength is defined as the ability of a material to resist fracture under applied stress which is applied at a high speed [67]. Kalia et al. [67] mention that impact properties relate to the toughness of a material and that composite fracture toughness is affected by interlaminar and interfacial strength properties. During an impact test the impactor hits the specimen, which absorbs energy until the point of fracture. The impactor then uses additional energy to propagate the crack until the specimen is split into two pieces and the impacted piece is projected away. The total energy dissipated in a composite consists of two components; the energy required to deform the material and the energy required to create new surfaces. Essentially the impact test provides an indication of the bond quality between the fibres and the matrix, as a weak bond would cause the fibres to pull-out from the matrix and would require more energy for the specimen to break, compared to a specimen with a strong bond which has no fibre pull-out and which uses less energy to break the specimen [68]. A small initial energy would indicate a good bond between fibres and matrix or conversely the least fibre pull-out. Mueller et al. [69] states that weak adhesion between fibre and polymer results in high impact energy as a result of the fibre pull-out. Li et al. [70] also observed that good interfacial bonding results in low impact energy and that good adhesion results in abrupt fibre fracture with low impact energy. Wambua et al. [9] mentioned that debonding and fibre pull-out results in an increase in the amount of impact energy compared to a composite that does not show these characteristics. Figure 5.15 shows the impact energy data obtained for different chemical treatments carried out on kenaf fibres in composites using two types of matrices, as previously mentioned.

By considering the composites consisting of a virgin polypropylene matrix, it is seen that composites made using sodium hydroxide treated fibres have a lower impact energy than composites manufactured using untreated fibres. This implies that fibres treated with a sodium hydroxide solution have a better bond to the virgin polypropylene matrix than untreated fibres. This improvement in mechanical properties is also seen in the tensile strength results in Figure 5.10 which were discussed earlier. It will be useful to view the fracture surfaces of the impact specimens to determine the quality of bond between the fibres and matrix. Figure 5.16 shows the fracture surface of an impact specimen consisting of untreated fibres with both types of matrices.

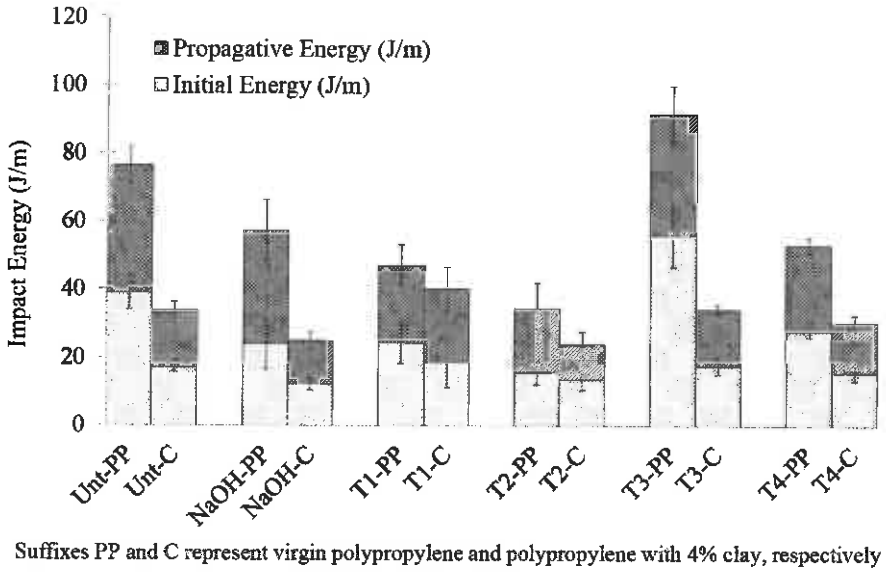

Figure 5.15: Impact energy - The effect of different MPS treatments on kenaf fibres using virgin PP and PP with 4% clay

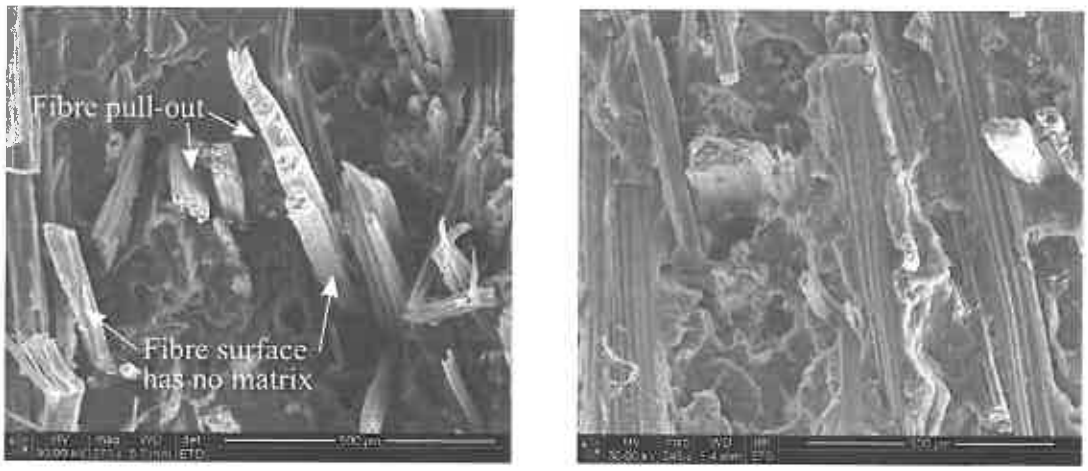

(a) Unt - PP Matrix (b) Unt - Clay Matrix

Figure 5.16: SEM images of impact specimens using untreated fibres with polypropylene matrix and clay matrix

Figure 5.16a shows the fracture surface of an impact specimen consisting of untreated fibres and a polypropylene matrix. An uneven surface fracture can be seen as well as fibres pulled from the surface of the composite. Fibre pull-out corresponds to a large energy dissipation [69] which can be seen in the impact results. The fibres are also clean of any matrix debris indicating a lack of adhesion between the fibres and the matrix. These surface characteristics

are associated with a large impact energy and are supported by the impact data seen in Figure 5.15. The impact data show that a composite consisting of untreated fibres has the second highest impact energy, with only a composite consisting of T3 fibres having a higher impact energy. Figure 5.17 show the fracture surfaces of impact specimens consisting of sodium hydroxide treated fibres and both types of matrices.

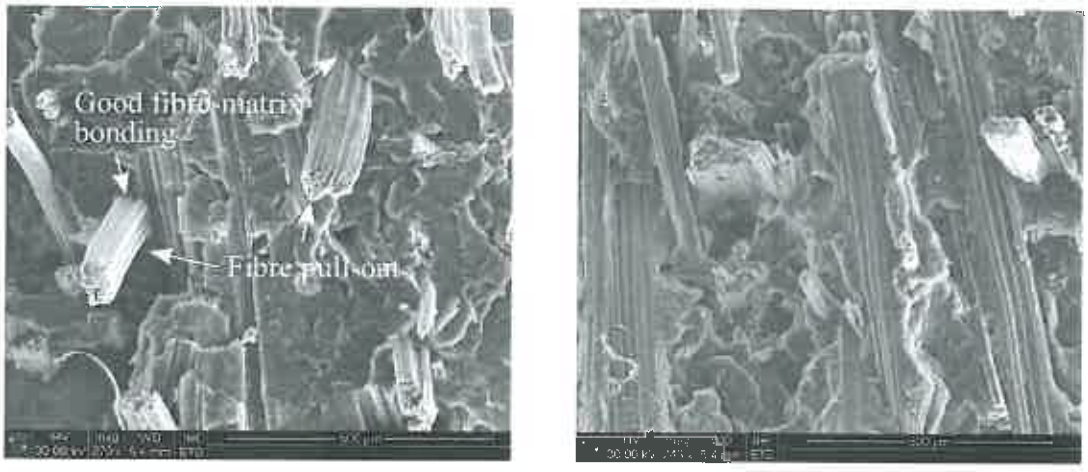

(a) NaOH - PP Matrix

(b) NaOH - Clay Matrix

Figure 5.17: SEM images of impact specimens using Sodium Hydroxide treated fibres with polypropylene matrix and clay matrix

Figure 5.17a shows the fracture surface of an impact specimen with a virgin polypropylene matrix reinforced with sodium hydroxide treated fibres. This figure shows better bonding of the matrix to the fibre and much less fibre pull-out compared to the same composite manufactured using untreated fibres, seen in Figure 5.16a. The composite with NaOH fibres shows evidence of improved bonding which supports the impact and tensile strength data as it shows less impact energy and more tensile strength than that of a composite using untreated fibres.

A composite consisting of untreated fibres and a virgin polypropylene matrix resulted in one of the highest impact energy, due to the poor interfacial strength between the matrix and the fibres, resulting in fibre pull-out. The relationship between poor bonding in the composite and high impact energy is consistent with the findings of Mueller et al. [69]. It will be useful to consider the shear data to obtain further insight into the interfacial bonding between the matrix and the fibres. The through-thickness shear strengths of composites made using different chemical treatments are presented in Figure 5.18.

Shear tests measure the apparent interlaminar shear strength of a composite, providing information regarding the quality of the adhesion at the fibre-matrix interface [71]. Twelve samples were used in calculating the mean of the shear results, however there is a large standard of deviation in the collected data. As seen in much of the previous results, all

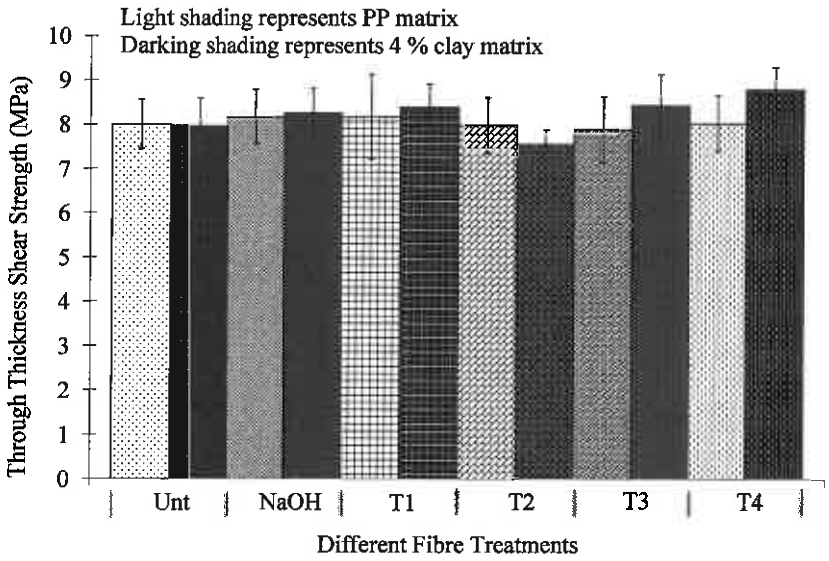

Figure 5.18: Through-thickness shear strength - The effect of different MPS treatments on kenaf fibres using virgin PP and PP with 4% clay

mechanical results show a general scatter in the data which is often associated with natural fibres. Considering the data obtained for composites manufactured using a virgin polypropylene matrix, no obvious improvements are noted in the through-thickness shear strength data for composites made using NaOH fibres, compared to untreated fibres.

Figure 5.19 shows the apparent shear modulus data and this data show a large variation in results compared to the shear strength data. Looking at the data of the composites made with a PP matrix, the data highlight that a composite made using sodium hydroxide fibres has a larger apparent shear modulus compared to the same composite made using untreated fibres. This agrees with the tensile modulus data seen earlier. This shear modulus data highlight that sodium hydroxide improves the modulus of the kenaf fibre. It will be interesting to consider the fracture surfaces of the shear specimens. Figure 5.20 show the shear specimens using untreated fibres with polypropylene matrix and clay matrix and Figure 5.21 shows the fracture surface of a shear specimen using sodium hydroxide treated fibres with a virgin polypropylene matrix.

Figures 5.20a and 5.21 show the fracture surfaces of the shear specimens consisting of a virgin polypropylene matrix with untreated fibre reinforcement and sodium hydroxide fibre reinforcement, respectively. Both fracture surfaces show fibre devoid of matrix material [72]

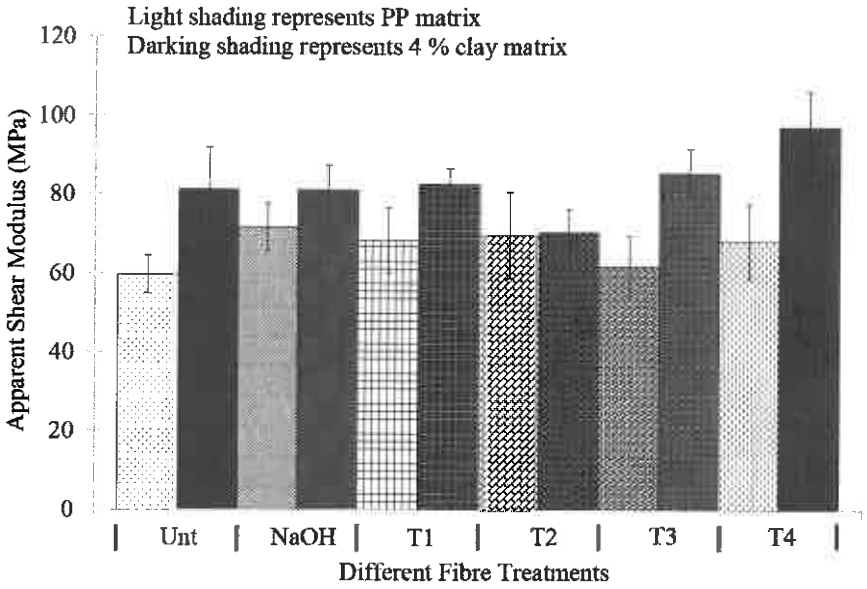

Figure 5.19: Approximate shear modulus - The effect of different MPS treatments on kenaf fibres using virgin PP and PP with 4% clay

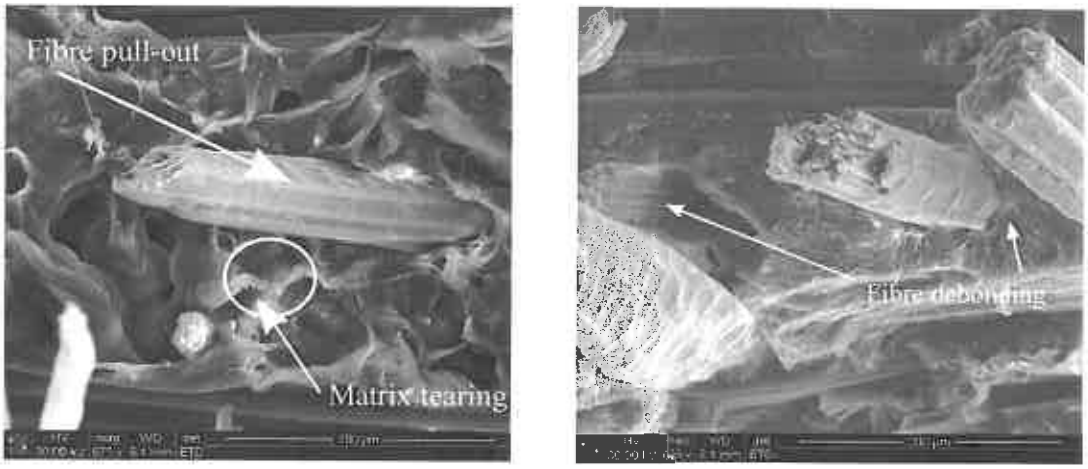

(a) Unt - PP Matrix

(b) Unt - Clay Matrix

Figure 5.20: SEM images of shear specimens using untreated fibres with polypropylene matrix and clay matrix

which is indicative of fibre-matrix interfacial failure. This is followed by extensive fibre pull-out. There is considerable matrix tearing in both fracture surfaces, however, the composite consisting of the sodium hydroxide treated fibres shows some fibre fibrillation. The sodium hydroxide fibre treatment causes fibrillation of the kenaf fibres, which according to Olayo et al. [73], results in a better fibre-matrix bond. An improvement in fibre-matrix bonding should

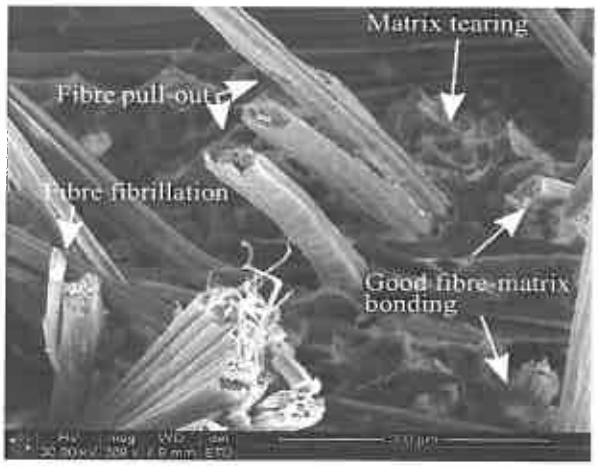

Figure 5.21: SEM images of shear specimens using NaOH treated fibres with virgin polypropylene matrix

have improved the shear strength of the composite using sodium hydroxide fibres compared to that using untreated fibres but this is not the case. The shear modulus data support the hypothesis that the modulus has improved in the fibres due to the sodium hydroxide treatment.

5.3.3 The Effect of different MPS Treatments

The following section focuses on the effect of different MPS treatments in composites consisting of a virgin polypropylene matrix.

Figure 5.10 shows that composites made using fibres subjected to treatments T1 and T4 have a similar tensile strength compared to those using sodium hydroxide treated fibres, whilst composites made using treatments T2 and T3 have a lower tensile strength. The MPS treatments are all a combination of a sodium hydroxide treatment used to clean the fibres and a MPS silane treatment used to bond the fibre to the matrix. Since treatments T1 and T4 have a similar strength to sodium hydroxide treated fibres, it could be argued that the MPS treatment had no effect on the tensile strength. However, based on the tensile results of the composites manufactured using treatments T2 and T3 fibres, it is seen that these MPS treatments had a negative effect on the tensile strength. This indicates that MPS is present on the kenaf fibre, and does influence the tensile strength of the composite. This is interesting as it implies that the addition of MPS silane does not improve the strength properties of the composite, contrary to the literature by Xie et al. [27]. The reasons for this discrepancy will be explored in greater detail in the next section.

Although there is no improvement in tensile strength of the composites manufactured using treatments T1 and T4, it will be interesting to look at the fracture surface of the tensile specimens to investigate the quality of the interfacial bonding due to the addition of silane. Figure 5.22 show the fracture surfaces of tensile specimens consisting of a virgin polypropylene matrix and clay matrix with treatment T4 fibres.

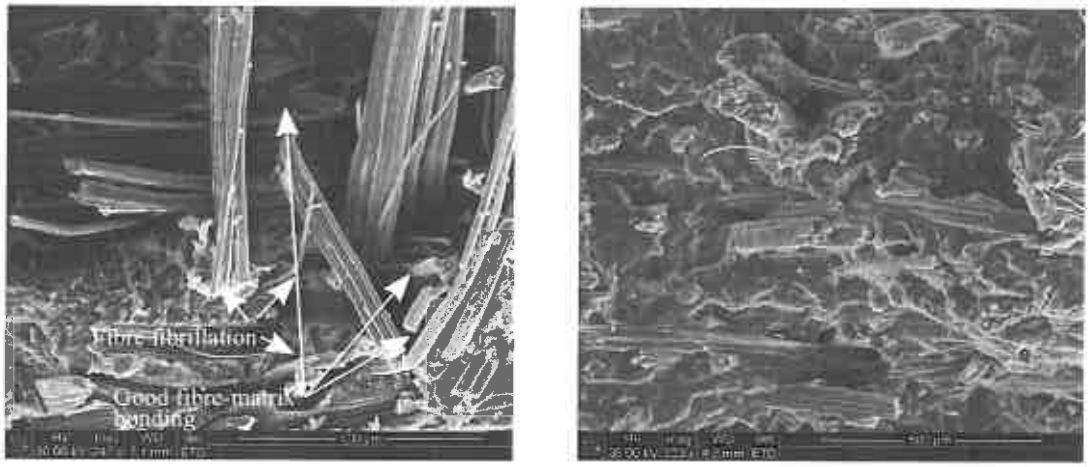

(a) T4 - PP Matrix (b) T4 - Clay Matrix

Figure 5.22: SEM images of tensile specimens using Treatment 4 treated fibres with virgin polypropylene matrix and clay matrix

The fracture surface shown in Figure 5.22a shows similar characteristics to that of a composite using the same matrix and sodium hydroxide treated fibres, seen in Figure 5.13a. Both fracture surfaces show similar characteristics which include fibre fibrillation and good bonding between the matrix and fibre. Both composites also show similar tensile strength values in Figure 5.10. No obvious surface characteristics can be seen for the silane treated fibres due to the silane working on a microscopic level to improve the bonding of the fibre to the matrix. Further consideration of the tensile modulus will provide a greater insight as to whether silane has improved the bonding between the matrix and fibres.

The tensile modulus data seen in Figure 5.11 shows that there is an improvement in modulus using sodium hydroxide treated fibres compared to untreated fibres, however, MPS treatments had no significant effect on the elastic modulus beyond this. These results resemble the data obtained by Herrera-Franco et al. [62] which also show no improvement in modulus for various silane treatments. However, they did not explain the reason for this trend.

The amount of MPS added to the fibre was very small and exists entirely in the interface between the matrix and the fibre. This interface has effectively no cross-sectional area and cannot affect the modulus of the composite. It can, however, influence the strength as indicated in Figure 5.10, where the tensile strength decreased for composites manufactured

with fibres treated with treatments T2 and T3, when compared to composites consisting of sodium hydroxide treated fibres.

To understand the influence of MPS in a composite, it will be interesting to look at the fracture surface of a tensile specimen using treatment T2 fibres. This can be seen in Figure 5.23.

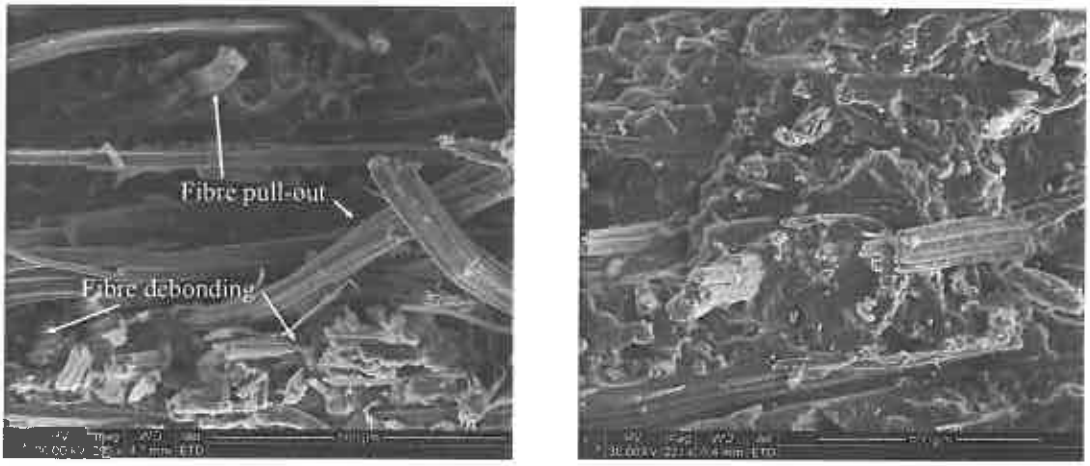

(a) T2 fibres - PP Matrix (b) T2 - Clay Matrix

Figure 5.23: SEM images of tensile specimens using Treatment 2 treated fibres with polypropylene matrix and clay matrix

Considering the fracture surface of the specimen using T2 fibres and a virgin polypropylene matrix, this fracture surface shows considerable fibre breakage, matrix tearing and fibre pull-out. A large amount of fibre pull-out is usually associated with low tensile properties and this supports the tensile strength data, which indicates poor mechanical properties.

Figure 5.15 shows the effect of different MPS treatments on the impact energy for two types of matrices. Focusing on the virgin polypropylene matrix, it is seen that composites manufactured using treatments T1, T2 and T4 display lower impact energy values compared to composites consisting of sodium hydroxide treated fibres, whilst the composite consisting of T3 fibres display a higher impact energy value. A high impact energy indicates that the bond between the fibres and matrix is poor and consequently has a considerable amount of fibre pull-out. This correlates well with the tensile strength data, as the composite consisting of T3 fibres has the lowest tensile strength. It is evident that T3 fibres are not worth further consideration in this investigation as they do not display good tensile strength properties or have a low impact energy.

The most interesting result is the low impact energy associated with the composite consisting of T2 fibres. This composite has the lowest impact energy which corresponds to a good fibre-matrix bond. This data does not correspond well to the poor tensile properties of this specimen seen earlier. The fracture surface of the impact specimen provides more detail

regarding the fibre-matrix bonding. Figure 5.24 shows the fracture impact surfaces of a specimen comprising of T2 fibres in a virgin polypropylene matrix and a clay matrix.

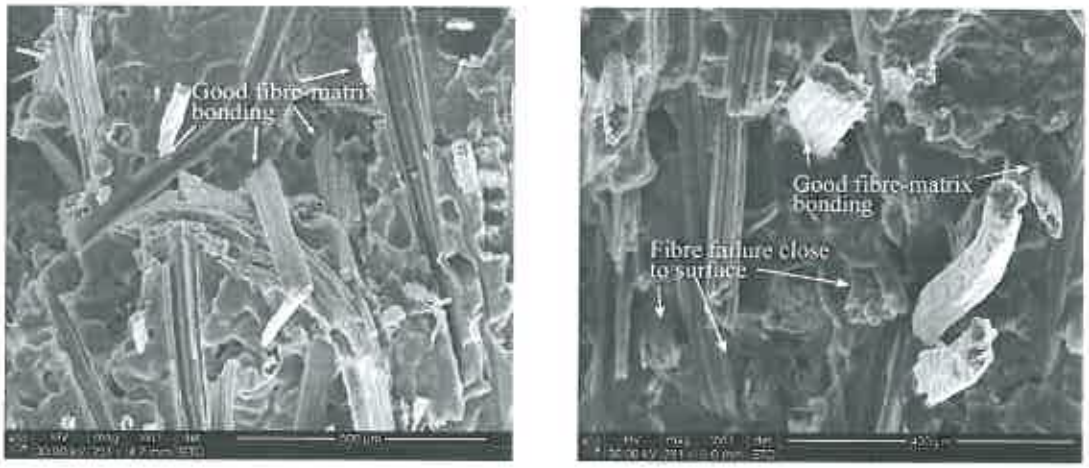

(a) T2 - PP Matrix (b) T2 - Clay Matrix

Figure 5.24: SEM images of impact specimens using Treatment 2 treated fibres with polypropylene matrix and clay matrix

The fracture surface of the impact specimen consisting of virgin polypropylene and T2 fibres is flat, resembling a brittle-like fracture and the surface shows good fibre-matrix bonding, which corresponds to the low impact energy of the composite. This consequently requires further investigation. Figure 5.25 shows images of impact specimens using Treatment 4 treated fibres with a polypropylene matrix and a clay matrix.

(a) T4 - PP Matrix (b) T4 - Clay Matrix

Figure 5.25: SEM images of impact specimens using Treatment 4 treated fibres with polypropylene matrix and clay matrix

Figure 5.25a shows the fracture surface of a specimen using T4 fibres with a virgin polypropylene matrix. The fracture surface shows an uneven surface fracture with fibres pulled from the surface and fibre holes. The fibre holes are evidence of fibre pull-out and not voids, which

is evidence of poor interfacial bonds. The uneven surface and the fibre pull-out corresponds well with the higher energy impact compared to the specimen using T2 fibres.

The effect of MPS treatments on the through-thickness shear strength of composites using kenaf fibres and a virgin polypropylene matrix is presented in Figure 5.18. The shear strength is approximately the same for all MPS treatments implying that the MPS treatments had no significant effect on shear strength, which is similar to the result obtained from the tensile strength data.

Figure 5.19 shows the apparent shear modulus data for different MPS treatments carried out on the kenaf fibres. Taking into consideration the scatter in the results presented, it is seen that the MPS treatments had no improvement in apparent shear modulus compared to the composites consisting of sodium hydroxide treated fibres. This result is the same as the tensile modulus data, emphasizing the fact that MPS treatments do not affect the modulus of the composites. The significant improvement is due to the NaOH treatment, as previously discussed.

Earlier it was seen that a composite consisting of T2 fibres provided interesting mechanical properties, thus it will be discussed in greater detail. The composite using T2 fibres displayed the lowest impact energy, implying good interfacial bonding between the matrix and fibres. A composite with good bonding between the matrix and fibres would imply good load transfer from the matrix to the fibre reinforcement and consequently should result in a large tensile strength and modulus, however, this was not the result obtained. The tensile strength data in Figure 5.10 shows that such a composite has a lower tensile strength than a composite using sodium hydroxide treated fibres. The fracture surface of the tensile specimen using T2 fibres, which can be seen in Figure 5.23a, shows that the surface has many snapped fibres as well as fibre pull-out. This fracture surface has characteristics of poor bonding and thus supports the tensile data.

The hypothesis is that the bond between the fibres and matrix is very strong which causes the composite to fail prematurely during tensile testing. Chawla [74] mentions that in an extreme case, when the interfacial strength is stronger than the reinforcement and the matrix, the interface has the lowest strain to failure, implying that the interface fails before the matrix and fibre do. The composite fails when any cracking occurs at a weak area along the brittle interface [74]. As a result, the interface between the matrix and fibres fails earlier during tensile testing than the other composites made using different fibre treatments. This causes the interfacial strength of the composite to be absent during the later part of the tensile testing. As soon as the interface fails, no load is transferred from the matrix to the fibres, which causes ultimate failure. The interfacial failure also results in the fibre pull-out seen in the fracture surface of the tensile specimen.

Although the composite using T2 fibres has a good bond between the matrix and fibres, it results in a tensile strength lower than a composite comprising of sodium hydroxide treated fibres. This particular treatment makes use of a large quantity of MPS, making it a very expensive treatment. The strength vs cost benefit is low and thus the treatment will not be investigated further.

In essence, a sodium hydroxide treatment is the most effective treatment with regards to improving the tensile strength and modulus as well as decreasing the impact energy of the composite as well as improving the shear modulus of the composite. This implies good bonding between the matrix and fibres. The MPS treatments however, did not improve the tensile strength of the composites when compared the sodium hydroxide treatments. In some instances, it was found that the MPS treatments decreased the mechanical properties of the composites. This implies that MPS does have some influence on the mechanical properties of the composite, however this influence is not of a positive nature. This will be discussed in greater depth in the next objective.

5.3.4 The Effect of the Clay on the different MPS treatments

The tensile strength and tensile modulus of composites using a 4% clay matrix can be seen in Figures 5.10 and 5.11, respectively. Figure 5.10 shows that the use of a clay matrix improves the strength of the composite when compared to composites using a virgin polypropylene matrix. The magnitude of the increase in strength is more or less the same for all the treatments, except for treatments T2 and T3. The strength improvement of T2 fibres is the smallest, whilst improvements for the composites consisting of T3 fibres show the greatest improvement in tensile strength. To gather further insight into the effect of the addition of clay on the polypropylene matrix, it is worthwhile to compare the fracture surfaces of tensile specimens of a particular fibre treatment for both types of matrices.

The fracture surfaces of composites consisting of untreated fibres with a virgin polypropylene matrix and clay matrix is presented in Figure 5.12. The composite consisting of a clay matrix displays a more even surface fracture compared to that using a virgin polypropylene matrix. This indicates that the introduction of clay into a polypropylene matrix causes a more brittle failure and this result has been noted by other authors [75, 76]. Fibre pull-out can also be seen in both fracture surfaces, indicating poor bonding between the fibres and both types of matrices. This implies that the use of a clay matrix does not improve the interfacial bonding between the matrix and the untreated fibre. Poor bonding leads to a low tensile strength for composites using untreated fibres, compared to all the other treatments, evidence for which can be seen in Figure 5.10.

To understand the effect of clay in a composite using sodium hydroxide treated fibres, the fracture surfaces of composites using sodium hydroxide fibres with both types of matrices are considered in Figure 5.13. The clay matrix shows a brittle failure surface which is similar to the results obtained for the composite consisting of untreated fibres and a clay matrix. The composite consisting of sodium hydroxide fibres and a virgin polypropylene matrix has a considerable amount of fibre pull-out and matrix tearing, compared to the composite consisting of a clay matrix. This is different to the composites manufactured using untreated fibres, which showed poor bonding for both types of matrices. Sodium hydroxide treated fibres show less fibre pull-out with a clay matrix than with a virgin polypropylene matrix. This is a result of better bonding between the fibres and matrix. The fracture surfaces support the tensile strength data, seen in Figure 5.10.

In general, fracture behaviour changes from being rather ductile with fibre deformation to exhibiting a featureless brittle cleavage when the matrix is changed from a virgin polypropylene matrix to a clay matrix. This is similar to the findings presented by Dong et al. [75]. The modulus data will provide further detail regarding the effects of the addition of clay in the polypropylene matrix.

Figure 5.11 shows the tensile modulus obtained for different chemical treatments carried out on the kenaf fibre reinforcement using the two types of matrices i.e virgin polypropylene matrix and the 4% clay polypropylene matrix. Although the tensile elastic modulus data is erratic with a large standard of deviation, there is an obvious improvement in modulus for clay based composites compared to those with a virgin polypropylene matrix. The data imply that clay improves the modulus of the matrix, a result seen by Hasegawa et al. [77]. This improves the stiffness of the overall composite. The improvement in stiffness is due the clay platelets restricting the motion of the polymer chains [37]. A comparison of tensile modulus values for the composites consisting of a clay matrix show that a composite using T4 fibres has the largest modulus. However, by taking the error bars into consideration, the different MPS treatments have no significant effect on the tensile modulus for composites using a clay matrix. This result is similar to the discussion earlier regarding the tensile results for composites using a virgin polypropylene matrix.

It is clear that clay improves the tensile strength and modulus for all composites regardless of the fibre treatment when compared to composites consisting of a virgin polypropylene matrix. Chen et al. [37] also presented similar improvements for clay based composites without fibre reinforcement. This result is attributed to the fact that clay has a high aspect ratio and therefore acts as further reinforcement to the polypropylene matrix. The clay platelets restrict the motion of the polymer chains, which results in a stiffer matrix [37], in addition to the rule of mixtures benefit from the clay. The mechanism that leads to the improved strength and modulus is the reduction of polymer chain mobility. Chen et al. [37] mentions

that debonding at the polymer-clay interface at the point of fracture appears to promote closure forces around the wake of a crack, which produces the crack growth resistance. This mechanism essentially delays fracture within the composite and the resistance created makes the composite stiffer, increasing its modulus. The rule of mixtures benefit is that the load applied to the composite follows the stiffest path in the composite, which in this case is the path consisting of clay, resulting in an increase in both the tensile strength and modulus.

To obtain a better understanding of the bonding between the clay matrix and kenaf fibre reinforcement, it is useful to look at the impact data seen in Figure 5.15. The composites made using a clay matrix show a decrease in impact energy compared to the same composites made with a virgin polypropylene matrix. This is interesting as other authors [78, 79, 80] show that impact energy increases with the introduction of clay in polypropylene without fibre reinforcement. The difference between their research and this investigation, is that this investigation uses kenaf fibre reinforcement. The fibres should, however, increase the impact energy as seen in the previous investigation using virgin polypropylene matrix. This could imply that the clay was not mixed well into the polypropylene, resulting in a tactoid, as seen in subsection 2.5.1. If this is true, the tactoid would act as a stress concentration which would result in poor mechanical properties of the composite. However, the clay and polypropylene used in this investigation were mixed using the very same equipment and procedure as Ray et al. [81]. These authors noted that they achieved intercalation. They mixed the matrix in two batches and compression moulded the mixture. Their X-ray diffraction results showed that the clay was intercalated, so there seems to be no reason why the clay/polypropylene mixture used in this investigation should not be properly intercalated.

The hypothesis to explain the low impact energy of the composites with a clay matrix is that the clay introduced into a PP matrix with kenaf fibres causes a transition from a ductile failure mode to a brittle failure mode. When the impactor hits the specimen, a crack starts in the matrix and propagates rapidly until it reaches a fibre. There is little deformation in the clay matrix around the fibre as the clay platelets restrict the motion of the polymer chains [37]. The high stress concentration at the tip of the crack dramatically increases the load applied to the fibre, thereby snapping it and creating a cutting effect. In the composites using a pure polypropylene matrix, the matrix can plastically deform around the fibre and allows fibre debonding and fibre pull-out which uses alot of energy. This hypothesis will be made more clear through the use of SEM images of the fracture surfaces of the impact specimens. Figure 5.26 shows the fracture surfaces of a composite using T1 fibres with a virgin polypropylene matrix and clay matrix.

The overview of the fracture surfaces show a large amount of fibre pull-out in the composite using a polypropylene matrix and the brittle fracture in the composite using a clay matrix. The composite using a clay matrix shows a flat surface indicating that the fibres and matrix

(a) T1 - PP Matrix

(b) T1 - Clay Matrix

Figure 5.26: Overview of impact specimens using T1 fibres with virgin polypropylene matrix and clay matrix

failed simultaneously in an even break. This supports the hypothesis that clay makes the composite brittle and reduces the impact energy for a composite when it is used in conjunction with polypropylene and kenaf fibres. The brittle fracture is also indicative of a lower fracture toughness for the composites using a clay matrix which is seen in terms of the impact results and SEM images. This is possibly due to the clay platelets in the matrix reducing the polymer chain mobility [37].

Considering the effects of the fibre treatments and looking at the standard of deviation associated with each of the results shown in Figure 5.15, it could be argued that the impact energy is the same for all treatments using a clay matrix, except for composites using T2 and T1 fibres, which exhibit the lowest and highest impact energy values respectively.

Composites manufactured using T2 and T3 fibres are proof that it is possible for MPS to influence the mechanical properties of a clay based composite. The composite using T2 fibres and a clay matrix has the lowest impact energy, similar to the composite made with a virgin polypropylene matrix. This is interesting as this is the only treatment that reduces the impact energy when using a clay matrix. This is not a coincidence, as an earlier discussion of a composite using T2 fibres combined with a virgin polypropylene matrix also has the lowest impact energy. The low impact energy is attributed to good chemical bonding between the matrix and the fibres. Consequently, it is necessary to investigate the fracture surface of this composite since it has the lowest impact energy and treatment T2 is influential in reducing the impact energy for a composite having a clay based matrix.

The fracture surfaces of impact specimens using a virgin polypropylene matrix and a clay matrix reinforced with T2 fibres can be seen in Figure 5.24. Both surfaces show very similar

surface characteristics such as good fibre-matrix bonding and fibre failure close to the surface of the matrix. The fracture surface for both types of matrices is indicative of a brittle fracture, which has an inherent characteristic of low impact energy. The impact results show that the composites manufactured using T2 fibres with both types of matrices have similar impact results and the lowest impact energy for their respective matrix types. This indicates that the fracture is dominated by the effect of the fibre treatment rather the effect of the clay matrix.

Figures 5.18 and 5.19 show the through-thickness shear strength and apparent modulus, respectively, for both types of matrices. Figure 5.18 shows that a composite consisting of T4 fibres and a clay matrix has the highest through-thickness shear strength whilst the composite using T2 fibres and a clay matrix has the lowest through-thickness shear strength. It could be argued that the shear strength for all the composites made from a clay matrix have a similar shear strength considering the large standards of deviation in the data. However, there is good confidence in the data as twelve specimens per configuration were used in calculating each result. Composites consisting of a clay matrix and fibres subjected to treatments T3 and T4 show distinct improvements in the through-thickness shear strength compared to the same composites made using virgin polypropylene matrix, whilst composite using T2 fibres showed a decrease in strength. The remaining treatments show the same shear strength for both types of matrices within the measurement of uncertainty. It is possible that the shear strength of the composites has improved through the addition of clay but if this were to be true, it would have resulted in all the composites with a clay matrix having a larger shear strength, when compared to those made using a virgin polypropylene matrix. It is proposed that the silane content influences the through-thickness shear strength as the MPS treatments have different MPS silane concentrations. This will be investigated further in the next section.

The apparent shear moduli are presented in Figure 5.19. Considering the data for the composites with a clay based matrix, this figure shows that the composite consisting of T4 fibres has the largest shear modulus whilst the composite made using T2 fibres has the lowest modulus. It also shows that the remaining treatments, within a measured uncertainty, show similar moduli. The figure shows that, across all samples, the clay matrix has a higher modulus than a virgin polypropylene matrix. As with the increase in tensile modulus, this increase in shear modulus is due to clay platelets hampering the motion of the polymer chains. It is also attributed to the rule of mixtures benefit from the clay. The increase in stiffness is also seen in the tensile modulus data. It is evident that clay stiffens the matrix, thereby increasing the modulus of the composite. It is useful to look at the fracture surfaces of the shear specimens to better understand the effect of clay.

Figure 5.20 shows the fracture surfaces of the shear specimens consisting of untreated fibres with a virgin polypropylene matrix and clay matrix. The fracture surface of the specimen comprising untreated fibres and a clay matrix shown in Figure 5.20b shows fibre debonding which is also evident in the same composite using a virgin polypropylene matrix. There is a considerable amount of matrix tearing in the virgin polypropylene matrix whilst the clay matrix shows no signs of tearing, rather it resembles brittle-like failure. The brittle-like fracture is seen in the fracture surfaces of the tensile specimens, impact specimens and shear specimens and this type of fracture is also seen by other authors [37, 44, 80].

It was seen earlier that the composite using T4 fibres and a clay matrix resulted in the largest shear strength and modulus values, it would thus be beneficial to investigate the fracture surface and compare it to that of a composite consisting of untreated fibres in a clay matrix. Figure 5.27 shows the fracture surfaces of composites made using T4 fibres with both types of matrices.

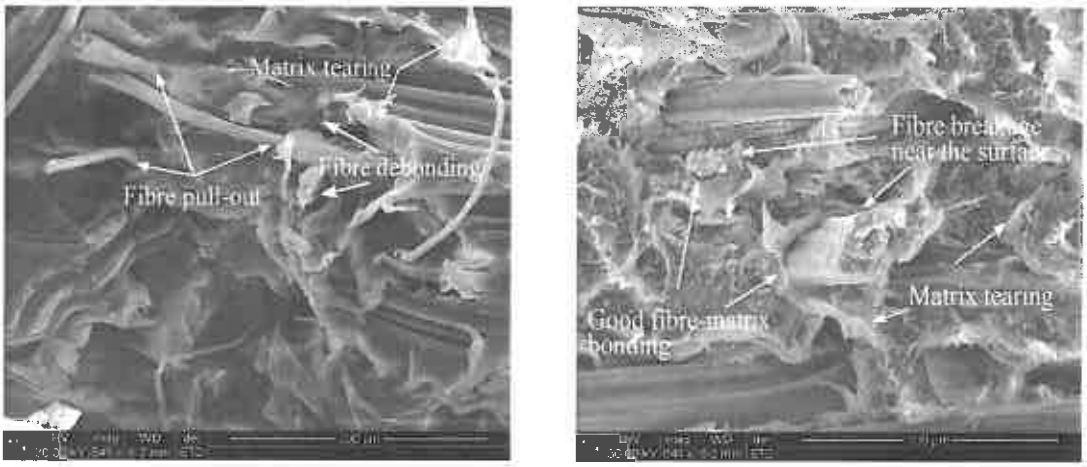

(a) T4 - PP Matrix (b) T4 - Clay Matrix

Figure 5.27: SEM images of shear specimens using treatment T4 fibres with polypropylene matrix and clay matrix

Referring to Figure 5.27, the composite using a virgin polypropylene matrix shows fibres pulled from the surface whilst the composite made from a clay matrix shows fibre breakage near the surface of the fibre and a good fibre-matrix bond. The fracture surface of the clay matrix is indicative of good bonding and is reflected in the shear strength results. A very peculiar sighting in the fracture surface of the clay matrix is the small amount of matrix tearing. This is not seen in Figure 5.20b which depicts the composite made from untreated fibres and a clay matrix. The hypothesis is that the increase in matrix tearing is a result of improved matrix-fibre bonding. Olayo et al. [73] investigated silane bonding using kenaf fibres and a polymer matrix. Although matrix tearing was not the focus of their research, it was observed that matrix tearing decreased when the bonding between the fibre and matrix improved. This resulted in an increase in tensile strength. However, they did not confirm any

direct relationship between matrix tearing and the tensile strength of a composite. Although this aspect is contradictory, it should be considered they did not make use of a clay matrix in their research. The matrix tearing is inconclusive and will not be investigated any further as it is not the focus of this research.

It is clear from the results discussed above that MPS treatments influence the mechanical properties of composites using both types of matrices. Although MPS did not lead to a significant improvement in the tensile strength results, it is possible that the no obvious trend could be seen in the tensile strength results due to the composites failing prematurely during testing. The hypothesis is that the introduction of clay reduces the fracture toughness, which results in brittle failure, reducing the allowable stress in the composite. This results in premature failure of the composite. Evidence of the reduction in fracture toughness can be seen in the impact results which show a large decrease in impact energy with the introduction of clay into the polypropylene matrix. It was seen earlier that tensile specimens consisting of a clay matrix have a matrix dominated failure surface, whilst the composites consisting of a virgin polypropylene generally show fibre snapping and matrix tearing. It is possible that composites using a polypropylene matrix with a 4% clay content result in an approximate allowable stress of 43 MPa, which limits the tensile strength of composites using treatments NaOH, T1 and T4 fibres to this stress. Based on this evidence, the hypothesis is true and will be further investigated in the following objective.

In essence, the effect of clay on a polypropylene matrix results in improved mechanical properties. The addition of clay into the matrix makes the matrix stiffer, which in turn increases the tensile strength and modulus of the composite. The clay also reduces the mobility of the polymer chains, which results in brittle-like failure which is indicative of a reduced fracture toughness. The impact data obtained shows that the failure in the composites consisting of clay is primarily matrix driven. The addition of clay to the composite matrix also causes premature failure during tensile testing.

One of the four MPS treatments is to be investigated further as the next objective considers the variation of the concentration of MPS silane in composites. Treatments T2 and T3 were discussed earlier and it was decided not to investigate these treatments further for reasons previously discussed. The MPS treatments, T1 and T4, show the most promise in improving the strength of the composites and show similar improvements for composites manufactured with a virgin polypropylene matrix. Since the nature of the investigation is based on the effect of adding clay to a polypropylene matrix, the fibre treatment which gave the best properties to the composite comprising of clay was selected. This was treatment T4 based on the tensile and shear results. The added benefit of choosing T4 over T1 is the cost saving associated with the treatment. T1 makes use of ethanol rather than methanol in the silane treatment,

which is an expensive alcohol. This is important as this investigation looks at developing a composite which not only displays good mechanical properties, but is also cost effective.

5.4 Variation of MPS Silane concentration using Treatment 4 on a Polypropylene Matrix and Polypropylene/Clay Matrix

It was found in section 5.3 that treatment T4 resulted in the best mechanical properties of the composite and was therefore used to investigate the remaining objectives. Following this, it was necessary to find the optimal MPS concentration to obtain the best mechanical properties. Silane works on a microscopic level to form a chemical bond between the matrix and the fibres. Clay mixed into a matrix also works on a microscopic level, with clay platelets acting as reinforcement within the nanocomposite. The combination of the two factors, percentage of silane and clay matrix, should have a different improvement compared to a no-clay matrix due to the complex interactions between silane and clay. Consequently, the silane was varied for both types of matrices; the virgin polypropylene matrix and 4 % clay matrix. Treatment T4 made use of 0.5% MPS silane for the fibre treatment, which may or may not be the optimum concentration. To investigate this possibility, the MPS silane concentration was varied to values below and above 0.5%, ranging from 0.25% MPS to 5% MPS. The fibre weight fraction of the composites were also kept constant at a value of 25%, as previously used.

The discussion can be broken into three sections; the effect of MPS concentration on kenaf fibres using a no-clay matrix, the effect of MPS concentration on kenaf fibres using a clay matrix and the discussion of the FTIR data. The abbreviations used for the different silane concentrations in this report can be seen in Table 5.2. The fibre weight fraction was kept constant at 25%.

Table 5.2: Abbreviation for the variation of MPS silane in treatment T4

Treatments	Abbreviation
Untreated fibres	Unt
6% Sodium Hydroxide	0M
6% Sodium Hydroxide + 0.25% MPS	0.25M
6% Sodium Hydroxide + 0.5% MPS	0.5M
6% Sodium Hydroxide + 1% MPS	1M
6% Sodium Hydroxide + 2% MPS	2M
6% Sodium Hydroxide + 5% MPS	5M

5.4.1 Effect of MPS silane on kenaf fibre using virgin polypropylene

Figure 5.28 shows the tensile strength results for the variation of MPS silane on kenaf fibres using both types of matrices. The focus in this section is the effect of MPS on a virgin polypropylene matrix composite.

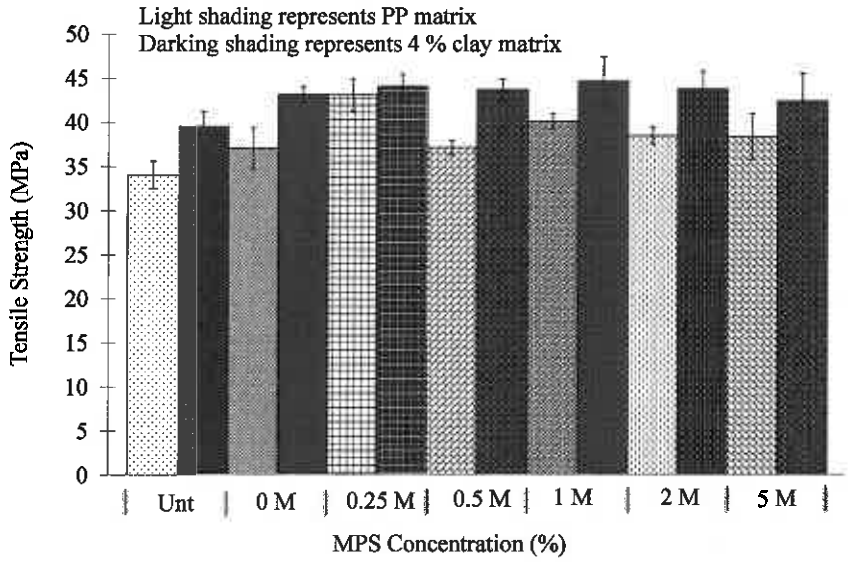

Figure 5.28: Tensile strength - Variation of MPS silane in treatment T4 on kenaf fibre using virgin PP and PP with 4% clay

Figure 5.28 shows that there is an increase in strength until a maximum value of 0.25% MPS of silane and thereafter a decrease to 0.5%, followed by an approximately constant value across the remaining percentages. It is no surprise that very little silane is required for optimal strength as Cho et al. [29] showed that an amount of as little as 0.5% MPS is enough to obtain the highest interfacial shear strength. Although this is double the amount of 0.25% MPS, it should be noted that their optimum concentration is for interfacial shear strength, and not for tensile strength. Their interfacial shear strength data had an increase in strength until 0.5% MPS followed by a decrease in strength across the remaining silane percentages.

It is assumed that having more than 0.25% MPS contributed to the development of the polysiloxane layer which added no strength benefit to the composite. Depending on the thickness of the layer, presumably it negatively affects the bonding capabilities of the kenaf fibres to the matrix, which in turn results in poor strength characteristics. This can be

investigated by looking at the fracture surfaces of the tensile specimens consisting of a virgin polypropylene matrix. Figures 5.29 and 5.30 show the fracture surface of tensile specimens consisting of 0.25% and 5% MPS treated fibres, respectively, with both types of matrices.

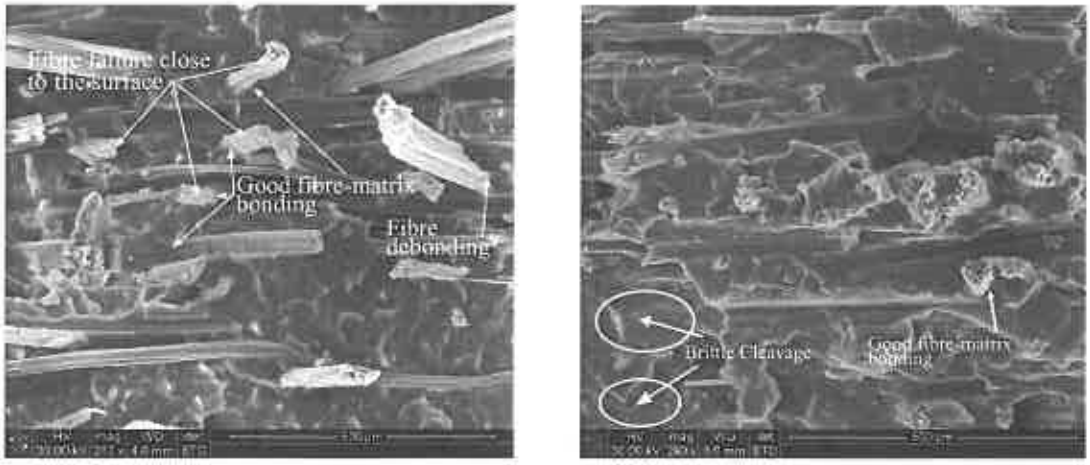

(a) 0.25% MPS - PP Matrix (b) 0.25% MPS - Clay Matrix

Figure 5.29: SEM images of tensile specimens using 0.25% MPS treated fibres with polypropylene matrix and clay matrix

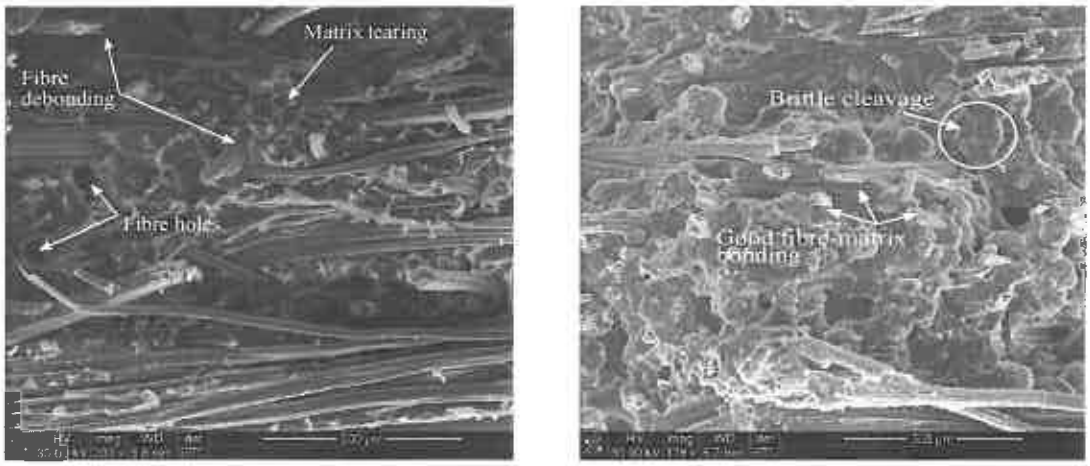

(a) 5% MPS - PP Matrix (b) 5% MPS - Clay Matrix

Figure 5.30: SEM images of tensile specimens using 5% MPS treated fibres with polypropylene matrix and clay matrix

Figures 5.29a and 5.30a show the fracture surface of tensile specimens using 0.25% MPS and 5% MPS fibres with a virgin polypropylene matrix, respectively. The fracture surface of the specimen using 0.25% MPS has little fibre pull-out and little fibre debonding compared to the composite using 5% MPS treated fibres. The composite using 5% MPS silane has a lot of matrix tearing with fibre holes, indicative of an inferior composite. The fracture surface of the composite using 0.25% MPS silane shows good fibre-matrix bonding and the fibres failed close to the interface, indicating a cohesive failure, the strongest interfacial adhesion between

fibre and matrix [29]. The fracture surface correlates well with the SEM image presented by Olayo et al. [73]. They found similar surface characteristics in their composite and such a composite had a large tensile strength. The fracture surface of the composites using 0.25% MPS fibres supports the tensile strength results in Figure 5.28, which indicates that such a composite has the highest tensile strength for a virgin polypropylene matrix, and that it has tensile strength higher than a composite using 5% MPS treated fibres. It would be beneficial to look at the tensile modulus data due to the improved fibre-matrix bonding for a composite using 0.25% MPS fibres.. The tensile modulus of composites having a variation of MPS silane concentration on kenaf fibres using both types of matrices is presented in Figure 5.31.

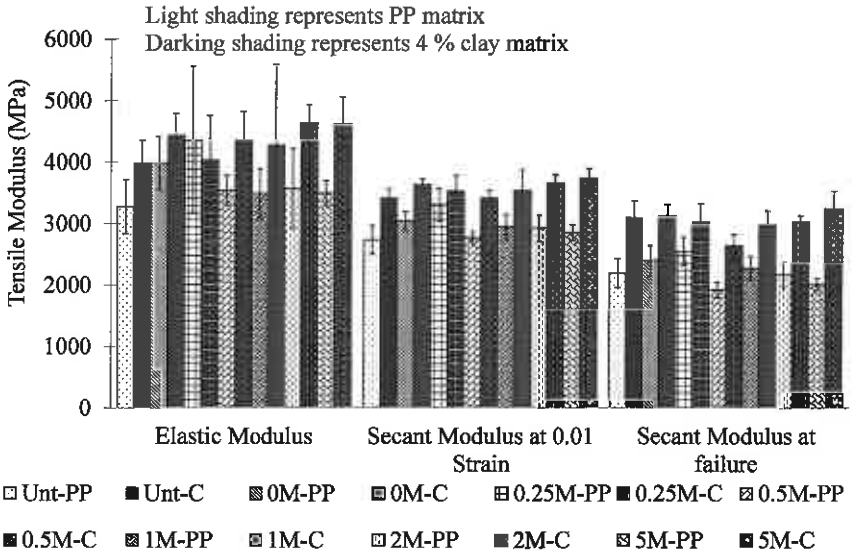

Figure 5.31: Tensile modulus - Variation of MPS silane in treatment T4 on kenaf fibre using virgin PP and PP with 4% clay

Considering the data corresponding to a virgin polypropylene matrix, it can be seen that there is an improvement in the tensile modulus for a MPS silane content of 0.25% compared to a composite using sodium hydroxide treated fibres. This implies that more load is being transferred to the fibres, resulting in an increase in the stiffness of the composite. This is a direct consequence of the improved bonding between the matrix and fibres. Since the fibre-matrix bond is stronger, a larger load can be transferred across the interface before the failure of the interface. The trend of increasing moduli up until 0.25% silane concentration is the same as the trend seen in the tensile strength data. Thereafter, there is a decrease and plateau in mechanical properties. The modulus data supports the hypothesis that the polysiloxane layer forms with the presence of silane concentrations above 0.25%. More details

regarding the formation of this layer can be found in subsubsection 2.4.2.2 of the literature review.

This finding is disturbing as it implies that a different MPS treatment might have been selected if the concentration of MPS silane in the different treatments had been lower. Nonetheless, the treatments implemented in this research were based on those found in the literature and it was assumed that the optimum concentration for the interfacial shear strength would also correspond with that for tensile strength and other mechanical properties. However, this is not the case. Despite this unfortunate finding, this treatment makes use of methanol which is cheaper than the other silane treatments, making it the most cost effective treatment.

Figure 5.32 shows the impact energy results for the variation of the concentration of MPS silane on kenaf fibres for composites using both types of matrices. With focus on the composites manufactured using a virgin polypropylene matrix, The figure shows a decrease in impact energy up until a concentration of 0.25% MPS on the kenaf fibres, followed by a plateau in the data. The energy results show that the sodium hydroxide treatment has the most significant effect in reducing the impact energy of the composite. Figure 5.32 shows that a content of 0.25% MPS marginally improves the fibre-matrix bonding compared to a composite using a NaOH treatment, resulting in a decrease in impact energy. This improvement in bonding is also noted in the tensile data. The impact energy for composites with a silane concentration higher than 0.25% is more or less constant. This lack of improvement of the fibre-matrix bonding at higher concentrations is possibly due to the development of a polysiloxane layer at concentrations above a 0.25% silane concentration. Nonetheless, the impact energy data show that MPS silane does affect the impact energy of composites using a virgin polypropylene matrix, although it is not significant compared to a composite using NaOH fibres. To investigate the bond improvement prevalent in composites using 0.25% MPS fibres, it will be useful to look at the fracture surface of the impact specimens. Figure 5.33 shows the fracture surfaces of impact specimens made using 0.25% MPS fibres with both types of matrices.

Figures 5.16a, 5.17a, 5.33a and 5.25a show the fracture surfaces of impact specimens manufactured with untreated fibres, 0% MPS, 0.25% MPS fibres and 0.5% MPS fibres, respectively, in a virgin polypropylene matrix. The impact fracture surfaces of composites consisting of 0% MPS, 0.25% and 0.5% MPS fibres show far less fibre pull-out and fibre holes than the impact specimen consisting of untreated fibres, as shown in Figure 5.16a. These fracture surfaces all look very similar, implying that similar processes occurred in these three specimens and that the resulting impact energies are thus similar. The effect of MPS is small, which is why the SEM images of the fracture surfaces of the composites using 0% MPS and composites using other MPS concentrations look similar. By investigating the interfacial strength data, insight can be obtained on whether fibre-matrix bonding is influenced by MPS concentrations.

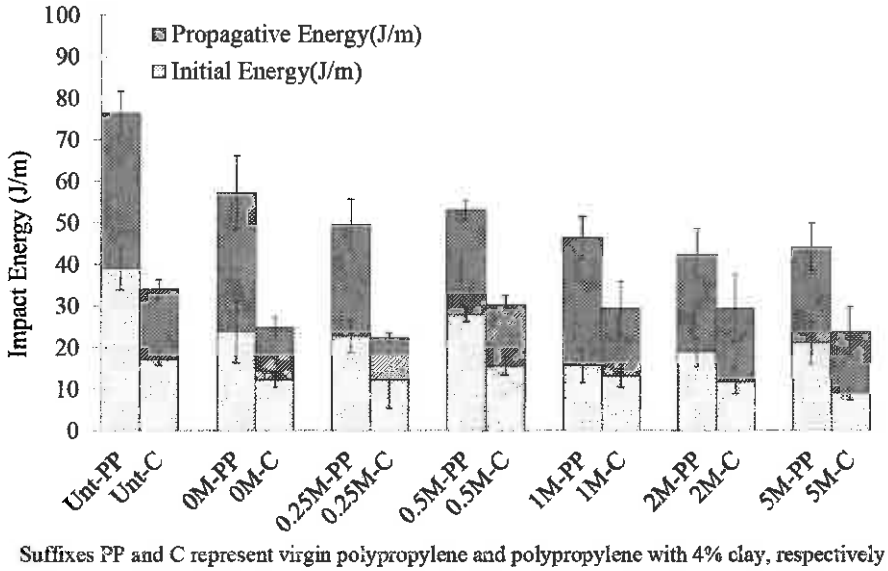

Figure 5.32: Impact energy - Variation of MPS silane in treatment T4 on kenaf fibre using virgin PP and PP with 4% clay

(a) 0.25% MPS - PP Matrix (b) 0.25% MPS - Clay Matrix

Figure 5.33: SEM images of impact specimens using 0.25% MPS treated fibres with polypropylene matrix and clay matrix

Figure 5.34 shows the through-thickness shear strength of composites using a variation of MPS silane concentrations on kenaf fibres for both types of matrices. By focusing on the composites using a virgin polypropylene matrix and taking into consideration the standards of deviation in the results, it is seen that the variation of MPS silane concentrations has no significant effect on the through-thickness shear strength. Further insight can be gathered

by looking at the fracture surfaces of the shear specimens. Figures 5.35 and 5.36 show the fracture surfaces of specimens made from 0.25% MPS and 0.5% MPS treated fibres, respectively, with both types of matrices.

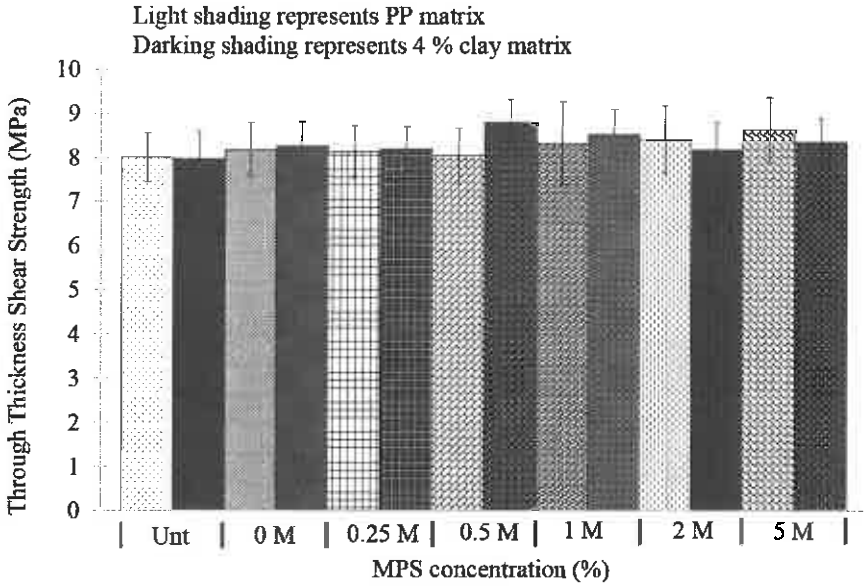

Figure 5.34: Through-thickness shear strength - Variation of MPS silane in treatment T4 on kenaf fibre using virgin PP and PP with 4% clay

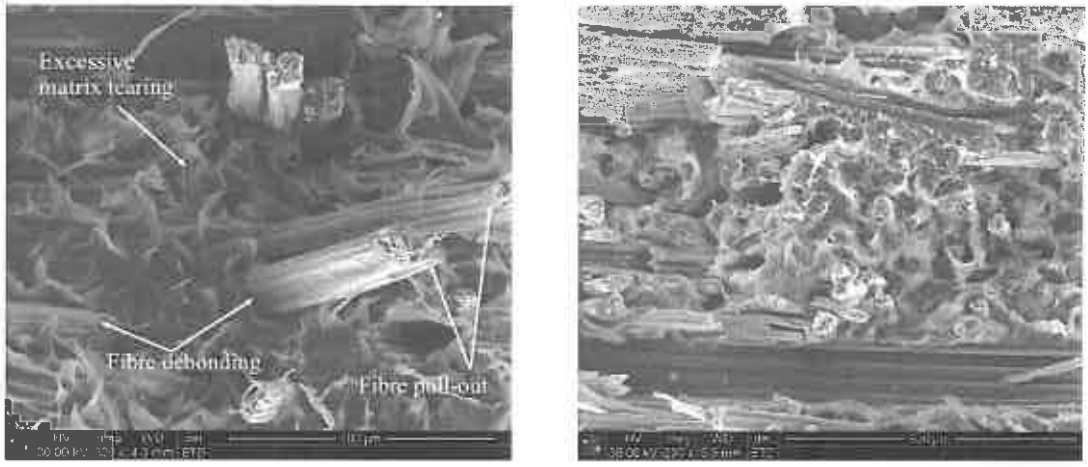

(a) 0.25% MPS - PP Matrix

(b) 0.25% MPS - Clay Matrix

Figure 5.35: SEM images of shear specimens using 0.25% MPS treated fibres with polypropylene matrix and clay matrix

Figures 5.35a and 5.36a show the fracture surfaces of shear specimens consisting of 0.25% MPS fibres and 5% MPS fibres in a virgin polypropylene matrix, respectively. Both fracture

(a) 5% MPS - Polypropylene Matrix

(b) 5% MPS - Clay Matrix

Figure 5.36: SEM images of shear specimens using 5% MPS treated fibres with polypropylene and clay matrix

surfaces have similar characteristics such as fibre pull-out and fibre debonding. The images imply that similar processes happen in the two specimens and that the resulting strength is therefore similar. This implies that MPS has no significant effect on the through-thickness shear strength of the composite using a virgin polypropylene matrix. This contrasts with the finding of Cho et al. [29], which showed an increase in interfacial shear strength for the variation of MPS silane up until a concentration of 0.5% followed by a decrease in strength across the higher concentrations for composites using a virgin polypropylene matrix and kenaf fibres. The difference between the results of this research and Cho et al. [29] would have been viewed as contradictory if the same test had been used to measure the interfacial shear strength. This research makes use of short beam shear testing to measure the through-thickness shear strength whilst Cho et al. [29] used the single fibre microbonding test to measure the interfacial shear strength between the matrix and fibre. The microbonding test essentially measures the shear strength locally whereas the short beam shear test, which was conducted in this report, measures the global shear strength. The global shear strength is a better representation of the strength of the composite. Since the improvements of MPS have been marginal in the shear strength data, it will be worthwhile to look at the shear modulus data.

The apparent modulus for a variation of MPS silane concentrations in composites using both types of matrices is presented in Figure 5.37. By looking at the data presented for composites manufactured with a virgin polypropylene matrix, it is seen that the shear modulus is approximately the same for a composite using sodium hydroxide treated fibres and composites using a variation of MPS concentrations. This implies that MPS has no significant effect on the shear modulus of the composite. The most significant improvement in shear modulus is

apparent in composites manufactured with sodium hydroxide treated fibres, when compared to composites containing untreated fibres.

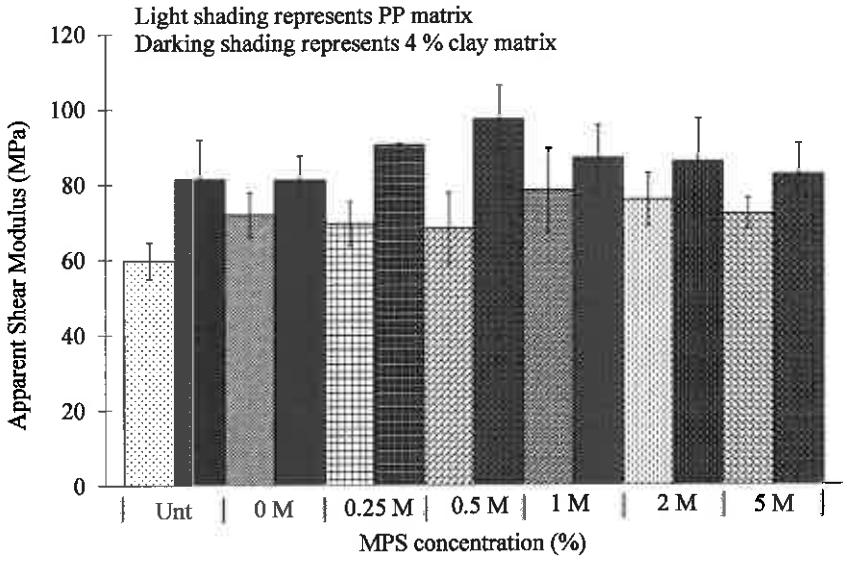

Figure 5.37: Approximate shear modulus - Variation of MPS silane in treatment T4 on kenaf fibre using virgin PP and PP with 4% clay

5.4.2 Effect of MPS silane concentration on kenaf fibre using clay matrix

Figure 5.28 shows the tensile strength for the variation of MPS silane on kenaf for both types of matrices. There is an improvement in tensile strength for composites using a clay matrix compared to the same composites made using a polypropylene matrix. This is similar to the results found in the previous investigation whereby clay improved the tensile strength results, highlighting the reinforcing effect of clay [37]. By considering the composites consisting of a clay matrix, it is evident that there is an improvement in tensile strength due to the sodium hydroxide treatment compared to a composite using untreated fibres. It is possible that there is a small increase in tensile strength with small amounts of silane and then a gradual decline, however the effect is not significant.

It is hypothesised that a small amount of silane does improve the tensile strength of a clay based composite, but the failure of the composite is primarily matrix driven. The matrix becomes brittle with the addition of clay resulting in premature failure, which was explained earlier. When the matrix fails, it causes failure of the composite, irrespective of whether

or not there is good bonding between the fibres and the matrix. A brittle failure will be noticeable in SEM images, as seen with previous results.

Figures 5.29b and 5.30b show the fracture surfaces of tensile specimens using 0.25% MPS fibres and 5% MPS fibres, respectively, in a clay matrix. Both fracture surfaces show no fibre debonding and no fibre pull-out, which is indicative of good fibre-matrix strength. These surfaces have similar characteristics implying that the resulting strength is similar. Both fracture surfaces are uniform with no matrix tearing, which is indicative of a brittle failure. The brittle failure helps support the hypothesis that the composites failed prematurely. It is possible that a clearer trend for the variation of MPS concentration would have been seen had the clay not made the matrix so brittle.

Figure 5.31 shows the variation in tensile modulus with MPS concentration using both types of matrices. The figure shows that clay increases the modulus of composites when compared to the same composites made using a virgin polypropylene matrix. The reinforcing effect of clay in improving modulus was explained in the previous investigation. By referring to the composites consisting of a clay matrix, the data show a small increase in modulus for 0% MPS compared to untreated fibres, whilst the addition of silane does not have a significant improvement in tensile modulus. This is in line with previous findings which show that the MPS treatments have no significant effect on the modulus of the composite consisting of a clay matrix.

Figure 5.32 shows the impact results for a variation of MPS concentrations for composites manufactured with the two types of matrices. A comparison between the two matrix types shows that the impact energy is greatly reduced with the presence of clay in the matrix, when compared to a virgin polypropylene matrix. A similar result was shown in Figure 5.15, which illustrates the impact results for different fibre treatments using two different types of matrices. Considering the composites made using the clay matrix, the data show a decrease in impact energy with 0.25% MPS silane in the composite, when compared to the same composite using sodium hydroxide treated fibres. This implies better bonding at the fibre-matrix interface. Thereafter, there is a slight increase in impact energy which remains more or less constant over the remaining MPS concentration. The increase in impact energy corresponds to a weaker fibre-matrix bond compared to the composite manufactured using 0.25% MPS silane. It will be useful to look at the fracture surfaces of the impact specimens to investigate the mechanism of failure.

Figures 5.17b, 5.33b, and 5.38 show the fracture surfaces of the impact specimens using 0% MPS silane, 0.25% MPS silane and 5% MPS silane, respectively, in a clay matrix. The lack of plastic deformation in these fracture surfaces in the form of matrix drawing is a consequence of the clay reducing the polymer chain mobility [37] and this results in a brittle fracture.

This is in line with the previous investigation of composites made using a clay matrix. The fracture surfaces of the specimens using 0% MPS and 0.25% MPS show good fibre-matrix bonding. These surfaces look similar and due to the small amount of MPS, the effect of the MPS is not noticeable. The composite consisting of 5% MPS shows slightly more fibre holes than the composite made using 0% MPS and 0.25% MPS. The fibre holes are a result of fibre pull-out which is a consequence of weak fibre-matrix bonding in a clay matrix. This results in an increase in impact energy, which can be seen in the impact data. The most significant decrease in impact energy is due to the sodium hydroxide treatment. As seen in Figure 5.32, this treatment reduces impact energy for composites using both types of matrices.

Figure 5.38: SEM images of impact specimens using 5% MPS treated fibres with clay matrix

A 0.25% MPS concentration improves the fibre-matrix bonding which results in a decrease in impact energy for composites made with a clay matrix. The increase in impact energy, which stays more or less constant with increasing MPS concentration, is possibly due to the development of the polysiloxane layer which develops at MPS concentrations greater than 0.25%. The increase after a 0.25% MPS concentration is more evident in the composites using the clay matrix compared to those using a virgin polypropylene matrix. A possible reason for the plateau of impact energy for MPS concentrations above 0.25% MPS is due to dominant matrix failure.

Figure 5.34 shows the through-thickness shear strength for a variation of MPS silane concentrations using both types of matrices. The figure has a considerable amount of scatter in the data making it difficult to comment on any specific trend. The trend is more or less constant in shear strength for composites using both types of matrices. However, there is a large improvement in shear strength for composites using a concentration of 0.5% MPS with a clay matrix, compared to the same composite consisting of a virgin polypropylene matrix. However, at 5% MPS concentration, the shear strength of the composite using a virgin polypropylene matrix is larger than the same composite made using a clay matrix.

This could possibly be due to the scatter in the data, thus the effect of the concentration of MPS silane is investigated further by looking at the fracture surfaces of these specimens.

The fracture surfaces of shear specimens using 0.5% MPS fibres and 5% MPS fibres in both a clay matrix and a virgin polypropylene matrix can be seen in Figures 5.27 and 5.36, respectively. Figure 5.27 was discussed in the previous investigation. The fracture surfaces of the composites manufactured with 0.5% MPS concentration show that there is a good fibre-matrix bond in the composite made with a clay matrix compared to the same composite made with a virgin polypropylene matrix. However, the fracture surfaces of the composites using 5% MPS concentration for both matrices show fibre debonding and fibre pull-out which is similar to the specimen consisting of 0.5% MPS and a virgin polypropylene matrix. This implies that these composites underwent similar processes in failure. Thus, these composites should have similar shear strengths and this can be seen in Figure 5.34. The shear strength data confirm the results obtained earlier which show that a variation of MPS has no significant effect on the through-thickness shear strength for composites using a virgin polypropylene matrix. The composite using a clay matrix with a lower MPS concentration shows better fibre-matrix bonding compared to the same composite with a higher MPS concentration. It will therefore be worthwhile to consider the shear modulus data for a composite using a clay matrix.

The apparent shear modulus data for a clay matrix can be seen in Figure 5.37. The data show an increase in shear modulus up until a MPS silane percentage of 0.5% MPS followed by a decrease across the remaining MPS percentages, indicating that MPS can influence the shear modulus of the composite. This local maximum agrees with the shear strength data which shows that a 0.5% MPS concentration results in the highest shear strength. This is similar to the result found by Cho et al. [29], even though their research involved composites consisting of virgin polypropylene and kenaf fibres. The shear strength data could have a similar trend to the shear modulus data which is hidden in the scatter of the data.

The possible reasoning behind the improvement of shear strength for a composite using a clay matrix at a 0.5% MPS silane concentration is that the silanols attached to the fibre are attracted to the surfactant used in the clay or the compatabiliser which is mixed into the polypropylene. This results in an improvement in strength. However, the addition of large amounts of silane weakens the fibre-matrix bond, resulting in lower shear strengths. The mechanism of interaction between silane and clay is not in the scope of this research, therefore, it will not be investigated further.

A MPS concentration above 0.25% was expected to result in inferior mechanical properties due to the development of the polysiloxane layer. However, it is interesting that 0.5% MPS is the optimum concentration for shear properties for a clay matrix, whilst a concentration

of 0.25% MPS is the optimum amount for tensile and impact properties for composites using both types of matrices. It is plausible that a concentration of 0.5% MPS results in a really strong fibre-matrix bond, which results in the interface having the lowest strain to failure [74], resulting in a brittle interface. This is a similar effect to that seen earlier for composites using T2 fibres. However, a good fibre-matrix bond should have resulted in a low impact energy but this was not the case. The improvement in shear strength at 0.5% MPS is specific for a composite having a clay matrix, and thus, this effect will be investigated in the next section of the discussion, which highlights the effect of clay content in a polypropylene matrix. A MPS silane concentration of 0.25% improved two of the three mechanical test results for composites consisting of both type of matrices. This concentration was thus used for all remaining investigations.

5.4.3 FTIR Data

FTIR spectroscopy was performed on the kenaf fibres to find evidence of the silane bonding. There is doubt as to whether the silane did effectively bind to the fibres as there was very little mechanical strength benefit. Figure 5.39 shows the FTIR results for the variation of MPS concentrations on kenaf fibres and Figure 5.40 shows a zoomed in section of interest of the same results. Figure 5.40 shows that there is a disappearance of peaks at 1239 cm^{-1} and 1730 cm^{-1}, corresponding to the lignin and hemicellulose components in the kenaf fibre, respectively [62, 82]. These peaks are present for untreated kenaf fibres that were heated to 25°C and 175°C, but no peaks were present for the remaining MPS treatments, including the 0% MPS fibres. This implies that untreated fibres loses these bonds during the NaOH chemical treatment. The removal of the peaks corresponds to the decomposition of two types of bonds, namely, the double and single bond between carbon and oxygen. Sgriccia et al. [83] showed similar results. They treated fibres with a combination of an alkali treatment and silane treatment and performed FTIR spectroscopy on the fibres. Their data showed a disappearance of the double and single carbon bond which is due to the alkali treatment [84]. However, there were no peaks at 766 cm^{-1} and 847 cm^{-1} which corresponds to silane [85]. Sgriccia et al. [83] concluded that it is possible that the concentration of silane on the fibre surfaces is too small to be detected by FTIR, which is possibly why silane was not detected in this investigation either.

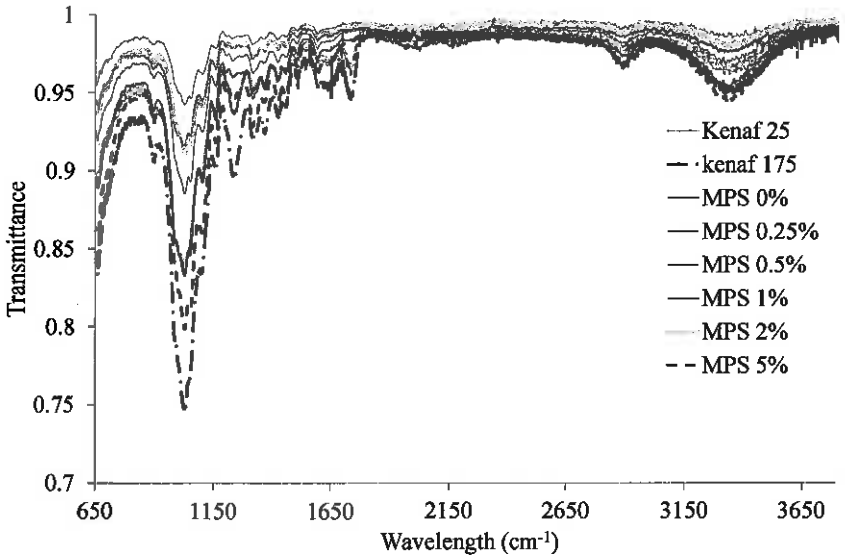

Figure 5.39: Full spectrum of FTIR results for variation MPS concentration on treated fibres

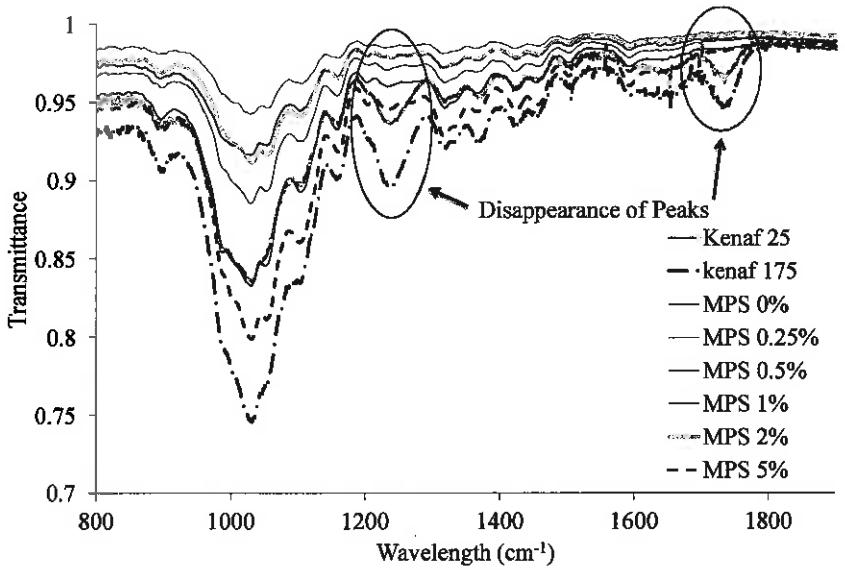

Figure 5.40: FTIR results for 800 cm^{-1} to 1900 cm^{-1} range for variation MPS concentration on treated fibres

5.5 The Effect of Clay on Mechanical Strength

The aim of this work is to find the clay content which gives the best mechanical properties. For the work done to this point, the clay matrix consisted of a clay content of 4%. Before proceeding with the discussion regarding the variation of clay content, it is useful to summarise the previous investigations leading up to the final fibre treatment.

Four MPS treatments were investigated with each treatment having a specific silane concentration and a particular type of alcohol which was used to liberate the silane and facilitate silane bonding to the fibre. These treatments were applied to the fibre. After mechanical testing, it was shown that treatment T4 yielded the best mechanical properties. Thereafter, the MPS silane concentration was varied in treatment T4 from a concentration of 0% to 5%. It was found that a silane concentration of 0.25% MPS results in the best mechanical properties. The previous investigation showed that higher concentrations of MPS silane led to the formation of a polysiloxane layer which results in inferior fibre-matrix bonding. SEM imagery was useful in justifying the fact that excessive amounts of silane result in a weaker composite, confirming earlier studies carried out by Cho et al. and Xie et al. [27, 29]. Consequently, the kenaf fibre treatment was fixed for the remaining objectives and consisted of 6% sodium hydroxide and 0.25% MPS. To find the best clay content, it was varied from 0% to 8% in a polypropylene matrix and three different mechanical tests were used to evaluate the effect of clay. Figures 5.41 and 5.42 show the effect of clay content on tensile strength and tensile modulus, respectively, for composites using 0.25% MPS treated fibres.

Figure 5.41 shows that a 2% clay content in a polypropylene matrix results in the largest tensile strength for the composite. The data have a large scatter which makes it difficult to comment on a trend. It seems that a small amount of clay improves the strength, however, a further increase in the clay content does not improve the tensile strength of the composite. From previous discussion, it is seen that the addition of clay makes the composite brittle, which is indicative of a lower fracture toughness which leads to premature failure. The reduction in fracture toughness of the composite results in a lower allowable stress according to the fracture toughness equation, seen in Equation 5.1. It is possible that a small amount of clay provides some benefit before the increase in strength is counteracted by the lower allowable stress resulting from the fracture of the specimen. It is useful to investigate the effect of different clay contents on the tensile modulus data and, in turn, interpret how that influences the tensile strength data.

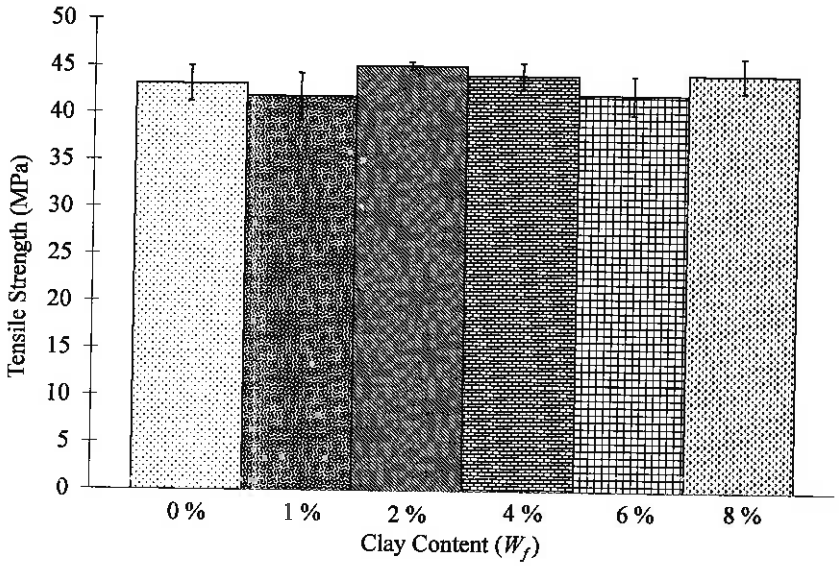

Figure 5.41: Tensile strength - Variation of clay content using 0.25% MPS on kenaf fibres

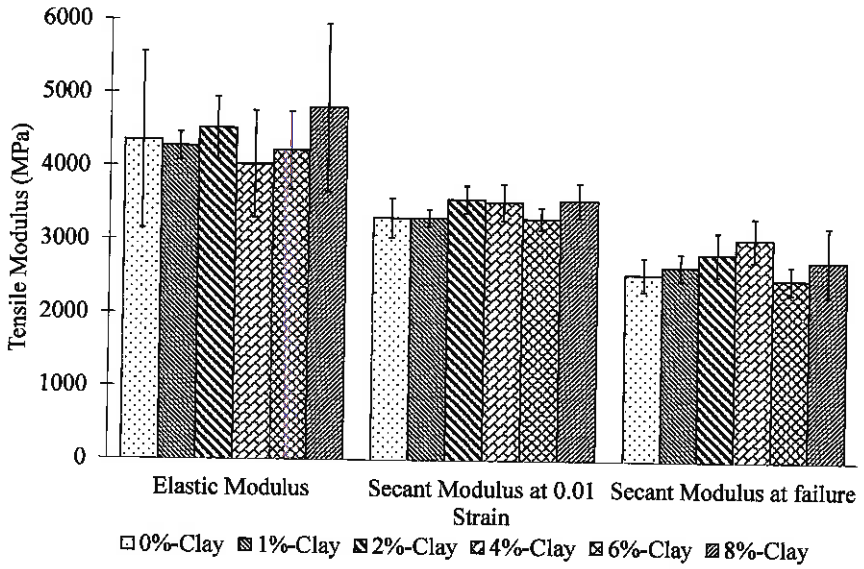

Figure 5.42: Tensile modulus - Variation of clay content using 0.25% MPS on kenaf fibres

$$K = B \cdot \sigma \cdot \sqrt{\pi \cdot a} \tag{5.1}$$

where K = fracture toughness (MPa$\sqrt{m}$)
B = crack length and component geometry factor
σ = applied stress (MPa)
a = crack length (m)

The modulus data shown in Figure 5.42 has no clear trend as the standards of deviation are very large. However, previous research done by Garcia-Lopez et al. [12] and Chen et al. [37] found that the tensile modulus increases with an increase in clay content in PP, but the composites tested by these researchers did not make use of fibre reinforcement. Despite the lack of fibre reinforcement in their composites, the modulus of their composites increased with increasing clay content. Using their results and applying it to this research, it would be expected that the modulus of the composite would increase with increasing clay content, since the matrix modulus is increasing. It is possible that there is a trend of an increase in elastic modulus with an increase in clay hidden in the standards of deviation in the results. The secant modulus at failure shows a better trend, highlighting that the secant modulus is increasing with clay content up until a concentration of 4% and followed by a decrease.

Jo et al. [86] investigated the effect of clay on tensile modulus using an unsaturated polyester matrix without fibre reinforcement. Their results showed that the modulus of the clay matrix increased up until a clay content of approximately 5% in the matrix and thereafter decreased. The decrease in modulus at higher clay concentrations was attributed to a lower degree of clay exfoliation/intercalation and lower degree of polymer-clay surface interactions, which is possibly the same reason for the decrease in the secant modulus observed in this research. Although exfoliation of clay occurs at a nano-level, it is useful to look at the fracture surfaces of the tensile specimens to investigate other possible reasons of failure. Figure 5.43 shows the fracture surface of of tensile specimens using 0.25% MPS treated fibres with a 1% clay, 2% clay, 6% clay, and 8% clay content in polypropylene matrix.

Figures 5.29a, 5.43a, 5.43b and 5.43d show the fracture surfaces of the tensile specimens using 0.25% MPS silane and clay matrix consisting of 0%, 1%, 2% and 8% clay content, respectively. The surface of the specimen containing 0% clay shows fibre debonding and fibre failure close to the surface, whilst the surfaces of the specimens that contain clay do not show any of these characteristics. All the surfaces consisting of clay show similar featureless brittle cleavage which is similar to the findings by Chen et al. [37] and Tarapow et al. [15]. The SEM imagery helps show that the addition of clay causes a transition from ductile failure

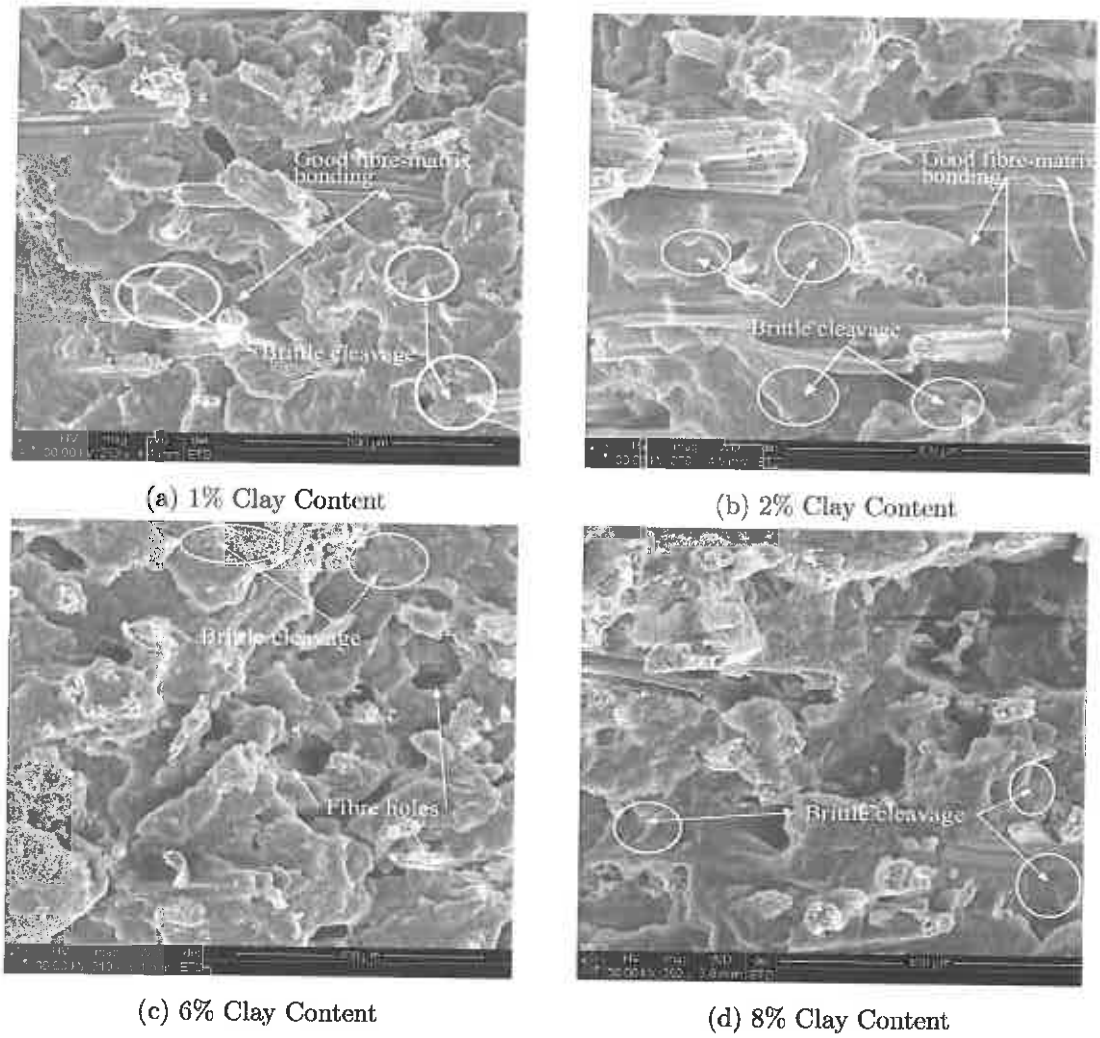

(a) 1% Clay Content

(b) 2% Clay Content

(c) 6% Clay Content

(d) 8% Clay Content

Figure 5.43: SEM images of tensile specimens using 0.25% MPS treated fibres with a 1%clay, 2%clay, 6%clay, and 8% clay content in polypropylene matrix

to brittle failure in the composites. To get further insight into the failure mechanism, it is beneficial to look at the impact results and imagery of the impact failure surfaces.

The impact energy data for the variation of clay content in a composite using 0.25% MPS is presented in Figure 5.44. This figure shows that an increase in clay content results in a decrease in impact energy. The increase in the clay content presumably results in an increase in brittleness in the clay matrix, subsequently decreasing the impact energy. This effect can be further explored by looking at the fracture surfaces of the impact specimens which can be seen in Figure 5.45.

Figures 5.33b, 5.45a, 5.45b and 5.45d show the fracture surfaces of impact specimens using 0.25% MPS and clay matrices consisting of 0%, 1%, 2% and 8% clay content, respectively. The composite having 0% clay content has an uneven surface fracture with small fibre lengths protruding from the surface, whereas all the specimens that contain clay show almost no fibre

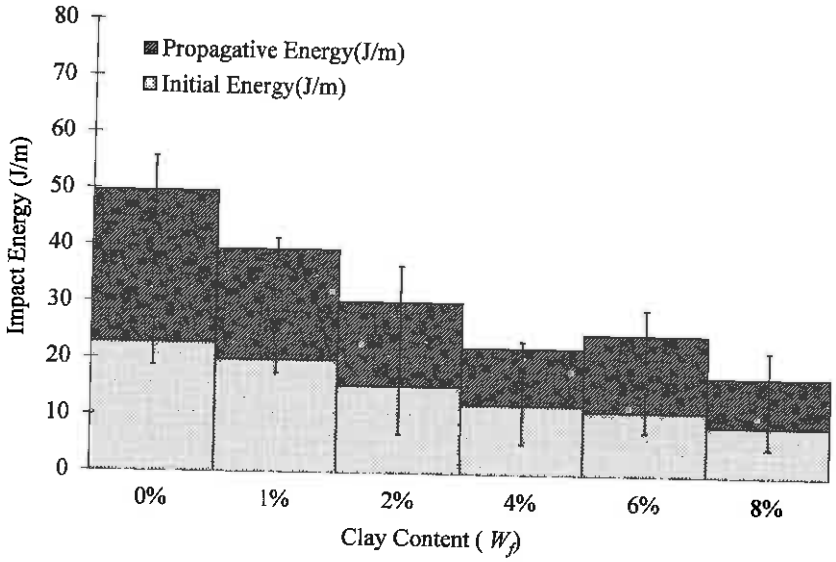

Figure 5.44: Impact energy - Variation of clay content using 0.25% MPS on kenaf fibres

pull-out and a brittle-like surface. This supports the hypothesis that failure is controlled by matrix fracture when it contains clay.

Figure 5.46 shows the through-thickness shear strength for a variation in clay content in composites using 0.25% MPS silane. It shows a gentle increase in shear strength up to a clay content of 2%, thereafter the data plateaus for the remaining clay percentages. This implies that there is a constant through-thickness shear strength for clay contents greater than 2% in the polypropylene matrix and presumably no effect brought about by matrix failure. In fibre reinforced ceramic matrix composites, shear stresses are less able to cause matrix cracking than axial stresses from tensile testing [87] and so the effect of a brittle matrix should be less pronounced in shear testing. This might allow failure to be controlled by the fibre-matrix bond strength. This hypothesis can be examined further by looking at the fracture surface of the shear specimens which can be seen in Figure 5.47.

Figures 5.35b, 5.47a, 5.47b and 5.47d show the fracture surfaces of shear specimens using 0.25% MPS and clay matrix consisting of 0%, 1%, 2% and 8% clay content, respectively. The composites consisting of 0%, 1% and 8% clay content show some fibre debonding whilst the composite having a 2% clay content has good fibre-matrix bonding. This supports the shear strength data, proving that the bonding between the matrix and fibres improves with a polypropylene matrix having a 2% clay content. There is a considerable amount of matrix tearing present in a composite that has 0% clay content, whilst there is little matrix drawing in

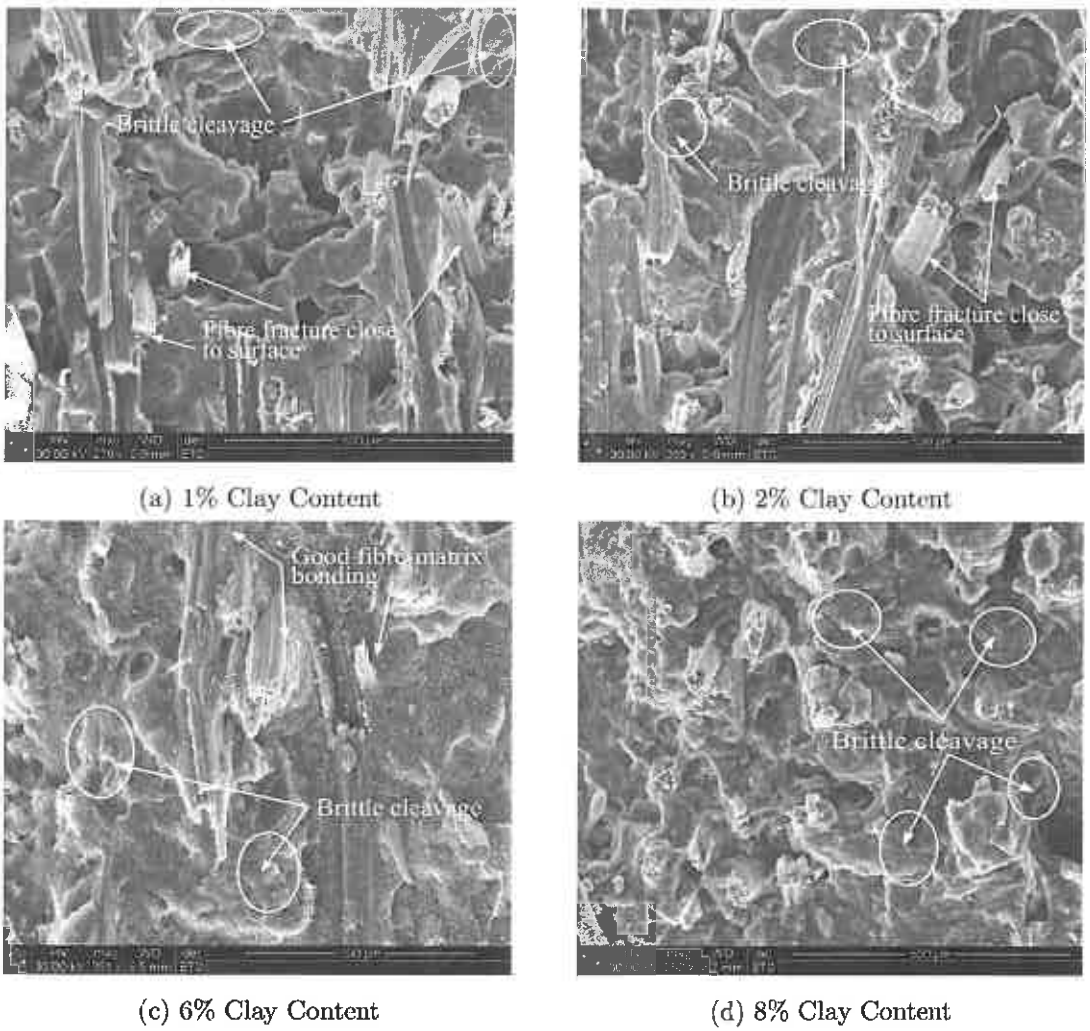

(a) 1% Clay Content

(b) 2% Clay Content

(c) 6% Clay Content

(d) 8% Clay Content

Figure 5.45: SEM images of impact specimens using 0.25% MPS treated fibres with a 1%clay, 2%clay, 6%clay, and 8% clay content in PP matrix

the composites containing clay. This implies that the matrix is less ductile with the presence of clay. It is interesting to note that the composite having an 8% clay content also shows some matrix drawing and does not have a flat surface. This surface does not resemblance a ductile fracture nor a brittle-like failure. The SEM images show less of a brittle-like fracture, compared to that seen for the tensile and impact specimens. This supports the hypothesis that, in shear testing, the matrix is less susceptible to matrix cracking.

The apparent shear modulus for the variation of clay concentrations in composites using 0.25% MPS silane is presented in Figure 5.48. The figure shows that the shear modulus increases up until a 2% clay content and thereafter has a plateau or subsequent decrease in modulus over the remaining clay concentrations. This increase in shear modulus with the increase in clay content corresponds to the shear strength data.

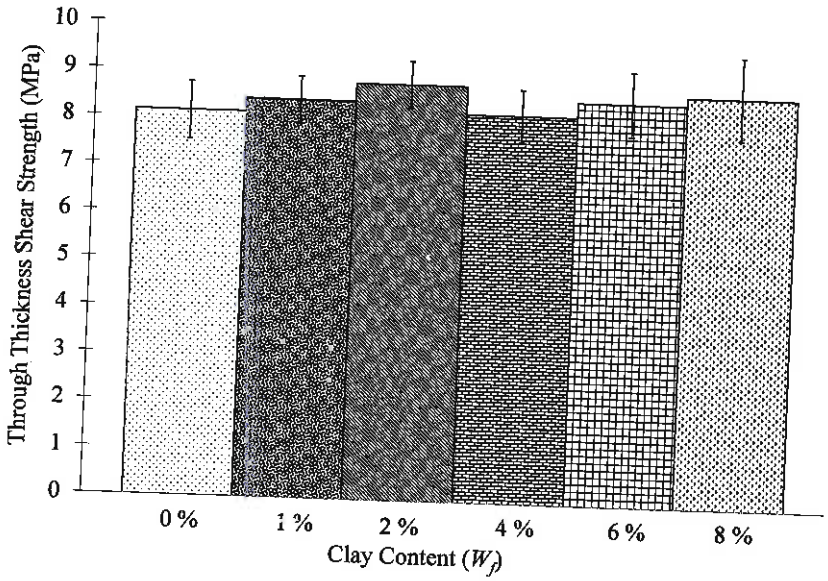

Figure 5.46: Through-thickness shear strength - Variation of clay content using 0.25% MPS on kenaf fibres

The increase in through-thickness shear strength with the increase in clay content is possibly related to the surface roughness of the composite. Ataeefard et al. [44] investigated the surface roughness of a composite consisting of polypropylene and montmorillonite clay. It was found that the surface roughness increases with clay content and leads to improved wettability. It was also found that the surface roughness can enhance the anchor effect and this in turn strongly influences adhesive properties. It is thus possible for the rough matrix surface to form a better mechanical bond with the fibres, resulting in an increase in the fibre-matrix bond. If the through-thickness shear strength increases with clay content, the tensile strength would be expected to increase in the same manner. However, the increase in clay content reduces the fracture toughness, thereby causing premature failure in the composite during tensile testing. Although the SEM images do not show evidence of an increase in surface roughness, evidence of surface roughness can be obtained through Atomic Force Microscopy (AFM) [44].

As mentioned previously, the shear modulus data show a plateau or possibly decrease after a 2% clay content. This is most likely a result of poor clay exfoliation and less polymer-clay interaction sites [86], which could make either of the two trends admissible. The only way to determine the correct trend would be to determine the degree of clay exfoliation. This could be done with transmission electron microscopy which is capable of viewing specimens on a nano-scale or alternatively by using X-Ray diffraction. However, such a detailed study was

(a) 1% Clay Content

(b) 2% Clay Content

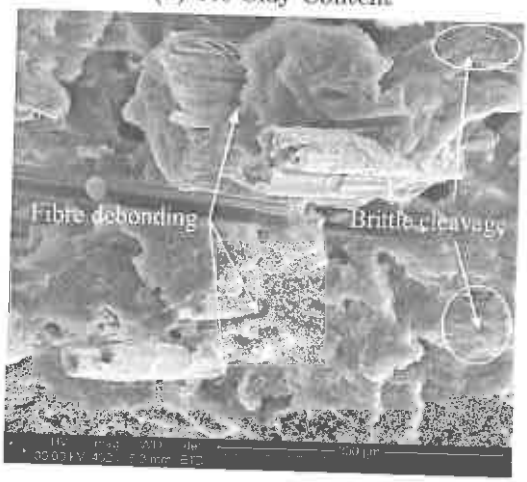

(c) 6% Clay Content

(d) 8% Clay Content

Figure 5.47: SEM images of shear specimens using 0.25% MPS treated fibres with a 1%clay, 2%clay, 6%clay, and 8% clay content in polypropylene matrix

not in the scope of this investigation. The reason for the shear modulus trend after a 2% clay content thus remains inconclusive.

From the mechanical results presented, a predominant trend is seen in the impact energy data. This shows that the increase of clay in a composite causes a corresponding decrease in impact energy. The tensile data and shear data show a small increase in strength using a 2% clay content in a polypropylene matrix when compared to a composite consisting of a virgin polypropylene matrix. The clay content in a polypropylene matrix was therefore fixed at 2% for the remaining investigation.

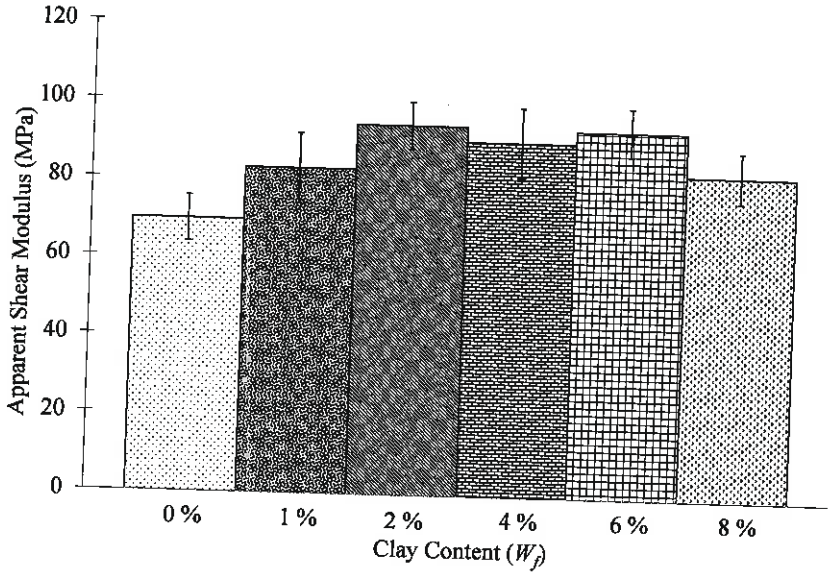

Figure 5.48: Approximate shear modulus - Variation of clay content using 0.25% MPS on kenaf fibres

5.6 Effect of Fibre Weight Fraction on Mechanical Strength

Based on the results presented in Section 5.5, a clay content of 2% by mass is the optimal amount to be mixed into polypropylene to form a clay matrix that yields the highest mechanical properties. All prior investigations were carried out on composites consisting of a constant W_f of 25%. The next investigation is aimed at finding the optimal fibre weight fraction which results in the best mechanical properties. The fibre weight fraction was varied from 15% to 30% for this investigation using both types of matrices; a virgin polypropylene matrix and a polypropylene matrix with 2% clay content.

5.6.1 Effect of W_f in pure PP matrix

The effect of the variation of fibre weight fraction on the tensile strength and tensile modulus of a composite using both types of matrices is presented in Figures 5.49 and 5.50, respectively. Only the data for pure polypropylene is considered in this section.

The tensile strength data show an increase in strength with increasing fibre weight fraction up until a value of 25% W_f,thereafter there is a decrease in strength. Asumani et al. [4]

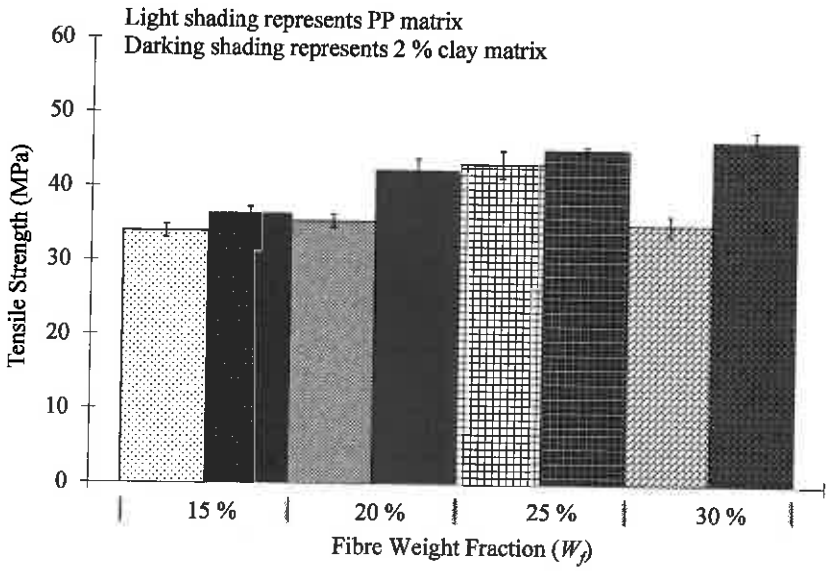

Figure 5.49: Tensile strength - Varying W_f using Polypropylene Matrix and 2% clay matrix with 0.25% MPS on Kenaf Fibre

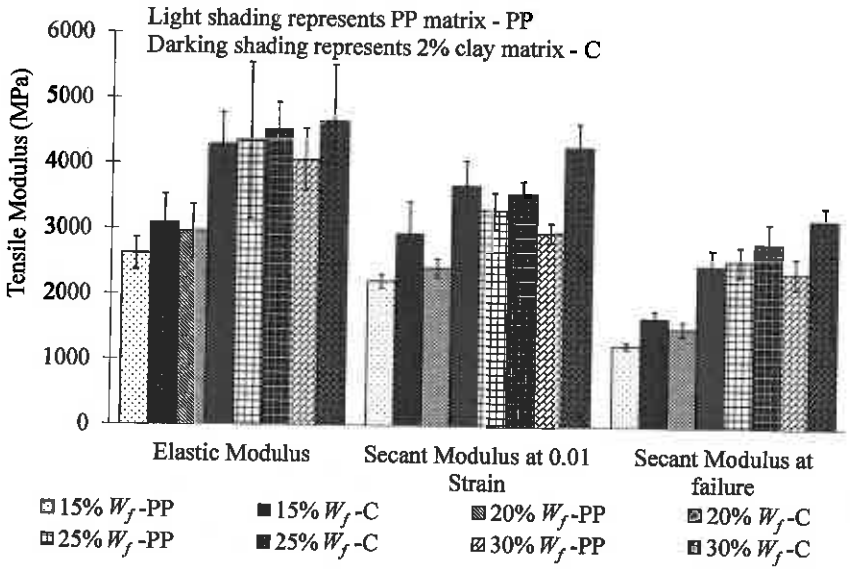

Figure 5.50: Tensile modulus - Varying W_f using Polypropylene Matrix and 2% clay matrix with 0.25% MPS on Kenaf Fibre

conducted a similar investigation, however they varied the fibre weight fraction from 15% to 35%. They found that the tensile strength and modulus increased with W_f up until 30% and thereafter a decrease in tensile strength and modulus was observed. They attributed these inferior results to the presence of voids in the composite which was seen in the fracture surface. The tensile strength data in this research also show that the composite with a 20% W_f has a strength that is lower than expected as it is marginally better than the composite with a 15% W_f. It would thus be useful to determine whether a similar result exists in the tensile modulus data and if voids can be seen in the SEM images, which can be seen in Figures 5.51 and 5.52.

(a) 15% W_f (b) 20% W_f

Figure 5.51: SEM images of tensile specimens using 15% W_f and 20% W_f with 0.25% MPS treated fibres with a PP matrix

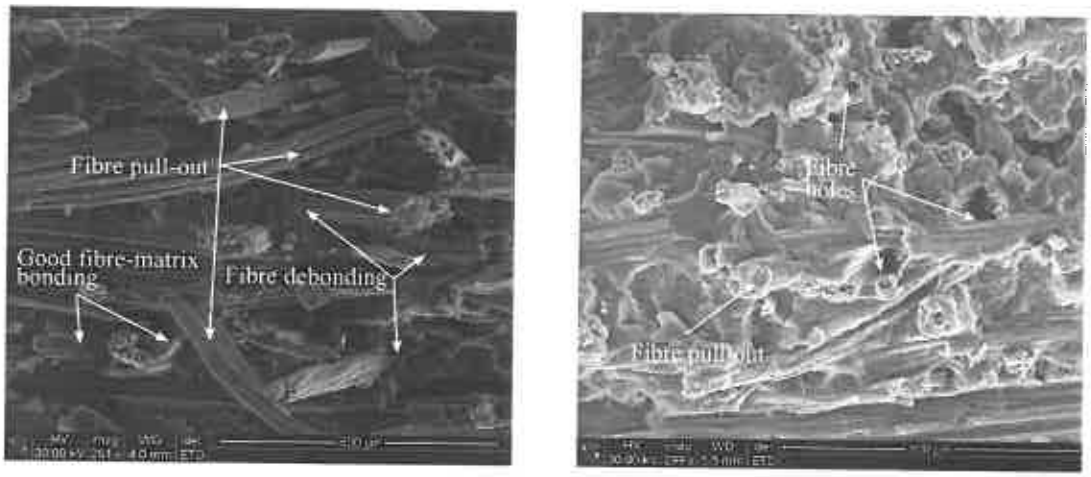

(a) PP Matrix (b) 2% Clay Matrix

Figure 5.52: SEM images of tensile specimens using 30% W_f with 0.25% MPS treated fibres with PP matrix and 2% clay matrix

Figures 5.51a, 5.51b, 5.29a and 5.52a show the fracture surfaces of composites consisting of a virgin polypropylene matrix with a weight fraction of 15%, 20%, 25% and 30%, respectively. The composite having a 30% W_f shows a considerable amount of fibre pull-out and fibre debonding compared to the other composites, which show good fibre-matrix bonding. The fracture surface of the composite with a 25% W_f, seen in Figure 5.29a, shows a flat fracture surface with almost no fibre debonding and fibre pull-out. This supports the tensile strength results which show that the tensile properties of a composite with a 25% W_f are better than the same composite with a 30% W_f. The poor results of the composite with a 30% W_f are possibly attributed to poor wetting of the fibre, as there is a surplus of fibre and possibly not enough matrix to properly wet out the fibres. Figure 5.53 shows a zoomed-out view of the fracture surface of a tensile specimen having a 30% W_f. The fracture surface shows a considerable amount of fibres in the centre that are not properly wetted out with matrix, indicating that the extra fibres make it difficult for the matrix to penetrate into the fibres. This results in voids in the composite which in turn reduce the load capability of the composite [4]. The poor wetting of the fibres prevents the formation of a good fibre-matrix bond, reducing the interfacial shear strength in the composite. Once the fibre weight fraction increases beyond 25% W_f, a large degree of fibre pull-out is evident in the SEM imagery. This is associated with a decrease in tensile strength.

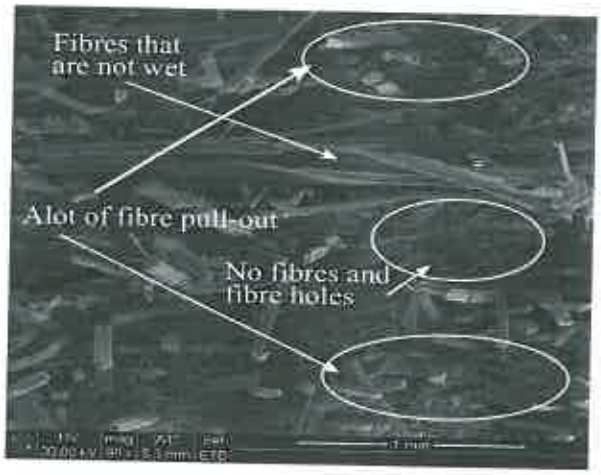

Figure 5.53: Zoomed in section of the composite with a 30% W_f using a PP matrix

Earlier it was shown that a composite with a 20% W_f has poor tensile properties. To understand the reason for these results, it is useful to discuss the fracture surfaces of the composites with a weight fraction of 15%, 20% and 25%. The composite with a 15% W_f has a considerable amount of matrix tearing and snapped fibres close to the fracture surface. The fracture surface of the composite having a 20% W_f shows resemblance to the fracture surface of the specimen having a 25% W_f. Both fracture surfaces show signs of a brittle-like failure. The fact that these composites show similar fracture surfaces implies that the composites underwent similar processes during failure and consequently should result in a similar tensile strength.

However, this is not the case. It is not apparent why the strength of the composite with a 20% W_f is lower than expected. Thus, this will be subject to further investigation.

Figure 5.50 shows the effect of a variation of fibre weight fraction on the tensile modulus of a composite with 0.25% MPS silane. As before, only the data for pure polypropylene are considered. The modulus increases with the increase in W_f [4, 63] up to 25% W_f and thereafter there is a decrease in modulus at 30% W_f. This is similar to the trend found in the tensile strength data. The increase in modulus with the increase in fibre content is a benefit from the rules of mixtures, since the fibres are stiffer than the matrix. The decrease in modulus for the composite with a 30% W_f is attributed to the weaker fibre-matrix bond which reduces the load transferred to the fibres, reducing the composite stiffness. The composite with a 20% W_f has a tensile modulus lower than expected, a similar result to that of the tensile strength results. If the composite with a 20% W_f has poor fibre-matrix bonding, it explains the lower tensile strength and modulus data, however, this does not correlate with the fracture surface image. The impact data provide more information regarding the quality of the fibre-matrix bonding.

Figure 5.54 shows the effect of a variation of fibre weight fraction on impact energy. Considering the data presented for a virgin polypropylene matrix, the data show a trend of increasing impact energy with an increase in fibre weight fraction. This is due to the fact that there are more fibres which result in more fibre pull-out and fibre debonding, which is an energy expensive mode of failure. However, there is a larger increase in impact energy for the composite with a 30% W_f compared to the other fibre weight fractions. This increase can be attributed to poor fibre-matrix bonding as there is not enough matrix to properly wet out the fibres, resulting in a significant amount of fibre pull-out, which uses a lot of energy during impact. This relates well to the lower tensile strength attributed to the composite with a 30% W_f. The composite having a 20% W_f has an impact energy within the trend seen earlier, implying that the fibre-matrix bonding in this composite is the same as the composites with a fibre weight fraction of 15% and 25%. To further investigate the impact energy, it is useful to look at the SEM imagery of the impact specimens which can be seen in Figure 5.55.

Figures 5.55a, 5.33a and 5.55b show the fracture surfaces of impact specimens consisting of a virgin polypropylene matrix with fibre weight fractions of 20%, 25% and 30%, respectively. The composite consisting of a 30% W_f has more fibre holes and fibre pull-out compared to the same composite with a fibre weight fraction of 20% and 25%, whilst the fracture surfaces of the impact specimens having a 20% W_f and 25% W_f show a flat fracture surface with good fibre-matrix bonding. This implies that composites with a 30% W_f have a larger impact energy than a composite having a 25% W_f, which agrees well with the measured data presented in Figure 5.54.

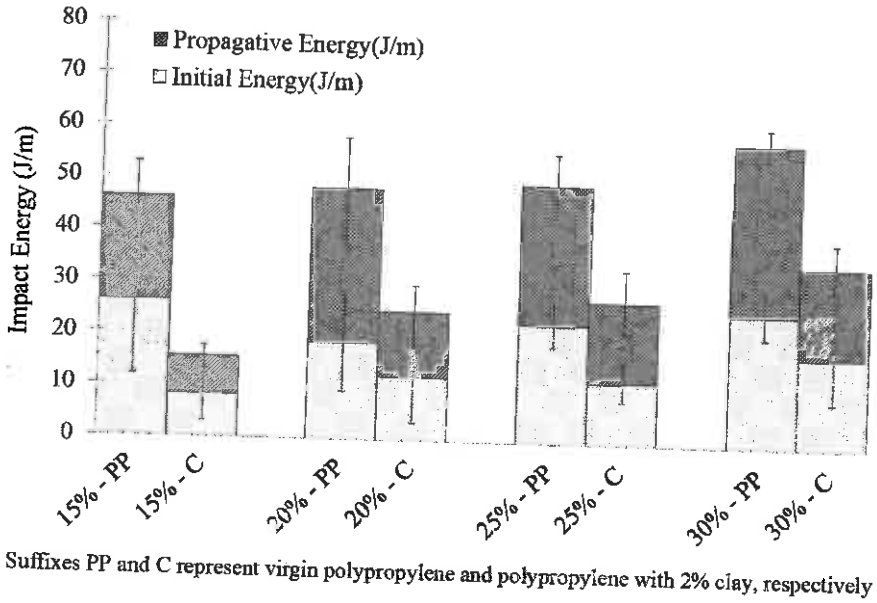

Figure 5.54: Impact energy - Varying W_f using Polypropylene Matrix and 2% clay matrix with 0.25% MPS on Kenaf Fibre

(a) 20% W_f

(b) 30% W_f

Figure 5.55: SEM images of impact specimens using 20% W_f and 30% W_f with 0.25% MPS treated fibres with a polypropylene matrix

Figure 5.56 shows the through-thickness shear strength for composites using 0.25% MPS fibre. Considering the data relating to composites made with virgin polypropylene, a fair degree of scatter can be noted, which makes it difficult to comment on a trend. Considering the data without the error bars, the trend shows a decrease in shear strength with an increase in the composite weight fraction from 15% to 20% followed by a gentle increase in shear

strength, with increasing fibre weight fraction. It is possible, however, that the shear strength is constant across all the fibre weight fractions. The through-thickness shear strength is considerably lower than the tensile strength for all the composites using virgin polypropylene, therefore an assumption can be made that the fibre-matrix interface is the weakest component of the composite, when compared to the matrix and fibres in the composite. Since failure in the tensile results is dominated by the fibre-matrix interface, it is expected that the composites should have a constant shear stress with the variation of the fibre weight fraction. This is further investigated by considering SEM imagery of the shear specimens failure surfaces which can be seen in Figures 5.57, 5.58 and 5.59.

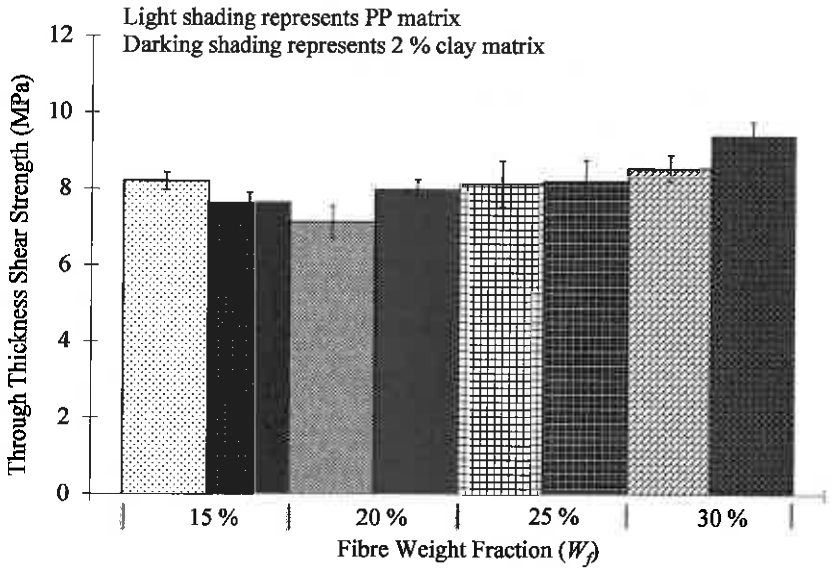

Figure 5.56: Through-thickness shear strength - Varying W_f using Polypropylene Matrix and 2% clay matrix with 0.25% MPS on Kenaf Fibre

Figures 5.57a, 5.58a and 5.59a show the fracture surfaces of shear specimens with a 15% W_f, 20% W_f and 30% W_f, respectively. These images do not show signs of shear failure at the fibre, however, failure at the fibre-matrix interface in the form of fibre debonding can be seen. This supports the hypothesis that failure in virgin polypropylene composites is primarily interface driven. These fracture images all show similar characteristics such as fibre debonding and matrix tearing. This implies that these surfaces underwent the same processes and should thus result in a similar shear strength amongst the specimens tested. This ultimately supports the previous argument which states that the shear strength remains constant for the variation of fibre weight fraction for composites consisting of a virgin polypropylene matrix.

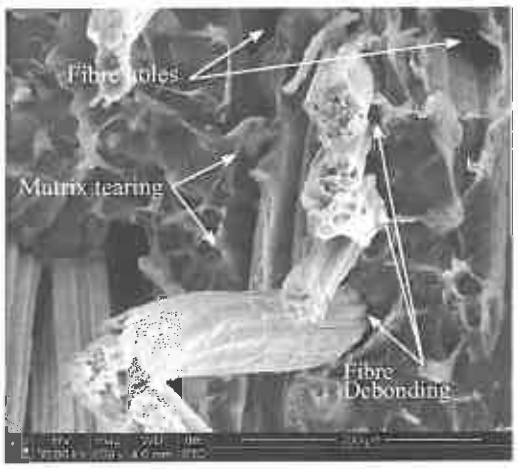

(a) PP Matrix

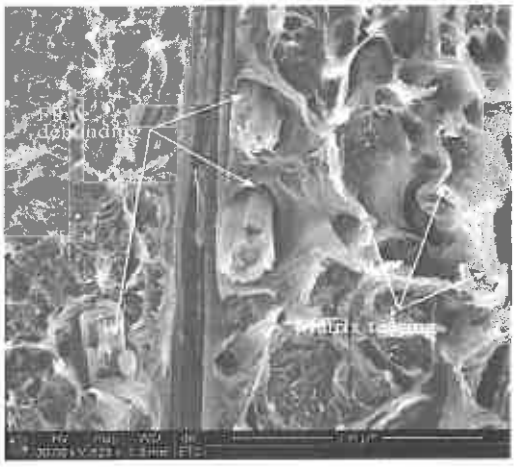

(b) 2% Clay Matrix

Figure 5.57: SEM images of shear specimens using 15% W_f with 0.25% MPS treated fibres with PP matrix and 2% clay matrix

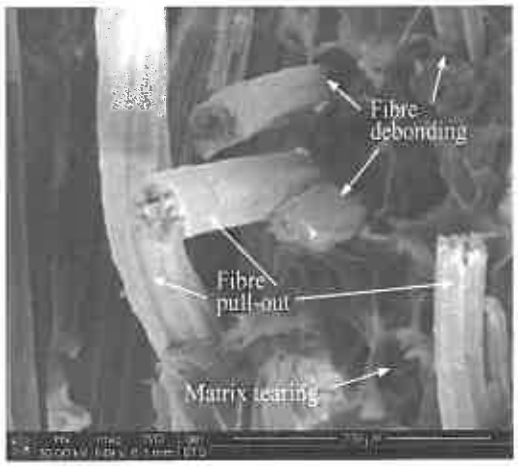

(a) Polypropylene Matrix

(b) 2% Clay Matrix

Figure 5.58: SEM images of shear specimens using 20% W_f with 0.25% MPS treated fibres with PP matrix and 2% clay matrix

Figure 5.60 shows the apparent shear modulus for composites with varying fibre weight fraction using a virgin polypropylene matrix. By focusing on the data of the composites using a virgin polypropylene matrix, it can be seen that the shear modulus shows an approximately constant modulus with a variation in fibre weight fraction, except for the composite with a 20% W_f, which has a modulus that is lower than the rest of the data. The composite with a 20% W_f displayed poor tensile and shear properties. It is possible that this particular composite was poorly manufactured, however, this is not reflected in the SEM images, which show fracture surfaces highlighting good fibre-matrix bonding. Taking into consideration the standards of deviation in the results, it is possible that all the moduli are the same across

(a) PP Matrix (b) 2% Clay Matrix

Figure 5.59: SEM images of shear specimens using 30% W_f with 0.25% MPS treated fibres with PP matrix and 2% clay matrix

the variation of fibre weight fractions. This supports the shear strength data as well as the SEM fracture images.

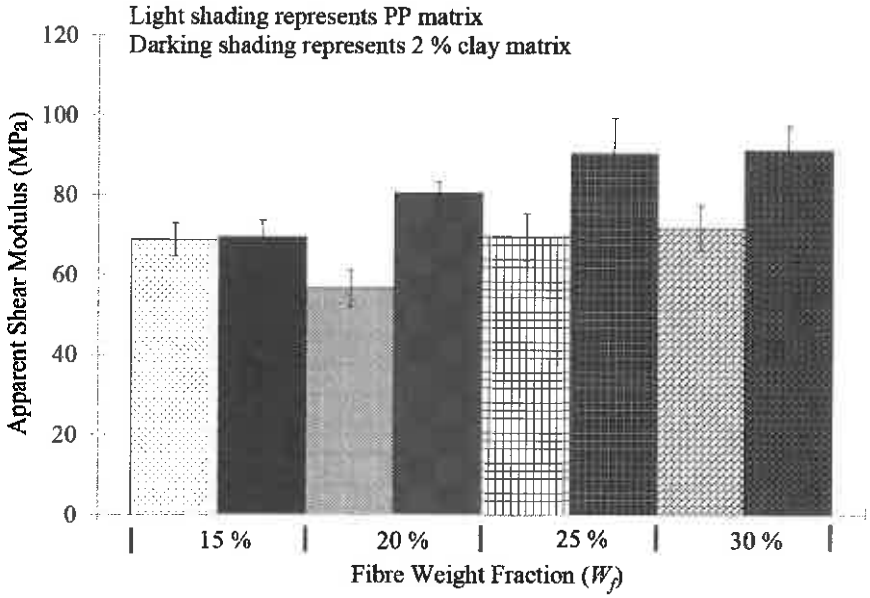

Figure 5.60: Approximate shear modulus - Varying W_f using Polypropylene Matrix and 2% clay matrix with 0.25% MPS on Kenaf Fibre

5.6.2 Effect of W_f on a clay matrix

The effect of the variation in fibre weight fraction on the tensile strength of a composite using both types of matrices are presented in Figure 5.49. The data show that composites with a clay matrix have a larger tensile strength than those with a virgin polypropylene matrix. This is a result that is seen in all the tensile data. Only the data for the composites with a clay matrix are considered in the following discussion. The trend seen in the data is similar to the tensile strength data for composites consisting of a virgin polypropylene matrix except for the composite consisting of a 30% W_f. In the previous discussion, the composite having a 30% W_f had a lower tensile strength than the composite with a 25% W_f, for composites using a virgin polypropylene. This reduction in strength was due to poor impregnation of the matrix. The fact that the strength of the 30% W_f composite with a clay matrix does not decrease from that of the 25% W_f composite is interesting in view of the results for the composites with a pure polypropylene matrix. It is necessary to look at the fracture surface of the tensile specimens consisting of clay to gain a further understanding.

Figures 5.29b and 5.52b show the fracture surfaces of composites consisting of a 2% clay matrix with a 25% and 30% W_f, respectively. The fracture surface of the composite having a 30% W_f has more fibre holes and fibre pull-out than the composite having a 25% W_f with a clay matrix. Generally, a composite that shows more fibre pull-out also shows a lower strength value. This is due to the fact that fibre pull-out is indicative of poor fibre-matrix bonding. This implies that the composite having a 25% W_f should have a larger tensile strength than the composite having a 30% W_f. Considering the scatter in the tensile strength data and the SEM images, it is possible that a composite with a 30% W_f has a lower or the same tensile strength compared to the composite with a 25% W_f. This is possibly due to poor impregnation of the fibres using a clay matrix in a composite with a 30% W_f. This result was also seen for the same composite using a virgin polypropylene matrix. The poor impregnation results in weak interfacial strength, which affects the tensile modulus of the composite.

Considering the tensile modulus data for the composites with a clay matrix, shown in Figure 5.50, the data show a trend of increasing tensile modulus with an increase in fibre weight fraction, as expected [4]. However the trend shows that modulus of the composite with a 30% W_f is lower than expected. The data have a large scatter which could imply that the moduli of the composites with a 25% W_f and 30% are similar. This corresponds to the tensile strength data and will help support the hypothesis regarding poor impregnation.

The impact energy data for the variation of fibre weight fraction using a 2% clay matrix is presented in Figure 5.54. The figure shows a trend of increasing impact energy with the increase in fibre weight fraction. There are two parameters that influence the impact energy

for a clay matrix, the first is the quantity of the matrix in the composite. With an increase in fibre weight fraction, the quantity of matrix in the composite decreases. The matrix containing clay is brittle and this reduces the impact energy of the composite. Decreasing the amount of clay matrix reduces the extent of brittle failure, which increases the impact energy. The second parameter that influences the impact energy is the quantity of fibre. A large amount of energy is required to pull fibres from the matrix therefore, the more fibres in the composite, the higher the impact energy. The figure shows that the impact energy of the composites is reduced for composites using a clay matrix compared to composites with virgin polypropylene matrix. However, the trend of increasing impact energy with increasing fibre weight fraction is dominated by the effect of fibre loading and fibre pull-out.

Figure 5.56 shows the through-thickness shear strength for composites varying in fibre weight fraction using a 2% clay matrix. The figure shows that the shear strength increases with increasing weight fraction. If failure in composites using a clay matrix was dominated by interfacial failure, it would be expected that there will be a constant shear strength with the variation in fibre weight fraction, as seen in the previous discussion. However, in composites having a clay matrix, the addition of clay causes the composite to be brittle, thereby resulting in the matrix being the critical component in the composite. Although it was shown in the previous discussion that shear test results for composites using a clay matrix are less susceptible to matrix cracking, the matrix still remains a critical component.

A possible hypothesis to explain the trend is as follows. In pure polypropylene, the interface is critical which results in a constant shear strength. In clay, the matrix is brittle, thus the matrix is critical. Therefore, with an increase in weight fraction, there is less matrix and more interface, which results in an increase in the shear strength of the composite. Another benefit of the increase in the fibre content are the crack closing forces. The fibres bridge the gap across the fracture and provide a crack closing force which reduces crack growth. It would be expected that as the fibre weight fraction increases, the failure of the composite will be dominated by interface failure, rather than the brittle failure of the matrix, and consequently the shear strength of the composites will increase. It should be kept in mind that the shear strength of a composite using a clay matrix should be larger than that of a virgin polypropylene due to the increased surface roughness in the clay matrix, which results in a better fibre-matrix bond. The images of shear failure are used to investigate this process at work.

Figures 5.57b and 5.59b show the fracture surface of shear specimens consisting of a 2% clay matrix with a 15% W_f and 30% W_f, respectively. The fracture surface of the composite having a 15% W_f shows matrix tearing and fibre debonding, whilst the composite having a 30% W_f shows a considerable amount of fibres (indicating the higher W_f) and fibre debonding. A

comparison of these two images does not aid in supporting the hypothesis, it is thus necessary to look at the shear modulus data.

Figure 5.60 shows the apparent shear modulus for composites varying in fibre weight fraction using a 2% clay matrix. The modulus data show an increase in modulus with an increase in fibre weight fraction. This trend ties up with the shear strength data for composites having a clay matrix. This also supports the hypothesis that the presence of clay and fibre helps increase shear strength. There is also the additional benefit from the rule of mixtures, as the quantity of fibres increases, thereby increasing the modulus of the composite.

In essence the results indicate that composites with a 25% W_f result in the best mechanical properties for both types of matrices. A higher W_f in the composite results in poor matrix impregnation, thereby resulting in an inferior composite. The effect of fibre loading is a dominant factor influencing impact energy, whereby a higher W_f in composite results in a higher impact energy. The through-thickness shear strength for a composite using a virgin polypropylene remains constant with a variation in W_f due to the interface being the critical failure mechanism, whereas the shear strength increases with W_f for a composite having a clay matrix as the matrix is the critical component and fibres help with crack closing.

6 Conclusions

1. Natural fibres show repeatability in strength testing, but moisture absorbed by the kenaf fibre from the atmosphere affects the strength of the composite. The moisture increases the elasticity of the fibre, delaying failure and allows the composite to reach a higher tensile strength.

2. Natural fibre composites should be conditioned for a set time before testing, as the environment affects the amount of moisture absorbed by the composite. This influences the mechanical properties.

3. 175°C is the optimum manufacturing temperature for making kenaf fibre composites consisting of a polypropylene matrix using the compression moulding technique.

4. A 6% sodium hydroxide treatment provides a significant improvement in mechanical properties for a composite consisting of kenaf fibres and both types of matrices and is the most cost effective treatment.

5. Methanol is a better choice than ethanol for administering MPS silane. This is due to the common functional groups in the methanol and MPS molecules. Methanol is also cheaper than ethanol, which adds an economic benefit.

6. As little as 0.25% MPS silane is needed to improve the strength of the composite.

7. Silane marginally improves the strength of a clay matrix composite reinforced with kenaf fibres.

8. 0.25% MPS is the optimum silane concentration for both a virgin polypropylene matrix and a clay/polypropylene matrix.

9. Montmorillonite clay improves the strength and modulus of a kenaf fibre based PP composite but decreases the ability to absorb impact energy.

10. Clay increases the surface roughness of the polypropylene matrix which improves the mechanical bond between the fibres and matrix.

11. The addition of montmorillonite clay to a PP matrix reinforced with kenaf fibres makes the overall composite brittle.

12. 2% is the optimum clay content to be mixed into a polypropylene matrix as it results in the highest tensile strength and modulus.

13. A 25% W_f is optimum for both a virgin PP matrix and a PP matrix with 2% clay content.

14. SEM is effective in validating the modes of failure for composites and identifying the effectiveness of bonding agents.

15. FTIR is useful for identifying the chemical bonds created and destroyed in the manufacturing process and can assist in identifying the effect of chemical treatments on kenaf fibres.

7 Recommendations

1. Manufacture a new thermal compression rig with a more accurate temperature control, whereby the exact moulding temperature can be maintained.
2. Make use of a pump and reservoir system for the manufacture of mats to save water.
3. Investigate the effect of the clay concentration on the water absorption properties of a kenaf reinforced composite.

References

[1] M.J. John and R.D. Anandjiwala. Recent Developments in Chemical Modification and Characterization of Natural Fiber-Reinforced Composites. *Polymer Composites*, 29(2): 187–207, 2008.

[2] A.K. Mohanty, M. Misra, and G. Hinrichsen. Biofibres, biodegradable polymers and biocomposites: An overview. *Macromolecular Materials and Engineering*, 276(1):1–24, 2000.

[3] R. Malkapuram and V. Kumar. Recent Development in Natural Fiber Reinforced Polypropylene Composites. *Journal of Reinforced Plastics and Composites*, 28(10):1169–1189, 2008.

[4] O.M.L. Asumani, R.G. Reid, and R. Paskaramoorthy. The effects of alkali silane treatment on the tensile and flexural properties of short fibre non-woven kenaf reinforced polypropylene composites. *Composites Part A*, 43(9):1431–1440, 2012.

[5] H.M. Akil, M.F. Omar, A.A.M. Mazuki, S. Safiee, Z.A.M. Ishak, and A. Bakar. Kenaf Fiber Reinforced Composites: A review. *Materials and Design*, 32(8):4107–4121, 2011.

[6] N.G. Danalatos and S.V. Archontoulis. Growth and Biomass Productivity of Kenaf (Hibiscus cannabinus, L.) Under Different Agricultural Inputs and Management Practices in Central Greece. *Industrial Crops and Products*, 32(3):231–240, 2010.

[7] A.K. Bledzki and J. Gassan. Composites Reinforced with Cellulose Based Fibres. *Progress in Polymer Science*, 24(2):221–274, 1999.

[8] J. Summerscales, N. Dissanayake, A. Virk, and W. Hall. A Review of Bast Fibres and their Composites. Part 2 Composites. *Composites Part A: Applied Science and Manufacturing*, 41(10):1336–1344, 2010.

[9] P. Wambua, J. Ivens, and I. Verpoest. Natural fibres: Can They Replace Glass in Fibre Reinforced Plastics? *Composites Science and Technology*, 63(9):1259–1264, 2003.

[10] M.M. Kabir, H. Wang, K.T. Lau, and F. Cardona. Chemical treatments on plant-based natural fibre reinforced polymer composites: An overview. *Composites Part B: Engineering*, 43(7):2883–2892, 2012.

[11] A.K. Mohanty, M. Misra, and L.T. Drzal. Surface Modifications of Natural Fibers and Performance of the Resulting Biocomposites: An overview. *Composite Interfaces*, 8(5): 313–343, 2001.

[12] D. García-López. Polypropylene Clay Nanocomposites: Effect of Compatibilizing Agents on Clay Dispersion. *European Polymer Journal*, 39(5):945–950, 2003.

[13] H. Shariatpanahi, F. Sarabi, M. Mirali, M. Hemmati, and F. Mahdavi. Polypropylene-Organoclay Nanocomposite : Preparation , Microstructure , and Mechanical Properties. *Journal of Applied Polymer Science*, 113(2):2–6, 2009.

[14] F.C. Chiu, S.M. Lai, J.W. Chen, and P.H. Chu. Combined Effects of Clay Modifications and Compatibilizers on the Formation and Physical Properties of Melt-mixed Polypropylene/Clay Nanocomposites. *Journal of Polymer Science Part B: Polymer Physics*, 42 (22):4139–4150, 2004.

[15] J.A. Tarapow, C.R. Bernal, and V.A. Alvarez. Mechanical Properties of Polypropylene / Clay Nanocomposites : Effect of Clay Content , Polymer / Clay Compatibility , and Processing Conditions. *Journal of Applied Polymer Science*, 111(2):768–778, 2008.

[16] R. Mahjoub, J.M. Yatim, A. Rahman, and S.H. Hashemi. Tensile properties of kenaf fiber due to various conditions of chemical fiber surface modifications. *Construction and Building Materials*, 55(1):103–113, 2014.

[17] T. Nishino. Natural fibre sources. In Caroline Baillie, editor, *Green Composites*, Woodhead Publishing Series in Composites Science and Engineering, pages 49 – 80. Woodhead Publishing, 2004.

[18] S. Blouw and D.A. Rajesh. Composites from Bast Fibres- Prospects and Potential in the Changing Market Environment. *Journal of Natural Fibres*, 4(2):37–41, 2007.

[19] D.N. Saheb and J.P. Jog. Natural Fiber Polymer Composites: A Review. *Advances in Polymer Technology*, 18(4):351–363, 1999.

[20] A. Bismarck, I. Aranbefwi-Askargorta, T. Lampkfc, and B. Wielage. Surface Characterization of Flax, Hemp and Cellulose Fibers; Surface Properties and the Water Uptake Behavior. *Polymer Composites*, 23(5):872–894, 2002.

[21] S. Deng, A. Beehag, W. Hillier, D. Zhang, and L. Ye. Kenaf-Polypropylene Composites Manufactured from Blended Fiber Mats. *Journal of Reinforced Plastics and Composites*, 32(16):1198–1210, 2013.

[22] N. Sallih, P. Lescher, and D. Bhattacharyya. Factorial Study of Material and Process Parameters on the Mechanical Properties of Extruded Kenaf Fibre/Polypropylene Composite Sheets. *Composites Part A: Applied Science and Manufacturing*, 61(2):91–107, 2014.

[23] T.T. Law and Z.A.M. Ishak. Water Absorption and Dimensional Stability of Short Kenaf Fiber-Filled Polypropylene Composites Treated with Maleated Polypropylene. *Journal of Applied Polymer Science*, 120(1):563–572, 2010.

[24] M. C. Symington, W.M. Banks, O. D. West, and R.A. Pethrick. Tensile Testing of Cellulose Based Natural Fibers for Structural Composite Applications. *Journal of Composite Materials*, 43(9):1083–1108, 2009.

[25] X. Li, L.G. Tabil, and S. Panigrahi. Chemical Treatments of Natural Fiber for Use in Natural Fiber-Reinforced Composites: A Review. *Journal of Polymers and the Environment*, 15(1):25–33, 2007.

[26] A.M.M. Edeerozey, H.M. Akil, A.B. Azhar, and M.I.Z. Ariffin. Chemical Modification of Kenaf Fibers. *Materials Letters*, 61(10):2023–2025, 2007.

[27] Y. Xie, S.A.C. Hill, A, Z. Xiao, H. Militz, and C. Mai. Silane Coupling Agents used for Natural Fiber/Polymer Composites: A Review. *Composites Part A: Applied Science and Manufacturing*, 41(7):806–819, 2010.

[28] M.S. Huda, L.T. Drzal, A.K. Mohanty, and M. Misra. Effect of Fiber Surface-Treatments on the Properties of Laminated Biocomposites from Poly(lactic acid) (PLA) and Kenaf Fibers. *Composites Science and Technology*, 68(2):424–432, 2008.

[29] D. Cho, H.S. Lee, and S. Han. Effect of Fiber Surface Modification on the Interfacial and Mechanical Properties of Kenaf Fiber-Reinforced Thermoplastic and Thermosetting Polymer Composites. *Composite Interfaces*, 16(7):711–729, 2009.

[30] M. Kawasumi, N. Hasegawa, M. Kato, and A. Usuki. Preparation and Mechanical Properties of Polypropylene - Clay Hybrids using a Maleic Anhydride-modified Polypropylene Oligomer. *Macromolecules*, 67(1):87–92, 1998.

[31] L. Delva, K. Ragaert, J. Degrieck, and L. Cardon. The Effect of Multiple Extrusions on the Properties of Montmorillonite Filled Polypropylene. *Polymers*, 6(12):2912–2927, 2014.

[32] A. Vermogen, K. Masenelli-Varlot, R. Se, S. Boucard, and P. Prele. Evaluation of the Structure and Dispersion in Polymer-Layered Silicate Nanocomposites. *Macromolecules*, 38(23):9661–9669, 2005.

[33] Y. Zhang and J. Lee. Science and Polypropylene : Clay Nanocomposites Prepared by in Situ Grafting-intercalating in Melt. *Composites Science and Technology*, 64(9): 1383–1389, 2004.

[34] F. Uddin. Clays, Nanoclays, and Montmorillonite Minerals. *Metallurgical and Materials Transactions A*, 39(12):2804–2814, 2008.

[35] C.O. Rohlmann, M.F. Horst, L.M. Quinzani, and M.D. Failla. Comparative Analysis of Nanocomposites Based on Polypropylene and Different Montmorillonites. *European Polymer Journal*, 44(9):2749–2760, 2008.

[36] M.L. López-Quintanilla, S. Sánchez-Valdés, L.F. Ramos de Valle, and R. Guedea Miranda. Preparation and Mechanical Properties of PP/PP-g-MA/Org-MMT Nanocomposites with Different MA Content. *Polymer Bulletin*, 57(3):385–393, 2006.

[37] L. Chen, S. Wong, and S. Pisharath. Fracture Properties of Nanoclay-Filled Polypropylene. *Journal of Applied Polymer Science*, 88(14):3298–3305, 2003.

[38] E.P. Giannelis, R. Krishnamoorthi, and E. Manias. Polmer-silicate Nanocomposites: Model Systems for Confined Polymers and Polymer Brushes. *Advances in Polymer Science*, 138(2):108–147, 1999.

[39] M.J. Solomon, A.S. Almusallam, K.F. Seefeldt, A. Somwangthanaroj, and P. Varadan. Rheology of Polypropylene/Clay Hybrid Materials. *Macromolecules*, 34(6):1864–1872, 2001.

[40] V. Mittal. Polypropylene-Layered Silicate Nanocomposites: Filler Matrix Interactions and Mechanical Properties. *Journal of Thermoplastic Composite Materials*, 20(6):575–599, 2007.

[41] M. Lewin, E.M. Pearce, K. Levon, A. Mey-Marom, M. Zammarano, C.A. Wilkie, and B.N. Jang. Nanocomposites at Elevated Temperatures : Migration and Structural Changes . *Polymers for Advanced Technologies*, 17(2):226–234, 2006.

[42] F. Ka and E. Fekete. Surface Characteristics of Layered Silicates : Influence on the Properties of Clay / Polymer Nanocomposites. *Langmuir*, 22(10):7848–7854, 2006.

[43] M. Alexandre and P. Dubois. Polymer-layered Silicate Nanocomposites : Preparation , Properties and Uses of a New Class of Materials. *Material Science and Engineering*, 28 (1):1–63, 2000.

[44] M. Ataeefard and S. Moradian. Polypropylene/Organoclay Nanocomposites: Effects of Clay Content on Properties. *Polymer-Plastics Technology and Engineering*, 50(7): 732–739, 2011.

[45] K. Kim, H. Kim, and J. Lee. Effect of Interlayer Structure , Matrix Viscosity and Composition of a Functionalized Polymer on the Phase Structure of Polypropylene-Montmorillonite Nanocomposites. *Polymer Engineering and Science*, 41(11):1963–1969, 2001.

[46] S.N. Sathe, S. Devi, G.S. Rao, and K.V. Rao. Relationship between Morphology and Mechanical Properties of Binary and Compatibilized Ternary Blends of Polypropylene and Nylon-6. *Journal of Applied Polymer Science*, 61(1):97–107, 1996.

[47] W.S. Chow, I. Mohd, J. Karger-Kocsis, A.A. Apostolov, and U.S. Ishiaku. Compatibilizing Effect of Maleated Polypropylene on the Mechanical Properties and Morphology of Injection Molded Polyamide 6/Polypropylene/Organoclay Nanocomposites. *Polymer*, 44(24):7427–7440, 2003.

[48] C. Ding, D. Jia, H. He, B. Guo, and H. Hong. How Organo-Montmorillonite Truly Affects the Structure and Properties of Polypropylene. *Polymer Testing*, 24(1):94–100, 2005.

[49] W. Xu, M. Ge, and P. He. Nonisothermal Crystallization Kinetics of Polypropylene/Montmorillonite Nanocomposites. *Journal of Polymer Science Part B: Polymer Physics*, 40(5):408–414, 2002.

[50] M. Abdelmouleh, S. Boufi, and M. Belgacem. Short Natural-Fibre Reinforced Polyethylene and Natural Rubber Composites: Effect of Silane Coupling Agents and Fibres Loading. *Composites Science and Technology*, 67(7):1627–1639, 2007.

[51] K. Sever, M. Sarikanat, Y. Seki, G. Erkan, and U. H. Erdogan. The Mechanical Properties of 3-Methacryloxypropyltrimethoxy Silane-Treated Jute/Polyester Composites. *Journal of Composite Materials*, 44(15):1913–1924, 2010.

[52] L. Paiken. The effects of alkali-silane treatment and filler materials on the tensile and water absorption properties of hemp fibre reinforced polypropylene. Master's thesis, School of Mechanical, Industrial and Aeronautical Engineering, University of Witwatersrand, 2012.

[53] Y. Dong and D. Bhattacharyya. Effects of Clay Type, Clay/Compatibiliser Content and Matrix Viscosity on the Mechanical Properties of Polypropylene/Organoclay Nanocomposites. *Composites Part A: Applied Science and Manufacturing*, 39(7):1177–1191, 2008.

[54] ASTM D638-14, Standard Test Method for Tensile Properties of Plastics, ASTM International, West Conshohocken, PA, 2014, viewed March 2017, www.astm.org , .

[55] ASTM D256-10, Standard Test Methods for Determining the Izod Pendulum Impact Resistance of Plastics, ASTM International, West Conshohocken, PA, 2010, viewed March 2017, www.astm.org, .

[56] ASTM D2344 / D2344M-00e1, Standard Test Method for Short-Beam Strength of Polymer Matrix Composite Materials and Their Laminates, ASTM International, West Conshohocken, PA, 2000, viewed March 2017, www.astm.org,

[57] A. Khan, T. Huq, M. Saha, R. A. Khan, M. A. Khan, and M. A. Gafur. Effect of Silane Treatment on the Mechanical and Interfacial Properties of Calcium Alginate Fiber Reinforced Polypropylene Composite. *Journal of Composite Materials*, 44(24):2875–2886, 2010.

[58] V.T. Ganesh (2016), What is shear stress?, viewed 30 January 2017, https://www.quora.com/What-is-shear-stress.

[59] D.R. Askeland. *Essential of Materials Science and Engineering.* CENGAGE learning, 2010.

[60] M. Ho, H. Wang, J. Lee, C. Ho, K. Lau, J. Leng, and D. Hui. Critical Factors on Manufacturing Processes of Natural Fibre Composites. *Composites Part B: Engineering*, 43(8):3549–3562, 2012.

[61] M.K. Thakur, R.K. Gupta, and V.K. Thakur. Surface Modification of Cellulose using Silane Coupling Agent. *Carbohydrate Polymers*, 111(1):849–855, 2014.

[62] P.J. Herrera-Franco and A. Valadez-González. A Study of the Mechanical Properties of Short Natural-Fiber Reinforced Composites. *Composites Part B: Engineering*, 36(8): 597–608, 2005.

[63] S. Ochi. Mechanical Properties of Kenaf Fibers and Kenaf/PLA Composites. *Mechanics of Materials*, 40(4):446–452, 2008.

[64] A. Espert, F. Vilaplana, and S. Karlsson. Comparison of Water Absorption in Natural Cellulosic Fibres from Wood and One-year Crops in Polypropylene Composites and Its Influence on their Mechanical Properties. *Composites Part A: Applied Science and Manufacturing*, 35(11):1267–1276, 2004.

[65] G.N. Farahani, I. Ahmad, and Z. Mosadeghzad. Effect of Fiber Content, Fiber Length and Alkali Treatment on Properties of Kenaf Fiber/UPR Composites Based on Recycled PET Wastes. *Polymer-Plastics Technology and Engineering*, 51(6):634–639, 2012.

[66] J. Summerscales and S. Grove. *Interface Engineering of Natural Fibre Composites for Maximum Performance.* Woodhead Publishing Limited, 2014.

[67] S. Kalia, B.S. Kaith, and I. Kaur. Pretreatments of Natural Fibers and their Application as Reinforcing Material in Polymer Composites A Review. *Polymer Engineering and Science*, 49(7):1253–1272, 2009.

[68] G. Canch-Escamilla, J. Rodriguez-Laviada, J.I. Cauich-Cupul, E. Mendizbal, J.E. Puig, and P.J. Herrera-Franco. Flexural, Impact and Compressive Properties of a Rigid-Thermoplastic Matrix/Cellulose Fiber Reinforced Composites . *Composites Part A: Applied Science and Manufacturing*, 33(4):539–549, 2002.

[69] D.H. Mueller and A. Krobjilowski. New Discovery in the Properties of Composites Reinforced with Natural Fibers. *Journal of Industrial Textiles*, 33(2):111–130, 2003.

[70] Y. Li, Y.W. Mai, and L. Ye. Effects of Fibre Surface Treatment on Fracture-Mechanical Properties of Sisal-Fibre Composites. *Composite Interfaces*, 12(1):141–163, 2005.

[71] J.M. Whitney and C.E. Browning. On Short-Beam Shear Tests for Composite Materials. *Experimental Mechanics*, 25(3):294–300, 1985.

[72] E. Lunsing. Biofiber-Reinforced Polypropylene Composites. *Polymer Engineering and Science*, 37(2):476–483, 1997.

[73] R. Olayo. Fibers with an Organosilane Coupling Chemical Modification of Heneque Agent. *Composites Part B: Engineering*, 30(3):321–331, 1999.

[74] K.K. Chawla. *Composite Materials - Science and Engineering*. Springer, Birmingham, Alabama, 2001.

[75] Y. Dong and D. Bhattacharyya. Investigation on the Competing Effects of Clay Dispersion and Matrix Plasticisation for Polypropylene /Clay Nanocomposites . Part I : Morphology and Mechanical Properties. *Journal of Materials Science*, 47(8):3900–3912, 2012.

[76] N.A. Ibrahim, B.W. Chieng, and W.M.Z. Yunus. Morphology, Thermal and Mechanical Properties of Biodegradable Poly(Butylene Succinate)/Poly(Butylene Adipate-co-terephthalate)/Clay Nanocomposites. *Polymer-Plastics Technology and Engineering*, 49 (15):1571–1580, 2010.

[77] N. Hasegawa, H. Okamoto, M. Kato, and A. Usuki. Preparation and Mechanical Properties of Polypropylene/Clay Hybrids based on Modified Polypropylene and Organophilic Clay. *Journal of Applied Polymer Science*, 78(11):1918–1922, 2000.

[78] K. Kalaitzidou, H. Fukushima, and L.T. Drzal. Mechanical Properties and Morphological Characterization of Exfoliated Graphite/Polypropylene Nanocomposites. *Composites Part A*, 38(7):1675–1682, 2007.

[79] Q. Yuan and R.D.K. Misra. Impact Fracture Behavior of Clay Reinforced Polypropylene Nanocomposites. *Polymer*, 47(12):4421–4433, 2006.

[80] C. Deshmane, Q. Yuan, R.S. Perkins, and R.D.K. Misra. On Striking Variation in Impact Toughness of Polyethylene/Clay and Polypropylene/Clay Nanocomposite Systems : The Effect of Clay/Polymer Interaction. *Materials Science and Engineering: A*, 458(1):150–157, 2007.

[81] S.S. Ray, M. Scriba, and J. Wesley-Smith. A Combined Experimental and Theoretical Approach to Establish the Relationship between Shear Force and Clay Platelet. *Polymer*, 55(9):2233–2245, 2015.

[82] Y.A. El-Shekeil. Influence of Chemical Treatment on the Tensile Properties of Kenaf Fiber Reinforced Thermoplastic Polyurethane Composite. *Express Polymer Letters*, 6 (12):1032–1040, 2012.

[83] N. Sgriccia, M.C. Hawley, and M. Misra. Characterization of Natural Fiber Surfaces and Natural Fiber Composites. *Composites Part A: Applied Science and Manufacturing*, 39 (10):1632–1637, 2008.

[84] L.Y. Mwaikambo and M.P. Ansell. Chemical Modification of Hemp, Sisal, Jute, and Kapok Fibers by Alkalization. *Applied Polymer Science*, 84(12):2222–2234, 2002.

[85] A.K. Mubarak and Lawrence T.D. Characterization of 2-hydroxyethyl Methacrylate (HEMA)-Treated Jute Surface Cured by UV Radiation. *Journal of Adhesion Science and Technology*, 18(3):381–393, 2004.

[86] B.W. Jo, S.K. Park, and D.K. Kim. Mechanical Properties of Nano-MMT Reinforced Polymer Composite and Polymer Concrete. *Construction and Building Materials*, 22(1): 14–20, 2008.

[87] V.P. Rajan and F.W. Zok. Matrix Cracking of Fiber-Reinforced Ceramic Composites in Shear. *Journal of the Mechanics and Physics of Solids*, 73(1):3–21, 2014.

Appendix A Data Specification Sheets

Product data sheet

HLR102

Polypropylene homopolymer

Technical Support:
Polymer Technology Services Centre
PO Box 72
Modderfontein 1645
South Africa

Tel: +27 (0)11 458 0700
Fax: +27 (0)11 458 0734

Sales office:
Sasol Polymers
PO Box 2525
Randburg 2125
South Africa

Tel: +27 (0)11 790 1413
Fax: +27 (0)11 344 0287

Date of Issue: January 2012

www.sasol.com/polymers

Sasol Polymers
Polyolefins Business

Sasol Polymers PP: HLR102

MFR: 5.3g/10min

Features

- Medium flow
- Low water carry over during the extrusion process
- Particularly suitable for processing on high speed tape extrusion lines

Applications

Extrusion

- Production of raffia tapes as used in the manufacture of woven fabric
- Block-bottom cement bags
- Sacks and bags
- Flexible intermediate bulk containers (FIBC's)

Injection moulding

- Domestic, industrial and general purpose articles

Additives

- High processing stabilisation

Material properties *(typical values not to be construed as specifications)*

	Value	Unit	Test method
Rheological properties			
Melt mass-flow rate - MFR (230/2.16)	5.3	g/10min	ISO 1133
Moulding Shrinkage - S_{Mp} / S_{Mn}	1.5 / 1.4	%	ISO 294-4
Mechanical properties			
Flexural modulus	1500	MPa	ISO 178
Tensile modulus of elasticity	1550	MPa	ISO 527-2/1A/1
Tensile stress at yield	34	MPa	ISO 527-2/1A/50
Tensile strain at yield	9.0	%	ISO 527-2/1A/50
Tensile strain at break	>50	%	ISO 527-2/1A/50
Charpy notched impact strength (23°C)	3.5	kJ/m^2	ISO 179-1/1eA
Ball indentation hardness - HB	72	N/mm^2	ISO 2039-1
Thermal properties			
Melting temperature - DSC	163	°C	ISO 11357-3
Heat deflection temperature - HDT/A (1.8 MPa)	53	°C	ISO 75-2
Heat deflection temperature - HDT/B (0.45 MPa)	85	°C	ISO 75-2
Vicat softening temperature - VST/A 120 (10N)	154	°C	ISO 306
Vicat softening temperature - VST/B 120 (50N)	90	°C	ISO 306
Other properties			
Density	0.905	g/cm^3	ISO 1183-1

SIGMA-ALDRICH®

sigma-aldrich.com

3050 Spruce Street, Saint Louis, MO 63103, USA
Website: www.sigmaaldrich.com
Email USA: techserv@sial.com
Outside USA: eurtechserv@sial.com

Product Specification

Product Name:
Nanoclay, surface modified - contains 35-45 wt. % dimethyl dialkyl (C14-C18) amine

Product Number: **682624**

TEST	Specification
Appearance (Color)	Beige
Appearance (Form)	Powder
Loss on Drying	≤ 3 %
Bulk Density	200 - 500 kg/m3
Size	≤ 20 micron
Average Particle Size	

Specification: PRD.0.ZQ5.10000023456

Sigma-Aldrich warrants, that at the time of the quality release or subsequent retest date this product conformed to the information contained in this publication. The current Specification sheet may be available at Sigma-Aldrich.com. For further inquiries, please contact Technical Service. Purchaser must determine the suitability of the product for its particular use. See reverse side of invoice or packing slip for additional terms and conditions of sale.

3050 Spruce Street, Saint Louis, MO 63103, USA
Website: www.sigmaaldrich.com
Email USA: techserv@sial.com
Outside USA: eurtechserv@sial.com

Product Specification

Product Name:
Polypropylene-graft-maleic anhydride - average Mw ~9,100 by GPC, average Mn ~3,900 by GPC, maleic anhydride 8-10 wt. %

Product Number:	**427845**
CAS Number:	25722-45-6
MDL:	MFCD00212584
Formula:	C7H8O3

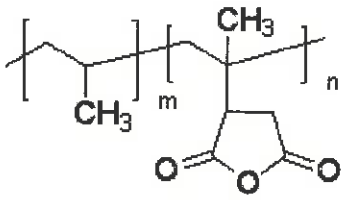

TEST	Specification
Appearance (Color)	Conforms to Requirements
Yellow or Tan	
Appearance (Form)	Beads or Pellets
Viscosity	150 - 700 cps
Acid Value	40.0 - 55.0
mg KOH/g	

Specification: PRD.0.ZQ5.10000038283

Sigma-Aldrich warrants, that at the time of the quality release or subsequent retest date this product conformed to the information contained in this publication. The current Specification sheet may be available at Sigma-Aldrich.com. For further inquiries, please contact Technical Service. Purchaser must determine the suitability of the product for its particular use. See reverse side of invoice or packing slip for additional terms and conditions of sale.

Model Number	ICP® ACCELEROMETER	Revision: G
353B03		ECN #: 35369

Performance	ENGLISH	SI	
Sensitivity(± 5 %)	10 mV/g	1.02 mV/(m/s²)	[2]
Measurement Range	± 500 g pk	± 4905 m/s² pk	
Frequency Range(± 5 %)	1 to 7000 Hz	1 to 7000 Hz	
Frequency Range(± 10 %)	0.7 to 11,000 Hz	0.7 to 11,000 Hz	
Frequency Range(± 3 dB)	0.35 to 20,000 Hz	0.35 to 20,000 Hz	
Resonant Frequency	≥ 38 kHz	≥ 38 kHz	
Broadband Resolution(1 to 10,000 Hz)	0.003 g rms	0.03 m/s² rms	[1]
Non-Linearity	≤ 1 %	≤ 1 %	[3]
Transverse Sensitivity	≤ 5 %	≤ 5 %	[4]
Environmental			
Overload Limit(Shock)	± 10,000 g pk	± 98,100 m/s² pk	
Temperature Range(Operating)	-65 to +250 °F	-54 to +121 °C	
Temperature Response	See Graph	See Graph	[1]
Base Strain Sensitivity	≤ 0.0005 g/με	≤ 0.005 (m/s²)/με	[1]
Electrical			
Excitation Voltage	18 to 30 VDC	18 to 30 VDC	
Constant Current Excitation	2 to 20 mA	2 to 20 mA	
Output Impedance	≤ 100 ohm	≤ 100 ohm	
Output Bias Voltage	8 to 12 VDC	8 to 12 VDC	
Discharge Time Constant	0.5 to 2.5 sec	0.5 to 2.5 sec	
Settling Time(within 10% of bias)	<5 sec	<5 sec	
Spectral Noise(1 Hz)	2800 µg/√Hz	27,468 (µm/sec²)/√Hz	[1]
Spectral Noise(10 Hz)	700 µg/√Hz	6867 (µm/sec²)/√Hz	[1]
Spectral Noise(100 Hz)	180 µg/√Hz	1766 (µm/sec²)/√Hz	[1]
Spectral Noise(1 kHz)	64 µg/√Hz	628 (µm/sec²)/√Hz	[1]
Physical			
Sensing Element	Quartz	Quartz	
Sensing Geometry	Shear	Shear	
Housing Material	Titanium	Titanium	
Sealing	Welded Hermetic	Welded Hermetic	
Size (Hex x Height)	0.50 in x 0.81 in	12.7 mm x 20.6 mm	
Weight	0.38 oz	10.5 gm	[1]
Electrical Connector	10-32 Coaxial Jack	10-32 Coaxial Jack	
Electrical Connection Position	Side	Side	
Mounting Thread	10-32 Female	10-32 Female	

CE [5]

Typical Sensitivity Deviation vs Temperature

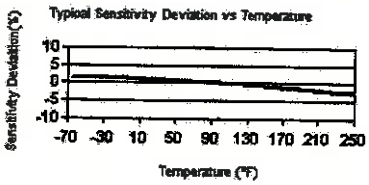

All specifications are at room temperature unless otherwise specified.
In the interest of constant product improvement, we reserve the right to change specifications without notice.

ICP® is a registered trademark of PCB Group, Inc.

OPTIONAL VERSIONS

Optional versions have identical specifications and accessories as listed for the standard model except where noted below. More than one option may be used.

B - Low bias electronics		
Output Bias Voltage	4.5 to 7.5 VDC	4.5 to 7.5 VDC
Excitation Voltage	12 to 30 VDC	12 to 30 VDC
Constant Current Excitation	1 to 20 mA	1 to 20 mA
Measurement Range	± 300 g pk	± 2943 m/s² pk
J - Ground Isolated		
Frequency Range(± 5 %)	1 to 5000 Hz	1 to 5000 Hz
Frequency Range(± 10 %)	0.7 to 9000 Hz	0.7 to 9000 Hz
Resonant Frequency	≥ 22 kHz	≥ 22 kHz
Electrical Isolation(Base)	≥ 10^8 ohm	≥ 10^8 ohm
Size - Hex x Height	0.50 in x 0.66 in	12.7 mm x 21.8 mm
Q - Extended discharge time constant		
Frequency Range(± 5 %)	0.1 to 7000 Hz	0.1 to 7000 Hz
Frequency Range(± 10 %)	0.07 to 11,000 Hz	0.07 to 11,000 Hz
Discharge Time Constant	>10 sec	>10 sec
Settling Time(within 10% of bias)	45 sec	45 sec
Supplied Accessory : Model ACS-4 Single axis, low frequency phase and amplitude response cal from 0.6 to 10 Hz (1)		
W - Water Resistant Cable		
Electrical Connector	Sealed Integral Cable	Sealed Integral Cable
Electrical Connection Position	Side	Side

NOTES:
[1] Typical
[2] B and Q options supplied with a sensitivity tolerance of ± 10 %.
[3] Zero-based, least-squares, straight line method.
[4] Transverse sensitivity is typically ≤ 3%.
[5] See PCB Declaration of Conformance PS023 for details.

SUPPLIED ACCESSORIES:
Model 080A Adhesive Mounting Base (1)
Model 080A109 Petro Wax (1)
Model 081B05 Mounting Stud (10-32 to 10-32) (1)
Model ACS-1 NIST traceable frequency response (10 Hz to upper 5% point). (1)
Model M081B05 Mounting Stud 10-32 to M6 X 0.75 (1)

Entered: Emm	Engineer: DAM	Sales: WDC	Approved: AB	Spec Number
Date: 3/24/11	Date: 3/24/11	Date: 3/24/11	Date: 3/24/11	353-2030-80

PCB PIEZOTRONICS VIBRATION DIVISION
3425 Walden Avenue, Depew, NY 14043
Phone: 716-684-0001
Fax: 716-685-3886
E-Mail: vibration@pcb.com

Appendix B Manufacturing Procedure

The aim of this investigation is to develop a manufacturing procedure to obtain a set internal mould temperature. The internal mould temperature is critical when manufacturing the composite. If the temperature is low, the polypropylene will not melt and it will not penetrate the fibres, whilst a high temperature will cause degradation to the composite. A temperature range can be derived from these limitations to ensure that the internal mould temperature is above the melting temperature of the polypropylene and below the thermal degradation temperature of the kenaf fibres. Three temperatures were considered, namely; 170°C, 175°C and 180°C.

The first part in obtaining this procedure is establishing the relationship between the oven temperature and the internal mould temperature. The method used in determining this relationship consisted of using a thermocouple to log the temperatures of the mould and another to log the temperature of the oven simultaneously. A thermocouple was placed in a mould which was then placed in the compression oven set at 280°C. A high thermal gradient between the oven and the mould will reduce the manufacturing time. The thermocouple could log temperature, and consequently the duration to reach a desired temperature was obtained from the log.

After reaching the moulding temperature, this temperature had to be maintained to allow for penetration of the resin into the fibres with pressure application. For this research, this temperature was maintained for half an hour as this was sufficient time according to the work done by Paiken [52]. The data log of the temperatures to obtain an internal mould temperature of 175°C can be seen in Figure B.1.

Figure B.1 shows the internal mould temperature, the surface temperature of the mould and the set oven temperature throughout the mould manufacturing cycle. This figure shows that the process takes approximately 52 min for the mould to obtain an internal mould temperature of 175°C using an oven temperature of 280°C. Thereafter, the fan was used reduce the thermal inertia of the mould to ensure that the internal mould temperature does not exceed 175°C. During the compression moulding, it is seen that the set temperature of

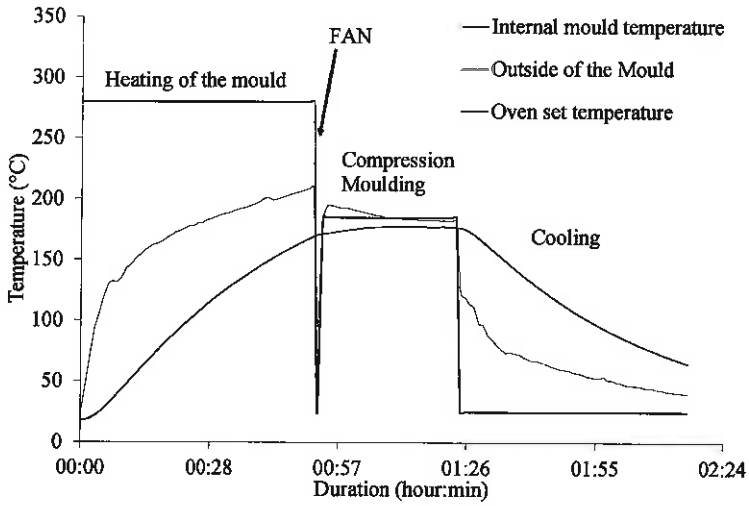

Figure B.1: Temperatures associated with internal mould temperature of 175°C

the oven is slightly higher than the internal mould temperature. This difference is the loss of heat from the oven to its surrounding. During the compression moulding section, the oven set temperature is effective in maintaining a constant internal mould temperature for half an hour. Thereafter it takes 1 hour for the mould to cool down to remove the composite. The moulding procedure for this internal mould temperature is summarised in Table 4.6. A similar procedure was done to obtain the internal mould temperatures of 170°C and 180°C and this can be seen in tables B.1 and tab:oven180, respectively.

Table B.1: Temperature of 170°C

Step	Duration (min)	Oven Temp(°C)	Oven Pressure(Bar)
1	49	280	0
2	1	Off- Place Fan	0
3	15	185	0
4	15	185	60
5	30	Off- Place Fan	200
6	110	Remove Mould and Cool	

Table B.2: Temperature of 180°C

Step	Duration (min)	Oven Temp(°C)	Oven Pressure(Bar)
1	55	280	0
2	1	Off- Place Fan	0
3	15	185	0
4	15	185	60
5	30	Off- Place Fan	200
6	116	Remove Mould and Cool	

Appendix C Matlab Codes

C.1 Image Processing

This matlab code calculated the velocity of the impact pendulum. A highspeed camera was used to obtain pictures of the motion of the impact pendulum and the camera took 4000 pictures/frames per second. The matlab code provided an interface for the user to input the pictures and track the motion of the pendulum. The distance moved by the pendulum between each frame was calculated by matlab. The frame rate was fixed by the camera, thereby establishing the time interval between each picture.Dividing the distance travelled by the pendulum by the time taken to travel the distance, gave the velocity of the pendulum. The code for this process can be seen below.

```
clear
clc
close all


prompt={'Do you want to do scaling analysis+Position Zero', 'No of iterations'}
default={'no', '5'};
title='Scaling analysis & position zero, yes or no';
lineNo=1;
user_input1=inputdlg(prompt,title,lineNo,default);
answer=(user_input1{1});
no_iter=str2num(user_input1{2});


prompt={'No of pics to be analysed'};
default={'10'};
title='Overal Analysis';
lineNo=1;
```

```
user_input2=inputdlg(prompt,title,lineNo,default);
no_of_pics=str2num(user_input2{1});

if strcmp('yes',answer)==1

    cd ('C:\Users\Sumi\Desktop\New folder\Impact Pictures for velocity\Test2_40
    [FileName,PathName] = uigetfile('*.tif','Select the File');
    TotalV=0;
    total=0;

    I = imread(FileName);
    [I3,rect] = imcrop(I);

    msgbox('Select the centre of the black strip','Zero Position')
    pause(3)
    imshow(I3)
    set(gcf,'Position',get(0,'Screensize'))%
    [zerox, zeroy]=ginput(1);


    msgbox('Please select the two points that define the specified dimension of
    pause(3)

     for i=1:no_iter
         imshow(I3)
            set(gcf,'Position',get(0,'Screensize'))%
         [a, b]=ginput(1);
         [c, d]=ginput(1);
         e(i)=sqrt((a-c)^2+(b-d)^2);
         total=total+e(i);

     end
     ratio=16/(total/i);
else
    ratio =16/90.3289;
end

cd ('C:\Users\Sumi\Google Drive\Impact Pictures for velocity\Test1_4000fps');
[FileName,PathName] = uigetfile('*.tif','Select the File');
```

```
namelength=length(FileName);
pic_no=str2num(FileName((namelength-9):end-4));


Name=[FileName(1:end-10),sprintf('%06d', pic_no),'.tif'];
B=1;
fps=4000;
TotalV=0;
total=0;

I = imread(Name);
[I3,rect] = imcrop(I);

msgbox('Select the centre of the black strip')
pause(3)
while B<no_of_pics

    A = imread(Name);
    I2 = imcrop(A, rect);
    figure, imshow(I2)
        set(gcf,'Position',get(0,'Screensize'))%


    [a(B), b(B)]=ginput(1);
    pic_no=pic_no+1;

    Name=[FileName(1:end-10),sprintf('%06d', pic_no),'.tif'];
    if B>1
       Cx=(a(B)+a(B-1));
       Cy=(b(B)+b(B-1));
       K=sqrt((a(B)-a(B-1))^2+(b(B)-b(B-1))^2)*ratio*fps/1000; %
       V(B-1)=K;
       TotalV=K+TotalV;
    end

    B=B+1;
end


```

```
97  close Figure 1 2 3 4 5 6 7 8 9 10
98
99
100 %%%%%printing
101
102 Titles={'Velocity(m/s)','Scaling'};
103 filename=strcat(num2str(FileName(1:5)),'result','.xls');
104 V=transpose(V);
105 ratio=transpose(ratio);
106
107 xlswrite(filename,Titles,1,'A1');
108 xlswrite(filename,V,1,'A2');
109 xlswrite(filename,ratio,1,'B2');
110 xlswrite(filename,TotalV/(B-2),1,['A',num2str(no_of_pics+1)]);
```

C.2 Impact data - finding the cutoff frequency

A matlab code was written to find the optimum cutoff frequency for the impact data.

The collected impact data had a lot of noise. A butterworth function was used in matlab to remove the noise. However, the function required a cutoff frequency and the degree of polynomial for the function to filter the noise. If the cutoff frequency is low, it removes energy from the impact, thereby lowering the impact energy. If the cutoff frequncy is high, it will not remove all the noise from the impact, thereby having a higher impact energy. A high degree of polynomial tends to remove more energy, whilst a low polynomial removes less energy. The matlab code to find the cutoff freqnecy can be seen below and the results of this code can be seen in Figure E.2.

```
1 %Finding the cutoff frequency
2 clear;
3 clf;
4 % DECLARATION OF CONSTANTS
5 mass1=4.65;              %Mass of striker/pendulum          1.9955
6 e0=0;
7 acc_const=100*10^(-3); %100mV is '1g' (9.81m/s^2)
8 rs=0.481;                %Distance to STRIKER             0.350
9 rg=0.408;                %Distance to CENTRE OF GRAVITY    0.2411
```

```
ra=0.490;                 %Distance to ACCELEROMETER       0.3875
v0=2.791;
Lstrike=20;
mefreq=3000;

%=======================================================
%   1.  IMPACT DATA FILE GETS OPENED

%prompt={'Time per division in Seconds'};
%totaltime=inputdlg(prompt);
%totaltime=str2num(totaltime{1});

% f=10;
prompt = {'Enter the Number of Specimens'};
number_of_specimens = inputdlg(prompt);
M = str2num(number_of_specimens{1});

for SB=1:1:M
    cd C:\Users\Sumi\Documents\MATLAB;                 %Set path to data files
    [FileName,PathName] = uigetfile('*.txt','Select the File');
    data=dlmread(FileName);
    timedivison=0.004; %%%%%%%%%%%%%%%%%%%%%%%%%%%%%%%%%%%%%%%%%%%%%%%%%%%%%%%%%%
    volts=data(:,1);                         %Acquire signal
    L=length(volts);                          %length of signal
    T=10*timedivison/(L-1);                     %each sample time
    Fs=1/T;                                   %sampling Frequency
    t=T*(0:(L-1));                             %time vector
    Fs2=Fs/2;
    [b a] = butter(2,0.018,'low');
    volts_filt=filter(b,a,volts);
    figure(1)
    plot(t,volts_filt-0.6)
    grid on
    [intial_time, zero_volts]=ginput(1);
    [final_time, finish_volts]=ginput(1);
    close fig 1
    n=1;
    for fg=1:mefreq
        clear b a
```

```
49          [b a] = butter(2,fg/Fs2,'low');
50          volts_filt=filter(b,a,volts);
51
52          ABC=ceil(intial_time/T);
53          BCD=ceil(final_time/T);
54          t3=t(ABC:BCD);
55          q=1;
56          %rearrganing the time to start from zero at the ginput point
57          while q<((BCD-ABC)+1)
58              t4(q)=t3(q)-t3(1);
59              q=q+1;
60          end
61          reducedvolts=volts_filt(ABC:BCD)-volts_filt(ABC);%%%Adjusting the volta
62
63          for f=1:length(t4)
64              accel(f)=(-1)*(9.81/acc_const)*reducedvolts(f);
65          end
66          accel=transpose(accel);
67          %
68          % figure(5)
69          %
70          % plot(t4(1:length(t4)),(reducedvolts(1:length(t4)))/0.1*9.81)
71          % grid on
72          %
73
74
75          %=======================================================
76          %    6.1.    DATA IS USED TO COMPUTE VELOCITY OF ACCELEROMETER VIA
77          %    NUMERICAL INTEGRATION
78
79          for g=1:length(t4)-1
80              vel(1)=v0*(ra/rg);
81              vel(g+1)=vel(g)+((accel(g)+accel(g+1))/2*(t4(g+1)-t4(g)));
82          end
83          vel=transpose(vel);
84
85
86          %=======================================================
87          %    7.  DATA IS USED TO COMPUTE FORCE FROM MOMENTS
```

```
88          %   AND PENDULUM PROPERTIES.
89          %   (F=MA)
90          %   Fg*rg=Fs*rs
91          %   Fs=(rg/rs)*Fg ------- (1)
92          %   but
93          %   Fg=Mg*ag ------- (2)
94          %   ag=(rg/ra)*aa ------- (3)
95          %
96          %  where ag= acc. of centre of gravity
97          %        as= acc. of striker
98          %        aa= acc. Of accelerometer
99          %  Fs=Mg*(rg/rs)*(rg/ra)*aa
100
101         for i=1:length(t4)
102             force(i)=(-1)*mass1*(rg/rs)*(rg/ra)*accel(i);
103         end
104         force=transpose(force);
105
106         %=====================================================
107         %   8.  DATA IS USED TO COMPUTE ENERGY VIA NUMERICAL INTEGRATION OF
108         %   MASS AND VELOCITY OF PENDULUM
109
110         for j=1:length(t4)     %j=1:N-1
111             %energy(1)=e0;
112             energy(j)=0.5*mass1*((vel(1)*(rg/ra))^2-(vel(j)*(rg/ra))^2);    %ene
113         end
114         energy=transpose(energy);
115
116         %%%%%%%%%%%%%%%%%%
117         j=1;
118         while abs(accel(j))<max(abs(accel))
119             j=j+1;
120         end
121         KP=energy(j);
122         Epeak(n)=KP;
123
124         K = max(force);
125         Fmax(n)=K;
126         n=n+1;
```

```
127
128         end
129         Fmax_all(SB,:)=Fmax;
130         Epeak_all(SB,:)=Epeak;
131         AGH1=find(Fmax==max(Fmax));
132         FGH2=find(Epeak==max(Epeak));
133 %         ffmax(OP)=AGH;
134 %         fEpeak(OP)=FGH;
135
136         clear Fmax Epeak t4 i j KP K volts_filt fg f t3 t4 g
137         clear vel accel force
138         clear volts
139 end
140
141
142 %
143 %
144 %
145         fg=1:mefreq;
146
147         figure()
148         [AX,H1,H2]=plotyy(fg, Fmax_all(1,:), fg, Epeak_all(1,:), 'plot');
149         title('Finding the maximum cutoff frequency')
150
151 %         grid on
152 %         set(get(AX(1), 'Ylabel'), 'String', 'Force [N]')
153 %             set(get(AX(2), 'Ylabel'), 'String', 'Energy [J]')
154 %             xlabel('Time [s]');
155 %
156 %         %         %Smax = (6*Fmax*Lstrike)/(thickness*width^2);
157 %         %
158 %         ffmax=find(Fmax==max(Fmax));
159 %         fEpeak=find(Epeak==max(Epeak));
160 % clf;
161 % figure(5)
162 % [AX,H1,H2]=plotyy(t4, force, t4, energy, 'plot');
163 % grid on
164 %
165 % annotation('textbox',...
```

```
166 %      [0.15 0.14 0.6 0.2],...
167 %      'String',{['Etot(J) =' num2str(max(energy))],['Ei(J) =' num2str(peakenerg
168 %      'FontSize',14,...
169 %      'FontName','Arial',...
170 %      'LineStyle','--',...
171 %      'EdgeColor',[1 1 0],...
172 %      'LineWidth',2,...
173 %      'BackgroundColor',[0.9  0.9 0.9],...
174 %      'Color',[0.84 0.16 0]);
175
```

C.3 Impact Testing Code

The following code was used to process the raw data from the impact rig to obtain the impact properties of a batch of specimens.

```
1  %Impact Code by Sumilan Govinden
2  %It requires a dimension file input with the names of specimens in number
3  %form. The test files should be .csv and be in the same folder of the dimension
4  %It can work out impact strenght(MPa), Initial Energy, Propagative
5  %Energy and Total Energy. It also takes into account the final angle of the
6  %pendulum, and works out the total energy that went into the impact. It
7  %should be noted, that total energy will comprise of sound energy, energy
8  %to throw the impacted piece, as well as the energy to break the specimen.
9  % close figure 1 2 3 4 5 6 7
10 clear
11 clc
12 % Change default axes fonts.
13 set(0,'DefaultAxesFontName', 'Times New Roman')
14 set(0,'DefaultAxesFontSize', 14)
15
16 % Change default text fonts.
17 set(0,'DefaultTextFontname', 'Times New Roman')
18 set(0,'DefaultTextFontSize', 14)
19 %to clear all previous data
20 %constants
21 %dimensions of the impact rig
```

```
22  mass1=4.112;              %Mass of striker/pendulum
23  e0=0;
24  rs=0.470;                 %Distance to STRIKER
25  rg=0.422;                 %Distance to CENTRE OF GRAVITY
26  ra=0.470;                 %Distance to ACCELEROMETER
27  v0=1.63582427448488;      %This needs to be changed depending on the point chosen
28  v0angle=49.5    ;          % This is the angle the striker is picked up too from a
29  Lstrike=22;               % distance of the specimen from the holder to the strik
30
31  %property of the accelerometer
32  acc_const=10*10^(-3);     %1mV is '1g' (9.81m/s^2)
33
34  prompt = {'Type the Directory Containing Impact Test Files'}; %choosing the dir
35  default = {'C:\Users\Sumi\Dropbox\Masters\Testings\Final Impact Test Data\Good
36  title = 'directory';
37  lineNo = 1;
38  directory = inputdlg(prompt, title, lineNo, default);
39  directory = char(directory);
40  cd(directory);
41  [file, pathname] = uigetfile('*.txt', ['Select File Containing Dimensions']);
42
43  dim = dlmread(file, '\t', 1, 0);
44  Specimen=dim(:,1);
45  width=dim(:,2);
46  thickness=dim(:,3);
47  angles=dim(:,8);
48  totaltime=0.004;%ms
49  noofspec=length(Specimen);    %Number of the specimens tested
50
51
52  %All the specimens will be automatically selected. It will be assumed that
53  %the impact occurs at 20ms, but it can be changed if it is otherwise.
54
55  for spec=1:length(Specimen)
56      clear vel energy volts_filt Timeregion Accregion
57      filename = strcat(num2str(Specimen(spec)),'.csv'); %automatic selection of
58      data=csvread(filename,2,0,'A3..A10242');
59
60
```

```
61      volts=data(:,1);                          %Acquire signal
62  %     if spec==2;
63  %        volts=-1*volts;
64  %
65  %
66  %     end
67      L=length(volts);                          %length of signal
68      T=10*totaltime/(L-1);                         %each sample time
69      Fs=1/T;                                   %sampling Frequency
70      t=T*(0:(L-1));                            %time vector
71      Fs2=Fs/2;
72      [b a] = butter(4,1000/Fs2,'low');         %Calculation of the filter coeffici
73                                                %this was found to be the best
74                                                %filtering frequency. Refer to
75                                                %appendix for code used to obtain
76                                                %the best filtering frequency and
77                                                %explanations.
78      volts_filt=filter(b,a,volts);             %Filtering of the signal
79
80      voltavg=mean(volts_filt(1000:2000));      %Finding the average voltage in the
81      volts_filt=volts_filt-voltavg;            %adjusting the voltage of the impac
82
83      %Selection of the start of the impact.
84      figure(spec)
85      plot(t*1000,volts/acc_const)        %volts_filt
86      xlabel('Time [ms]');
87      ylabel('Acceleration [g]');
88      grid on
89
90      prompt={'Is the start of the impact occur at 20ms'};
91      default={'yes'};
92      title='Selecting the start of the impact, yes or no';
93      lineNo=1;
94      user_input1=inputdlg(prompt,title,lineNo,default);
95      answer=(user_input1{1});
96      volt_pos1=ceil((totaltime*10/2)/T);
97
98
99      if strcmp('no',answer)==1
```

```
100
101         figure(spec)
102         plot(t,volts_filt/acc_const)
103         xlabel('Time [s]');
104         ylabel('Acceleration [g]');
105         grid on
106
107         [intial_time, zero_volts]=ginput(1);
108         [final_time, finish_volts]=ginput(1);
109         volt_pos1=ceil(intial_time/T);
110
111
112     end
113
114 %     volts_filt=volts_filt-volts_filt(volt_pos1);
115
116     N=volt_pos1+350; %200 points is a rough estimate away from the start of the
117     while volts_filt(N)>0.3*max(volts_filt)      % finding the end point of the
118         %                               impact is that the 'g' value is 1 again .
119         N=N+1;
120     end
121     volt_pos2=N;
122     if strcmp('no',answer)==1
123         volt_pos2=ceil(final_time/T);
124     end
125
126     clear Timeregion Accregion
127
128     %plotting the region of the impact.
129     Timeregion=t(volt_pos1:volt_pos2)-t(volt_pos1);
130     Accregion=(volts_filt(volt_pos1:volt_pos2)/acc_const)*9.81;%%taking the imp
131     figure(spec)
132     plot(Timeregion,Accregion)
133     xlabel('Time [s]');
134     ylabel('Acceleration [m/s2]');
135     grid on
136
137     %%%%readjusting to reduce the propagative energy
138     MaxP=max(Accregion);
```

```
139     Q=1;
140     while Accregion(Q)<MaxP
141         Q=Q+1;
142     end
143     W=Q;
144     state=1;
145     while state==1
146
147
148
149         if Accregion(W)>0.4*MaxP
150             counter1=W;
151         end
152
153         if Accregion(W)>0.6*MaxP
154             counter2=W;
155
156         end
157
158         if Accregion(W)<0.35*MaxP
159             state=0;
160         end
161         W=W+1;
162
163      end
164    m=(Accregion(counter2)-Accregion(counter1))/(Timeregion(counter2)-Timeregion
165    c=Accregion(counter2)-Timeregion(counter2)*m;
166
167    counter=counter1;
168    state=1;
169    while state==1
170        counter=counter+1;
171        Timeregion(counter)=Timeregion(counter-1)+T;
172        Accregion(counter)=m*Timeregion(counter)+c;
173        if Accregion(counter)<0
174            state=0;
175        end
176
177    end
```

```
178
179
180
181
182     figure(spec)
183     plot(Timeregion(1:counter),Accregion(1:counter))
184
185
186
187      %finding max peak
188      N=1;
189      while Accregion(N)+0.000001<max(Accregion)
190          N=N+1;
191      end
192      Peak=N;
193
194      %Integrating the acceleration to find the velocity profile of the
195      %impact.
196      for g=1:counter-1
197          vel(1)=v0;
198          vel(g+1)=vel(g)-((Accregion(g)+Accregion(g+1))/2*(Timeregion(g+1)-Timer
199      end
200      vel=transpose(vel);
201  %       figure(spec)
202  %       plot(Timeregion,vel)
203  %       xlabel('Time [s]');
204  %       ylabel('Velocity [m/s]');
205  %       grid on
206
207      %Using energy =1/2mv^2 to find the energy throughout the impact.
208       for j=1:counter
209
210                  energy(j)=0.5*mass1*((vel(1))^2-(vel(j))^2);
211       end
212       %plotting the energy profile throughout the impact.
213  %       figure(spec)
214  %       plot(Timeregion,energy)
215  %       xlabel('Time [s]');
216  %       ylabel('Energy [J]');
```

```
217 %     grid on
218     %storing of data of the impact
219     TotalEnergy(spec)=(max(energy)/thickness(spec))*1000                ;          %
220     TotalEnergy2(spec)=(max(energy)/(thickness(spec)*width(spec)))*1000        ;
221     Ei(spec)=(energy(Peak)/thickness(spec))*1000                        ;
222     Ep(spec)=(TotalEnergy(spec)-Ei(spec))                               ;        %J/m
223
224     Stress(spec)=(6*mass1*max(Accregion)*Lstrike)/(thickness(spec)*(width(spec)
225     %%These last to energy calculations to compare the energy worked out by
226     %%the accelerometer to the energy taken from the dial indicator on the
227     %%impact rig
228     TheoretEnergy(spec)=sqrt(rg*(1-cos(degtorad((v0angle-angles(spec))))))*9.81*
229     MaxEnergy(spec)=max(energy);
230
231
232
233 end
234
235
236 %%Working out averages and standard of deviation and printing to excel.
237 Avwidth=mean(width);
238 Avthickness=mean(thickness);
239 AvTotalEnergy=mean(TotalEnergy);
240 AvTotalEnergy2=mean( TotalEnergy2);
241 AvEi=mean(Ei);
242 AvEp=mean(Ep);
243 AvMaxstress=mean(Stress);
244 AvTheoretEnergy=mean(TheoretEnergy);
245 AvMaxEnergy=mean(MaxEnergy);
246
247 Stwidth=std(width);
248 Stthickness=std(thickness);
249 StTotalEnergy=std(TotalEnergy);
250 StTotalEnergy2=std(TotalEnergy2);
251 StEi=std(Ei);
252 StEp=std(Ep);
253 StMaxstress=std(Stress);
254 StTheoretEnergy=std(TheoretEnergy);
255 StMaxEnergy=std(MaxEnergy);
```

```
256
257 Varwidth=Stwidth/Avwidth*100;
258 Varthickness=Stthickness/Avthickness*100;
259 VarTotalEnergy=StTotalEnergy/AvTotalEnergy*100;
260 VarTotalEnergy2=StTotalEnergy2/AvTotalEnergy2*100;
261 VarEi=StEi/AvEi*100;
262 VarEp=StEp/AvEp*100;
263 VarMaxstress=StMaxstress/AvMaxstress*100;
264 VarTheoretEnergy=StTheoretEnergy/AvTheoretEnergy*100;
265 VarMaxEnergy=StMaxEnergy/AvMaxEnergy*100;
266
267 mean1=[Avwidth Avthickness AvTotalEnergy AvTotalEnergy2 AvEi AvEp AvMaxstress A
268 standard=[Stwidth Stthickness StTotalEnergy StTotalEnergy2 StEi StEp StMaxstres
269 variance=[Varwidth Varthickness VarTotalEnergy VarTotalEnergy2 VarEi VarEp VarM
270 Titles2={'average'; 'standard deveation';'variance'};
271 fileout=strcat(file(1:length(file)-4),'finalresult');
272 Titles={'Specimen','Width','Thickness','Total Energy(J/m)','Total Energy(kJ/m2)
273 Matrix=[Specimen width thickness transpose(TotalEnergy) transpose(TotalEnergy2)
274
275 xlswrite(fileout,Titles,1,'A1');
276 xlswrite(fileout,Titles2,1,'A10');
277 xlswrite(fileout,Matrix,1,'A2');
278 xlswrite(fileout,mean1,1,'B10');
279 xlswrite(fileout,standard,1,'B11');
280 xlswrite(fileout,variance,1,'B12');
281
282
283
```

Appendix D Shortcoming with Tensile Testing

As explained previously in subsection 4.6.1, there was shortcomings in processing the tensile data, an example of which can be seen in Figure 4.16. This figure shows that the strain data has an initial negative gradient and negative strain at the start of the test which is a result of clamping the specimen. This results in erroneous values of distance being measured, as the laser extensometer can not measure out-of-plane bending.

One of the limits of the extensometer is that the laser of the extensometer has to be perpendicular to the specimen. The extensometer thus provides erroneous results for a specimen in bending until the specimen is flat and in pure tension. The erroneous results are a consequence of the laser not being perpendicular to the specimen and hence not reflecting the laser light directly back to the extensometer.

To overcome this shortcoming, the data had to be considered from a specific reference point. This was chosen to be a force of 7 N as it exhibited a positive gradient in all the data obtained.

The elastic modulus was calculated by determining the gradient between two points that lie on the linear region of the stress-strain curve, and this was calculated for all specimens in the batch. Thereafter, the standard of deviation of the elastic modulus was calculated for each batch of specimens. Deviations as high as 20% of the elastic modulus were calculated, which made it difficult to find trends in the data.

It can be seen in Figure 4.16, that there is a gentle curve in the stress-strain data, which comprises several different gradients. The stress-strain curve has high gradients towards the start of the test, and lower gradients towards the end of the test. Calculating the modulus using two random points in the approximated linear region of the stress-strain curve was not a repeatable method, as it resulted in large values of the standard of deviation. A new procedure to calculate the elastic modulus had to be developed to reduce this deviation.

An iterative approach was thus adopted to find the optimal region in the stress-strain curve which resulted in the smallest standard of deviation of the elastic modulus. The investigation carried out considered two methods of calculating the gradient of the stress-strain curve, which

represents the elastic modulus; finding the gradient using two points in the linear region of the stress-strain graph, or curve fitting a series of points in the linear region.

Calculating the modulus using two random points in the approximated linear region of the stress-strain curve was not a repeatable method, as it resulted in large values of the standard of deviation. A new procedure to calculate the elastic modulus had to be developed in order to reduce the deviation. An iterative approach was thus adopted to find an optimal region in the stress-strain curve to calculate the elastic modulus. This approach showed that the optimal region for calculating the elastic modulus is between 7 MPa and 15 MPa. Figure D.1 shows the force-deflection data collected from the tensile testing machine.

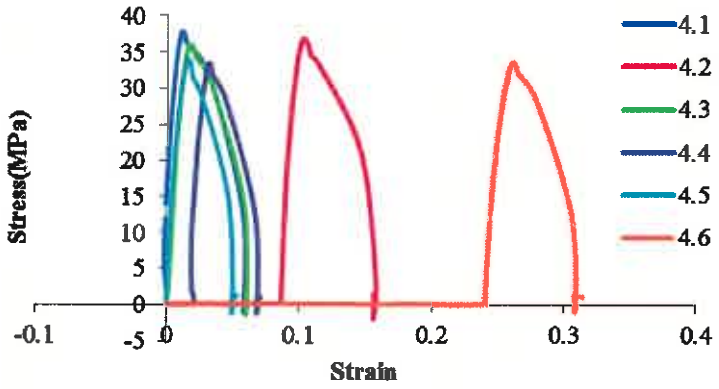

Figure D.1: Raw tensile data

Figure D.1 shows that the data for each specimen is laterally displaced. The tensile testing specimens exhibited strain for zero force until the specimen did not slip with respects to the grips holding the specimen. This is a big issue for calculating the secant modulus as it is calculated from the strain values. To shift all the specimen stress-strain data to pass through the origin, a repeatable method was required. It had to take into consideration the fact that the strain data below the 7 MPa line was not quite linear. This could be attributed to the specimen being held in slight compression in the beginning of the testing as the laser extensometer only gives repeatable results when there is sufficient tension in the specimen. A line is passed through 7 MPa and 15 MPa of all the specimens. The x-intercept of these lines is used to shift the stress-strain data to pass through the origin. The results of these modifications can be seen in Figure D.2.

The gradient of the curves in the data which corresponds to the elastic modulus is calculated at the points corresponding to 7 MPa and 15 MPa. The results of this can be seen in Table D.1.

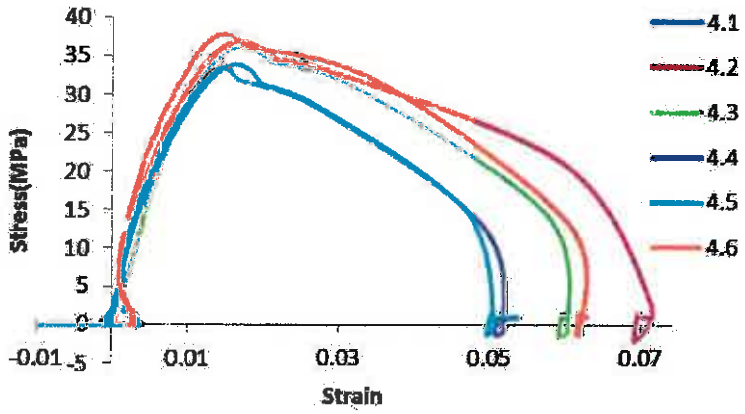

Figure D.2: Overview of the Multilayer Cast System

Table D.1: Approximation of the Elastic Modulus using points 7 MPa and 15 MPa

Specimen	Approximated Elastic Modulus(MPa)
4.1	5947
4.2	4322
4.3	3548
4.4	3770
4.5	3729
4.6	2713
Average	4005
STD	1085

Table D.1 shows that there is a standard of deviation of 1 GPa and this is significant compared to the elastic modulus. Due to the parabolic shape of the tensile stress-strain curve, it is difficult to approximate the curve using a linear relationship and shifting it to overlap. Consequently, another method is considered. To accommodate the slight parabolic shape in the stress-strain data, it is useful to fit a line using the least squares method between the range of 7 MPa and 15 MPa of the data. The x-intercept from the least squares method will be used to shift the curve to the origin. This method of line fitting the data was applied to two specimens of the same batch. The results of this can be seen in Figure D.3 and in Table D.2.

Table D.2: Elastic modulus for different orders of curve fitting

	Elastic Modulus(MPa)		
Specimen	Order 1	Order 2	Order 3
1	5121	1310	11372
2	2631	90525	-4788496

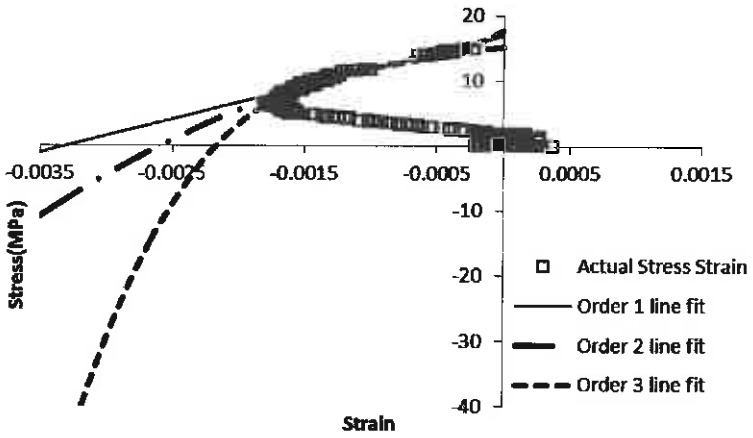

Figure D.3: Different orders of line fitting

Table D.2 shows that using a high order polynomial results in a large elastic modulus. Consequently, a polynomial order of 1 was used to fit the data, the results of which can be seen in Table D.3.

Table D.3: Curve fitting with order 1

Specimen	Approximated Elastic Modulus(MPa)
4.1	5121
4.2	4225
4.3	3517
4.4	3534
4.5	3574
4.6	2631
Average	3767
STD	835

Table D.3 shows that the standard of deviation for the elastic modulus reduced from approximately 1 GPa to 0.83 GPa. This confirms that least squares method is better approximation of the elastic modulus than line fitting with two points.

However, this best fit line did not pass through the origin of the stress-strain data. The stress-strain curve was accordingly shifted horizontally to ensure that the best fit line passed through the origin. The adjusted stress-strain data can be seen in Figure 4.16. The secant moduli at 0.01 strain and at failure were calculated using the recorded stress at 0.01 strain and at failure, respectively.

Appendix E Shortcomings with Impact Testing

It was seen in Figure 4.18 that the collected raw impact data had a lot of noise which made it difficult to differentiate between the impact and noise data. For this reason, a Fast Fourier Transform (FFT) was performed on the data. A FFT is a Matlab function which converted the raw impact data from a time domain to a frequency domain which aids in differentiating between the impact data and noise. The FFT can be seen in Figure E.1. The figure shows the raw data broken up into its frequencies.

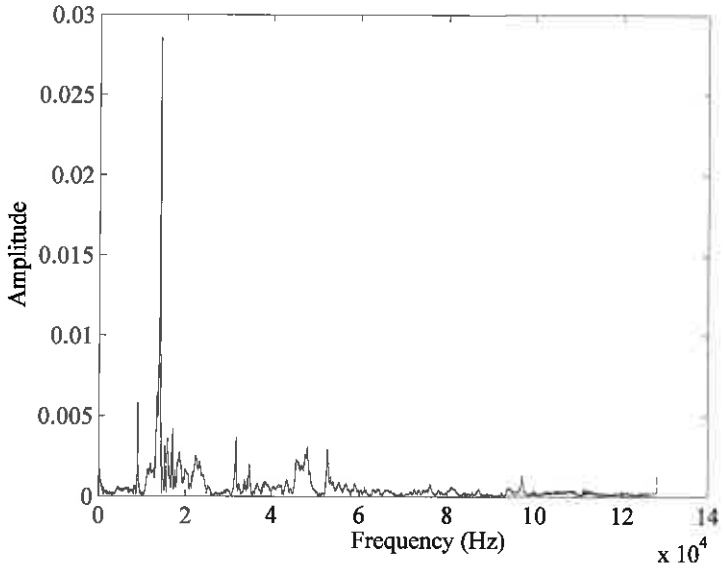

Figure E.1: Fast Fourier Transform on Impact Data

Large amount of noise was present above the 1 kHz mark, as shown in Figure E.1. To remove this noise, the data was analysed using a MATLAB code which can be found in Appendix E. The code employed a Butterworth function to filter the data and the function was set to a cutoff frequency of 1 kHz. This caused the filter to remove all the frequencies above 1 kHz, thus removing the noise. The result of which was seen earlier in Figure 4.19.

It is useful to provide an overview of the processes involved in obtaining the impact energy before explaining the filter.

The impact region seen in Figure 4.19 and can be identified by a sudden increase in acceleration until a maximum acceleration is reached followed by a drop in acceleration back to a value of zero. The impact energy can be calculated from the impact region by using the acceleration to obtain the velocity and then using Equation 4.3 to determine the energy. This is further explained later in this section. The filter mentioned above essentially influences the calculated impact energy. If the filter is set to a low cutoff frequency, it will not only remove the noise but also the frequency components relating to the breaking of the specimen. If the cutoff frequency is set very high, the filter will not remove all the noise from the impact data. The impact energy will seem higher than it actually is, because it will be a combination of the impact energy used to break the specimen as well as noise and vibration energy in the hammer. The Butterworth filter is thus a key factor in this test which will be investigated further.

The Butterworth function has two parameters that can be adjusted, namely, the degree of the polynomial curve to filter the data, and the cutoff frequency. It was difficult to determine the exact frequency at which noise exists, as well as what degree polynomial to filter the noise. Consequently, an iterative approach of varying the two factors was used to determine the optimum stress. The impact specimen experiences a stress during impact. Although the impact test is meant to measure impact energy, finding the correct cutoff frequency is difficult, as this frequency directly influences the measured impact energy. As mentioned earlier, a low cutoff frequency could remove more than just the noise of the impact, and a high cutoff frequency will add more noise energy to the impact energy value. Stress is less sensitive to changes in the cutoff frequency compared to impact energy, hence it was used to determine a cutoff frequency. The stress experienced during impact of the specimen was calculated using the maximum acceleration multiplied by the mass of the hammer, divided by the cross sectional area behind the notch of the specimen.

The iterative approach made use of a cutoff frequency range from 0 Hz to 6000 Hz with polynomials of degree of 2,3 and 4 for the Butterworth function. The code of this process can be found in Appendix D and the results from this analysis can be seen in Figure E.2.

A low cutoff frequency removes essential frequency components of the impact resulting in a low peak stress. A larger cutoff frequency will filter out less noise energy, resulting in a large impact energy. The aim of this investigation is to find a low cutoff frequency to remove as much noise of the impact as possible, without removing essential frequency components of the impact. Figure E.2 shows that up until a value of 900 Hz, the order of the polynomial did not matter. The data show an approximate maximum peak stress for the different order of polynomials around 1000 Hz. Consequently this was used as the cutoff frequency. Although there is little difference between the peak stress for the different order of polynomial, an order of polynomial had to be chosen. Order 2 shows that the peak stress is rising with increasing

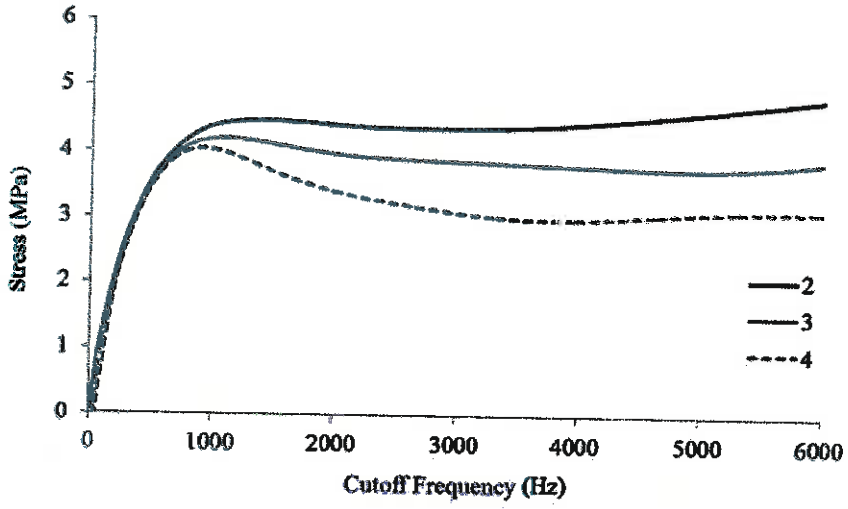

Figure E.2: Variation of cutoff frequency with different degree butterworth function

cutoff frequencies which indicates that the noise contributes to a higher peak stress. Order 3 is constant, independent of cutoff frequencies implying that noise has no effect. Order 4 shows a distinct maximum peak stress at 1000 Hz and was thus used in filtering the impact data.

The filtered data in Figure 4.19 highlights the acceleration through the impact of the specimen. The impact occurs at 20 ms which is represented by the increase in acceleration. The acceleration increases to a maximum value at which the specimen fractures, thereafter the acceleration decreases back to a minimum value. The end of the impact can be approximated to occur at 24 ms, at which the acceleration returns back to zero.

The acceleration vs time data had to be converted to velocity vs time data to determine the energy of the impact. This required integration of the acceleration data using the trapezium rule, and also required the initial impact velocity of the hammer which was determined both experimentally and theoretically.

Preliminary testing was done to determine an angle of releasing the hammer to result in complete fracture of the impact specimen. This angle corresponded to a value of 43.5°with an impact speed of 1.52 m/s, which was determined experimentally using a high speed camera.

The camera is capable of measuring a maximum of 200 000 pictures per second It was determined that a frame rate of 4 000 pictures per second was ideal for this application, through a trial and error process. A vertical mark was made on the hammer as a point of moving reference and the edge of the impact specimen holder was used as the stationery reference. A light source was placed near the impactor to help increase visibility of the vertical

references. The pendulum was released from each of the five markings, and the camera took a series of pictures of the motion of the pendulum before any specimen was placed in the rig. These pictures were imported into MATLAB, where the distance travelled for each picture was obtained using the 'ginput' function of MATLAB. The time between each picture was determined merely from the fact that 4 000 pictures were taken in one second. Using the distance and time, the velocity of the hammer was thus calculated. The codes used to process the images can be found in the Appendix D whilst pictures from the high speed camera can be seen in Figure E.3.

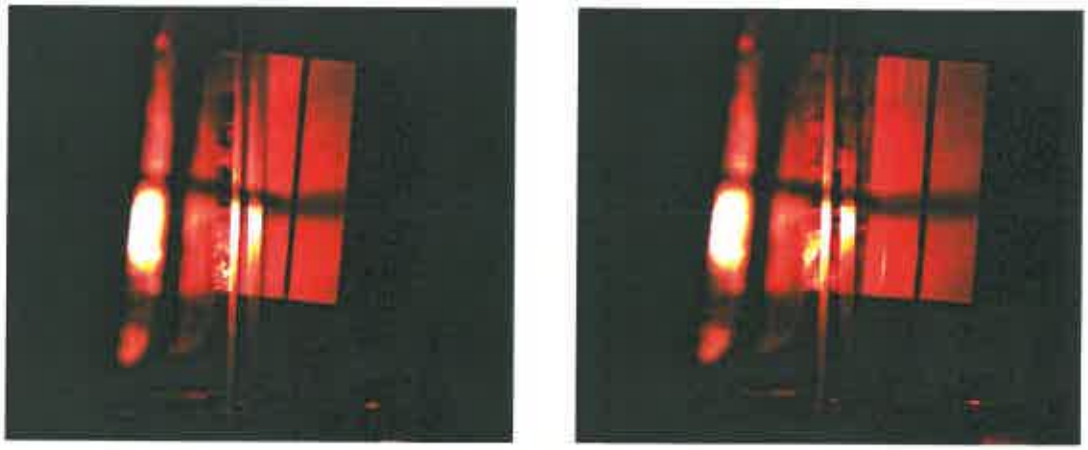

Figure E.3: Motion of the Impactor captured by the High Speed Camera

The speed of the impactor was used in the integration calculation to determine the impact energy. Figure 4.20 shows the final impact data for an impact specimen. It highlights the acceleration and energy through the duration of the impact. The energy absorbed prior to the peak acceleration was considered to be the initial energy whilst the remaining energy is considered to be the propagative energy.

Appendix F Processed Data

Table F.1: Raw Results - Tensile 1

Single fibre sheet - 170						
Specimen	Width (mm)	Thickness (mm)	Max Stress (MPa)	Elastic Modulus (MPa)	Secant Modulus at 0.01 Strain	Secant Modulus at failure (MPa)
1.1	1.49	12.59	30.09	2695.90	2331.78	1900.40
1.2	1.55	12.56	34.98	4318.50	3042.12	2383.54
1.3	1.55	12.51	36.32	3961.74	3072.48	2599.04
1.4	1.55	12.46	34.58	3449.25	2851.00	2424.21
1.5	1.59	12.42	25.60	6767.75	2559.87	4970.22
1.6	1.59	13.33	30.66	3620.76	2837.70	2616.70
average	1.55	12.65	32.04	4135.65	2782.49	2815.69
STD	0.04	0.34	4.01	1400.05	287.03	1086.86
Single fibre sheet - 175						
Specimen	Width (mm)	Thickness (mm)	Max Stress (MPa)	Elastic Modulus (MPa)	Secant Modulus at 0.01 Strain	Secant Modulus at failure (MPa)
2.1	1.34	12.63	40.96	4095.74	3223.96	2793.31
2.2	1.35	12.58	36.39	3308.68	3347.78	3291.56
2.3	1.38	12.54	33.56	3260.84	3006.80	2662.84
2.4	1.40	12.48	32.33	6367.59	3224.70	3914.47
2.5	1.40	12.44	39.82	5082.34	3691.89	3404.67
2.6	1.40	13.06	34.47	3968.27	3021.41	2479.10
average	1.38	12.62	36.25	4347.24	3252.76	3090.99
STD	0.03	0.23	3.48	1190.62	251.99	540.94
Single fibre sheet - 180						
Specimen	Width (mm)	Thickness (mm)	Max Stress (MPa)	Elastic Modulus (MPa)	Secant Modulus at 0.01 Strain	Secant Modulus at failure (MPa)
3.1	1.61	12.64	32.56	5601.23	3256.13	4327.35
3.2	1.47	12.58	33.27	3579.52	2898.69	2660.20
3.3	1.43	12.51	31.48	3611.92	2995.85	2916.68
3.4	1.36	12.48	28.21	2695.71	2522.37	2265.19
3.5	1.30	12.46	33.60	4444.69	3360.24	3439.93
3.6	1.30	13.16	31.44	3249.26	2809.26	2550.95
average	1.41	12.64	31.76	3863.72	2973.76	3026.72
STD	0.12	0.26	1.95	1023.96	305.30	750.35

Table F.2: Raw Results - Tensile 2

Double fibre sheet - 170						
Specimen	Width (mm)	Thickness (mm)	Max Stress (MPa)	Elastic Modulus (MPa)	Secant Modulus at 0.01 Strain	Secant Modulus at failure (MPa)
5.1	3.14	12.59	31.49	2997.59	2673.01	2519.01
5.2	3.14	12.60	28.21	2535.71	2277.52	1843.64
5.3	3.15	12.63	24.63	3877.77	2462.68	2729.64
5.4	3.11	12.63	25.64	3837.68	2537.56	2360.68
5.5	3.10	12.57	36.13	4334.67	3028.97	2385.80
5.6	3.08	12.46	31.91	3427.68	2649.03	2077.37
average	3.12	12.58	29.67	3501.85	2604.79	2319.36
STD	0.03	0.06	4.33	654.35	252.34	315.97
Double fibre sheet - 175						
Specimen	Width (mm)	Thickness (mm)	Max Stress (MPa)	Elastic Modulus (MPa)	Secant Modulus at 0.01 Strain	Secant Modulus at failure (MPa)
6.1	3.17	12.56	35.22	4293.50	3151.53	2849.16
6.2	3.08	12.42	37.43	5543.41	3512.11	3108.94
6.3	3.14	12.39	31.79	3176.20	2748.78	2472.87
6.4	3.02	12.69	29.24	2311.33	2160.30	1783.29
6.5	3.06	12.61	30.73	3047.56	2437.29	1789.56
6.6	3.06	12.51	37.20	3648.60	3060.14	2450.18
average	3.09	12.53	33.60	3670.10	2845.02	2409.00
STD	0.06	0.11	3.49	1129.26	495.90	541.23
Double fibre sheet - 180						
Specimen	Width (mm)	Thickness (mm)	Max Stress (MPa)	Elastic Modulus (MPa)	Secant Modulus at 0.01 Strain	Secant Modulus at failure (MPa)
7.1	3.14	12.48	37.04	5499.39	3397.74	3061.88
7.2	3.09	12.43	26.11	4167.56	2610.82	3108.96
7.3	3.07	12.74	21.52	1886.51	1922.05	1890.69
7.4	2.91	12.63	31.80	2826.12	2559.04	2174.79
7.5	2.87	12.57	28.73	2965.40	2686.87	2563.00
7.6	2.75	12.54	34.98	3931.84	3056.60	2757.69
average	2.97	12.57	30.03	3546.13	2705.52	2592.83
STD	0.15	0.11	5.77	1261.76	499.40	486.26

Table F.3: Raw Results - Tensile 3

Untreated fibre and polypropylene (Unt - PP)						
Specimen	Width (mm)	Thickness (mm)	Max Stress (MPa)	Elastic Modulus (MPa)	Secant Modulus at 0.01 Strain	Secant Modulus at failure (MPa)
13.1	3.01	12.79	34.86	3117.67	2747.88	2164.92
13.2	3.19	12.63	32.10	3066.53	2673.73	2303.58
13.3	3.22	12.81	33.41	3515.83	2818.83	2229.28
13.4	3.13	12.65	33.90	3012.75	2561.93	1943.45
13.5	3.06	12.72	33.45	2879.91	2462.79	1965.54
13.6	2.95	12.79	36.73	4059.58	3123.26	2572.19
average	3.09	12.73	34.07	3275.38	2731.40	2196.49
STD	0.11	0.08	1.58	439.69	230.51	233.26
Sodium hydroxide treated fibres and polypropylene (NaOH - PP)						
Specimen	Width (mm)	Thickness (mm)	Max Stress (MPa)	Elastic Modulus (MPa)	Secant Modulus at 0.01 Strain	Secant Modulus at failure (MPa)
14.1	3.15	12.67	38.15	3662.52	3027.52	2376.04
14.2	3.20	12.77	39.53	3860.31	3019.08	2223.03
14.3	3.03	12.90	37.56	3921.29	2927.13	2093.62
14.4	3.12	12.56	37.67	4852.62	3342.72	2721.36
14.5	3.25	12.89	36.98	3714.73	2971.23	2341.92
14.6	3.30	12.82	32.66	3902.60	2954.80	2661.08
average	3.18	12.77	37.09	3985.68	3040.41	2402.84
STD	0.10	0.13	2.34	437.31	152.94	245.16
T1 treated fibres and polypropylene (T1 - PP)						
Specimen	Width (mm)	Thickness (mm)	Max Stress (MPa)	Elastic Modulus (MPa)	Secant Modulus at 0.01 Strain	Secant Modulus at failure (MPa)
7.1	3.19	12.80	39.33	3175.76	2854.89	2154.54
7.2	3.14	12.73	37.31	3616.72	2929.47	2269.82
7.3	3.09	12.76	38.00	3324.49	2886.12	2065.99
7.4	3.05	12.65	36.13	3293.06	2699.74	1870.98
7.5	3.00	12.57	36.55	3013.45	2557.31	1856.19
7.6	2.95	12.51	36.65	3660.34	3081.44	2394.70
average	3.07	12.67	37.33	3347.30	2834.83	2102.04
STD	0.09	0.11	1.18	250.97	183.34	215.26

Table F.4: Raw Results - Tensile 4

T2 treated fibres and polypropylene (T2 - PP)						
Specimen	Width (mm)	Thickness (mm)	Max Stress (MPa)	Elastic Modulus (MPa)	Secant Modulus at 0.01 Strain	Secant Modulus at failure (MPa)
8.1	3.13	12.76	34.00	3490.67	3249.69	1880.08
8.2	3.11	12.64	34.63	3730.95	2937.51	2369.34
8.3	3.11	12.64	35.42	3368.37	3144.28	2498.38
8.4	3.09	12.67	36.83	3872.64	3032.08	2328.88
8.5	3.06	12.59	36.10	3016.73	2829.16	2223.39
8.6	3.03	12.62	35.42	2962.77	2820.35	2237.83
average	3.09	12.65	35.40	3407.02	3002.18	2256.32
STD	0.04	0.06	1.01	368.76	172.94	209.58
T3 treated fibres and polypropylene (T3 - PP)						
Specimen	Width (mm)	Thickness (mm)	Max Stress (MPa)	Elastic Modulus (MPa)	Secant Modulus at 0.01 Strain	Secant Modulus at failure (MPa)
5.1	3.05	12.83	34.10	4008.75	2932.79	2098.04
5.2	3.03	12.65	35.64	3633.59	2982.74	2220.53
5.3	2.99	12.73	31.73	2387.86	2194.65	1485.64
5.4	3.00	12.70	31.99	3976.82	2917.34	2486.05
5.6	2.95	12.87	31.55	3269.10	2716.48	2121.45
average	3.00	12.76	33.00	3455.22	2748.80	2082.34
STD	0.04	0.09	1.80	667.87	326.00	367.39
T4 treated fibres and polypropylene (T4 - PP)						
Specimen	Width (mm)	Thickness (mm)	Max Stress (MPa)	Elastic Modulus (MPa)	Secant Modulus at 0.01 Strain	Secant Modulus at failure (MPa)
6.1	3.31	12.84	37.94	3774.49	3401.79	2237.03
6.2	3.22	12.74	38.19	3217.78	3138.91	1871.71
6.3	3.13	12.68	34.43	5011.56	3239.25	2784.44
6.4	3.05	12.59	35.55	3764.49	3530.20	2239.31
6.5	2.96	12.64	35.64	4142.07	2935.91	2342.10
average	3.13	12.70	36.35	3982.08	3249.21	2294.92
STD	0.14	0.10	1.64	663.33	230.58	326.88

Table F.5: Raw Results - Tensile 5

Untreated fibre and 4% clay (Unt - C)						
Specimen	Width (mm)	Thickness (mm)	Max Stress (MPa)	Elastic Modulus (MPa)	Secant Modulus at 0.01 Strain	Secant Modulus at failure (MPa)
13.1	2.88	12.48	37.68	3958.48	3414.32	3114.81
13.2	2.85	12.70	39.53	4276.94	3494.08	3218.92
13.3	2.91	12.66	38.25	4468.85	3577.36	3462.98
13.4	2.85	12.54	42.39	3412.32	3388.58	3027.31
13.5	2.83	12.72	39.73	3991.81	3483.30	3167.02
13.6	2.85	12.78	39.92	3825.89	3156.95	2649.27
average	2.86	12.65	39.58	3989.05	3419.10	3106.72
STD	0.03	0.11	1.64	366.95	144.55	267.87
Sodium hydroxide treated fibres and 4% clay (NaOH - C)						
Specimen	Width (mm)	Thickness (mm)	Max Stress (MPa)	Elastic Modulus (MPa)	Secant Modulus at 0.01 Strain	Secant Modulus at failure (MPa)
14.1	2.89	12.48	43.14	4475.49	3647.52	3131.20
14.2	2.91	12.69	44.02	3892.51	3553.46	3137.06
14.3	2.86	12.61	41.70	4704.08	3674.91	3337.43
14.4	2.92	12.54	44.16	4919.05	3789.86	3337.87
14.5	2.94	12.52	42.61	4370.47	3563.51	2898.66
14.6	2.92	12.59	43.56	4209.18	3557.42	2944.99
average	2.91	12.57	43.20	4428.46	3631.11	3131.20
STD	0.03	0.07	0.93	362.64	93.19	186.56
T1 treated fibres and 4% clay (T1 - C)						
Specimen	Width (mm)	Thickness (mm)	Max Stress (MPa)	Elastic Modulus (MPa)	Secant Modulus at 0.01 Strain	Secant Modulus at failure (MPa)
6.1	2.92	12.80	44.55	4388.42	4292.88	2560.37
6.2	2.76	12.85	43.91	6016.28	4031.74	3579.72
6.3	2.69	12.60	43.40	3941.27	4024.89	3028.94
6.4	3.02	12.63	42.52	5415.33	3982.14	3617.93
6.5	2.85	12.82	42.52	4445.72	3579.01	3016.80
6.6	3.10	13.04	43.10	4721.83	3801.24	3268.11
average	2.89	12.79	43.33	4821.48	3951.98	3178.64
STD	0.16	0.16	0.80	760.74	241.09	398.17

Table F.6: Raw Results - Tensile 6

T2 treated fibres and 4% clay (T2 - C)						
Specimen	Width (mm)	Thickness (mm)	Max Stress (MPa)	Elastic Modulus (MPa)	Secant Modulus at 0.01 Strain	Secant Modulus at failure (MPa)
5.1	2.84	12.51	39.30	4456.94	3403.57	2945.82
5.2	2.92	12.55	39.36	4292.45	3361.56	2692.91
5.3	3.11	12.79	39.58	4743.18	3737.15	3089.02
5.4	3.22	12.77	37.83	5134.79	3543.32	3193.48
5.5	2.83	12.61	37.34	3903.58	3562.46	2655.45
5.6	3.03	12.48	38.08	3741.95	3563.63	3251.31
average	2.99	12.62	38.58	4378.81	3528.61	2971.33
STD	0.16	0.13	0.95	519.47	133.88	252.80
T3 treated fibres and 4% clay (T3 - C)						
Specimen	Width (mm)	Thickness (mm)	Max Stress (MPa)	Elastic Modulus (MPa)	Secant Modulus at 0.01 Strain	Secant Modulus at failure (MPa)
7.1	2.98	12.80	44.14	3940.68	3515.86	2845.74
7.2	3.08	12.73	37.79	4078.50	3384.68	2943.09
7.3	3.05	12.94	43.46	5465.28	4037.64	3691.20
7.4	2.91	12.70	41.65	4102.30	3317.89	2710.75
7.5	2.91	12.83	40.98	4403.02	3537.33	2992.35
7.6	2.96	12.64	43.02	3718.35	4247.20	2543.00
average	2.98	12.77	41.84	4284.69	3673.43	2954.36
STD	0.07	0.11	2.30	620.11	378.15	396.20
T4 treated fibres and 4% clay (T4 - C)						
Specimen	Width (mm)	Thickness (mm)	Max Stress (MPa)	Elastic Modulus (MPa)	Secant Modulus at 0.01 Strain	Secant Modulus at failure (MPa)
8.1	2.98	12.78	43.69	5246.98	3815.38	3177.12
8.2	3.10	12.59	45.03	4704.08	3927.38	3325.56
8.3	2.84	12.52	43.82	7387.25	3797.12	3067.40
8.5	2.93	12.74	43.52	4727.99	3670.47	3098.90
8.6	2.77	12.61	41.84	4119.46	3569.76	3038.91
average	2.93	12.65	43.58	5237.15	3756.02	3141.58
STD	0.13	0.11	1.14	1266.46	138.37	115.08

Table F.7: Raw Results - Tensile 7

0.25% treated fibres with polypropylene (0.25M - PP)						
Specimen	Width (mm)	Thickness (mm)	Max Stress (MPa)	Elastic Modulus (MPa)	Secant Modulus at 0.01 Strain	Secant Modulus at failure (MPa)
2.1	3.23	12.63	45.85	6729.07	3815.55	2984.09
2.2	3.12	12.99	43.11	4076.25	3201.34	2354.00
2.3	2.78	12.86	41.52	3532.10	3032.88	2359.74
2.4	2.67	13.06	40.71	4115.22	3230.84	2478.62
2.5	3.04	12.99	44.21	3510.04	3185.91	2535.54
2.6	2.90	12.82	43.54	4162.03	3375.46	2582.96
average	2.96	12.89	43.16	4354.12	3307.00	2549.16
STD	0.21	0.16	1.85	1199.98	272.06	232.14

1% treated fibres with polypropylene (1M - PP)						
Specimen	Width (mm)	Thickness (mm)	Max Stress (MPa)	Elastic Modulus (MPa)	Secant Modulus at 0.01 Strain	Secant Modulus at failure (MPa)
1.1	3.11	12.99	39.09	3735.20	3082.95	2404.97
1.2	3.26	12.94	39.57	3696.28	3001.11	2301.25
1.3	3.22	12.82	40.07	3846.56	3086.84	2418.02
1.4	3.03	12.64	40.64	3612.56	3095.35	2440.82
1.5	2.95	13.09	40.25	3270.45	2802.83	2006.31
1.6	3.31	13.16	41.43	2763.18	2605.85	2042.30
average	3.15	12.94	40.17	3487.37	2945.82	2268.94
STD	0.14	0.19	0.82	405.28	200.07	195.78

2% treated fibres with polypropylene (2M - PP)						
Specimen	Width (mm)	Thickness (mm)	Max Stress (MPa)	Elastic Modulus (MPa)	Secant Modulus at 0.01 Strain	Secant Modulus at failure (MPa)
7.1	3.42	12.70	39.14	4227.66	3125.91	2329.74
7.2	3.15	12.89	38.11	3323.06	2819.72	1921.47
7.3	3.26	13.18	38.72	4466.26	3191.36	2429.59
7.4	2.96	13.10	37.22	2742.50	2604.23	1945.67
7.5	2.87	12.93	38.11	3445.35	2901.40	2126.36
7.6	3.07	12.76	39.98	3231.92	2918.80	2238.87
average	3.12	12.93	38.55	3572.79	2926.90	2165.28
STD	0.20	0.19	0.96	649.82	212.54	205.67

Table F.8: Raw Results - Tensile 8

0.25% treated fibres with 4% clay (0.25M - C)						
Specimen	Width (mm)	Thickness (mm)	Max Stress (MPa)	Elastic Modulus (MPa)	Secant Modulus at 0.01 Strain	Secant Modulus at failure (MPa)
2.1	3.06	12.78	41.90	3484.79	3437.81	3129.01
2.2	2.97	12.68	45.48	4675.59	3940.57	3505.19
2.3	3.14	13.19	44.92	3410.53	3312.11	2799.02
2.4	2.87	13.01	44.21	4953.74	3576.65	2779.21
2.6	3.29	12.73	44.19	3629.41	3370.86	2972.21
average	3.07	12.88	44.14	4030.81	3527.60	3036.93
STD	0.16	0.21	1.36	726.56	251.00	297.89

1% treated fibres with 4% clay (1M - C)						
Specimen	Width (mm)	Thickness (mm)	Max Stress (MPa)	Elastic Modulus (MPa)	Secant Modulus at 0.01 Strain	Secant Modulus at failure (MPa)
4.1	2.71	12.88	44.41	2834.01	3137.93	2659.83
4.2	3.00	13.13	46.38	6325.95	3994.64	3317.48
4.3	2.82	12.76	44.40	4605.83	3732.35	3122.59
4.4	3.08	13.07	41.08	4576.91	3403.04	2746.36
4.5	2.76	13.04	43.33	2790.78	3217.12	2940.18
4.6	3.04	12.95	49.00	4489.51	3732.20	3036.52
average	2.90	12.97	44.76	4270.50	3536.21	2970.49
STD	0.16	0.14	2.70	1321.53	336.22	243.13

2% treated fibres with 4% clay (2M - C)						
Specimen	Width (mm)	Thickness (mm)	Max Stress (MPa)	Elastic Modulus (MPa)	Secant Modulus at 0.01 Strain	Secant Modulus at failure (MPa)
7.1	3.27	12.86	45.76	4737.42	3830.20	3152.61
7.2	3.34	12.66	44.20	4594.64	3662.84	3026.89
7.3	3.04	12.99	41.75	4578.57	3506.25	2917.15
7.4	2.99	13.13	41.30	5135.19	3556.32	2932.85
7.5	3.19	13.04	46.23	4544.71	3799.09	3141.59
7.6	3.12	13.00	44.02	4208.59	3620.86	3043.15
average	3.16	12.95	43.88	4633.19	3662.60	3035.71
STD	0.13	0.16	2.02	301.81	129.77	99.65

Table F.9: Raw Results - Tensile 9

5% MPS treated fibres with polypropylene (5M - PP)						
Specimen	Width (mm)	Thickness (mm)	Max Stress (MPa)	Elastic Modulus (MPa)	Secant Modulus at 0.01 Strain	Secant Modulus at failure (MPa)
8.1	2.95	12.95	34.68	3326.80	2744.43	2089.18
8.2	2.94	13.12	39.45	3714.36	2973.89	1993.97
8.3	2.96	12.89	40.36	3661.66	2976.60	2019.38
8.4	2.89	13.18	37.14	3212.95	2686.45	1824.03
8.5	2.97	13.16	37.05	3613.23	2814.29	1994.79
8.6	3.02	13.33	41.89	3446.83	2953.16	2107.14
average	2.96	13.10	38.43	3495.97	2858.13	2004.75
STD	0.04	0.16	2.62	200.02	127.11	100.70

5% MPS treated fibres with 4% clay (5M - 4C)						
Specimen	Width (mm)	Thickness (mm)	Max Stress (MPa)	Elastic Modulus (MPa)	Secant Modulus at 0.01 Strain	Secant Modulus at failure (MPa)
6.1	3.23	12.51	45.02	4676.82	3766.72	3150.41
6.2	3.11	12.87	45.69	5172.26	3872.12	3223.85
6.3	3.06	12.78	40.43	4661.62	3658.65	3238.93
6.4	3.11	12.61	39.53	4330.96	3427.28	2877.41
6.5	3.16	12.58	45.29	3925.50	3811.87	3249.00
6.6	3.00	12.77	39.03	4942.32	3828.73	3740.54
average	3.11	12.69	42.50	4618.25	3727.56	3246.69
STD	0.08	0.14	3.14	442.65	164.13	279.32

0.25% MPS treated fibres with 1% clay (0.25M - 1C)						
Specimen	Width (mm)	Thickness (mm)	Max Stress (MPa)	Elastic Modulus (MPa)	Secant Modulus at 0.01 Strain	Secant Modulus at failure (MPa)
2.1	2.88	12.44	43.06	4050.31	3182.10	2401.90
2.2	2.88	12.50	41.10	4458.01	3358.46	2687.78
2.3	2.94	12.59	43.51	4222.24	3240.30	2481.99
2.4	2.91	12.53	44.39	4541.24	3470.70	2780.96
2.5	2.93	12.70	41.57	4255.42	3391.51	2878.02
2.6	2.92	12.65	37.44	4116.80	3212.82	2713.45
average	2.91	12.57	41.85	4274.01	3309.31	2657.35
STD	0.03	0.10	2.48	191.34	114.43	181.14

Table F.10: Raw Results - Tensile 10

0.25% MPS treated fibres with 2% clay (0.25M - 2C)						
Specimen	Width (mm)	Thickness (mm)	Max Stress (MPa)	Elastic Modulus (MPa)	Secant Modulus at 0.01 Strain	Secant Modulus at failure (MPa)
12.1	2.91	12.73	45.29	4225.09	3432.41	2580.47
12.2	2.88	12.82	44.68	4861.08	3693.76	3051.75
12.3	2.95	12.63	44.74	4600.59	3582.40	2781.17
12.4	2.99	12.56	44.86	3968.93	3342.77	2541.47
12.5	2.83	12.60	45.72	5108.76	3857.19	3317.57
12.6	2.84	12.57	45.48	4344.27	3473.63	2731.29
average	2.90	12.65	45.13	4518.12	3563.69	2833.95
STD	0.06	0.10	0.43	422.13	188.45	298.14

0.25% MPS treated fibres with 6% clay (0.25M - 6C)						
Specimen	Width (mm)	Thickness (mm)	Max Stress (MPa)	Elastic Modulus (MPa)	Secant Modulus at 0.01 Strain	Secant Modulus at failure (MPa)
11.1	2.91	12.60	38.28	3864.53	3073.62	2301.20
11.2	2.85	12.87	43.26	4121.59	3248.52	2320.60
11.3	2.75	12.63	41.48	3964.74	3271.63	2581.16
11.4	2.82	12.80	43.95	3955.07	3422.17	2639.55
11.5	2.98	12.63	42.69	5288.35	3511.70	2738.18
11.6	3.04	12.53	43.09	4099.43	3288.16	2354.75
average	2.89	12.68	42.12	4215.62	3302.63	2489.24
STD	0.11	0.13	2.06	534.26	151.36	187.03

0.25% MPS treated fibres with 8% clay (0.25M - 8C)						
Specimen	Width (mm)	Thickness (mm)	Max Stress (MPa)	Elastic Modulus (MPa)	Secant Modulus at 0.01 Strain	Secant Modulus at failure (MPa)
7.1	2.90	12.71	44.13	3807.48	3323.87	2382.17
7.2	2.99	12.93	44.32	4220.33	3438.55	2505.45
7.3	2.87	12.65	46.02	4625.21	3589.78	2664.91
7.4	2.94	12.85	41.64	6996.46	3959.40	3674.12
7.5	3.03	12.70	46.68	4957.67	3641.48	2712.42
7.6	2.98	12.60	42.96	4213.57	3389.30	2492.38
average	2.95	12.74	44.29	4803.45	3557.06	2738.58
STD	0.06	0.13	1.87	1144.10	230.93	473.99

Table F.11: Raw Results - Tensile 11

0.25% MPS treated fibres with polypropylene using 15% FWF (15FWF - PP)						
Specimen	Width (mm)	Thickness (mm)	Max Stress (MPa)	Elastic Modulus (MPa)	Secant Modulus at 0.01 Strain	Secant Modulus at failure (MPa)
8.1	5.33	12.54	33.53	2338.94	2069.49	1169.97
8.2	5.35	12.71	34.58	2776.62	2283.39	1224.38
8.3	5.37	12.62	32.50	2420.49	2129.02	1303.67
8.4	5.37	12.80	33.78	2529.95	2178.13	1210.52
8.5	5.37	12.60	34.42	3011.24	2351.46	1286.09
8.6	5.35	12.83	34.94	2633.66	2240.19	1277.04
average	5.36	12.68	33.96	2618.49	2208.61	1245.28
STD	0.02	0.11	0.88	246.85	103.55	51.77
0.25% MPS treated fibres with polypropylene using 20% FWF (20FWF - PP)						
Specimen	Width (mm)	Thickness (mm)	Max Stress (MPa)	Elastic Modulus (MPa)	Secant Modulus at 0.01 Strain	Secant Modulus at failure (MPa)
3.1	3.95	12.56	36.57	2938.39	2490.64	1544.00
3.2	4.03	12.82	34.50	2595.14	2278.15	1410.62
3.3	4.05	12.71	34.45	3054.53	2420.95	1644.66
3.4	4.07	12.51	34.91	2625.99	2272.57	1368.17
3.5	4.04	12.74	35.63	2839.11	2366.86	1481.90
3.6	4.02	12.69	36.18	3715.19	2655.73	1615.44
average	4.03	12.67	35.37	2961.39	2414.15	1510.80
STD	0.04	0.12	0.89	409.64	144.94	110.62
0.25% MPS treated fibres with polypropylene using 30% FWF (30FWF - PP)						
Specimen	Width (mm)	Thickness (mm)	Max Stress (MPa)	Elastic Modulus (MPa)	Secant Modulus at 0.01 Strain	Secant Modulus at failure (MPa)
2.1	2.68	12.81	35.29	4548.13	3201.36	2803.77
2.2	2.44	12.63	35.60	3428.21	2794.12	2128.48
2.3	2.70	12.65	36.12	3979.43	2982.23	2408.88
2.4	2.63	12.84	33.26	3782.54	2896.23	2356.76
2.5	2.51	12.84	36.33	4702.45	3061.38	2192.00
2.6	2.58	12.91	33.51	3904.79	2873.64	2315.28
average	2.59	12.78	35.02	4057.59	2968.16	2367.53
STD	0.10	0.11	1.32	481.19	146.74	237.83

Table F.12: Raw Results - Tensile 12

0.25% MPS treated fibres with 2% clay using 15% FWF (15FWF - 2C)						
Specimen	Width (mm)	Thickness (mm)	Max Stress (MPa)	Elastic Modulus (MPa)	Secant Modulus at 0.01 Strain	Secant Modulus at failure (MPa)
6.1	4.54	12.91	35.57	3948.58	2745.18	1855.96
6.2	4.44	12.74	36.24	2968.14	3573.00	1694.54
6.3	4.54	12.76	37.14	2807.14	3562.06	1598.23
6.4	4.47	12.93	37.27	3084.75	2613.00	1646.70
6.5	4.35	12.69	35.17	2846.15	2480.47	1688.40
6.6	4.60	12.66	37.02	2904.77	2675.05	1561.72
average	4.49	12.78	36.40	3093.26	2941.46	1674.26
STD	0.09	0.11	0.89	430.29	492.72	102.79

0.25% MPS treated fibres with 2% clay using 20% FWF (20FWF - 2C)						
Specimen	Width (mm)	Thickness (mm)	Max Stress (MPa)	Elastic Modulus (MPa)	Secant Modulus at 0.01 Strain	Secant Modulus at failure (MPa)
4.1	3.62	13.01	43.83	5142.38	3677.59	2965.07
4.2	3.68	12.66	43.68	3896.17	4132.48	2525.96
4.3	3.31	12.79	41.23	4080.41	3869.88	2279.77
4.4	3.47	13.08	41.04	3983.33	3945.51	2283.04
4.5	3.55	12.86	40.39	4628.19	3204.75	2372.83
4.6	3.41	12.72	43.58	3995.19	3229.90	2391.33
average	3.51	12.86	42.29	4287.61	3676.69	2469.67
STD	0.14	0.16	1.56	494.14	384.63	258.84

0.25% MPS treated fibres with 2% clay using 30% FWF (30FWF - 2C)						
Specimen	Width (mm)	Thickness (mm)	Max Stress (MPa)	Elastic Modulus (MPa)	Secant Modulus at 0.01 Strain	Secant Modulus at failure (MPa)
2.1	2.48	12.65	44.64	4607.03	3791.16	3078.17
2.2	2.66	12.76	46.85	4273.57	4639.62	3241.81
2.3	2.54	13.00	46.51	3909.40	4562.48	3068.93
2.4	2.45	12.86	45.31	4407.25	4284.36	2953.67
2.5	2.64	13.07	46.40	6366.18	4499.67	3548.47
2.6	2.59	12.89	48.49	4364.49	3865.29	3198.06
average	2.56	12.87	46.37	4654.65	4273.76	3181.52
STD	0.09	0.15	1.33	869.21	365.54	206.80

Table F.13: Raw Results - Impact 1

Untreated fibre and polypropylene (Unt - PP)							
Specimen	Width (mm)	Thickness (mm)	Total Energy (J/m)	Total Energy (kJ/m2)	Initial Energy (J/m)	Propagative Energy (J/m)	Stress (MPa)
11.1	10.18	2.83	69.85	6.86	39.22	30.63	7.35
11.2	10.23	2.98	88.45	8.65	45.33	43.11	7.48
11.3	10.29	2.96	83.73	8.14	41.91	41.81	4.55
11.4	10.37	2.91	61.65	5.95	30.51	31.14	5.45
11.5	10.31	2.88	74.95	7.27	37.20	37.74	5.03
11.6	10.23	2.78	79.53	7.77	40.18	39.35	6.51
average	10.27	2.89	76.36	7.44	39.06	37.30	6.06
STD	0.07	0.08	9.71	0.97	5.01	5.31	1.23

Sodium hydroxide treated fibres and polypropylene (NaOH - PP)							
Specimen	Width (mm)	Thickness (mm)	Total Energy (J/m)	Total Energy (kJ/m2)	Initial Energy (J/m)	Propagative Energy (J/m)	Stress (MPa)
10.1	10.06	2.79	38.33	3.81	17.43	20.90	4.94
10.2	9.69	2.49	54.12	5.59	23.88	30.24	6.11
10.3	10.14	2.59	51.36	5.07	24.40	26.97	5.48
10.4	10.08	2.61	56.80	5.64	14.16	42.63	4.20
10.5	10.14	2.68	78.19	7.72	34.86	43.33	4.79
10.6	10.07	2.74	64.63	6.42	28.46	36.16	6.11
average	10.03	2.65	57.24	5.71	23.87	33.37	5.27
STD	0.17	0.11	13.38	1.31	7.45	8.93	0.77

T1 treated fibres and polypropylene (T1 - PP)							
Specimen	Width (mm)	Thickness (mm)	Total Energy (J/m)	Total Energy (kJ/m2)	Initial Energy (J/m)	Propagative Energy (J/m)	Stress (MPa)
11.1	10.26	2.35	48.20	4.70	25.49	22.71	5.14
11.2	10.26	2.70	44.13	4.30	16.99	27.15	3.13
11.3	10.26	2.42	52.65	5.13	23.47	29.17	5.17
11.4	10.31	2.52	62.08	6.02	33.12	28.96	5.96
11.5	10.28	2.56	46.58	4.53	24.45	22.13	4.35
11.6	10.25	2.66	53.84	5.26	29.82	24.02	4.64
average	10.27	2.53	51.25	4.99	25.56	25.69	4.73
STD	0.02	0.14	6.45	0.62	5.56	3.14	0.96

Table F.14: Raw Results - Impact 2

T2 treated fibres and polypropylene (T2 - PP)							
Specimen	Width (mm)	Thickness (mm)	Total Energy (J/m)	Total Energy (kJ/m2)	Initial Energy (J/m)	Propagative Energy (J/m)	Stress (MPa)
13.1	10.22	3.39	39.97	3.91	15.37	24.61	2.78
13.2	10.24	2.86	33.41	3.26	14.84	18.56	3.66
13.3	10.24	3.21	55.63	5.43	21.75	33.87	4.74
13.4	10.13	3.13	31.41	3.10	15.04	16.37	4.07
13.5	10.20	3.04	28.74	2.82	14.00	14.75	3.64
13.6	10.23	2.95	26.02	2.54	12.72	13.30	4.02
average	10.21	3.10	35.86	3.51	15.62	20.24	3.82
STD	0.04	0.19	10.78	1.05	3.15	7.76	0.64

T3 treated fibres and polypropylene (T3 - PP)							
Specimen	Width (mm)	Thickness (mm)	Total Energy (J/m)	Total Energy (kJ/m2)	Initial Energy (J/m)	Propagative Energy (J/m)	Stress (MPa)
14.1	10.37	2.53	81.96	7.90	50.43	31.53	7.15
14.2	10.45	2.63	83.14	7.96	54.40	28.74	5.65
14.3	10.39	2.69	86.29	8.31	51.38	34.92	5.12
14.4	10.32	2.74	75.49	7.31	47.33	28.16	5.33
14.5	10.31	2.81	114.36	11.10	72.81	41.55	5.51
14.6	10.42	2.90	108.41	10.40	58.91	49.50	6.29
average	10.38	2.71	91.61	8.83	55.87	35.73	5.84
STD	0.06	0.13	15.83	1.54	9.18	8.34	0.75

T4 treated fibres and polypropylene (T4 - PP)							
Specimen	Width (mm)	Thickness (mm)	Total Energy (J/m)	Total Energy (kJ/m2)	Initial Energy (J/m)	Propagative Energy (J/m)	Stress (MPa)
12.1	10.37	3.11	50.11	4.83	26.84	23.27	6.37
12.2	10.27	3.35	56.86	5.54	30.34	26.52	7.58
12.3	10.36	3.29	52.73	5.09	27.73	25.01	6.47
12.4	10.40	3.23	48.29	4.64	25.56	22.73	6.24
12.5	10.46	3.22	53.17	5.08	28.76	24.41	6.37
12.6	10.29	3.14	57.27	5.57	28.07	29.20	6.84
average	10.36	3.22	53.07	5.13	27.88	25.19	6.65
STD	0.07	0.09	3.57	0.37	1.63	2.37	0.50

Table F.15: Raw Results - Impact 3

Untreated fibre and polypropylene (Unt - PP)							
Specimen	Width (mm)	Thickness (mm)	Total Energy (J/m)	Total Energy (kJ/m2)	Initial Energy (J/m)	Propagative Energy (J/m)	Stress (MPa)
12.1	10.22	3.08	29.70	2.91	16.81	12.88	3.19
12.2	10.27	2.76	36.50	3.56	19.51	16.98	4.72
12.3	10.30	2.84	33.13	3.22	16.77	16.37	2.89
12.4	10.25	2.88	33.02	3.22	16.24	16.79	4.17
12.5	10.39	2.93	38.47	3.70	18.12	20.35	3.94
12.6	10.26	2.97	33.07	3.22	15.63	17.44	2.86
average	10.28	2.91	33.98	3.31	17.18	16.80	3.63
STD	0.06	0.11	3.08	0.28	1.41	2.39	0.76

Sodium hydroxide treated fibres and 4% clay (NaOH - 4C)							
Specimen	Width (mm)	Thickness (mm)	Total Energy (J/m)	Total Energy (kJ/m2)	Initial Energy (J/m)	Propagative Energy (J/m)	Stress (MPa)
10.1	10.24	3.36	30.06	2.94	14.44	15.62	3.90
10.2	10.38	3.32	24.77	2.39	10.94	13.83	3.40
10.3	10.48	3.42	18.82	1.80	10.08	8.75	2.76
10.4	10.30	3.36	27.90	2.71	13.68	14.22	3.89
10.5	10.40	3.37	24.08	2.32	13.40	10.68	2.73
10.6	10.36	3.38	22.92	2.21	10.98	11.94	3.11
average	10.36	3.37	24.76	2.39	12.25	12.51	3.30
STD	0.08	0.03	3.92	0.40	1.80	2.54	0.52

T1 treated fibres and 4% clay (T1 - 4C)							
Specimen	Width (mm)	Thickness (mm)	Total Energy (J/m)	Total Energy (kJ/m2)	Initial Energy (J/m)	Propagative Energy (J/m)	Stress (MPa)
2.1	10.29	3.32	35.73	3.47	17.76	17.96	4.06
2.2	10.31	3.29	52.81	5.12	31.59	21.22	4.22
2.3	10.27	3.02	40.65	3.96	21.06	19.59	5.18
2.4	10.26	3.22	46.10	4.49	16.87	29.23	3.51
2.5	10.31	3.15	26.99	2.62	15.21	11.78	4.54
2.6	10.33	3.10	37.77	3.66	9.79	27.98	4.75
average	10.29	3.18	40.01	3.89	18.71	21.29	4.38
STD	0.02	0.12	8.88	0.86	7.32	6.51	0.58

Table F.16: Raw Results - Impact 4

T2 treated fibres and 4% clay (T2 - 4C)							
Specimen	Width (mm)	Thickness (mm)	Total Energy (J/m)	Total Energy (kJ/m2)	Initial Energy (J/m)	Propagative Energy (J/m)	Stress (MPa)
3.1	10.29	2.80	19.91	1.94	10.61	9.31	2.49
3.2	10.32	2.83	23.64	2.29	16.58	7.06	2.47
3.3	10.32	2.85	33.43	3.24	17.53	15.90	3.83
3.4	10.34	2.98	16.91	1.64	10.74	6.16	2.84
3.5	10.31	3.03	25.07	2.43	11.68	13.39	2.54
3.6	10.35	2.98	24.62	2.38	13.89	10.73	3.28
average	10.32	2.91	23.93	2.32	13.51	10.42	2.91
STD	0.02	0.09	5.61	0.54	3.00	3.73	0.55

T3 treated fibres and 4% clay (T3 - 4C)							
Specimen	Width (mm)	Thickness (mm)	Total Energy (J/m)	Total Energy (kJ/m2)	Initial Energy (J/m)	Propagative Energy (J/m)	Stress (MPa)
4.1	10.41	3.29	36.88	3.54	19.26	17.62	5.33
4.2	10.32	2.93	28.62	2.77	14.16	14.46	4.49
4.3	10.33	2.99	35.89	3.47	18.33	17.56	5.13
4.4	10.34	3.01	33.00	3.19	16.40	16.60	4.87
4.5	10.35	3.10	31.32	3.03	16.16	15.16	4.92
4.6	10.40	3.15	38.30	3.68	21.22	17.09	5.82
average	10.36	3.08	34.00	3.28	17.59	16.41	5.09
STD	0.04	0.13	3.67	0.35	2.52	1.32	0.45

T4 treated fibres and 4% clay (T4 - 4C)							
Specimen	Width (mm)	Thickness (mm)	Total Energy (J/m)	Total Energy (kJ/m2)	Initial Energy (J/m)	Propagative Energy (J/m)	Stress (MPa)
1.1	10.47	3.64	32.82	3.13	17.44	15.39	5.10
1.2	10.28	3.61	28.16	2.74	15.03	13.12	4.18
1.3	10.37	3.53	27.56	2.66	14.04	13.53	4.28
1.4	10.40	3.51	24.22	2.33	12.16	12.06	3.48
1.5	10.37	3.38	32.62	3.15	17.06	15.56	5.19
1.6	10.36	3.35	36.12	3.49	17.70	18.42	4.66
average	10.37	3.50	30.25	2.92	15.57	14.68	4.48
STD	0.06	0.12	4.35	0.42	2.21	2.27	0.64

Table F.17: Raw Results - Impact 5

0.25% MPS treated fibres and polypropylene (0.25M - PP)							
Specimen	Width (mm)	Thickness (mm)	Total Energy (J/m)	Total Energy (kJ/m2)	Initial Energy (J/m)	Propagative Energy (J/m)	Stress (MPa)
3.1	10.41	3.35	37.96	3.65	18.05	19.91	3.86
3.2	10.20	3.43	54.59	5.36	22.55	32.04	4.92
3.3	10.26	3.43	58.58	5.71	27.64	30.94	5.17
3.4	10.36	3.36	54.37	5.25	21.63	32.75	4.57
3.5	10.34	3.33	38.41	3.72	19.29	19.12	4.44
3.6	10.33	3.32	53.67	5.20	27.58	26.09	5.35
average	10.31	3.37	49.60	4.81	22.79	26.81	4.72
STD	0.08	0.05	9.01	0.89	4.06	6.11	0.54

1% MPS treated fibres and polypropylene (1M - PP)							
Specimen	Width (mm)	Thickness (mm)	Total Energy (J/m)	Total Energy (kJ/m2)	Initial Energy (J/m)	Propagative Energy (J/m)	Stress (MPa)
5.1	10.43	3.33	50.46	4.84	14.75	35.72	3.48
5.2	10.44	3.26	37.77	3.62	10.39	27.37	2.41
5.3	10.39	2.96	39.24	3.78	13.50	25.74	3.22
5.4	10.46	3.14	48.02	4.59	19.82	28.20	3.72
5.5	10.35	2.81	56.40	5.45	19.72	36.68	4.34
average	10.41	3.10	46.38	4.45	15.64	30.74	3.43
STD	0.04	0.22	7.82	0.76	4.09	5.07	0.71

2% MPS treated fibres and polypropylene (2M - PP)							
Specimen	Width (mm)	Thickness (mm)	Total Energy (J/m)	Total Energy (kJ/m2)	Initial Energy (J/m)	Propagative Energy (J/m)	Stress (MPa)
6.1	10.28	2.74	46.18	4.49	20.63	25.55	5.01
6.2	10.34	2.83	47.97	4.64	23.77	24.19	5.20
6.3	10.14	2.91	39.96	3.94	16.19	23.77	3.82
6.4	10.46	3.44	33.51	3.20	16.95	16.56	4.17
6.5	10.38	3.12	54.36	5.24	21.09	33.26	4.13
6.6	10.36	3.20	33.44	3.23	14.85	18.59	3.26
average	10.32	3.04	42.57	4.12	18.91	23.65	4.27
STD	0.11	0.26	8.41	0.81	3.44	5.87	0.73

Table F.18: Raw Results - Impact 6

0.25% MPS treated fibres and 4% clay (0.25M - 4C)							
Specimen	Width (mm)	Thickness (mm)	Total Energy (J/m)	Total Energy (kJ/m2)	Initial Energy (J/m)	Propagative Energy (J/m)	Stress (MPa)
3.1	10.10	3.28	20.76	2.06	10.38	10.38	2.24
3.2	10.12	3.24	23.24	2.30	11.89	11.36	2.88
3.3	10.12	3.20	17.39	1.72	7.70	9.69	2.35
3.4	10.15	3.08	33.83	3.33	25.00	8.84	2.56
3.5	10.23	3.06	21.38	2.09	12.64	8.74	2.17
3.6	10.19	3.02	17.30	1.70	5.75	11.54	1.68
average	10.15	3.14	22.32	2.20	12.23	10.09	2.31
STD	0.05	0.10	6.10	0.60	6.77	1.21	0.40

1% MPS treated fibres and 4% clay (1M - 4C)							
Specimen	Width (mm)	Thickness (mm)	Total Energy (J/m)	Total Energy (kJ/m2)	Initial Energy (J/m)	Propagative Energy (J/m)	Stress (MPa)
1.1	10.13	3.14	21.83	2.16	10.91	10.91	3.20
1.2	10.27	3.24	18.68	1.82	9.90	8.78	3.06
1.3	10.21	3.27	33.97	3.33	16.99	16.99	4.24
1.4	10.20	3.30	26.11	2.56	12.60	13.51	3.62
1.5	10.24	3.35	37.21	3.63	15.25	21.96	3.53
1.6	10.20	3.45	38.72	3.80	13.47	25.25	3.53
average	10.20	3.29	29.42	2.88	13.19	16.23	3.53
STD	0.05	0.10	8.39	0.82	2.65	6.42	0.41

2% MPS treated fibres and 4% clay (2M - 4C)							
Specimen	Width (mm)	Thickness (mm)	Total Energy (J/m)	Total Energy (kJ/m2)	Initial Energy (J/m)	Propagative Energy (J/m)	Stress (MPa)
8.1	10.31	3.29	31.37	3.04	12.78	18.60	2.55
8.2	10.40	3.26	20.32	1.95	10.39	9.93	2.56
8.3	10.16	3.34	16.18	1.59	7.70	8.48	2.06
8.4	10.29	3.32	40.06	3.89	15.69	24.37	3.65
8.5	10.23	3.29	39.50	3.86	13.11	26.38	3.55
average	10.28	3.30	29.49	2.87	11.93	17.55	2.87
STD	0.09	0.03	10.92	1.07	3.02	8.15	0.69

Table F.19: Raw Results - Impact 7

5% MPS treated fibres and polypropylene (5M - PP)							
Specimen	Width (mm)	Thickness (mm)	Total Energy (J/m)	Total Energy (kJ/m2)	Initial Energy (J/m)	Propagative Energy (J/m)	Stress (MPa)
4.1	10.25	3.34	44.68	4.36	21.09	23.59	4.66
4.2	10.27	3.33	58.20	5.67	27.40	30.80	5.83
4.3	10.41	3.30	47.43	4.56	21.84	25.59	4.23
4.4	10.40	3.23	41.26	3.97	22.14	19.12	4.58
4.5	10.36	3.20	29.45	2.84	13.23	16.22	3.31
average	10.34	3.28	44.20	4.28	21.14	23.06	4.52
STD	0.07	0.06	10.40	1.02	5.08	5.68	0.91

5% MPS treated fibres and 4% clay (5M - 4C)							
Specimen	Width (mm)	Thickness (mm)	Total Energy (J/m)	Total Energy (kJ/m2)	Initial Energy (J/m)	Propagative Energy (J/m)	Stress (MPa)
5.1	10.11	3.00	15.83	1.57	6.96	8.87	2.76
5.2	10.12	2.82	19.94	1.97	9.91	10.02	3.10
5.3	10.20	2.85	32.13	3.15	10.38	21.75	2.52
5.4	10.01	2.82	27.97	2.80	7.64	20.34	2.56
5.5	10.08	2.79	22.52	2.23	10.37	12.15	3.37
average	10.10	2.85	23.68	2.34	9.05	14.63	2.86
STD	0.07	0.08	6.46	0.63	1.63	5.99	0.37

0.25% MPS treated fibres and 1% clay (0.25M - 1C)							
Specimen	Width (mm)	Thickness (mm)	Total Energy (J/m)	Total Energy (kJ/m2)	Initial Energy (J/m)	Propagative Energy (J/m)	Stress (MPa)
1.1	10.34	2.99	44.97	4.35	22.50	22.48	5.65
1.2	10.35	2.95	37.23	3.60	18.99	18.23	5.47
1.3	10.38	2.97	41.52	4.00	20.56	20.96	5.69
1.4	10.37	2.95	33.43	3.22	16.26	17.17	4.92
1.5	10.33	2.96	36.52	3.54	18.38	18.14	5.11
1.6	10.37	2.96	42.54	4.10	22.42	20.12	5.70
average	10.35	2.96	39.37	3.80	19.85	19.52	5.42
STD	0.02	0.01	4.34	0.42	2.44	2.01	0.33

Table F.20: Raw Results - Impact 8

0.25% MPS treated fibres and 2% clay (0.25M - 2C)							
Specimen	Width (mm)	Thickness (mm)	Total Energy (J/m)	Total Energy (kJ/m2)	Initial Energy (J/m)	Propagative Energy (J/m)	Stress (MPa)
3.1	10.30	3.38	33.01	3.20	11.57	21.43	2.67
3.2	10.19	3.33	36.09	3.54	15.22	20.87	3.52
3.3	10.21	3.33	25.11	2.46	12.27	12.84	2.53
3.4	10.18	3.38	12.61	1.24	6.04	6.58	2.02
3.5	10.21	3.35	29.93	2.93	14.59	15.33	3.52
average	10.22	3.35	27.35	2.68	11.94	15.41	2.85
STD	0.05	0.02	9.18	0.90	3.64	6.14	0.66

0.25% MPS treated fibres and 6% clay (0.25M - 6C)							
Specimen	Width (mm)	Thickness (mm)	Total Energy (J/m)	Total Energy (kJ/m2)	Initial Energy (J/m)	Propagative Energy (J/m)	Stress (MPa)
5.1	10.23	3.09	25.41	2.48	11.07	14.35	4.29
5.2	10.23	3.05	12.39	1.21	6.34	6.05	1.78
5.3	10.22	2.91	22.10	2.16	7.63	14.47	1.79
5.4	10.36	2.98	33.64	3.25	14.79	18.86	3.69
5.5	10.26	2.93	30.46	2.97	13.75	16.70	2.95
5.6	10.19	2.92	25.10	2.46	13.80	11.30	2.98
average	10.25	2.98	24.85	2.42	11.23	13.62	2.92
STD	0.06	0.08	7.37	0.71	3.53	4.49	1.01

0.25% MPS treated fibres and 8% clay (0.25M - 8C)							
Specimen	Width (mm)	Thickness (mm)	Total Energy (J/m)	Total Energy (kJ/m2)	Initial Energy (J/m)	Propagative Energy (J/m)	Stress (MPa)
8.1	10.06	3.39	28.01	2.78	13.71	14.30	3.50
8.2	10.11	3.29	11.57	1.14	7.17	4.40	2.02
8.3	10.18	3.27	7.60	0.75	4.41	3.19	1.52
8.4	10.16	3.12	26.81	2.64	12.90	13.91	3.64
8.5	10.11	3.10	12.58	1.24	5.69	6.88	2.14
8.6	10.06	3.15	18.18	1.81	9.40	8.78	2.34
average	10.11	3.22	17.46	1.73	8.88	8.58	2.52
STD	0.05	0.12	8.43	0.84	3.81	4.70	0.85

Table F.21: Raw Results - Impact 9

0.25% MPS treated fibres with polypropylene using 15% FWF (15FWF - PP)							
Specimen	Width (mm)	Thickness (mm)	Total Energy (J/m)	Total Energy (kJ/m2)	Initial Energy (J/m)	Propagative Energy (J/m)	Stress (MPa)
7.1	10.26	4.44	23.07	2.25	10.58	12.49	2.91
7.2	10.38	4.55	24.22	2.33	12.84	11.38	3.26
7.3	10.32	4.68	43.07	4.17	17.60	25.47	2.68
7.4	10.22	4.76	62.45	6.11	36.00	26.45	3.23
7.5	10.25	4.84	56.34	5.50	37.54	18.79	4.01
7.6	10.32	5.31	67.89	6.58	43.64	24.25	4.97
average	10.29	4.76	46.17	4.49	26.37	19.81	3.51
STD	0.06	0.30	19.31	1.89	14.32	6.65	0.84

0.25% MPS treated fibres with polypropylene using 20% FWF (20FWF - PP)							
Specimen	Width (mm)	Thickness (mm)	Total Energy (J/m)	Total Energy (kJ/m2)	Initial Energy (J/m)	Propagative Energy (J/m)	Stress (MPa)
6.1	10.16	4.08	42.90	4.22	17.80	25.10	4.00
6.2	10.21	4.11	46.42	4.55	13.68	32.74	3.34
6.3	10.28	4.11	41.70	4.06	13.96	27.73	3.82
6.4	10.29	4.26	26.44	2.57	12.57	13.87	3.41
6.5	10.30	4.14	76.50	7.43	37.22	39.28	8.67
6.6	10.26	4.21	56.13	5.47	16.57	39.55	4.11
average	10.25	4.15	48.35	4.72	18.63	29.71	4.56
STD	0.05	0.07	16.80	1.63	9.31	9.73	2.04

0.25% MPS treated fibres with polypropylene using 30% FWF (30FWF - PP)							
Specimen	Width (mm)	Thickness (mm)	Total Energy (J/m)	Total Energy (kJ/m2)	Initial Energy (J/m)	Propagative Energy (J/m)	Stress (MPa)
1.1	10.31	2.68	64.99	6.31	29.56	35.43	4.90
1.2	10.29	2.72	53.89	5.24	22.97	30.92	4.80
1.3	10.28	2.75	69.03	6.72	31.26	37.76	6.08
1.4	10.33	2.67	55.71	5.40	25.85	29.87	3.97
1.5	10.31	2.70	55.49	5.38	23.45	32.04	4.98
1.6	10.33	2.68	50.90	4.93	19.53	31.37	4.52
average	10.31	2.70	58.34	5.66	25.44	32.90	4.88
STD	0.02	0.03	7.05	0.69	4.38	3.04	0.70

Table F.22: Raw Results - Impact 10

0.25% MPS treated fibres with 2% clay using 15% FWF FWF (15FWF - 2C)							
Specimen	Width (mm)	Thickness (mm)	Total Energy (J/m)	Total Energy (kJ/m2)	Initial Energy (J/m)	Propagative Energy (J/m)	Stress (MPa)
5.1	10.29	4.16	14.05	1.37	7.32	6.73	2.69
5.2	10.29	4.34	13.13	1.28	6.71	6.41	1.93
5.3	10.31	4.21	29.33	2.84	18.26	11.07	2.10
5.4	10.32	4.26	12.72	1.23	6.37	6.35	2.24
5.5	10.22	4.29	9.62	0.94	4.32	5.30	1.54
5.6	10.26	4.30	14.95	1.46	6.75	8.20	2.11
average	10.28	4.26	15.63	1.52	8.29	7.34	2.10
STD	0.04	0.07	6.95	0.67	4.99	2.05	0.38

0.25% MPS treated fibres with 2% clay using 20% FWF (20FWF - 2C)							
Specimen	Width (mm)	Thickness (mm)	Total Energy (J/m)	Total Energy (kJ/m2)	Initial Energy (J/m)	Propagative Energy (J/m)	Stress (MPa)
3.1	10.11	4.33	43.25	4.28	28.71	14.54	3.62
3.2	10.17	4.22	17.54	1.72	6.28	11.25	1.80
3.3	10.14	4.22	28.90	2.85	14.12	14.78	2.78
3.4	10.15	4.13	19.84	1.96	10.25	9.59	2.15
3.5	10.13	4.05	10.49	1.04	5.56	4.93	1.91
3.6	10.16	4.01	28.48	2.80	8.30	20.18	2.23
average	10.14	4.16	24.75	2.44	12.20	12.54	2.42
STD	0.02	0.12	11.43	1.13	8.65	5.21	0.68

0.25% MPS treated fibres with 2% clay using 30% FWF (30FWF - 2C)							
Specimen	Width (mm)	Thickness (mm)	Total Energy (J/m)	Total Energy (kJ/m2)	Initial Energy (J/m)	Propagative Energy (J/m)	Stress (MPa)
1.1	10.21	2.68	47.81	4.68	30.52	17.29	4.81
1.2	10.27	2.67	22.98	2.24	8.07	14.91	2.05
1.3	10.26	2.65	33.58	3.27	11.04	22.53	2.63
1.4	10.27	2.66	32.06	3.12	18.53	13.52	3.14
1.5	10.18	2.66	25.43	2.50	12.89	12.54	3.09
1.6	10.31	2.64	47.34	4.59	23.81	23.53	6.20
average	10.25	2.66	34.87	3.40	17.48	17.39	3.65
STD	0.05	0.01	10.61	1.03	8.51	4.67	1.55

Table F.23: Raw Results - Shear 1

Untreated fibres with polypropylene (Unt - PP)					Untreated fibres with 4% clay (Unt - 4C)				
Specimen	Width (mm)	Thick (mm)	Shear Str (MPa)	Shear Mod (MPa)	Specimen	Width (mm)	Thick (mm)	Shear Str (MPa)	Shear Mod (MPa)
11.1	5.84	3.01	7.95	57.15	12.1	5.82	3.06	8.24	77.14
11.2	5.75	3.01	7.75	51.60	12.2	5.73	3.09	8.45	78.46
11.3	5.83	2.99	8.63	65.91	12.3	5.82	3.06	8.13	77.80
11.4	5.74	2.97	7.53	64.04	12.4	5.82	3.07	7.50	75.25
11.5	5.82	2.96	7.56	64.96	12.5	5.78	3.01	7.49	72.28
11.6	5.73	2.96	6.94	57.88	12.6	5.79	3.02	8.34	99.78
11.7	5.82	2.92	8.50	60.20	12.7	5.79	2.94	8.23	96.63
11.8	5.70	2.92	8.51	61.85	12.8	5.75	2.93	7.54	75.87
11.9	5.82	2.86	8.17	62.28	12.9	5.81	2.92	9.37	96.63
11.1	5.76	2.89	8.87	61.85	12.101	5.74	2.87	7.14	71.16
11.11	5.81	2.82	7.72	57.52	12.11	5.76	2.84	8.11	85.00
11.12	5.79	2.84	7.92	51.31	12.12	5.83	2.79	7.26	71.72
Avg	5.78	2.93	8.00	59.71	Avg	5.79	2.97	7.98	81.48
STD	0.05	0.07	0.55	4.79	STD	0.03	0.10	0.63	10.46

NaOH fibres with polypropylene (NaOH - PP)					NaOH fibres with 4% clay (NaOH - 4C)				
Specimen	Width (mm)	Thick (mm)	Shear Str (MPa)	Shear Mod (MPa)	Specimen	Width (mm)	Thick (mm)	Shear Str (MPa)	Shear Mod (MPa)
10.1	6.12	3.38	8.97	80.48	10.1	6.05	3.11	8.37	78.40
10.2	6.16	3.30	8.28	76.24	10.2	6.08	3.19	8.36	84.82
10.3	6.21	3.29	9.27	71.91	10.3	6.03	3.13	7.30	66.64
10.4	6.11	3.19	7.77	71.41	10.4	6.08	3.19	9.09	88.02
10.5	6.18	3.22	7.21	67.15	10.5	6.03	3.04	8.26	87.20
10.6	6.12	3.11	8.47	72.95	10.6	6.08	3.14	8.81	84.05
10.7	6.18	3.10	8.05	72.43	10.7	6.04	3.04	8.55	81.84
10.8	6.06	2.99	7.68	60.72	10.8	6.07	3.11	8.86	84.05
10.9	6.18	3.00	8.22	77.40	10.9	6.03	2.98	7.62	74.05
10.1	6.12	2.88	8.70	76.24	10.101	6.04	3.11	8.31	81.13
10.11	6.20	2.95	7.41	61.83	10.11	6.09	3.01	7.49	75.85
10.12	6.10	2.83	8.23	73.48	10.12	6.07	3.06	8.20	88.02
Avg	6.15	3.10	8.19	71.85	Avg	6.06	3.09	8.27	81.17
STD	0.05	0.18	0.61	5.99	STD	0.02	0.07	0.56	6.45

Table F.24: Raw Results - Shear 2

T1 fibres with polypropylene (T1 - PP)					T1 fibres with 4% clay (T1 - 4C)				
Specimen	Width (mm)	Thick (mm)	Shear Str (MPa)	Shear Mod (MPa)	Specimen	Width (mm)	Thick (mm)	Shear Str (MPa)	Shear Mod (MPa)
11.1	5.53	3.03	8.90	66.84	2.1	5.83	3.03	8.73	86.57
11.2	5.64	2.94	8.37	65.87	2.2	5.76	3.10	9.21	90.90
11.3	5.57	3.01	9.06	80.44	2.3	5.81	2.98	8.37	85.75
11.4	5.60	2.90	9.47	74.51	2.4	5.70	3.07	8.49	84.95
11.5	5.56	2.93	8.80	72.14	2.5	5.79	2.92	8.43	77.03
11.6	5.60	2.85	8.58	75.12	2.6	5.73	2.98	9.06	79.04
11.7	5.57	2.85	8.27	64.47	2.7	5.78	2.83	8.48	80.44
11.8	5.56	2.73	7.01	59.80	2.8	5.73	2.88	8.24	81.89
11.9	5.57	2.72	6.78	52.54	2.9	5.76	2.75	7.49	77.69
11.1	5.62	2.67	8.03	68.86	2.101	5.75	2.86	8.15	81.89
11.11	5.56	2.71	8.62	79.04	2.11	5.78	2.71	8.71	82.64
11.12	5.55	2.61	6.43963	60.6	2.12	5.74	2.81	7.50	82.64
Avg	5.58	2.83	8.19	68.35	Avg	5.76	2.91	8.40	82.62
STD	0.03	0.14	0.96	8.34	STD	0.04	0.12	0.53	3.97

T2 fibres with polypropylene (T2 - PP)					T2 fibres with 4% clay (T2 - 4C)				
Specimen	Width (mm)	Thick (mm)	Shear Str (MPa)	Shear Mod (MPa)	Specimen	Width (mm)	Thick (mm)	Shear Str (MPa)	Shear Mod (MPa)
13.1	5.94	3.35	8.22	88.16	3.1	5.95	3.11	7.85	70.68
13.2	5.90	3.27	9.31	87.39	3.2	6.19	3.18	7.55	72.89
13.3	5.86	3.19	8.10	79.76	3.3	6.09	3.14	7.70	67.61
13.4	5.89	3.15	7.76	70.28	3.4	6.25	3.27	7.48	76.48
13.5	5.83	3.07	8.72	72.30	3.5	6.12	3.13	7.56	74.05
13.6	5.91	3.03	7.62	70.77	3.6	6.24	3.14	7.51	79.74
13.7	5.87	2.95	8.45	65.69	3.7	6.05	3.06	7.19	59.43
13.8	5.91	2.92	7.66	59.47	3.8	6.20	3.13	7.85	71.22
13.9	5.85	2.80	8.07	66.56	3.9	6.06	3.09	7.86	71.22
13.1	5.88	2.74	7.19	60.91	3.101	6.15	3.07	7.92	67.12
13.11	5.89	2.68	7.81	60.54	3.11	6.11	3.02	7.62	74.05
13.12	5.92	2.70	7.07	54.03	3.12	6.13	3.03	6.74	61.79
Avg	5.89	2.99	8.00	69.66	Avg	6.13	3.11	7.57	70.52
STD	0.03	0.23	0.63	10.87	STD	0.09	0.07	0.33	5.81

Table F.25: Raw Results - Shear 3

T3 fibres with polypropylene (T3 - PP)					T3 fibres with 4% clay (T3 - 4C)				
Specimen	Width (mm)	Thick (mm)	Shear Str (MPa)	Shear Mod (MPa)	Specimen	Width (mm)	Thick (mm)	Shear Str (MPa)	Shear Mod (MPa)
14.1	6.01	3.17	6.79	64.69	4.1	6.10	3.35	8.40	83.75
14.2	6.00	3.28	8.38	77.32	4.2	6.09	3.31	8.93	97.57
14.3	5.99	3.12	8.93	60.96	4.3	6.14	3.36	8.75	88.94
14.4	6.00	3.23	8.08	70.97	4.4	6.12	3.28	7.57	87.39
14.5	5.92	3.00	8.95	67.93	4.5	6.16	3.27	7.80	81.71
14.6	6.01	3.11	7.98	56.27	4.6	6.15	3.20	8.69	88.94
14.7	5.99	2.92	7.96	55.61	4.7	6.22	3.20	10.20	88.16
14.8	6.00	3.00	7.73	60.57	4.8	6.19	3.05	8.17	75.00
14.9	5.94	2.90	8.38	65.59	4.9	6.19	3.01	8.25	88.94
14.1	5.98	2.91	6.60	51.41	4.101	6.08	2.95	8.21	83.06
14.11	5.99	2.79	7.43	55.94	4.11	6.11	2.89	8.04	78.52
14.12	6.05	2.90	7.61	55.61					
Avg	5.99	3.03	7.90	61.91	Avg	6.14	3.17	8.45	85.63
STD	0.03	0.15	0.73	7.61	STD	0.05	0.17	0.71	6.12

T4 fibres with polypropylene (T4 - PP)					T4 fibres with 4% clay (T4 - 4C)				
Specimen	Width (mm)	Thick (mm)	Shear Str (MPa)	Shear Mod (MPa)	Specimen	Width (mm)	Thick (mm)	Shear Str (MPa)	Shear Mod (MPa)
12.1	5.82	3.08	8.03	72.76	1.1	5.80	3.20	9.09	94.12
12.2	5.78	3.13	8.86	87.17	1.2	5.85	3.07	8.87	103.23
12.3	5.81	3.06	7.59	58.85	1.3	5.80	3.11	9.07	101.05
12.4	5.79	3.05	9.16	69.47	1.4	5.84	2.98	8.54	90.57
12.5	5.73	2.98	8.24	66.96	1.5	5.86	3.01	9.25	104.35
12.6	5.78	3.02	7.60	64.62	1.6	5.83	2.93	9.58	111.63
12.7	5.73	2.96	8.18	75.74	1.7	5.83	2.98	8.45	93.20
12.8	5.78	2.95	8.88	75.12	1.8	5.81	2.85	8.55	104.35
12.9	5.74	2.84	7.76	71.08	1.9	5.87	2.92	9.13	94.12
12.1	5.81	2.91	7.29	68.96	1.101	5.84	2.80	9.26	103.23
12.11	5.82	2.78	7.71	57.39	1.11	5.87	2.88	8.04	89.72
12.12	5.75	2.80	7.28	51.62	1.12	5.81	2.78	7.92	78.05
Avg	5.78	2.96	8.05	68.31	Avg	5.83	2.96	8.81	97.30
STD	0.03	0.11	0.63	9.48	STD	0.03	0.13	0.51	9.04

Table F.26: Raw Results - Shear 4

0.25% MPS fibres with PP (0.25M - PP)					0.25% MPS fibres with 4% clay (0.25M - 4C)				
Specimen	Width (mm)	Thick (mm)	Shear Str (MPa)	Shear Mod (MPa)	Specimen	Width (mm)	Thick (mm)	Shear Str (MPa)	Shear Mod (MPa)
3.1	5.89	3.09	8.22	77.90	3.1	6.16	3.48	8.72	100.38
3.2	5.84	2.97	7.86	63.93	3.2	6.09	3.49	8.56	92.39
3.3	5.87	3.09	8.32	67.66	3.3	6.29	3.37	8.69	100.38
3.4	5.85	2.96	7.82	57.58	3.4	6.26	3.37	8.95	100.38
3.5	5.88	3.07	8.00	69.18	3.5	6.25	3.25	7.78	84.19
3.6	5.88	2.98	8.40	66.21	3.6	6.28	3.27	7.67	93.21
3.7	5.92	3.08	8.30	77.25	3.7	6.33	3.17	8.57	94.05
3.8	5.86	2.94	8.76	69.18	3.8	6.26	3.16	8.20	87.73
3.9	5.92	3.05	9.40	74.16	3.9	6.32	3.10	8.45	93.21
3.101	5.88	2.92	7.92	66.21	3.101	6.32	3.08	8.12	90.00
3.11	5.93	3.06	6.92	73.57	3.11	6.10	3.02	7.18	77.33
3.12	5.88	2.89	7.72	72.42	3.12	6.23	2.97	7.52	72.50
Avg	5.88	3.01	8.14	69.61	Avg	6.24	3.23	8.20	90.48
STD	0.03	0.07	0.60	5.84	STD	0.08	0.17	0.55	8.89

1% MPS fibres with PP (1M - PP)					1% MPS fibres with 4% clay (1M - 4C)				
Specimen	Width (mm)	Thick (mm)	Shear Str (MPa)	Shear Mod (MPa)	Specimen	Width (mm)	Thick (mm)	Shear Str (MPa)	Shear Mod (MPa)
5.1	5.87	3.35	9.20	89.73	1.1	6.14	3.30	8.95	87.61
5.2	5.95	3.33	10.24	97.57	1.2	6.29	3.30	8.65	86.09
5.3	5.88	3.19	9.00	91.36	1.3	6.08	3.29	8.72	103.13
5.4	5.93	3.19	8.23	86.64	1.4	6.23	3.23	9.15	96.12
5.5	5.88	3.06	8.78	77.31	1.5	6.15	3.21	9.38	98.02
5.6	5.89	3.05	8.72	78.52	1.6	6.24	3.16	9.15	92.52
5.7	5.90	2.98	8.08	72.83	1.7	6.20	3.14	8.55	83.90
5.8	5.88	2.97	8.29	81.05	1.8	6.24	3.09	8.00	74.44
5.9	5.91	2.89	7.03	64.84	1.9	6.18	3.03	8.04	80.49
5.101	5.87	2.84	8.21	69.79	1.101	6.22	3.02	8.28	81.82
5.11	5.90	2.73	7.25	68.37	1.11	6.20	3.11	7.83	76.15
5.12	5.88	2.73	6.98	62.81	1.12	6.26	2.94	7.79	83.19
Avg	5.90	3.03	8.33	78.40	Avg	6.20	3.15	8.54	86.96
STD	0.02	0.21	0.95	11.17	STD	0.06	0.12	0.55	8.87

Table F.27: Raw Results - Shear 5

2% MPS fibres with PP (2M - PP)					2% MPS fibres with 4% clay (2M - 4C)				
Specimen	Width (mm)	Thick (mm)	Shear Str (MPa)	Shear Mod (MPa)	Specimen	Width (mm)	Thick (mm)	Shear Str (MPa)	Shear Mod (MPa)
6.1	6.05	3.34	8.61	79.52	8.1	6.10	3.22	7.99	78.54
6.2	6.07	3.40	9.22	75.34	8.2	6.11	3.12	6.98	71.03
6.3	6.10	3.21	8.86	85.64	8.3	6.16	3.27	9.29	106.15
6.4	6.04	3.25	8.00	82.81	8.4	6.16	3.14	8.14	86.25
6.5	6.06	3.10	8.86	75.34	8.5	6.13	3.19	8.29	88.62
6.6	6.02	3.14	10.04	82.13	8.6	6.16	3.11	8.37	96.60
6.7	6.01	2.99	8.22	74.22	8.7	6.15	3.16	8.95	97.58
6.8	6.05	3.02	8.21	80.81	8.8	6.16	3.08	7.98	85.49
6.9	6.04	2.86	7.65	73.68	8.9	6.14	3.14	8.49	87.82
6.101	6.04	2.90	8.40	74.22	8.101	6.13	3.06	7.97	87.03
6.11	6.06	2.73	7.20	63.82	8.11	6.11	3.09	7.45	63.14
6.12	6.01	2.72	7.77	63.02	8.12	6.17	3.06	8.27	84.00
Avg	6.05	3.06	8.42	75.88	Avg	6.14	3.14	8.18	86.02
STD	0.03	0.23	0.77	7.02	STD	0.02	0.06	0.61	11.56

5% MPS fibres with PP (5M - PP)					5% MPS fibres with 4% clay (5M - 4C)				
Specimen	Width (mm)	Thick (mm)	Shear Str (MPa)	Shear Mod (MPa)	Specimen	Width (mm)	Thick (mm)	Shear Str (MPa)	Shear Mod (MPa)
4.1	5.90	3.00	10.04	72.58	5.1	6.18	3.31	7.91	71.44
4.2	5.87	3.08	7.52	65.22	5.2	6.23	3.24	7.76	75.80
4.3	5.90	2.97	8.85	75.00	5.3	6.32	3.28	9.45	91.10
4.4	5.83	3.05	8.67	80.36	5.4	6.30	3.26	8.35	77.58
4.5	5.88	2.95	9.92	76.27	5.5	6.31	3.23	8.72	99.30
4.6	5.88	3.06	8.41	72.00	5.6	6.30	3.20	8.18	86.35
4.7	5.88	2.92	8.63	72.00	5.7	6.34	3.21	8.25	85.60
4.8	5.87	2.99	8.65	70.31	5.8	6.27	3.24	9.25	91.10
4.9	5.87	2.88	7.68	70.31	5.9	6.37	3.25	8.65	80.08
4.101	5.88	3.00	8.32	74.38	5.101	6.27	3.21	8.04	80.08
4.11	5.89	2.85	8.54	66.18	5.11	6.29	3.14	7.71	75.80
4.12	5.89	2.97	8.49	71.43	5.12	6.27	3.14	8.02	75.80
Avg	5.88	2.98	8.64	72.17	Avg	6.29	3.23	8.36	82.50
STD	0.02	0.07	0.74	4.14	STD	0.05	0.05	0.56	8.24

Table F.28: Raw Results - Shear 6

0.25% MPS fibres with 1% clay (0.25M - 1C)					0.25% MPS fibres with 2% clay (0.25M - 2C)				
Specimen	Width (mm)	Thick (mm)	Shear Str (MPa)	Shear Mod (MPa)	Specimen	Width (mm)	Thick (mm)	Shear Str (MPa)	Shear Mod (MPa)
1.1	6.07	3.15	8.14	72.14	3.1	6.09	3.17	7.70	64.69
1.2	6.10	3.08	8.13	84.37	3.2	5.85	3.19	8.09	71.50
1.3	6.14	3.17	8.41	71.59	3.3	6.17	3.13	6.99	70.44
1.4	6.08	3.04	7.76	80.77	3.4	5.99	3.16	7.55	76.08
1.5	6.10	3.09	8.65	73.26	3.5	6.16	3.11	6.97	68.42
1.6	6.09	3.04	7.85	76.83	3.6	6.15	3.20	7.29	76.69
1.7	6.13	3.14	8.33	75.60	3.7	6.15	3.13	8.35	80.59
1.8	6.12	3.07	8.86	95.45	3.8	6.14	3.14	8.27	80.59
1.9	6.07	3.10	8.49	90.87	3.9	6.09	3.12	7.62	76.69
1.101	6.11	3.07	9.62	92.65	3.101	6.15	3.17	8.10	80.59
1.11	6.10	3.06	8.16	90.87	3.11	6.06	3.06	7.18	63.40
1.12	6.08	3.04	8.60	90.87	3.12	6.14	3.15	8.05	73.72
Avg	6.10	3.09	8.42	82.94	Avg	6.10	3.14	7.68	73.62
STD	0.02	0.04	0.50	8.93	STD	0.09	0.04	0.49	6.00

0.25% MPS fibres with 6% clay (0.25M - 6C)					0.25% MPS fibres with 8% clay (0.25M - 8C)				
Specimen	Width (mm)	Thick (mm)	Shear Str (MPa)	Shear Mod (MPa)	Specimen	Width (mm)	Thick (mm)	Shear Str (MPa)	Shear Mod (MPa)
5.1	5.69	3.06	7.19	86.60	8.1	6.10	3.19	7.97	84.69
5.2	5.79	3.03	7.96	90.89	8.2	6.11	3.13	8.38	82.50
5.3	5.77	2.95	8.34	94.64	8.3	6.11	3.23	8.19	77.80
5.4	5.79	2.91	8.40	88.27	8.4	6.11	3.22	9.03	83.95
5.5	5.80	2.86	8.96	99.78	8.5	6.12	3.16	10.62	89.44
5.6	5.77	2.84	9.30	102.00	8.6	6.10	3.02	7.81	71.42
5.7	5.71	2.97	9.23	100.88	8.7	6.11	3.06	9.58	89.44
5.8	5.68	2.92	9.16	96.63	8.8	6.10	3.02	8.17	83.95
5.9	5.70	2.88	7.97	84.22	8.9	6.10	3.08	9.46	91.14
5.101	5.70	2.87	8.68	92.73	8.101	6.09	2.99	8.78	77.18
					8.11	6.06	3.03	8.81	87.80
					8.12	6.08	2.95	7.58	73.62
Avg	5.74	2.93	8.52	93.66	Avg	6.10	3.09	8.70	82.74
STD	0.05	0.07	0.68	6.20	STD	0.02	0.09	0.87	6.46

Table F.29: Raw Results - Shear 7

15% FWF with polypropylene (15%F - PP)					15% FWF with 2% clay (15%F - 2C)				
Specimen	Width (mm)	Thick (mm)	Shear Str (MPa)	Shear Mod (MPa)	Specimen	Width (mm)	Thick (mm)	Shear Str (MPa)	Shear Mod (MPa)
7.1	9.26	4.98	8.38	70.47	5.1	8.80	4.45	7.70	71.01
7.2	9.15	4.94	8.47	72.52	5.2	8.58	4.49	7.90	74.17
7.3	9.27	4.82	8.15	71.83	5.3	8.64	4.43	7.85	69.53
7.4	9.24	4.75	8.23	71.48	5.4	8.66	4.48	7.62	71.01
7.5	9.28	4.60	8.32	69.81	5.5	8.65	4.37	7.81	73.76
7.6	9.21	4.59	8.26	70.14	5.6	8.67	4.40	7.68	66.42
7.7	9.24	4.40	8.11	63.04	5.7	8.65	4.26	7.45	68.11
7.8	9.19	4.36	7.71	61.48	5.8	8.62	4.37	7.11	61.24
Avg	9.23	4.68	8.20	68.85	Avg	8.66	4.41	7.64	69.41
STD	0.04	0.23	0.23	4.18	STD	0.06	0.07	0.26	4.21

20% FWF with polypropylene (20%F - PP)					20% FWF with 2% clay (20%F - 2C)				
Specimen	Width (mm)	Thick (mm)	Shear Str (MPa)	Shear Mod (MPa)	Specimen	Width (mm)	Thick (mm)	Shear Str (MPa)	Shear Mod (MPa)
6.1	7.92	4.17	7.65	61.93	3.1	7.24	4.07	8.05	80.86
6.2	8.12	4.06	6.92	56.10	3.2	7.63	4.05	7.92	80.86
6.3	8.03	4.14	7.77	62.86	3.3	7.68	4.02	7.99	84.21
6.4	8.17	4.03	7.30	58.19	3.4	7.67	3.99	8.56	84.21
6.5	7.98	4.06	7.06	56.35	3.5	7.67	3.94	7.51	76.31
6.6	8.01	3.94	6.65	54.16	3.6	7.69	3.92	7.79	79.80
6.7	7.93	3.96	6.84	48.30	3.7	7.66	3.84	7.97	80.86
6.8	8.05	3.85	6.72	55.11	3.8	7.66	3.82	7.93	77.77
Avg	8.03	4.03	7.11	56.62	Avg	7.61	3.96	7.96	80.61
STD	0.09	0.11	0.42	4.59	STD	0.15	0.09	0.29	2.76

Table F.30: Raw Results - Shear 8

30% FWF with polypropylene (30%F - PP)					30% FWF with 2% clay (30%F - 2C)				
Specimen	Width (mm)	Thick (mm)	Shear Str (MPa)	Shear Mod (MPa)	Specimen	Width (mm)	Thick (mm)	Shear Str (MPa)	Shear Mod (MPa)
1.1	5.11	2.61	8.89	79.09	1.1	4.88	2.53	9.30	80.74
1.2	5.14	2.56	8.76	66.36	1.2	4.94	2.61	8.76	83.41
1.3	5.14	2.61	8.53	77.52	1.3	5.02	2.53	9.93	94.88
1.4	5.13	2.57	8.57	75.29	1.4	5.01	2.63	9.21	89.29
1.5	5.12	2.59	9.01	81.56	1.5	4.97	2.51	9.28	97.31
1.6	5.12	2.56	7.90	71.83	1.6	5.00	2.60	9.12	94.88
1.7	5.14	2.55	8.62	73.18	1.7	5.00	2.50	9.64	93.70
1.8	5.09	2.56	8.67	71.18	1.8	5.01	2.55	9.65	98.57
1.9	5.18	2.53	8.73	64.71	1.9	5.03	2.49	10.07	97.31
1.101	5.11	2.57	8.71	66.92	1.101	5.01	2.53	9.06	93.70
1.11	5.16	2.53	7.86	64.71	1.11	5.04	2.48	9.34	88.26
1.12	5.11	2.57	8.35	69.29	1.12	4.87	2.54	9.28	84.33
Avg	5.13	2.57	8.55	71.80	Avg	4.98	2.54	9.39	91.36
STD	0.02	0.03	0.35	5.69	STD	0.06	0.05	0.37	6.01

Appendix G Repeatability of Manufacturing

The repeatability of the manufacturing was tested by making two specimens of the same configuration and performing tensile testing. Each configuration comprised a particular chemical treatment. The first plate manufactured using a particular fibre chemical treatment was tested immediately whilst the remaining plate was tested approximately one week later. The tensile strength and tensile modulus data can be seen in figures G.1 and G.2, respectively. The abbreviations for the treatments employed in this investigation can be seen in Table 5.1.

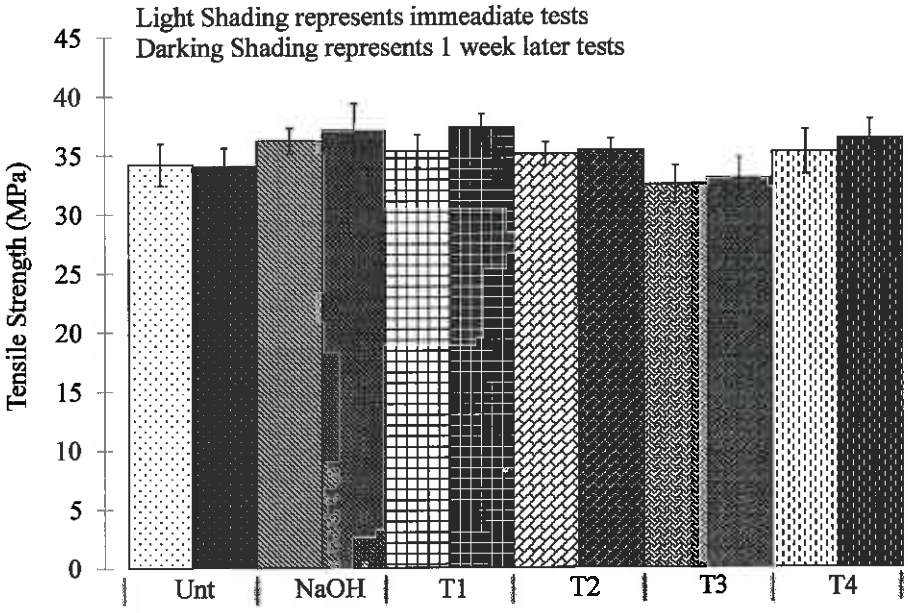

Figure G.1: Tensile Strength - Effect of conditioning in two composites

The tensile strength of composites tested a week after manufacture compared to immediately shows improved strength in comparison to those test immediately after manufacture and this

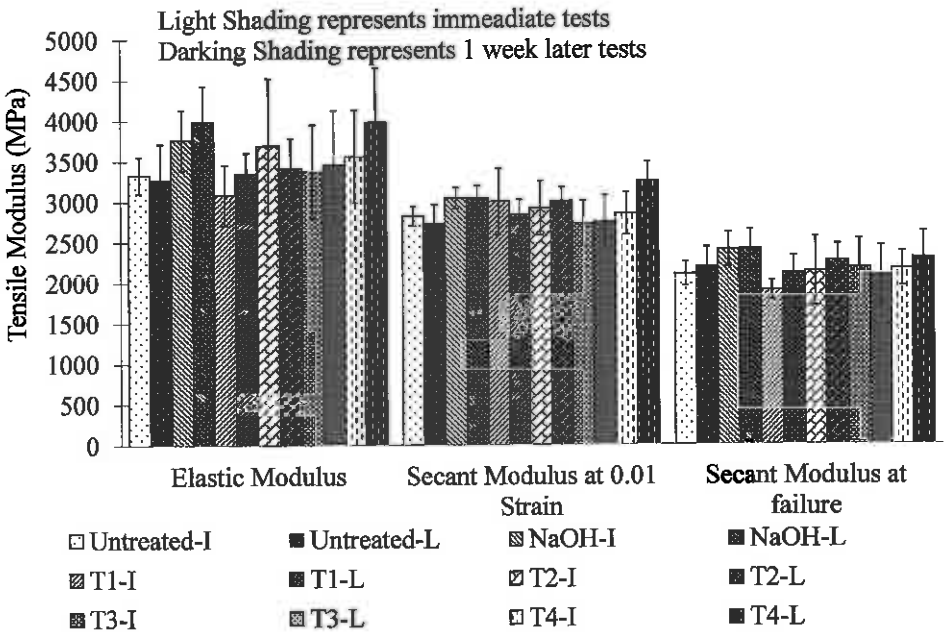

Figure G.2: Tensile Modulus - Effect of conditioning in two composites

effect can be seen in Figure G.1. The factor that was varied was time, which would imply conditioning of the composite.